Západočeská univerzita v Plzni
Fakulta aplikovaných věd

Bifurkace v reakčně–difuzních problémech

Mgr. Martin Fencl

disertační práce
k získání akademického titulu doktor (Ph.D.)
v oboru Aplikovaná matematika

Školitel: prof. RNDr. Milan Kučera, DrSc.

Katedra matematiky

Plzeň 2021

University of West Bohemia in Pilsen
Faculty of Applied Sciences

Bifurcations in reaction–diffusion problems

Mgr. Martin Fencl

dissertation thesis
for taking academic degree Doctor of Philosophy (Ph.D.)
in the specialization Applied mathematics

Supervisor: prof. RNDr. Milan Kučera, DrSc.

Department of mathematics

Pilsen 2021

Declaration:

I declare that the presented thesis is my original work. It is based on the scientific results which I have authored or co-authored and on cited sources which are contained in the list of references.

.....
Martin Fencl

Abstrakt

Náplní této práce je studium bifurkací v superlineárních neurčitých problémech a systémech reakce–difuze, které vykazují Turingovu difuzí řízenou nestabilitu. Při zkoumání těchto problémů využíváme metod matematické a numerické analýzy.

Tato disertace je rozdělena na dvě části. V první se věnujeme již zmíněným superlineárním problémům. Jednak jde o studium globální struktury pozitivních řešení pomocí numerické kontinuace a objasnění domněnky o počtu těchto řešení. Dále se pak zabýváme superlineárním problémem s váhovou funkcí. Zde jsme se věnovali nečekaným spektrálním vlastnostem tohoto problému a jejich důsledkům na chování bifurkačních větví. V druhé části této práce shrneme naše výsledky týkající se vlivu jednostranných členů a jednostranných členů obsahujících integrální průměr v rovnici pro aktivátor u systému reakce–difuze na vznik prostorových vzorků. Ukážeme, že množina difuzních parametrů, pro které je bifurkace z konstantního řešení možná, je v takovém případě menší, než u problému bez jednostranných členů. Zároveň prozkoumáme tvorbu vzorků u problému se Schnakenbergovou kinetikou pomocí numerických experimentů pro různé jednostranné členy a okrajové podmínky.

Závěrem přikládáme ve čtyřech apendixech články s výsledky, které prezentujeme v textu této disertační práce.

Klíčová slova:

bifurkace, superlineární neurčitý problém, numerická analýza, bifurkační diagramy, reačně–difuzní systémy, Turingova nestability, jednostranné členy, pozitivně homogenní operátory, prostorové vzorky, numerické experimenty

Abstract

This dissertation thesis presents our recent results concerning bifurcations in superlinear indefinite problems and in reaction-diffusion systems exhibiting Turing's diffusion-driven instability. All problems in the thesis are studied both by analytical and numerical methods.

We divided the thesis into two main parts. The first one is focused on superlinear indefinite problems. We study the global structure of positive solutions using numerical continuation and solve the conjecture about number of positive solutions under some additional conditions. Subsequently, we explore a weighted superlinear indefinite problem with unexpected spectral properties, which lead to complex behaviour of branches of nodal solutions. The second part contains results concerning a system of two reaction-diffusion equations exhibiting Turing's instability. We show that adding unilateral terms or unilateral terms involving integral average to the activator equation of the system results in a smaller set of positive diffusion parameters, for which the bifurcation from the trivial solution can occur. All analytical results in the part are accompanied by numerical experiments with Schnakenberg reaction kinetics. The main aim of these experiments is to observe changes in pattern formation provoked by various unilateral terms and boundary conditions.

The last part of the thesis is composed of four appendices containing our original publications with all details and technicalities for any interested readers.

Keywords:

bifurcation, superlinear indefinite problems, numerical analysis, bifurcation diagrams, reaction–diffusion systems, Turing's instability, unilateral terms, positively homogeneous operators, pattern formation, numerical experiments

Résumé

Cette thèse présente nos résultats récents concernant les problèmes de bifurcations superlinéaires indéfinis et les systèmes de réaction-diffusion présentant l'instabilité de Turing induite par la diffusion. Tous les problèmes de la thèse sont étudiés à la fois par des méthodes analytiques et numériques.

Nous avons divisé la thèse en deux parties principales. Le premier est axé sur les problèmes superlinéaires indéfinis. Nous étudions la structure globale des solutions positives en utilisant la continuation numérique et résolvons la conjecture sur le nombre de solutions positives dans certaines conditions d'addition. Par la suite, nous explorons un problème indéfini superlinéaire pondéré avec des propriétés spectrales inattendues, qui conduisent à un comportement complexe des branches de solutions nodales. La deuxième partie contient des résultats concernant un système de deux équations de réaction-diffusion présentant l'instabilité de Turing. Nous montrons que l'ajout de termes unilatéraux ou de termes unilatéraux impliquant une moyenne intégrale à l'équation activatrice du système entraîne un ensemble plus petit de paramètres de diffusion positifs, pour lesquels la bifurcation de la solution triviale peut se produire. Tous les résultats analytiques de la pièce sont accompagnés d'expériences numériques avec la cinétique de réaction de Schnakenberg. L'objectif principal de ces expériences est d'observer les changements dans la formation des motifs provoqués par divers termes unilatéraux et conditions aux limites.

La dernière partie de la thèse est composée de quatre annexes contenant nos publications originales avec tous les détails et détails techniques pour tous les lecteurs intéressés.

Mots clés:

bifurcation, problèmes indéfinis super-linéaires, analyse numérique, diagrammes de bifurcation, systèmes de réaction–diffusion, instabilité de Turing, termes unilatéraux, opérateurs positivement homog?nes, formation de motifs, expériences numériques

Acknowledgements

Firstly, I would like to thank very much to my supervisor Milan Kučera. I appreciate his scientific leadership, advices and a lot of patience, especially during the writing of our first paper.

I would also like to express gratitude to my co-author Julian López-Gómez for his many valuable advices and support during my stay at Madrid as well as expanding my mathematical thinking.

Further, let me thank Petr Stehlík for suggestions and comments after reading my master thesis and preliminary version of this thesis submitted to the state doctoral exam.

Many thanks also belong to Marek Brandner as he taught me much about numerical mathematics and was always open to discussions.

At the end, I would like to thank my family, friends and colleagues for their support, which helped me in the most challenging moments of my doctoral study.

This thesis and papers included in appendices were supported by Ministry of Education, Youth, and Sports of the Czech Republic under the program NPU I, Project No. LO1506 (PUNTIS) and Grant Agency of the Czech Republic, project no. 18-03253S (principal investigator prof. RNDr. Pavel Drábek, DrSc.). Also I would like to acknowledge the financial support of the research centre NTIS and the program Erasmus+, which allowed me to spend four amazing months at Universidad Complutense de Madrid.

Contents

1 | Introduction

The main focus of this thesis are bifurcations in two types of problems. The first one is a superlinear indefinite problem and the second one is a system of two reaction–diffusion equations, which exhibits so called Turing's instability. Every problem is approached by both methods of mathematical analysis and numerical mathematics as it fits the author's interest in both of these areas of mathematics during his doctoral study.

The further text of this work is composed of two chapters. In the former chapter, we present our new results concerning superlinear indefinite problems. The first section (Section 2.1) contains results from our joint paper with Julián López-Gómez:

[FLG21] M. Fencl and J. López-Gómez. *Global bifurcation diagrams of positive solutions for a class of 1-d superlinear indefinite problems.* arXiv:2005.09369v3[math.AP] 7Mar2021, Submitted to Nonlinearity.

We study there a superlinear indefinite problem

$$\begin{cases} -u'' = \lambda u + a(x)u^2 & \text{in } (0,1), \\ u(0) = u(1) = 0, \end{cases} \tag{1.1}$$

where $a(x)$ is a continuous function that changes the sign in the interval $(0,1)$ and the parameter $\lambda \in \mathbb{R}$ is regarded as a bifurcation parameter.

We study the conjecture (see, e.g., Conjecture 2.3) about the number of positive solutions of the problem (1.1) for sufficiently negative λ with dependence on the character of the function $a(x)$. This conjecture was originally presented in [GRnLG00]. We show that the conjecture holds true under some additional conditions on boundedness of solutions. Further we study the structure of positive solutions by methods of numerical analysis in four special cases of the function $a(x)$. Besides observing the confirmation of the conjecture, we show that the structure of branches of positive solutions can be very complex.

The next section (Section 2.2) summarizes results of the joint paper with Julián López-Gómez:

[FLG20] M. Fencl and J. López-Gómez. *Nodal solutions of weighted indefinite problems.* Journal of Evolution Equations, 2020, published on-line at doi:10.1007/s00028-020-00625–7

The problem of interest here is

$$\begin{cases} -u'' - \mu u = \lambda m(x)u - a(x)u^2 & \text{in } (0,1), \\ u(0) = u(1) = 0, \end{cases} \tag{1.2}$$

where functions a, m are continuous and change the sign in the interval $(0,1)$ and $\lambda, \mu \in \mathbb{R}$ are regarded as bifurcation parameters with λ being the primary one and μ being the secondary parameter.

It is known that the eigencurve of this problem associated with bifurcation points of branches of positive solutions is always concave. Hence, the branches of positive solutions bifurcate from up to two bifurcation points. We prove that for a special class of functions $m(x)$, the eigencurves of this problem associated with bifurcation points of branches of nodal solutions are not always concave, which has a significant impact on the number of bifurcation points of these branches. Further, we use numerical methods to compute branches of solutions and we show how these branches behave as we increase the parameter μ. The most interesting aspect here is the recombination of these branches due to non-concavity of the associate eigencurve and the change of the number of bifurcation points.

In the latter chapter, we incorporate our results concerning reaction–diffusion systems exhibiting Turing's instability. The well–known conditions on this effect are presented in Section 3.1. The new results on this topic were published in two papers, first one being in collaboration with Milan Kučera:

[FK19] M. Fencl and M. Kučera. *Unilateral sources and sinks of an activator in reaction-diffusion systems exhibiting diffusion-driven instability.* Nonlinear Anal., 187:71–92, 2019, doi:10.1016/j.na.2019.04.001

[Fen20] M. Fencl. *An influence of unilateral sources and sinks in reaction-diffusion systems exhibiting Turing's instability on bifurcation and pattern formation.* Nonlinear Anal., 196:111815, 2020, doi:10.1016/j.na.2020.111815

These two papers are very intertwined, because the numerical experiments published in the latter one are also completing the topic of the former one. The numerical methods, Schnakenberg's reaction kinetics we are using and boundary conditions are described in Section 3.2.

Sections 3.3 and 3.4 summarize the analytical and the numerical results concerning problems

$$\begin{aligned} \frac{\partial u}{\partial t} &= d_1 \Delta u + f(u,v) + \tilde{f}_-(\mathbf{x}, u^-) - \tilde{f}_+(\mathbf{x}, u^+), \\ \frac{\partial v}{\partial t} &= d_2 \Delta v + g(u,v) \quad \text{in } \Omega \times [0, +\infty)\,, \end{aligned} \tag{1.3}$$

and

$$\begin{aligned} \frac{\partial u}{\partial t} &= d_1 \Delta u + f(u,v) \\ &\quad + \sum_{i=1}^{n} \chi^{K_i^-}(x) f_-^i \left(\left(\int_{K_i^-} \frac{u}{|K_i^-|}\, dK_i^- \right)^- \right) - \sum_{j=1}^{m} \chi^{K_j^+}(x) f_+^j \left(\left(\int_{K_j^+} \frac{u}{|K_j^+|}\, dK_j^+ \right)^+ \right), \\ \frac{\partial v}{\partial t} &= d_2 \Delta v + g(u,v) \quad \text{in } \Omega \times [0, +\infty)\,, \end{aligned} \tag{1.4}$$

respectively. The numbers d_1, d_2 are positive diffusion parameters, $f, g : \mathbb{R}^2 \mapsto \mathbb{R}$ are functions of the class C^1 and $\Omega \in \mathbb{R}^N$ is a bounded domain with Lipschitz boundary. The system (1.3) contains functions $\tilde{f}_-, \tilde{f}_+ : \Omega \times \mathbb{R} \to \mathbb{R}$, which are the unilateral source and the sink with u^-, u^+ being the negative and the positive part of the function u. The system (1.4) on the

other hand contains multiple unilateral sources and sinks, which involve the integral average over some subset K_i^-, K_j^+ of the domain Ω. Let us note that $\chi(x)$ is always a characteristic function of the set in its superscript. We always assume the existence of a constant steady state of systems (1.3) and (1.4) completed by some boundary conditions. For more detailed description of the problem itself and assumptions, see Chapter 3.

We show that under some conditions the set of points $[d_1, d_2] \in \mathbb{R}^2_+$, for which the bifurcation from the constant steady state of (1.3) and (1.4) (with some boundary conditions) can occur, is smaller than in the classical case when there are no unilateral sources or sinks (with or without integral average) present in the system. This assertion is proved for a rather general combination of Dirichlet and Neumann boundary conditions. We also get specific results in some special cases of, e.g., only Neumann boundary conditions etc.

Both problems (1.3) and (1.4) with Neumann and periodic boundary conditions are also studied by numerical experiments in some specific situation concerning unilateral terms. We study the quantitative change of the area of points $[d_1, d_2]$, for which a pattern can develop from small perturbations of the constant steady state. We are also interested in the shape of created patterns and the effect of spatial dependence of unilateral terms on this shape. The discussion of numerical results is in Section 3.5.

To conclude this introduction, let us note that all four papers are attached in appendices of this thesis.

2 | Bifurcations in superlinear indefinite problems

This chapter summarizes results of two papers [FLG20] and [FLG21] (see also Appendices C, D). We study a superlinear indefinite problem in both of them. These two papers are good examples how numerics and analysis can aid each other. Actually, all analytical results here were motivated by a thorough numerical analysis and observations based on in. We devote each of following sections to results of one paper.

Firstly, we briefly summarize ideas of the numerical bifurcation analysis, which is the main tool used to study problems in this chapter, and used methods. The main goal of this approach is to compute and plot bifurcation diagrams, which describe both local and global behaviour of the problem under consideration. Hence, we want to compute branches of solutions of the problem

$$\mathcal{F}(\lambda, u) = 0, \tag{2.1}$$

where $\mathcal{F} : \mathbb{R} \times X \to Y$ is a nonlinear operator on general Banach spaces X, Y and $\lambda \in \mathbb{R}$ is regarded as a bifurcation parameter. Let us assume that there exists $\lambda_0 \in \mathbb{R}$ and $\delta > 0$ such that

$$\mathcal{F}(\lambda, 0) = 0 \quad \text{for all } \lambda \in I := (\lambda_0 - \delta, \lambda_0 + \delta) \tag{2.2}$$

and $\mathcal{F}(\lambda, u)$ is the operator of the class C^r, $r \geq 2$ in an open neighbourhood of $(\lambda_0, 0)$. Hence, the problem (2.1) now has the trivial solution for any $\lambda \in I$. We present here the following definition of a *bifurcation point*, which we use in this chapter. Let us mention that in Chapter 3 we use a different definition of a *bifurcation point* related to a system of reaction-diffusion equations with two diffusion parameters.

Definition 2.1.
We call the pair $(\lambda_0, 0)$ a *bifurcation point* of the problem (2.1) if there exists a sequence $(\lambda_n, u_n) \in I \times X \setminus \{0\}$ with $n \in \mathbb{N}$ such that $\mathcal{F}(\lambda_n, u_n) = 0$ for all n and

$$\lim_{n \to +\infty} (\lambda_n, u_n) = (\lambda_0, 0).$$

We built our own code in MATLAB to study all problems presented in this chapter and to compute all bifurcation diagrams. There are of course available bifurcation solver packages such as AUTO-07P, but our problems require very strict control of all step sizes, tolerances and other technical properties, which makes these usually "black box" solvers less useful.

Most of the numerical bifurcation analysis theory and the numerical continuation can be found, e.g., in [LG88], [AG03], [Mei00] or [Kel86]. Let us point out that we have used the idea of *pseudo-arclength parametrization* of a curve and *expanded system* (see, e.g., [Kel86,

Chapter 4]). In the predictor-corrector mechanism of the numerical continuation of a curve we have adopted either the secant or the tangent predictor and classical Newton's method as the corrector (see, e.g., [Kel86, Chapter 2]). The very important part of this approach is the approximation of the problem of the type (2.1). The operator contained in (2.1) is $-\frac{d^2}{dx^2}$ in all cases in this thesis. We have used two methods here, *finite differences* and *pseudo-spectral* method of Eilbeck (see [Eil86]). One could use either of these two methods to detect bifurcation points and continue branches. However, pseudo-spectral method respects spectral properties of the operator included in the problem (2.1) and provides much more accurate approximation of bifurcation points than finite differences in our experience. On the other hand, the numerical continuation of branches of solutions using finite differences is usually faster due to the fact that the matrix provided by finite differences is three-diagonal, while the approximation by pseudo-spectral method gives us full matrix. Hence, we decided to combined these two methods to achieve both the high accuracy, when looking for bifurcation points, and the low computation time, when computing large pieces of branches.

All problems in this thesis are studied by this approach in one spatial dimension. The numerical bifurcation analysis and the continuation of branches of solutions can be, of course, expanded to higher spatial dimension. However, this approach is very time demanding even in 1D and the computation cost increases significantly as we increase the dimension. It is also worth mentioning that the discretization gets more technically complicated and working with eigenfunctions of Laplacian for shooting directions at bifurcation points would be quite a difficult task in higher dimensions.

Remark 2.2.
The eigenvalues of the operator $-\frac{d^2}{dx^2}$ subject to homogeneous Dirichlet conditions form the positive increasing sequence $\lambda_n = (n\pi)^2$ with $n \in \mathbb{N}$ and the orthonormal basis composed of corresponding eigenfunctions can be chosen as $\varphi_n = \sin(n\pi x)$ with $n \in \mathbb{N}$.

2.1 | Global structure of positive solutions

This section summarizes results of the paper [FLG21] (see also Appendix D). We study both analytically and numerically the superlinear indefinite problem

$$\begin{cases} -u'' = \lambda u + a(x)u^2 & \text{in } (0,1), \\ u(0) = u(1) = 0, \end{cases} \tag{2.3}$$

where $a(x)$ is a continuous function that changes the sign in the interval $(0,1)$ and the parameter $\lambda \in \mathbb{R}$ is regarded as a bifurcation parameter.

This problem was studied by many authors, we refer the reader to [FLG21] and references therein for some historical background. Our interest here is the study of the global structure of positive solutions of the problem (2.3). This study is motivated mainly by the conjecture of Gómez-Reñasco and López-Gómez originated from [GRnLG00], which says that there exists some $\lambda_c < \pi^2$ such that, for every $\lambda < \lambda_c$, the problem (2.3) has, at least,

$$\sum_{j=1}^{n+1} \binom{n+1}{j} = 2^{n+1} - 1$$

positive solutions, where $n+1$ is the number of positive peaks of $a(x)$. Actually, $n+1$ of them have a single peak around one of the maxima of $a(x)$, $\frac{(n+1)n}{2}$ have two peaks, and in general, $\frac{(n+1)!}{j!(n+1-j)!}$ have j peaks for every $j \in \{1, ..., n+1\}$. Hence, if we have $a(x) = \sin(3\pi x)$, which has two positive peaks, then by this conjecture we expect three positive solutions for $\lambda < \lambda_c$, one with the peak localized around the left local maximum of $\sin(3\pi x)$, one with the peak localized around the right local maximum and one with both of these peaks. For the purpose of this thesis, we formulate here this conjecture in the following form.

Conjecture 2.3 (see also Conjecture 1.1 of [FLG21] in Appendix D).
Suppose that $a(x)$ possesses $n+1$ intervals, where it is positive, separated away by n intervals, where it is negative. Then, there exists $\lambda_c < \pi^2$ such that, for every $\lambda < \lambda_c$, the problem (2.3) admits, at least, $2^{n+1} - 1$ positive solutions.

The most of analytic results about local and global behaviour of positive solutions of the problem (2.3), that was already known, is collected in Section 2 of [FLG21]. We point out here only the most important features in the following remark.

Remark 2.4.
The problem (2.3) possesses a component of positive solutions $\mathscr{C}^+ \subset \mathbb{R} \times C([0,1])$ bifurcating from the bifurcation point $(\lambda_0, u_0) = (\pi^2, 0)$, where $\lambda_0 = \pi^2$ is the smallest eigenvalue of $-\frac{d^2}{dx^2}$ subject to homogeneous Dirichlet boundary conditions (see Remark 2.2). The component $\mathscr{C}^+$ is unbounded in $\mathbb{R} \times C([0,1])$ and there does not exist a positive solution for an arbitrary large $\lambda > \pi^2$. Let $\mathscr{P}_\lambda$ be the projection defined by

$$\mathscr{P}_\lambda(\lambda, u) = \lambda, \quad (\lambda, u) \in \mathbb{R} \times C([0,1]).$$

There are two options here, either $\mathscr{P}_\lambda(\mathscr{C}^+) = (-\infty, \pi^2)$ or there exists $\lambda_t > \pi^2$ and $\mathscr{P}_\lambda(\mathscr{C}^+) = (-\infty, \lambda_t)$. If we consider the latter case, then for every $\lambda \in (\pi^2, \lambda_t)$ there exist, at least, two positive solutions, one linearly stable and another one unstable and there is a subcritical turning point at λ_t. The bifurcation at $\lambda_0 = \pi^2$ is supercritical in that case and the branch emanating from this bifurcation point is filled with linearly stable solutions. Moreover, any positive solution of (2.3) is linearly unstable for $\lambda \leq \pi^2$.

Firstly, we present main analytical results of [FLG21], which support the conjecture about number of positive solutions of (2.3) for sufficiently negative λ. These results are contained in Section 3 of [FLG21] together with Theorem 1.1 from Section 1. The important feature here is the relation of (2.3) and its corresponding parabolic problem

$$\begin{cases} \frac{\partial u}{\partial t} = \frac{\partial^2 u}{\partial x^2} + \lambda u + a(x)u^2, & t > 0, \quad x \in (0,1), \\ u(0,t) = u(1,t) = 0, & t > 0, \\ u(x,0) = u_0(x), & x \in [0,1]. \end{cases} \tag{2.4}$$

Now, let us consider two open sets

$$\Omega_- = \text{int}(\text{supp } a^-) \quad \text{and} \quad \Omega_+ = \text{int}(\text{supp } a^+).$$

The next theorem gives us a behaviour of positive solutions of (2.3) for x, where the function $a(x)$ is negative.

Theorem 2.5 (see also Theorem 3.1 of [FLG21] in Appendix D).
For every $\lambda < \pi^2$, let u_λ be a positive solution of (2.3). Then,

$$\lim_{\lambda \to -\infty} u_\lambda(x) = 0 \quad \text{for all } x \in \Omega_- \tag{2.5}$$

uniformly on compact subintervals of Ω_-.

Let us denote the solution of the parabolic problem (2.4), with the initial data u_0 and defined in $[0, T]$ for some $T > 0$, by $u(x, t; u_0, \lambda)$. The following theorem provide us with the behaviour of solutions of the problem (2.4) in the case, when the initial data u_0 is a subsolution of (2.3).

Theorem 2.6 (see also Theorem 3.2 of [FLG21] in Appendix D).
Suppose that $u_0 \geq 0$, $u_0 \not\equiv 0$ is a subsolution of (2.3). Then, for every $x \in \Omega_-$ and $t \in (0, T_{\max}(u_0))$,

$$\lim_{\lambda \to -\infty} u(x, t; u_0, \lambda) = 0.$$

Moreover, the limit is uniform on compact subsets of Ω_-.

Looking at Theorems 2.5 and 2.6, we can see that the behaviour of solutions of the parabolic problem is copying the behaviour of solutions of (2.3) as $\lambda \to -\infty$. Further let us form the following assumption:

(H_a) The open sets Ω_- and Ω_+ consist of finitely many (non-trivial) intervals, I_j^-, $j \in \{1, ..., r\}$, and I_i^+, $i \in \{1, ..., s\}$, respectively, and $a(x)$ vanishes at the ends of these intervals in such a way that each interior interval $I_i^\pm$ is surrounded by two intervals of the form $I_j^\mp$. In such case, we will denote, $I_j^- = (\alpha_j, \beta_j)$, with $\alpha_j < \beta_j$ for all $j \in \{1, ..., r\}$, and $I_i^+ = (\gamma_i, \varrho_i)$, with $\gamma_i < \varrho_i$ for all $i \in \{1, ..., s\}$.

Let us denote $\theta_{\lambda,i}$ a positive solution of

$$\begin{cases} -u'' = \lambda u + a^+(x) u^2 & \text{in } (\gamma_i, \varrho_i), \\ u(\gamma_i) = u(\varrho_i) = 0. \end{cases} \tag{2.6}$$

for i as in (H_a). Further, we will consider the subsolution

$$u_0 := \begin{cases} \theta_{\lambda,i} & \text{in } [\gamma_i, \varrho_i], \ i \in \{1, ..., n+1\}, \\ 0 & \text{in } [0,1] \setminus \bigcup_{i=1}^{n+1} [\gamma_i, \varrho_i]. \end{cases} \tag{2.7}$$

If the solution $u(x, t; u_0, \lambda)$ is globally bounded in time as $\lambda \to -\infty$, one can prove Conjecture 2.3 (see the following theorem). However, the boundedness of solutions in time remains the open problem in [FLG21].

Theorem 2.7 (see also Theorem 3.3 of [FLG21] in Appendix D).
Suppose (H_a) with $s = n + 1$ and $r = n$, and u_0 (see (2.7)). Assume, in addition, that there exists $\mu > 0$ such that, for every $\lambda < \mu$, $T_{\max}(u_0, \lambda) = +\infty$ and there is a constant $C(\lambda) > 0$ such that

$$u(x, t; u_0, \lambda) \leq C(\lambda) \ \text{ for all } \ (x, t) \in [0, 1] \times [0, \infty). \tag{2.8}$$

Then, there exists $\lambda_c < 0$ such that (2.3) has, for every $\lambda < \lambda_c$, $2^{n+1} - 1$ positive solutions.

We have used special choices

$$a(x) = \sin\left((2n+1)\pi x\right), \text{ for } n \in \{1,2,3\}, \tag{2.9}$$

as well as

$$a(x) = \begin{cases} \mu \sin(5\pi x) & \text{if} \quad x \in [0, 0.2) \cup (0.8, 1], \\ \sin(5\pi x) & \text{if} \quad x \in [0.2, 0.8], \end{cases} \tag{2.10}$$

where $\mu \geq 1$ is regarded as a secondary bifurcation parameter in our numerical analysis. Let us mention that these special choices satisfy the condition (H_a). In next four subsections we present results of the numerical bifurcation analysis of the problem (2.3) with these four special choices of $a(x)$ and then we conclude this section with discussion about results.

Before we proceed to numerical results, we define a $n+1$ digit code

$$T \equiv d_1 d_2 \dots d_{n+1}, \tag{2.11}$$

where $n+1$ is the number of positive peaks of $a(x)$ and we assume $d_j \in \{0,1\}$ for every $j = 1, \dots, n+1$. This code T is referred to as the type of the solution, where 1 means there is emphasized bump in the solution localized around the positive peak of $a(x)$ indicated by the position of 1 in the code T and 0 means there is no bump on this position. For example let us consider the case $a(x) = \sin(3\pi x)$. This function has two positive peaks, hence, the code T has two digits. Hence, the solution with bump on the left will be represented by the code 10, the solution with bump on the right by 01 and the solution with both these bumps by 11 (see three positive solutions in Figure 2.1a). The trivial solution is then represented by 00. At the end of this code, we add a positive integer in parenthesis, which represents the Morse index, that is the dimension of the unstable manifold of the positive solution as a steady state of the parabolic problem (2.4).

In all subsequent bifurcation diagrams we plot the parameter λ versus the derivative of the solution in the zero $u'(0)$. It is not appropriate to use L^2 norm or max norm to represent a solution in these cases due to symmetries around 0.5, because, e.g., the solution with a bump on the left and the solution with a bump on the right can have the same maximum and also the same L^2 norms. Hence, if we used one of these representations, we would not be able to differentiate between these solutions.

2.1.1 | The case $n = 1$

Let us consider the case

$$a(x) = \sin(3\pi x), \quad x \in [0,1]. \tag{2.12}$$

In the process of finding first few points on the bifurcating branch from the bifurcation point $(\lambda_0, u_0) = (\pi^2, 0)$, it is very useful to compute the bifurcation direction. We can compute the first coefficient D_1 of the expansion of the mapping $\lambda(s)$ (s being a parameter of the curve bifurcating from the trivial solution) provided by Crandall-Rabinowitz theorem (see [CR71] or Section 2 of [FLG21]). In this case it is

$$D_1 = -2\int_0^1 a(x)\sin^3(\pi x)\,dx = -2\int_0^1 \sin(3\pi x)\sin^3(\pi x)\,dx = \frac{1}{4} > 0. \tag{2.13}$$

Hence, the bifurcation from $u_0 = 0$ at $\lambda_0 = \pi^2$ is supercritical. Thus we can expect a

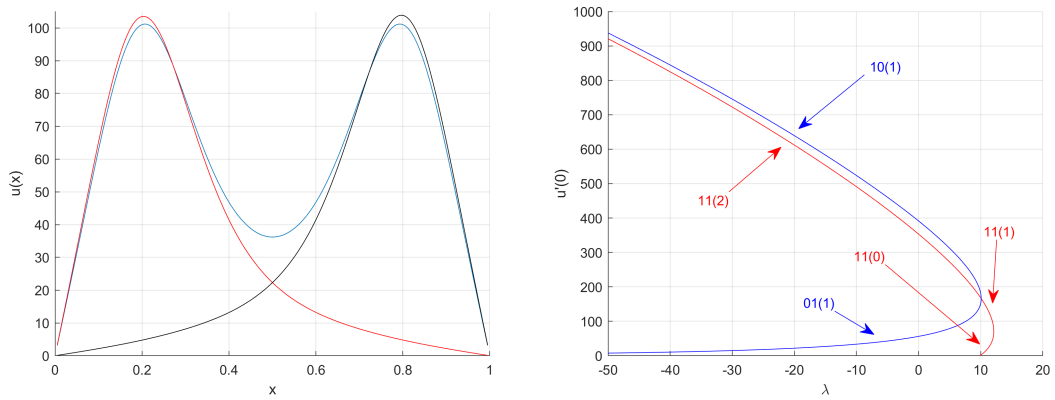

(a) Positive solutions for $\lambda \approx -21$: 10(1) in red, 01(1) in black, and 11(2) in blue.

(b) Global bifurcation diagram.

Figure 2.1: Numerical results for $a(x) = \sin(3\pi x)$.

turning point at some $\lambda_t > \pi^2$ as was stated in Remark 2.4. The global bifurcation diagram is plotted in Figure 2.1b. We can see that the set of positive solution of (2.3) with (2.12) consists of the component $\mathscr{C}^+$, which exhibits a turning point at $\lambda_t \approx 12.1$ and a secondary bifurcation at $\lambda_s \approx 10.1$. As expected by Crandall-Rabinowitz exchange of stability principle (see [CR73]), the positive solution bifurcating from $(\lambda_0, u_0) = (\pi^2, 0)$ is stable until it reaches the turning point at λ_t. As we can see in the diagram in Figure 2.1b, the Morse index jumps to one as we pass through the turning point and then it also increases after the secondary bifurcation. At λ_s two new branches of positive solutions bifurcate subcritically from the branch of 11 solutions. We can see that for sufficiently negative λ, there are three types of positive solutions, i.e., the peak on the left 10, the peak on the right 01 and both peaks 11, which we plotted for $\lambda \approx -21$ in Figure 2.1a. There seems to be no other change in the structure of branches and these solutions seem to be globally defined for every $\lambda < \lambda_s$. Hence, the number of positive solutions $2^2 - 1 = 3$ is in the perfect agreement with Conjecture 2.3. Let us mention that Morse indices of solutions on every branch for any $\lambda < \lambda_s$ are the same as the number of bumps of solutions, i.e., as the sum of ones in the type T of the solution.

2.1.2 | The case $n = 2$

Let us consider the case

$$a(x) = \sin(5\pi x), \quad x \in [0, 1]. \tag{2.14}$$

Since we have

$$D_1 = 2 \int_0^1 \sin(5\pi x) \sin^3(\pi x)\, dx = 0,$$

it is necessary to expand the mapping $\lambda(s)$ even more and compute D_2 to get the bifurcation direction. This computation is quite lengthy and technical and the reader can find it in Section 2 of [FLG21]. The second coefficient is

$$D_2 = -\frac{5}{256\pi^2} < 0,$$

hence, the bifurcation from $(\pi^2, 0)$ is subcritical. The global bifurcation diagram is plotted in Figure 2.2. Since there is quite large difference between the derivative in zero for, e.g., the solution 001 and the solution 111, the global diagram is very spread out. Therefore, we split it into the lower part, whose magnification is plotted in Figure 2.3b and the upper part, which is plotted in Figure 2.3a. Now we can see that the set of positive solutions consists of three branches with turning points, two in the upper part and one in the lower part, and the branch $\mathscr{C}^+$ bifurcating from the trivial solution at $\lambda = \pi^2$.

We can see that along the blue branch plotted in Figure 2.3b, the solution changes its

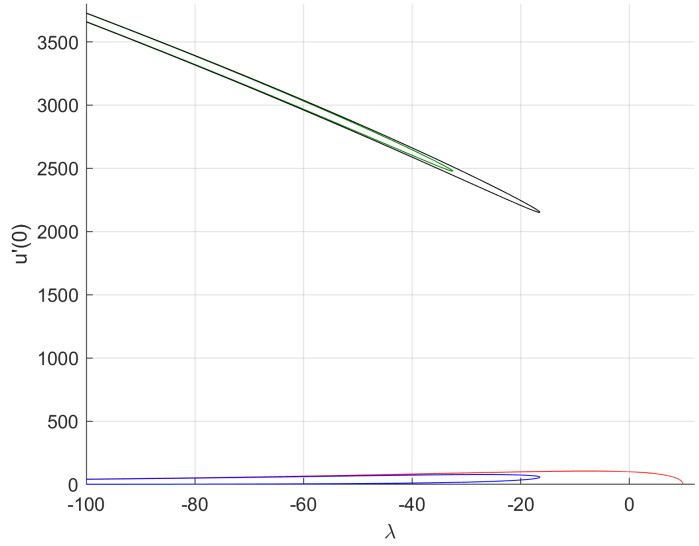

Figure 2.2: Global bifurcation diagram for $a(x) = \sin(5\pi x)$.

type from 001 to 011 as we pass through the turning point. In the upper part plotted in Figure 2.3a, the solution 111 on the green branch changes its type to 101 as we cross the turning point, while the solution on the black branch is changing from 110 to 101. In all cases there is also a jump in Morse index too as usual. The component $\mathscr{C}^+$ does not exhibit any secondary bifurcation as far as we know and neither does any other component. Hence, we have here $2^3 - 1 = 7$ positive solutions for sufficiently negative λ, which is again in the agreement with Conjecture 2.3. All positive solutions are unstable in this case as was predicted by results collected in Remark 2.4. Let us notice here that Morse indices of solutions on every single branch are equal to number of peaks of the solution.

2.1.3 | The case $n = 3$

Let us consider the case

$$a(x) = \sin(7\pi x), \qquad x \in [0, 1]. \tag{2.15}$$

Similarly as in the previous section, the first coefficient of $\lambda(s)$ is zero in this case:

$$D_1 = -2 \int_0^1 \sin(7\pi x) \sin^3(\pi x)\, dx = 0. \tag{2.16}$$

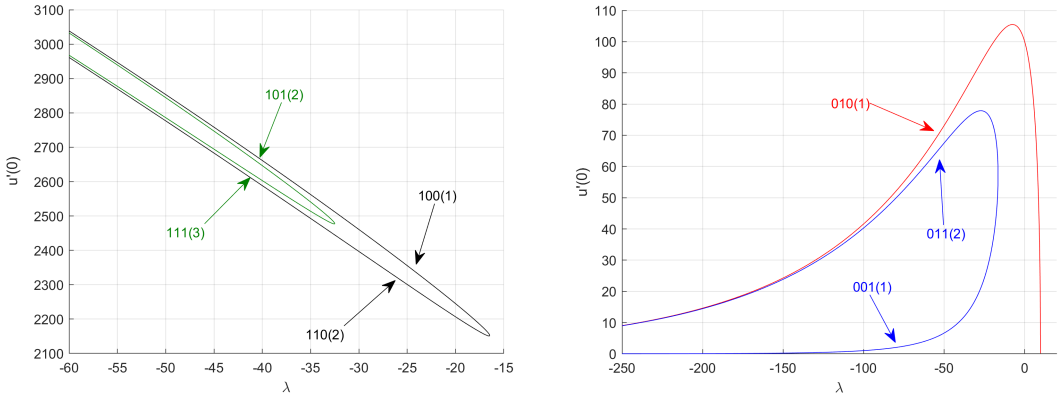

(a) Upper part magnification.

(b) Lower part magnification.

Figure 2.3: Two significant magnifications of Figure 2.2.

The second one is

$$D_2 = \frac{1}{128\pi^2} > 0, \tag{2.17}$$

thus $\mathscr{C}^+$ bifurcates from $(\pi^2, 0)$ supercritically as in the case $n = 1$. We have seen in the previous section, that branches in the bifurcation diagram were quite spread apart. In this case, the situation is even worse, therefore we do not present here the global bifurcation diagram, because it would not have any representative value. We rather show directly magnified significant parts of this diagram. Hence, the lower part containing branches of solutions with rather small $u'(0)$ is plotted in Figure 2.4a and the upper part containing branches of solutions with large $u'(0)$ is plotted in Figure 2.4b. Since the upper part is quite complicated, we present even more magnified diagram in Figure 2.4c.

The component $\mathscr{C}^+$ most likely possesses a turning point, but since the bifurcation from the trivial solution is very vertical, we were not able to find it. The solution on this branch is of the type 0110. There is again the secondary bifurcation on $\mathscr{C}^+$ at $\lambda_s \approx -2.85$ and the solutions on bifurcating branches have types 0100 and 0010. If we restrict x onto the interval $\left[\frac{2}{7}, \frac{5}{7}\right]$, then in fact $a(x)$ has the same behaviour here as in the case $n = 1$ and one can see that on the character of the component $\mathscr{C}^+$ (again a secondary bifurcation, compare Figures 2.4a and 2.1b). Actually, even solutions on this component are of types 10, 01 and 11 for $x \in \left[\frac{2}{7}, \frac{5}{7}\right]$. In the rest of the lower part we can see two branches with turning points. One with solutions of the type 0001 changing to 0011 and the other with the type 0111 changing to 0101. As far as we know, there is no other secondary bifurcation in the lower part of the bifurcation digram than the one on the component $\mathscr{C}^+$.

We can see that the situation in the upper part is more complicated than in the previous case $n = 2$. In Figure 2.4b, there are two branches with turning points, one internal in terms of other branches (green) and one external (red). The solutions on the internal branch are changing their type from 1110 to 1010 as we cross the turning point and on the external branch they are changing from 1100 to 1000. Between the red branch and the green branch there is another component composed of the black and the blue branch. The magnification of this part is plotted in Figure 2.4c. There is the secondary bifurcation at $\lambda_s \approx -44.05$ on the black branch of solutions of the type 1001 changing to 1111. The bifurcating branch is filled with solutions of the type 1011 changing to 1101 as we cross the bifurcation point. Hence,

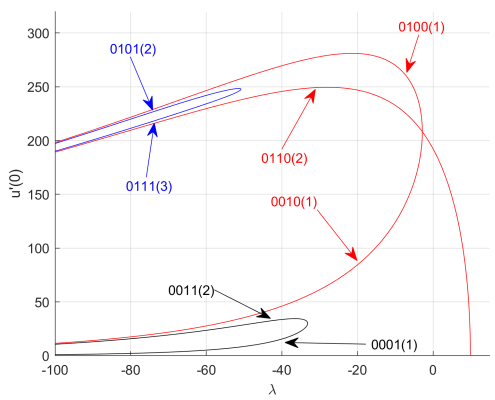

(a) Small positive solutions.

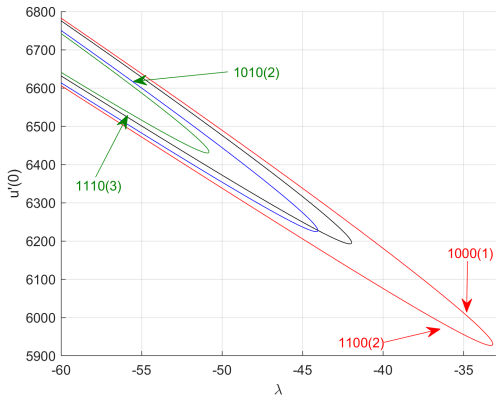

(b) Large positive solutions.

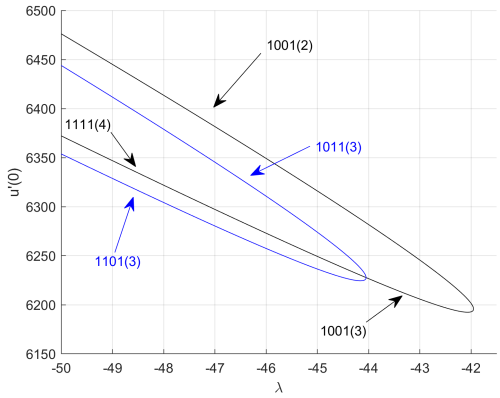

(c) A magnification of Figure 2.4b.

Figure 2.4: Scattered bifurcation diagrams for $a(x) = \sin(7\pi x)$.

we have $15 = 2^4 - 1$ solutions in the overall for sufficiently negative λ, which is again in the complete agreement with Conjecture 2.3. We can observe that the Morse index, i.e., the dimension of the unstable manifold of solution, is almost always equal to number of peaks, the solution is composed of. The only exceptions are solutions on the right side of bifurcation points. However, for sufficiently negative λ, this is always true. The example of solutions along one of branches in this case is plotted in Figure 7 of [FLG21] (see also Appendix D).

2.1.4 | The case $n = 2$ with an additional parameter μ

Let us consider the modification of (2.14) from Subsection 2.1.2 as

$$a(x) = \begin{cases} \mu \sin(5\pi x) & \text{if} \quad x \in [0, 0.2) \cup (0.8, 1], \\ \sin(5\pi x) & \text{if} \quad x \in [0.2, 0.8], \end{cases} \tag{2.18}$$

where the additional parameter $\mu \geq 1$ is a secondary bifurcation parameter. If there is $\mu = 1$, then (2.18) and (2.14) coincides and so does the structure of positive solutions of the problem

(2.3). The bifurcation direction depending on the parameter μ is

$$D_1 = -\frac{\sqrt{\frac{1}{2}\left(5-\sqrt{5}\right)}\left(5-\sqrt{5}\right)^2(\mu-1)}{128\pi}. \tag{2.19}$$

We can see that for $\mu = 1$, there is $D_1 = 0$ as in Subsection 2.1.2 and for any $\mu > 1$ we have $D_1 < 0$. Hence, the bifurcation is subcritical for any value of the parameter μ in this section. Let us mention that we will denote the positive component bifurcating at $(\pi^2, 0)$ from the trivial solution by $\mathscr{C}^+_\mu$ with some μ instead of $\mathscr{C}^+$ in this subsection.

The structure of branches in the global bifurcation diagram remains the same as in Figure 2.2 in Section 2.1.2 for $\mu < \mu_1 \approx 3.895$. As we increase μ from $\mu = 1$ to μ_1, the branches with turning points move closer to the component $\mathscr{C}^+_\mu$. This behaviour is indicated by arrows in Figure 2.5a. The diagram in Figure 2.5b shows the situation right before the collision of two branches with $\mathscr{C}^+_\mu$.

At the value $\mu_1 \approx 3.895$, two branches with turning points touch the branch bifurcating

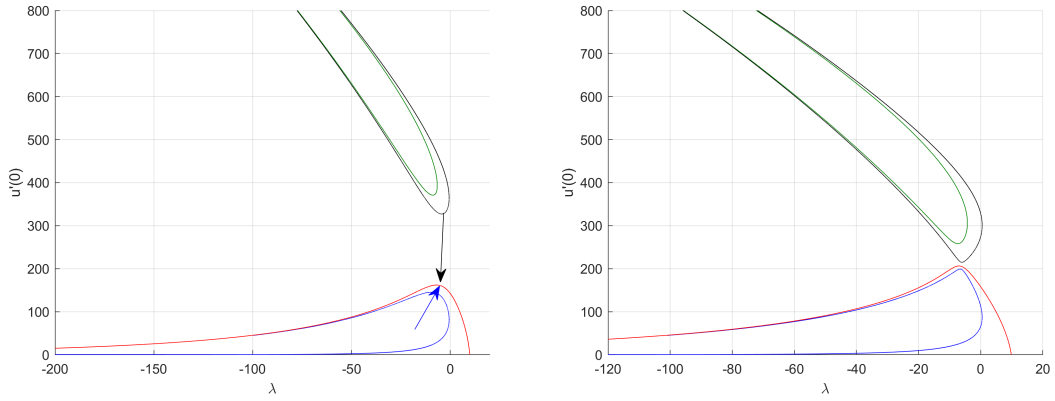

(a) $\mu = 3.5 < \mu_1$ (b) $\mu = 3.89 < \mu_1$

Figure 2.5: Global bifurcation diagrams for $\mu < \mu_1$.

from the trivial solution. In this moment, the global bifurcation diagram consists of only two components. One is the component $\mathscr{C}^+_{\mu_1}$, which is composed of the main branch bifurcating from $(\pi^2, 0)$ and two previously isolated branches, and the other is the remaining green branch with a turning point. The touching point of all three previous components acts here as some sort of organizing center with respect to the parameter μ. As μ separates away from μ_1, the touching point separates into two secondary bifurcation points as we can see in Figure 2.6a. This structure is persistent for μ in the interval (μ_1, μ_2), where $\mu_2 \approx 3.925$. Let us denote values of the parameter λ of these two secondary bifurcation points as $\lambda_1(\mu) \geq \lambda_2(\mu)$ with the dependence on the parameter μ. We have observed that as we increase the parameter μ from μ_1 to μ_2, these two secondary bifurcation points are moving away from each other. This behaviour is well illustrated by Table 2.1 with computed values of $\lambda_1(\mu)$, $\lambda_2(\mu)$ for three different values of $\mu \in (\mu_1, \mu_2)$.

At the next critical value $\mu_2 \approx 3.925$ occurs another reorganization of branches. The remaining isolated branch touches the main branch bifurcating from the trivial solution, hence, in this situation the global bifurcation diagram consists of a single component $\mathscr{C}^+_{\mu_2}$. As the parameter μ separates away from μ_2, the component splits into two, see the diagram plotted

μ	3.9	3.91	3.92
$\lambda_1(\mu)$	-5.1186	-4.4513	-3.9938
$\lambda_2(\mu)$	-7.5845	-8.4129	-9.0284

Table 2.1: $\lambda_i(\mu)$ for three values of $\mu \in (\mu_1, \mu_2)$.

in Figure 2.6b. One is the component $\mathscr{C}_\mu^+$ consisting of the main branch bifurcating from the trivial solution with the secondary bifurcation. The other is the branch with turning point and the secondary bifurcation of the next branch with similar structure. As far as we know, this structure persists even for large values of μ.

In Figure 2.7a we present the diagram for the larger value of μ and its magnification with

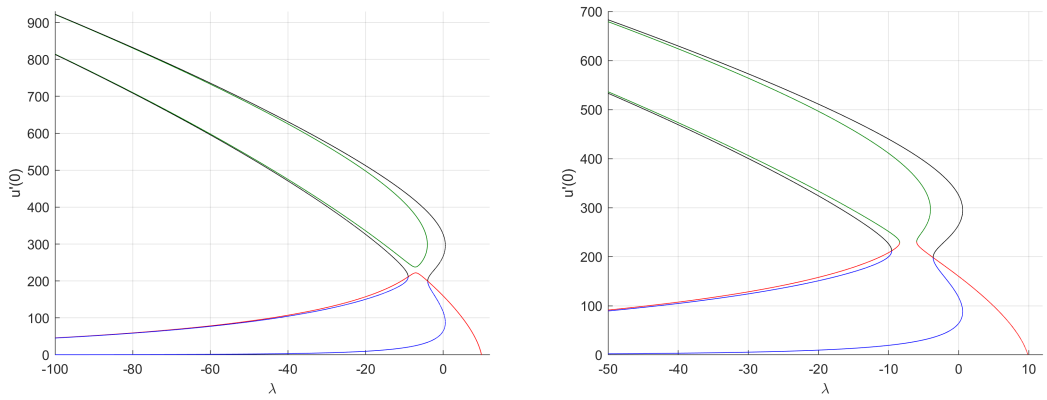

(a) $\mu_1 < \mu = 3.92 < \mu_2$ (b) $\mu_2 < \mu = 3.93$

Figure 2.6: Two significant global bifurcation diagrams

types of solutions on each branch is plotted in Figure 2.7b. We can see that for any $\mu > 1$, there exists sufficiently negative $\lambda(\mu)$ such that the problem (2.3) with the special choice (2.18) possesses $2^3 - 1 = 7$ positive solutions, which is in full agreement with Conjecture 2.3. The example of solutions along one of branches in this case is plotted in Figure 11 of [FLG21] (see also Appendix D).

2.1.5 | Discussion of numerical results

All our numerical experiments in every case support the validity of Conjecture 2.3, i.e., there exists a sufficiently negative λ such that the problem (2.3) has $2^{n+1} - 1$ positive solutions. We also made several other observations:

- For a sufficiently negative λ, the Morse index of any positive solution u of the type (2.11) is given by

$$\mathscr{M}(u) = \sum_{j=1}^{n+1} d_j.$$

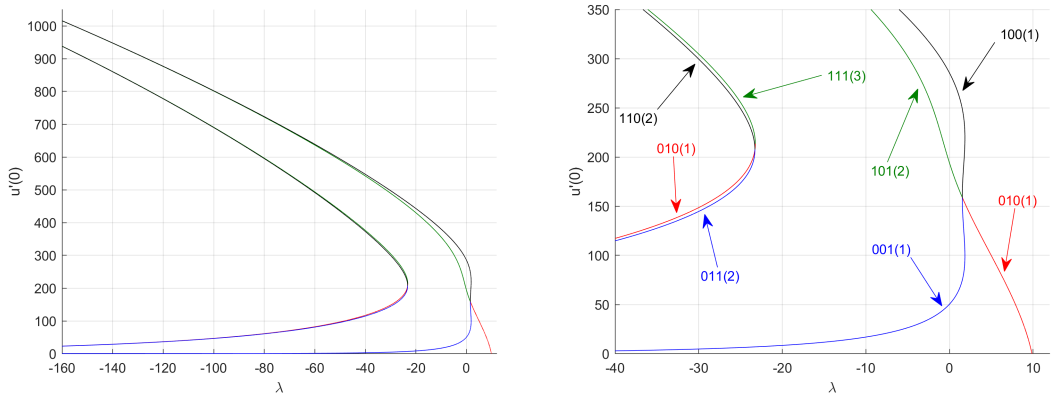

(a) $\mu_2 < \mu = 4.5$ (b) A zoom of the plot on the left

Figure 2.7: Global bifurcation diagram for $\mu > \mu_2$

- The only way, how to pass from the symmetric solution around $x = 0.5$ to the asymmetric one, is through the bifurcation point of a secondary bifurcation. That means any component that does not include a bifurcation point is filled only either with symmetric solutions or asymmetric ones.
- If n is even in (2.9), then $a(0.5)$ is negative, while if n is odd, then $a(0.5)$ is positive. We can see the for $n = 1, 3$, the component $\mathscr{C}^+$ includes a secondary bifurcation, while in the case $n = 2$ it does not. Assuming that there is some kind of a pattern for general n here is incorrect, which is supported by the case presented in Subsection 2.1.4, where there exists a bifurcation point on the component $\mathscr{C}^+$ for sufficiently large μ (e.g., $\mu = 4.5$).

2.2 | Nodal solutions and the concavity of eigencurves in weighted problems

In this section we collect both analytical and numerical results of our paper [FLG20]. Let us consider the superlinear indefinite problem

$$\begin{cases} -u'' - \mu u = \lambda m(x)u - a(x)u^2 & \text{in } (0,1), \\ u(0) = u(1) = 0, \end{cases} \tag{2.20}$$

where functions a, m are continuous and change the sign in the interval $(0,1)$ and $\lambda, \mu \in \mathbb{R}$ are regarded as bifurcation parameters with λ being the primary one and μ being the secondary parameter. We are interested in the case of the special class of functions

$$m(x) = \sin(j\pi x) \qquad \text{for } j \in \mathbb{N} \setminus \{1\}\,. \tag{2.21}$$

Both positive solutions and nodal solutions of the problem (2.20) were studied mostly in special cases $m \equiv 1$, $\mu = 0$. For some historical results we refer the reader to [FLG20] and references therein. We were mainly inspired by the paper [LGMM05], where positive solutions of the problem (2.20) with $m(x)$ changing the sign were studied. As far as we know, our paper

[FLG20] is the first one that studies nodal solutions of this problem, when $m(x)$ changes the sign.

The positive solutions were studied for a special choice of $a(x)$ by the methods of numerical analysis in [LGMM05]. We have studied numerically the nodal solutions for the same choice of $a(x)$ during which we have observed an unexpected behaviour of bifurcation points of the trivial solution and consequently of the eigenvalues of the operator $\left[-\frac{d^2}{dx^2} - \lambda m(x)\right]$ subject to Dirichlet boundary conditions. These numerical observations led to analytical results for the class of problems (2.20) with (2.21).

Firstly, let us consider the eigenvalue problem

$$\begin{cases} -\varphi'' - \mu\varphi - \lambda m(x)\varphi = \sigma\varphi \quad \text{in } (0,1), \\ \varphi(0) = \varphi(1) = 0. \end{cases} \tag{2.22}$$

This problem possesses a sequence of algebraically simple eigenvalues

$$\Sigma_n(\lambda,\mu) := \sigma_n\left[-\frac{d^2}{dx^2} - \mu - \lambda m(x); (0,1)\right] = \sigma_n\left[-\frac{d^2}{dx^2} - \lambda m(x); (0,1)\right] - \mu, \qquad n \in \mathbb{N}.$$

Hence, the set of bifurcation points $(\lambda(\mu), 0)$ from the trivial solution of the problem (2.20) is given by values of parameters λ, μ for which $\Sigma_n(\lambda,\mu) = 0$. Let us denote

$$\Sigma_n(\lambda) := \Sigma_n(\lambda, 0) = \sigma_n\left[-\frac{d^2}{dx^2} - \lambda m(x); (0,1)\right], \qquad n \in \mathbb{N}. \tag{2.23}$$

The function $\Sigma_n(\lambda)$ is called an eigencurve. We can see that there is $\Sigma_n(\lambda,\mu) = \Sigma_n(\lambda) - \mu$ and $\Sigma_n(0) = (n\pi)^2$ for all $n \in \mathbb{N}$. Hence, every bifurcation point $(\lambda(\mu), 0)$ satisfies the equation

$$\Sigma_n(\lambda) = \mu. \tag{2.24}$$

It is already known that every eigencurve is analytic and the first eigencurve $\Sigma_1(\lambda)$ is strictly concave function (see, e.g., [LG13, Chapter 9]). As such there is

$$\Sigma_1'(\lambda) > 0 \text{ for } \lambda < 0, \quad \Sigma_1'(0) = 0 \text{ for } \lambda = 0, \quad \Sigma_1'(\lambda) < 0 \text{ for } \lambda > 0 \quad \text{and } \Sigma_1''(\lambda) < 0 \text{ for } \lambda \in \mathbb{R},$$

where Σ_1' denotes the first derivative of $\Sigma_1(\lambda)$ in the parameter λ.

The local maximum of this eigencurve is at the zero with the function value $\Sigma_1(0) = \pi^2$. Hence, for every $\mu < \pi^2$, there exist two values of the parameter λ,

$$\lambda_-(\mu) < 0 < \lambda_+(\mu), \tag{2.25}$$

which satisfy the equation (2.24) and therefore are values λ of bifurcation points $(\lambda(\mu), 0)$. For more details about eigencurves see Section 1 of [FLG20].

We have numerically computed the eigencurves for the case $j = 2$ in (2.21), i.e., we chose $m(x) = \sin(2\pi x)$. The eigencurves are plotted in Figure 2.8 and we can see that the first one is indeed strictly concave. Surprisingly, the other eigencurves are not. Actually, this means that while the positive solutions bifurcate from the trivial solution at two values of λ (for $\mu < \pi^2$), the nodal solutions can bifurcate at two, three or even four bifurcation points depending on the value of μ.

Our numerical computations of eigencurves suggest that, the higher is the frequency

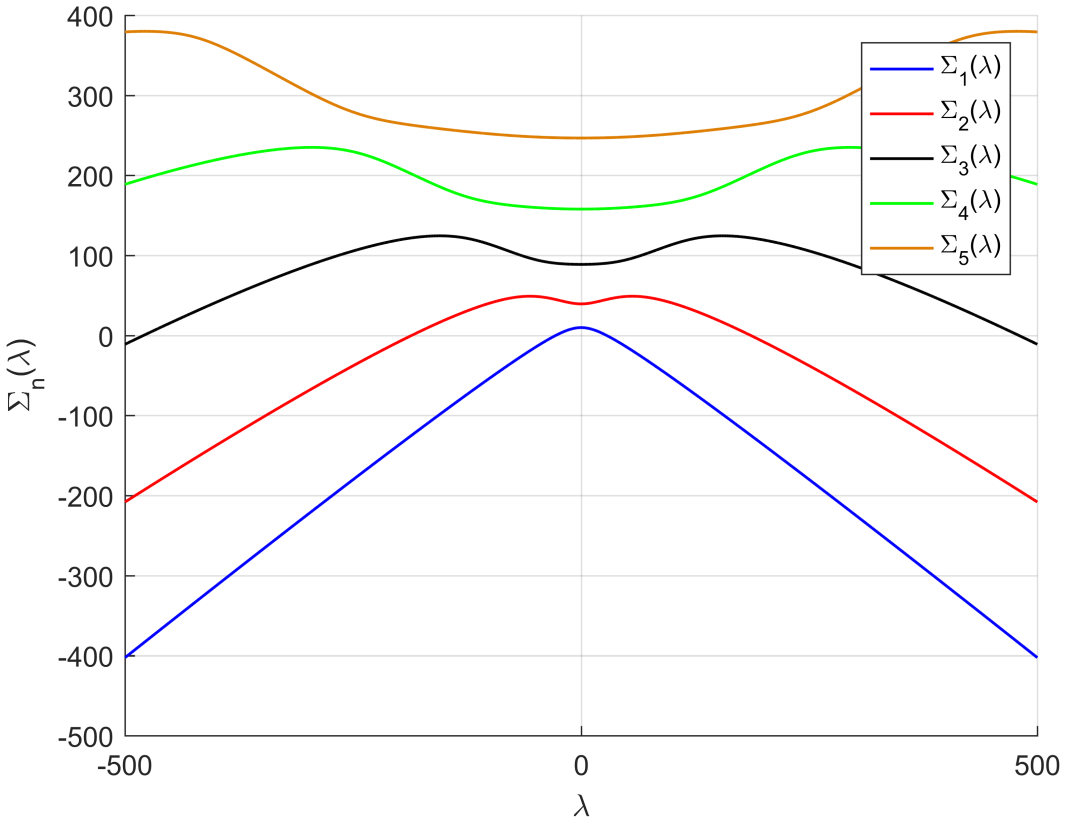

Figure 2.8: The curves $\Sigma_n(\lambda)$ for $1 \leq n \leq 5$ and $m(x) = \sin(2\pi x)$.

of the weight function $m(x)$, the larger number of eigencurves is concave. We can see the computed eigencurves in the cases $m(x) = \sin(4\pi x)$ and $m(x) = \sin(6\pi x)$ in Figure 2.9. Clearly, for $j = 4$ there is the first and the second eigencurve concave, while for $j = 6$ there are already first three eigencurves concave. We can see the systematic behaviour here, the one we can prove analytically.

We start with a proposition about the behaviour of the eigencurves as $|\lambda| \to \infty$ for a function $m(x)$ more general than in (2.21).

Proposition 2.8 (see also Proposition 2.1 of [FLG20] in Appendix C).
Suppose that there exist $x_\pm \in (0,1)$ *such that* $\pm m(x_\pm) > 0$, *i.e.,* $m(x)$ *changes the sign in* $(0,1)$. *Then, for every* $n \geq 1$,

$$\lim_{\lambda \to -\infty} \Sigma_n(\lambda) = -\infty, \qquad \lim_{\lambda \to \infty} \Sigma_n(\lambda) = -\infty. \tag{2.26}$$

The following proposition clarifies that if $m(x)$ is odd by the center of the interval $(0,1)$, then the eigencurves have always a stationary point in the zero and are symmetric.

Proposition 2.9 (see also Proposition 2.2 of [FLG20] in Appendix C).
Suppose that $m \neq 0$ *is a continuous function changing the sign in* $[0,1]$ *such that*

$$m(1-x) = -m(x) \quad \textit{for all } x \in [0,1]. \tag{2.27}$$

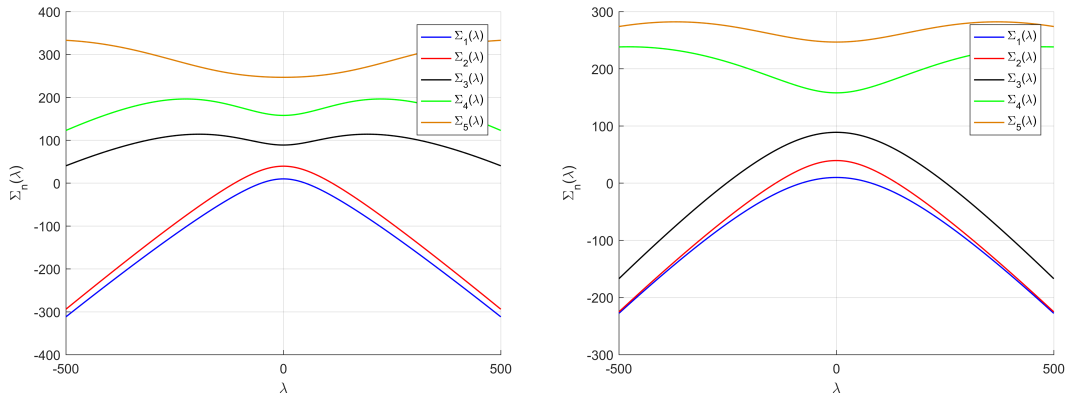

Figure 2.9: The curves $\Sigma_n(\lambda)$ for $1 \leq n \leq 5$ with $m(x) = \sin(j\pi x)$, $j = 4, 6$.

Then, $\Sigma_n(-\lambda) = \Sigma_n(\lambda)$ *for all* $\lambda \in \mathbb{R}$ *and any integer* $n \geq 1$. *In particular,*

$$\Sigma_n'(0) = 0 \quad \textit{for all} \;\; n \geq 1, \tag{2.28}$$

where we are denoting $\Sigma_n' = \frac{d\Sigma_n}{d\lambda}$.

If there is j odd in (2.21), then the assumptions of Proposition 2.9 are not satisfied and indeed the eigencurves, that we have computed, are not symmetric in this case (see Figure 2.10). We will restrict ourselves to the class of functions $m(x)$ of (2.21) that are odd around $x = 0.5$, for which we can prove even more. Hence, we have

$$m(x) = \sin(2k\pi x) \text{ with } k \in \mathbb{N}. \tag{2.29}$$

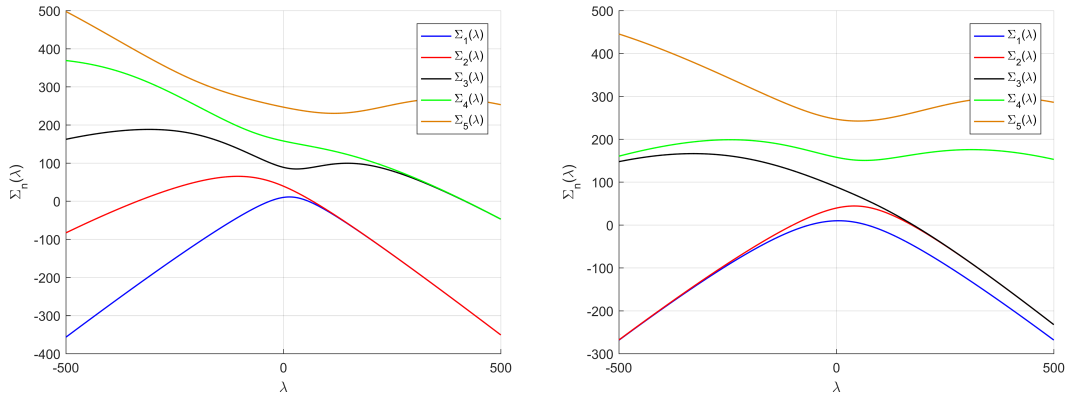

Figure 2.10: The curves $\Sigma_n(\lambda)$ for $1 \leq n \leq 5$ with $m(x) = \sin(j\pi x)$, $j = 3, 5$.

Remark 2.10.
Let us consider (2.29), *i.e., the case when assumptions of Proposition 2.9 are satisfied and the eigencurves are symmetric. The bifurcation points always come in pairs* $(\lambda_{-i}, 0)$ *and* $(\lambda_{+i}, 0)$, *where* $\lambda_{-i} = -\lambda_{+i}$ *and* $i \in \{1, 2\}$.

The next theorem is the main analytical result of [FLG20]. It confirms our numerical observations about concavity of eigencurves.

Theorem 2.11 (see also Theorem 2.1 of [FLG20] in Appendix C).
Assume (2.29) *for some integer* $k \geq 1$. *Then, as soon as* $n \geq k+1$,

$$\Sigma_n'(0) > 0 \quad \textit{for all } n \geq k+1. \tag{2.30}$$

Therefore, by (2.28), $\lambda = 0$ *is a local minimum of* $\Sigma_n(\lambda)$ *and, in particular,* $\Sigma_n(\lambda)$ *cannot be concave.*

In next subsections we present results of numerical analysis of 1-node solutions and 2-node solutions. The positive solutions were already studied numerically in [LGMM05] and we use the same function $a(x)$ as they did:

$$a(x) := \begin{cases} -0.2 \sin\left(\frac{\pi}{0.2}(0.2 - x)\right) & \text{if } 0 \leq x \leq 0.2, \\ \sin\left(\frac{\pi}{0.6}(x - 0.2)\right) & \text{if } 0.2 < x \leq 0.8, \\ -0.2 \sin\left(\frac{\pi}{0.2}(x - 0.8)\right) & \text{if } 0.8 < x \leq 1. \end{cases} \tag{2.31}$$

We discuss in the behaviour of the branch of positive solutions in the next subsection for the completeness. In the end, we also add our own observation of the behaviour of this branch for large values of μ, which was not discussed before.

We have studied the problem (2.20) by the methods of numerical analysis for the special case $k = 1$ in (2.29), i.e., we considered $m(x) = \sin(2\pi x)$. Let us note that in all bifurcation diagrams in this section we plot the value of the parameter λ versus the L^2 norm of the solution.

2.2.1 | Branch of positive solutions

Since the first eigencurve is concave, there can be maximally two bifurcation points from the trivial solution. The maximum of $\Sigma_1(\lambda)$ is π^2 attained in the zero. Hence, for any $\mu < \pi^2$, there are exactly two bifurcation points. The bifurcation diagram for $\mu = 0$ is plotted in Figure 2.11a. Indeed, we can see that the "fish-like" branch of positive solutions is bifurcating from two points. Let us mention that the intersection point is not a bifurcation point here, there is only the same L^2 norm of solutions in this point. As we increase the parameter μ in the interval $(0, \pi^2)$, those two bifurcation points are closing to each other until they collide in the zero for $\mu = \pi^2$. As μ separates from the critical value π^2, the branch of positive solutions separates from the trivial solution and becomes isolated. The bifurcation diagram of the branch in the case $\mu = 30 > \pi^2$ is plotted in Figure 2.11b.

This behaviour was already observed in [LGMM05]. As we have found out, the component of positive solutions is shrinking as we increase the parameter μ and it collides at $\mu \approx 54$ and eventually disappears. The values of the parameter λ of two bifurcation points from the trivial solution are in Table 2.2 for a few values of μ.

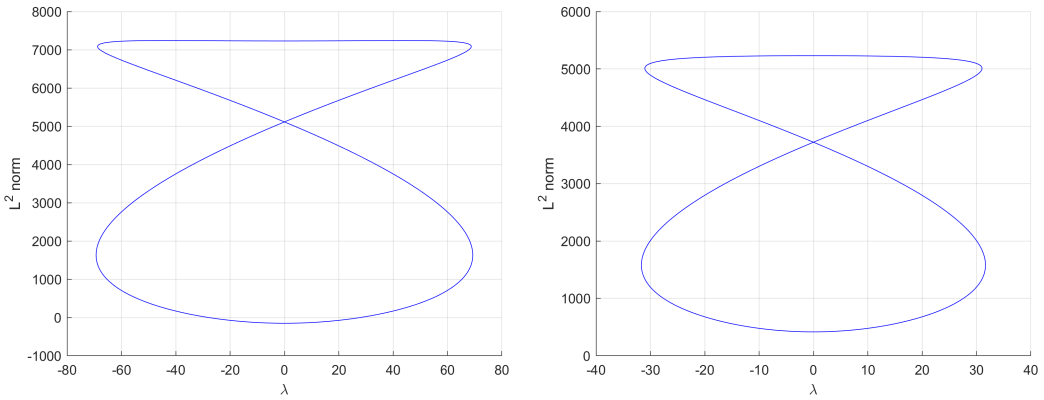

(a) $\mu = 0$ (b) $\mu = 30$

Figure 2.11: Bifurcation diagrams of branches of positive solutions.

μ	0	5	9	π^2	10
$\lvert\lambda_{-1}(\mu)\rvert$	28	18.64	7.49	0	–

Table 2.2: The absolute value of λ of bifurcation points $|\lambda_{-1}(\mu)| = |\lambda_{+1}(\mu)|$ depending on the parameter μ.

2.2.2 | Global behaviour of branches of 1-node solutions

According to Theorem 2.11, the second eigencurve $\Sigma_2(\lambda)$ is not concave (see also Figure 2.8). The local minimum is attained in the zero and $\Sigma_2(0) = (2\pi)^2$. Hence, for every $\mu < (2\pi)^2 \approx 39.4784$ there are two values $\lambda_{-1}(\mu) < 0 < \lambda_{+1}(\mu)$, which satisfy (2.24). It can be shown that assumptions of Crandall-Rabinowitz theorem hold at $(\lambda_{-1}(\mu), 0)$ and $(\lambda_{+1}(\mu), 0)$, hence, there is a branch emanating from the trivial solution at each of these two values of λ. We plot these two branches in Figure 2.12a for $\mu = 35$. The branches are closing to each other as we increase the value of the parameter μ from zero to $(2\pi)^2$.

At the critical value $\mu = (2\pi)^2$, these two branches touch at $\lambda = 0$ and the set of values of λ of bifurcation points from the trivial solution consist of $\lambda_{-1}(\mu)$, $\lambda_{+1}(\mu)$ and $\lambda = 0$. The bifurcation diagram for $\mu = 39.6 > 39.4786 \approx (2\pi)^2$, which is very close to the digram at the critical value of μ, where the branches touch, is plotted in Figure 2.12b.

If we have $\mu \in ((2\pi)^2, \mu_c)$, where $\mu_c \approx 49.5$, then there are four values of λ satisfying the equation (2.24), i.e.,

$$\lambda_{-1}(\mu) < \lambda_{-2}(\mu) < 0 < \lambda_{+2}(\mu) < \lambda_{+1}(\mu). \tag{2.32}$$

Once again it can be shown that there are bifurcating branches of solutions with one interior node from $u = 0$ at these four values of the parameter λ. As we increase the parameter $\mu \in ((2\pi)^2, \mu_c)$, the values $\lambda_{-2}(\mu)$, $\lambda_{+2}(\mu)$ separate away from the zero. The bifurcation diagram plotted in Figure 2.12c shows two components of 1-node solutions and four bifurcation points for $\mu = 45$. Clearly, as we pass through the critical value $\mu = (2\pi)^2$, the branches of solutions recombine. The more we increase the value of $\mu \in ((2\pi)^2, \mu_c)$, the closer are the bifurcation points with $\lambda_{-2}(\mu)$, $\lambda_{-1}(\mu)$ and the bifurcation points with $\lambda_{+1}(\mu)$, $\lambda_{+2}(\mu)$.

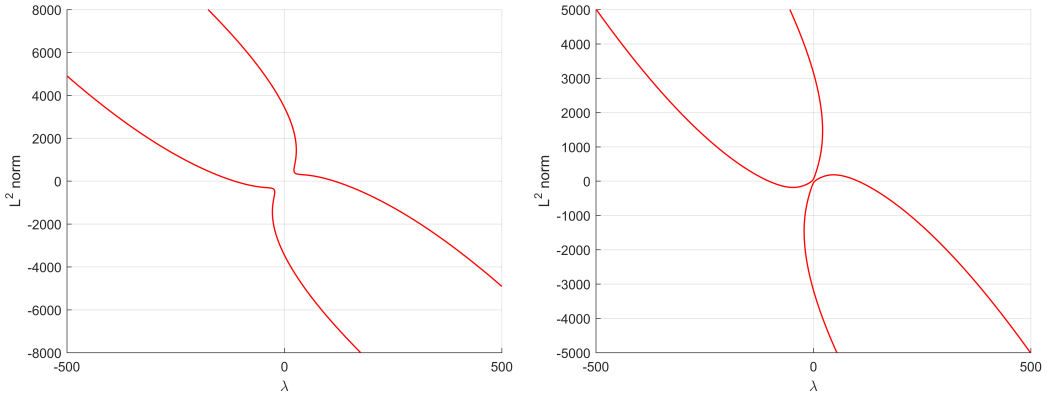

(a) $\mu = 35$

(b) $\mu = 39.6$

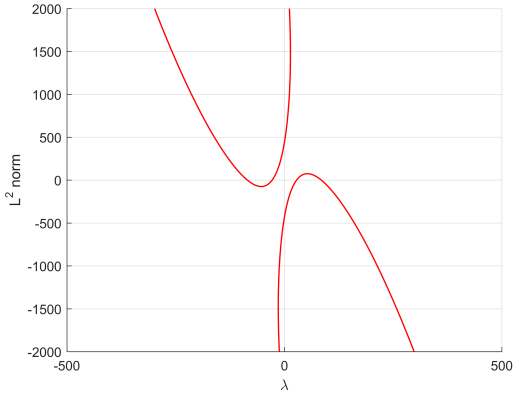

(c) $\mu = 45$

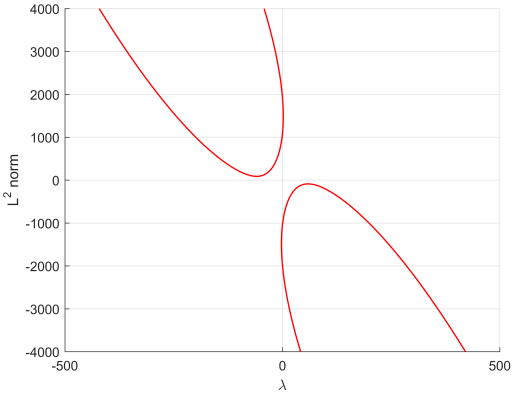

(d) $\mu = 54$

Figure 2.12: Four representative bifurcation diagrams of 1-node solutions.

μ	0	20	35	$(2\pi^2)$	40	45	49	50
$\lvert\lambda_{-1}(\mu)\rvert$	185	148	114	102	101	85	59	–
$\lvert\lambda_{-2}(\mu)\rvert$	–	–	–	0	7.15	28	52	–

Table 2.3: The absolute value of λ of bifurcation points $|\lambda_{-1}(\mu)| = |\lambda_{+1}(\mu)|$ and $|\lambda_{-2}(\mu)| = |\lambda_{+2}(\mu)|$ depending on the parameter μ.

Eventually, these pairs collide for $\mu = \mu_c$ and the components become isolated for $\mu > \mu_c$ (see Figure 2.12d). We present the values of bifurcation points with dependence on μ in Table 2.3, which illustrates how the bifurcation points are closing to each other as we increase μ. As far as we know, there are no secondary bifurcations on branches of 1-node solutions. The example of solutions along two branches 1-node solutions is plotted in Figure 5 of [FLG20] (see also Appendix C).

2.2.3 | Global behaviour of branches of 2-node solutions

Similarly as in the previous section, we know that the eigencurve $\Sigma_3(\lambda)$ is not concave by Theorem 2.11 (see also Figure 2.8). The local minimum of $\Sigma_3(\lambda)$ is again in the zero and $\Sigma_3(0) = (3\pi)^2 \approx 88.8264$. The situation with bifurcation points from the trivial solutions is more or less the same here as for 1-node solutions. Hence, for $\mu < (3\pi)^2$ there are two bifurcation points from the trivial solution. As we cross with μ the critical value $(3\pi)^2$, we have four of them

$$\lambda_{-1}(\mu) < \lambda_{-2}(\mu) < 0 < \lambda_{+2}(\mu) < \lambda_{+1}(\mu) \tag{2.33}$$

for $\mu \in ((3\pi)^2, \mu_c)$, where $\mu_c \approx 124.5$. The pairs $\lambda_{-1}(\mu)$, $\lambda_{-2}(\mu)$ and $\lambda_{+1}(\mu)$, $\lambda_{+2}(\mu)$ again collide as they did in the case of bifurcation points of 1-node solutions. The values of the parameter λ at these bifurcation points for several values of μ are in the Table 2.4.

While the behaviour of bifurcation points is the same as in the case of 1-node solutions,

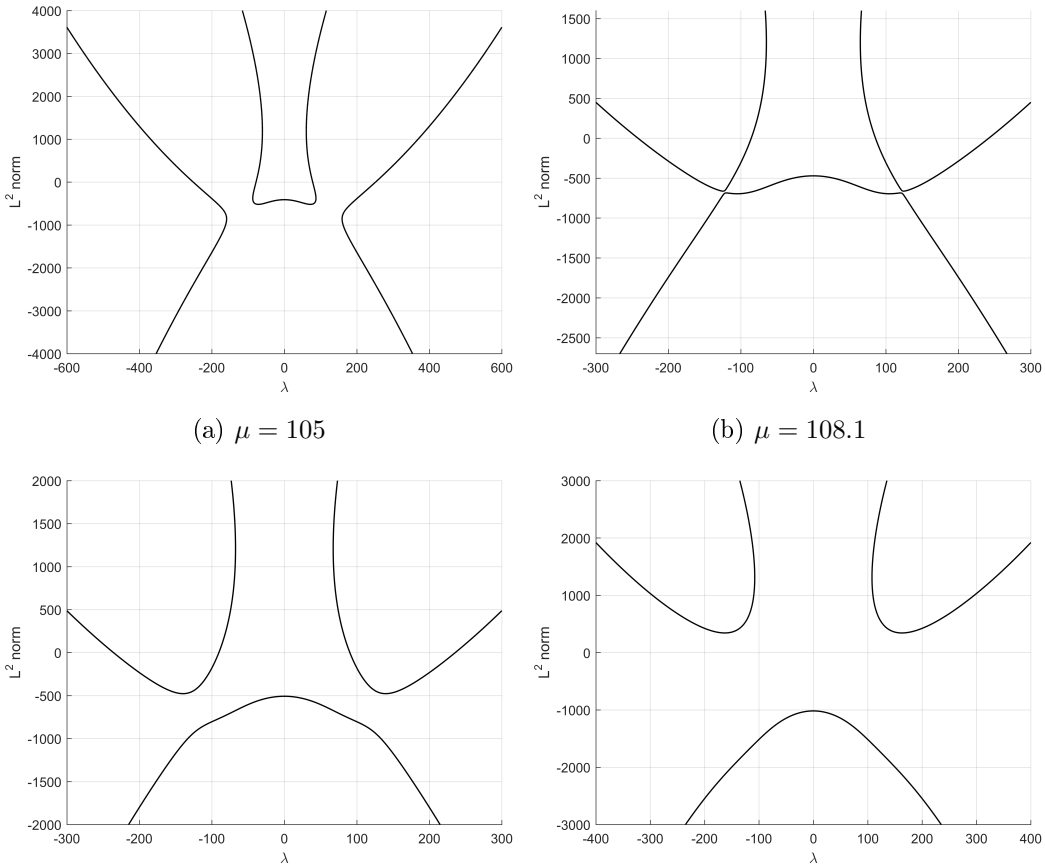

(a) $\mu = 105$ (b) $\mu = 108.1$

(c) $\mu = 110$ (d) $\mu = 140$

Figure 2.13: Four representative bifurcation diagrams of 2-node solutions.

branches behave very differently here. At the beginning for $\mu < (3\pi)^2$ there are again two components bifurcating from $u = 0$ at $\lambda_{-1}(\mu)$ and $\lambda_{+1}(\mu)$. As we increase the value of the parameter μ, these components are moving closer to each other. However, this time instead of touching, as they did in Figure 2.12b in the case of 1-node solutions, there appears en-

μ	50	80	$(3\pi^2)$	90	100	120	125
$\lvert\lambda_{-1}(\mu)\rvert$	382	317	290	292	266	196	–
$\lvert\lambda_{-2}(\mu)\rvert$	–	–	0	25	65	119	–

Table 2.4: The absolute value of λ of bifurcation points $|\lambda_{-1}(\mu)| = |\lambda_{+1}(\mu)|$ and $|\lambda_{-2}(\mu)| = |\lambda_{+2}(\mu)|$ depending on the parameter μ.

tirely new component for $\mu \in ((3\pi)^2, \mu_c)$ (see Figure 2.13a). The new component expands into space between other components as we increase μ and it, eventually, touches other two components for $\mu \approx 108.1 \in ((3\pi)^2, \mu_c)$ (see Figure 2.13b) and then become one component. At this value of μ occurs the reorganization of branches and for larger μ there are three components again (see Figure 2.12c), two of them bifurcating from the trivial solution and one being isolated. At the value $\mu = \mu_c$, where the pairs of bifurcation points collide, the two components previously bifurcating from $u = 0$ separate from the trivial solution and become isolated too (see Figure 2.13d). The example of solutions along two branches 2-node solutions is plotted in Figure 7 of [FLG20] (see also Appendix C).

2.2.4 | Bifurcation diagrams of superimposed branches of positive, 1-node and 2-node solutions

We conclude this section with superimposed diagrams of positive, 1-node and 2-node solutions in Figure 2.14. They are plotted in the same colors as individually in previous figures. We can see here, that the behaviour of branches for these three types of solutions is dramatically different. The component of positive solutions does not recombine with any other component, it get isolated, shrinks (see the trace of the component in the middle of Figure 2.14b) and eventually disappears. The branches of two components of 1-node solutions first recombine due to the fact that there are two more bifurcation points in the play and then get isolated too. The branches of 2-node solutions behave even more sophistically. Firstly, there appears the third component of 2-node solutions, which subsequently recombine with other two. Then two of these components get isolated, which results in three isolated components of 2-node solutions.

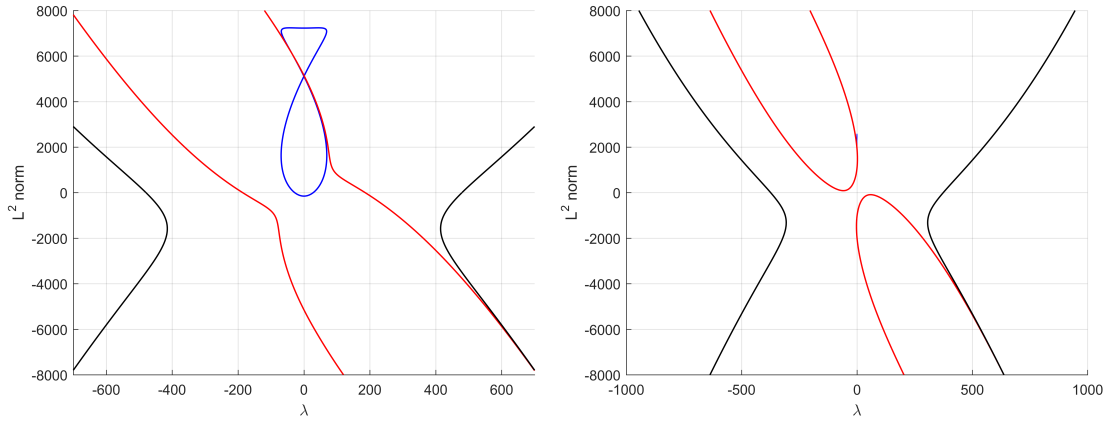

(a) $\mu = 0$ (b) $\mu = 54$

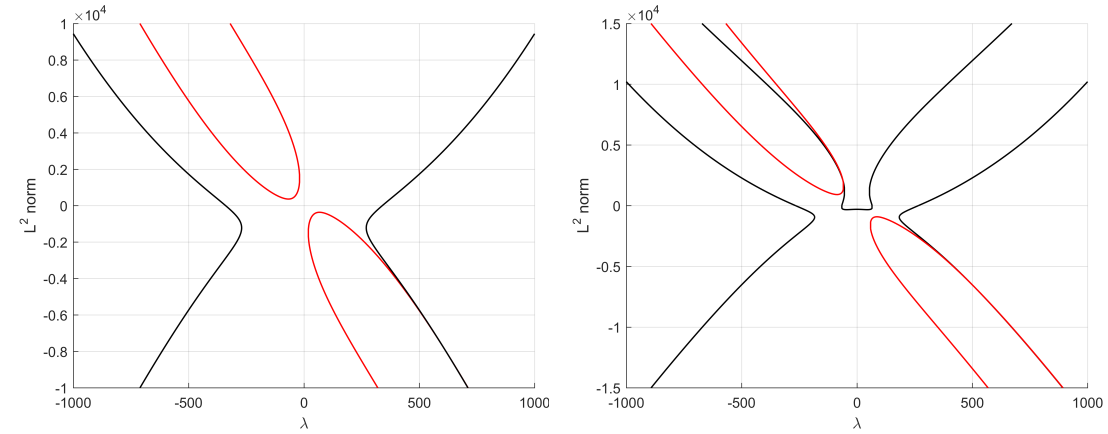

(c) $\mu = 70$ (d) $\mu = 100$

Figure 2.14: Some bifurcation diagrams with superimposed branches of positive (blue), 1-node (red) and 2-node (black) solutions.

3 | Bifurcations in reaction-diffusion systems with unilateral terms and unilateral integral terms in the activator equation

In 1952 Alan M. Turing wrote his paper *"The Chemical Basis of Morphogenesis"* [Tur52] on biological pattern formation, in which he described that a reaction of two chemicals and their diffusion in the space can lead to the production of a spatially heterogeneous structure. That means, the spatially homogeneous steady state of the system, that is stable in the absence of diffusion, could be destabilized by diffusion and produce a spatially heterogeneous state, usually called a "pattern". This behaviour is quite counter-intuitive since diffusion is often perceived as a stabilization effect. Twenty years later, Gierer and Meinhardt published their paper [GM72], in which they analysed this problem in more detail and introduced so called "short range activation-long range inhibition" mechanism. Their research was completely independent, because they did not know about Turing's paper. This effect is also often called Turing's instability, Turing's effect or diffusion-driven instability. The theory and applications are very thoroughly summarized, e.g., in the second instalment of Murray's *"Mathematical biology"* [Mur03].

A pattern formation is not a process exclusive to reaction-diffusion equations, but they are one of common mathematical models for pattern formation problems. Gierer and Meinhardt specified two types of reaction kinetics in [GM72]. The first one is "activator-inhibitor", that means an activator is activating the production of both chemicals, while an inhibitor is inhibiting the production of both chemicals. The other type is called "positive feedback" or "substrate depletion". In this case both activator and inhibitor activate an activator and inhibit an inhibitor.

We devote Section 3.1 to the introduction of known theory, which we use later in this chapter. Section 3.2 consists of introduction of periodic boundary conditions from our paper [Fen20] together with reaction kinetics, which we used for our numerical experiments in the same paper. New results collected from paper [FK19] and [Fen20] are presented in Sections 3.3 and 3.4.

3.1 | Conditions of Turing's instability

Let us consider a general two component reaction-diffusion system

$$\begin{aligned} \frac{\partial u}{\partial t} &= d_1 \Delta u + f(u,v), \\ \frac{\partial v}{\partial t} &= d_2 \Delta v + g(u,v), \end{aligned} \qquad \text{in } \Omega \times [0,+\infty) \tag{3.1}$$

where the domain $\Omega \subset \mathbb{R}^N$ is bounded with Lipschitz boundary, d_1, d_2 are real positive diffusion parameters and $f, g : \mathbb{R}^2 \mapsto \mathbb{R}$ are functions of the class C^1 such that there exist two real constant $\overline{u}, \overline{v}$ satisfying

$$f(\overline{u}, \overline{v}) = g(\overline{u}, \overline{v}) = 0. \tag{3.2}$$

The functions u, v describe concentrations of chemical substances. The reaction-diffusion system (3.1) can be completed by various types of boundary conditions, e.g., homogeneous or non-homogeneous Dirichlet, Neumann boundary conditions, periodic boundary conditions etc. Let us consider here the mixed, Dirichlet-Neumann, boundary conditions

$$\begin{aligned} u = \overline{u},\ v = \overline{v} \text{ on } \Gamma_D, \\ \frac{\partial u}{\partial n} = \frac{\partial v}{\partial n} = 0 \text{ on } \Gamma_N. \end{aligned} \tag{3.3}$$

where n is the unit outward-pointing normal vector of the boundary and Γ_D, Γ_N are open disjoint subsets of $\partial\Omega$ such that $\partial\Omega = \overline{\Gamma_D} \cup \overline{\Gamma_N}$.

The pair $[\overline{u}, \overline{v}]$ is the constant steady state of the problem (3.1),(3.3). Since the functions u, v describe concentrations of some chemicals, this steady state is positive in applications. However, it is only natural to shift it to the origin for the sake of the simpler analysis. Therefore, we will assume $\overline{u} = \overline{v} = 0$ from the beginning. Hence, the functions u, v describe differences from the original positive steady state rather than concentrations themselves.

The stationary system of (3.1) with expanded functions f, g around the constant steady state $[\overline{u}, \overline{v}] = [0, 0]$ has the form

$$\begin{aligned} d_1 \Delta u + b_{1,1} u + b_{1,2} v + n_1(u,v) = 0, \\ d_2 \Delta v + b_{2,1} u + b_{2,2} v + n_2(u,v) = 0, \end{aligned} \tag{3.4}$$

where $b_{i,j}$ for $i, j = 1, 2$ are elements of Jacobi matrix $\mathcal{J}$ of mappings f, g at $[0, 0]$ and n_1, n_2 are higher order terms such that

$$n_{1,2}(u,v) = o(|u| + |v|) \text{ as } |u| + |v| \to 0. \tag{3.5}$$

The corresponding linearized system is then

$$\begin{aligned} d_1 \Delta u + b_{1,1} u + b_{1,2} v = 0, \\ d_2 \Delta v + b_{2,1} u + b_{2,2} v = 0. \end{aligned} \tag{3.6}$$

Remark 3.1.
In this chapter we mostly work in the space

$$H^1_D(\Omega) := \{\phi \in W^{1,2}(\Omega) : \phi = 0 \text{ on } \Gamma_D \text{ in the sense of traces}\}. \tag{3.7}$$

If $\Gamma_D = \emptyset$, then the space H^1_D is actually the whole space $W^{1,2}$ equipped with the standard inner product

$$(u,\varphi)_{H^1_D} = (u,\varphi)_{W^{1,2}} = \int_\Omega (\nabla u \nabla \varphi + u\varphi)\ d\Omega \tag{3.8}$$

and the norm $\|u\|_{W^{1,2}} = \left(\int_\Omega \left((\nabla u)^2 + u^2\right)\ d\Omega\right)^{\frac{1}{2}}$. If $\Gamma_D \neq \emptyset$, then we will use the inner product

$$(u,\varphi)_{H^1_D} = \int_\Omega \nabla u \nabla \varphi\ d\Omega \tag{3.9}$$

and the norm $\|u\|_{H^1_D} = \left(\int_\Omega (\nabla u)^2\ d\Omega\right)^{\frac{1}{2}}$ equivalent to the classical Sobolev norm. Every time we talk about steady states in this chapter, we mean weak solutions from $H^1_D(\Omega)$.

The stability of the steady state $\overline{W} = [\overline{u}, \overline{v}]$ is considered in the norm $\|W\| = \|u\|_{H^1_D} + \|v\|_{H^1_D}$ of the space $H^1_D \times H^1_D$. The stability or the instability is decided by signs of eigenvalues λ of the eigenvalue problem

$$\begin{aligned} d_1 \Delta u + b_{1,1} u + b_{1,2} v &= \lambda u, \\ d_2 \Delta v + b_{2,1} u + b_{2,2} v &= \lambda v, \end{aligned} \tag{3.10}$$

completed by (3.3).

The set of four conditions

$$\begin{aligned} \mathrm{tr}(\mathcal{J}) < 0, \quad \det(\mathcal{J}) > 0, \\ b_{1,1} d_2 + b_{2,2} d_1 > 0, \quad \det(\mathcal{J}) < \frac{(b_{1,1} d_2 + b_{2,2} d_1)^2}{4 d_1 d_2}, \end{aligned}$$

is commonly presented in scientific papers as conditions of Turing's instability. These necessary conditions are derived, e.g., in [Mur03, Chapter 2] in the case $\Gamma_D = \emptyset$. The first and the third condition already imply that diffusion parameters must be different. Moreover, if we consider the first component u as the activator ($b_{1,1} > 0$) and v as the inhibitor ($b_{2,2} < 0$), then it is necessary to have $d_1 < d_2$.

We prefer a different approach introduced in [MNY79] and [Nis82], which is crucial for our new results in Section 3.3 and 3.4. Let us assume in the rest of this chapter that the conditions

$$b_{1,1} > 0,\ b_{2,2} < 0,\ b_{1,2} b_{2,1} < 0,\ \mathrm{tr}(\mathcal{J}) < 0,\ \det(\mathcal{J}) > 0. \tag{3.11}$$

are satisfied. The first two conditions of (3.11) characterize the first equation of (3.1) as the equation for the activator and the second equation as the equation for the inhibitor. The sign of $b_{1,2} b_{2,1}$ decides whether the system (3.1) is of the activator-inhibitor type or of the substrate-depletion type. The last two conditions provide us with the stability of the constant steady state $[\overline{u}, \overline{v}] = [0, 0]$ of (3.1) in the absence of diffusion.

The following remark describes eigenvalues and eigenfunctions of Laplace operator subject to mixed boundary conditions.

Remark 3.2.
Let us consider the problem

$$\begin{aligned} -\Delta u &= \kappa u, \\ u &= 0 \ \text{ on } \Gamma_D, \\ \frac{\partial u}{\partial n} &= 0 \ \text{ on } \Gamma_N. \end{aligned} \tag{3.12}$$

The eigenvalues of (3.12) *form a non-negative non-decreasing sequence* κ_k *with* $k = 1, 2, \ldots$ *(for* $\Gamma_D \neq \emptyset$*) or* $k = 0, 1, 2, \ldots$ *(for* $\Gamma_D = \emptyset$*). The first eigenvalue is always simple. In the case* $\Gamma_D \neq \emptyset$*, the eigenfunction* e_1 *corresponding to the first eigenvalue* κ_1 *does not change the sign on the domain* Ω*. In the case* $\Gamma_D = \emptyset$*, the eigenfunction* e_0 *corresponding to the first eigenvalue* $\kappa_0 = 0$ *is constant. Other eigenfunctions change the sign in both cases. We can choose an orthonormal basis* e_k *in* H^1_D*,* $k = 1, 2, \ldots$ *(for* $\Gamma_D \neq \emptyset$*) or* $k = 0, 1, 2, \ldots$ *(for* $\Gamma_D = \emptyset$*) composed of the eigenfunctions of* (3.12)*.*

Let us define sets of points $[d_1, d_2]$ such that an eigenvalue λ of (3.10) is zero as

$$C_k := \left\{ [d_1, d_2] \in \mathbb{R}^2_+ : \; d_1 = \frac{1}{\kappa_k} \left(\frac{b_{1,2} b_{2,1}}{d_2 \kappa_k - b_{2,2}} + b_{1,1} \right) \right\}, \; k = 1, 2, \ldots, \tag{3.13}$$

(for details see, e.g., [Nis82]). These sets are hyperbolas (or their parts) in $\mathbb{R}^2_+$ (see Figure 3.1). Let us mention here that the sets C_k are often presented in the equivalent form with respect to d_2 instead of d_1. However, the form we present here is much more suitable for our results.

Let us define the envelope of all hyperbolas C_k as

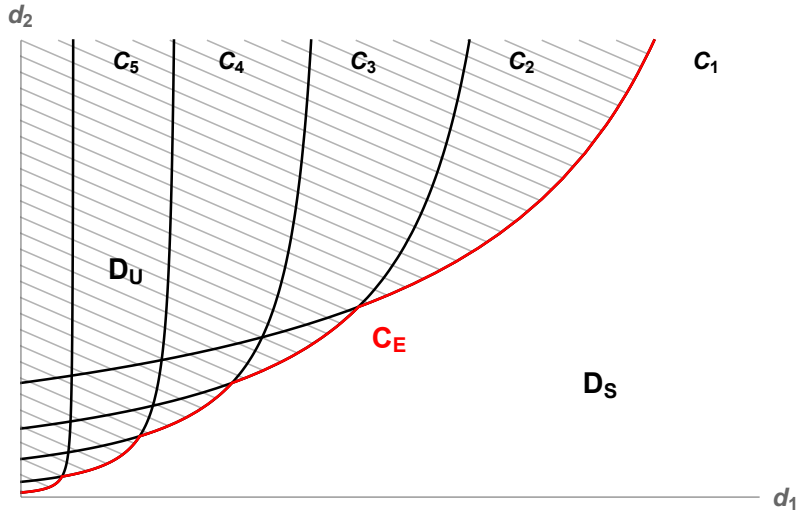

Figure 3.1: Illustration of hyperbolas C_k, the envelope C_E and domains of stability D_S and instability D_U (hatched) in the case when all eigenvalues κ_k are simple.

$$C_E := \left\{ d = [d_1, d_2] \in \mathbb{R}^2_+ : \; d_1 = \max_{\tilde{d}_1 \in \mathbb{R}_+} \left\{ \tilde{d}_1 : [\tilde{d}_1, d_2] \in \bigcup_{k=1}^{\infty} C_k \right\} \right\}. \tag{3.14}$$

This envelope divides the positive quadrant of points $[d_1, d_2]$ onto two regions

$$\begin{aligned} D_S &:= \{ d \in \mathbb{R}^2_+ : d \text{ lies on the right of } C_E \}, \\ D_U &:= \{ d \in \mathbb{R}^2_+ : d \text{ lies on the left of } C_E \}, \end{aligned} \tag{3.15}$$

which we call the domain of stability and the domain of instability, respectively (see Figure 3.1).

Remark 3.3 (see [MNY79],[Nis82] for the case $N = 1$ and [EK97] for the general case).

- *If all eigenvalues of* (3.12) *are simple, i.e.,* $\kappa_k < \kappa_{k+1}$ *for all* $k \in \mathbb{N}$, *then* $C_k \neq C_{k+1}$ *for all* $k > 0$. *If an eigenvalue* κ_k *has a multiplicity* l, *then* $\kappa_{k-1} < \kappa_k = \ldots = \kappa_{k+l-1} < \kappa_{k+l}$ *and* $C_{k-1} \neq C_k = \ldots = C_{k+l-1} \neq C_{k+l}$.

- *If we have* $[d_1, d_2] \in D_U$, *then there exists at least one eigenvalue* λ *of* (3.10) *with positive real part and if* $[d_1, d_2] \in D_S$, *then all eigenvalues* λ *have negative real parts.*

- *If we consider* $\Gamma_D = \emptyset$, *then we have* $C_0 = \emptyset$.

Definition 3.4 (Critical point).
A pair $d = [d_1, d_2] \in \mathbb{R}^2_+$ will be called a critical point of (3.6),(3.3) if there exists a non-trivial (weak) solution of (3.6),(3.3).

Observation 3.5.
We can see that there exists a non-trivial solution of the problem (3.6),(3.3) *for some* d *if and only if* $\lambda = 0$ *is an eigenvalue of the problem* (3.10),(3.3), *that means if and only if* d *lies on some hyperbola* C_k. *Hence,* d *is a critical point of the problem* (3.6),(3.3) *if and only if* $d \in C_k$ *for some* k. *Consequently, the domain of stability* D_S *does not contain any critical point of the problem* (3.6),(3.3).

Remark 3.6 (see, e.g., [EK97]).
If $d \in C_i$ *for* $i = k, \ldots, k+l-1$ *(either* l *is the multiplicity of the eigenvalue* κ_k *or* d *is in the intersection of two hyperbolas* C_k,C_m *and* l *is the sum of multiplicities of* κ_k, κ_m, *see Remark 3.3), then span* $\left(\left[\frac{d_2\kappa_k - b_{2,2}}{b_{2,1}} e_k, e_k \right]_{i=k}^{k+l-1} \right)$ *is the set of solutions of* (3.6),(3.3).

In Chapter 2 of this thesis we have used Definition 2.1 of a bifurcation point for a pair (λ_0, u_0), i.e., the value of the parameter and the solution. From now on, when we talk about bifurcation points, we mean the couple of diffusion parameters in the sense of the following definition.

Definition 3.7 (Bifurcation point).
A pair $d^0 = [d_1^0, d_2^0] \in \mathbb{R}^2_+$ will be called a bifurcation point of (3.4),(3.3) if in any neighbourhood of $[d^0, 0, 0] \in \mathbb{R}^2_+ \times W^{1,2} \times W^{1,2}$ there exists $[d, W] = [d, u, v]$, $\|W\| \neq 0$ satisfying (3.4),(3.3).

The following lemma provides us with the relation between critical points of (3.6),(3.3) and bifurcation points of (3.4),(3.3).

Lemma 3.8 (see, e.g., Lemma A.2 of [FK19] in a special case without unilateral terms).
Every bifurcation point $[d_1, d_2]$ *of* (3.4),(3.3) *is also a critical point of* (3.6),(3.3).

Combining Lemma 3.8 and Observation 3.5 yields the following consequence.

Corollary 3.9.
There are no bifurcation points of (3.4),(3.3) *in the domain of stability* D_S.

3.2 | Periodic boundary conditions and reaction kinetics for numerical experiments

Firstly, we introduce periodic boundary conditions as we did in [Fen20]. We believe that this type of boundary conditions can be more natural in many cases than Neumann boundary conditions (for more details see [Fen20, Section 2.1]). While setting periodic boundary conditions on the interval is quite straightforward, it can be less obvious for domains in higher dimensions. We do not claim the following approach to be novel, rather more specific, because this topic is not very well described in scientific papers. We suppose here that the domain Ω satisfies following properties:

$$\begin{aligned} &\textit{for } N=2:\Omega \textit{ is convex and its boundary is composed of } n \textit{ pairs of edges } \Gamma^i \textit{ and } \Gamma^i_P \\ &\qquad\qquad \textit{with } i=1,\dots n, \textit{ which are parallel and of the same length,} \\ &\textit{for } N\neq 2:\Omega \textit{ is a hypercube with } N \textit{ pairs of parallel facets } \Gamma^i \textit{ and } \Gamma^i_P \textit{ with } i=1,\dots N, \end{aligned} \tag{3.16}$$

where N is the dimension of the domain Ω. Let us denote $\overrightarrow{p_i}$ the vector of the line connecting the center of Γ^i and the center of Γ^i_P. For every point $\mathbf{x}\in\Gamma^i$ there exists a point $\mathbf{x}_P\in\Gamma^i_P$ such that $\mathbf{x}_P$ lies in the intersection of Γ^i_P and the line given by $\overrightarrow{p_i}$ and $\mathbf{x}$. By periodic boundary conditions we will mean boundary conditions of the type

$$u(\mathbf{x}) = u(\mathbf{x}_P) \quad , \qquad v(\mathbf{x}) = v(\mathbf{x}_P) \tag{3.17a}$$

$$-\frac{\partial u}{\partial n}(\mathbf{x}) = \frac{\partial u}{\partial n}(\mathbf{x}_P) \quad , \qquad -\frac{\partial v}{\partial n}(\mathbf{x}) = \frac{\partial v}{\partial n}(\mathbf{x}_P) \tag{3.17b}$$

for every pair of $\mathbf{x}\in\Gamma^i, \mathbf{x}_P\in\Gamma^i_P$. The illustration of these conditions on two examples is in Figure 2 in [Fen20].

Remark 3.10.
When we consider reaction-diffusion system with periodic boundary conditions (3.17)*, by solution we will always mean weak solution in the space of periodic functions*

$$H^1_{per}(\Omega) := \left\{\varphi\in W^{1,2}(\Omega) : \varphi(\mathbf{x}) = \varphi(\mathbf{x}_P)\right\}. \tag{3.18}$$

The space is equipped with the same norm and inner product as $W^{1,2}$ (see Remark 3.1).

The Laplace eigenvalue problem

$$-\Delta u = \kappa u \tag{3.19}$$

with periodic boundary conditions has similar structure of eigenvalues and eigenfunctions as if pure Neumann boundary conditions were considered. Hence, there is the eigenvalue $\kappa_0 = 0$ and the corresponding eigenfunction e_0 is constant. Other eigenvalues are positive. Let us note that hyperbolas and their properties are the same.

Our numerical experiments from [Fen20], which we present in this chapter, are realized using well-known Schnakenberg kinetics (see [Sch79])

$$\begin{aligned} f(u,v) &= a - u + u^2 v, \\ g(u,v) &= b - u^2 v, \end{aligned} \tag{3.20}$$

where a, b are positive reaction coefficients. The reaction-diffusion system (3.1) with this kinetics and either homogeneous Neumann or periodic boundary conditions has a single constant steady state $[\overline{u}, \overline{v}] = \left[a + b, \frac{b}{(a+b)^2}\right]$. We will always assume that

$$a = 0.2, \quad b = 2. \tag{3.21}$$

One can easily verify that conditions (3.11) are satisfied in such case.

We consider the square computation domain $\Omega = [-25, 25]^2$ and we always use a random noise around the constant steady state $[\overline{u}, \overline{v}]$ with the range $\left[-10^{-2}, 10^{-2}\right]$ as the initial condition. We say that we have found a stationary solution, when the difference of solutions in the maximum norm in two consecutive times is smaller than 10^{-3}. We call $[\overline{u}, \overline{v}]$ unstable if the solution $u(\mathbf{x})$ that evolved from perturbations of the constant homogeneous steady state satisfy

$$\frac{\max\limits_{\mathbf{x}\in\Omega} |u(\mathbf{x}) - \overline{u}|}{\overline{u}} > 0.1. \tag{3.22}$$

The value 0.1 is ten times bigger than the range of the initial perturbation, hence, we assume that the solution has evolved enough and it suggests the instability of $[\overline{u}, \overline{v}]$. We use the relative difference from $\overline{u}$ here, because the constant $\overline{u}$ is quite bigger that $\overline{v}$ and the stationary solution u is in general much bigger than v. It does not seem to be the best idea to look for some exact value of d_1, where the stability changes. We will rather look for a critical interval $I_{crit} := (d_1^U, d_1^S)$ such that $|d_1^U - d_1^S| < 0.01$ and $[\overline{u}, \overline{v}]$ is unstable for $[d_1^U, d_2]$ and stable for $[d_1^S, d_2]$ (in the sense of (3.22)).

We built our own code in MATLAB for numerical experiments. The main idea is the

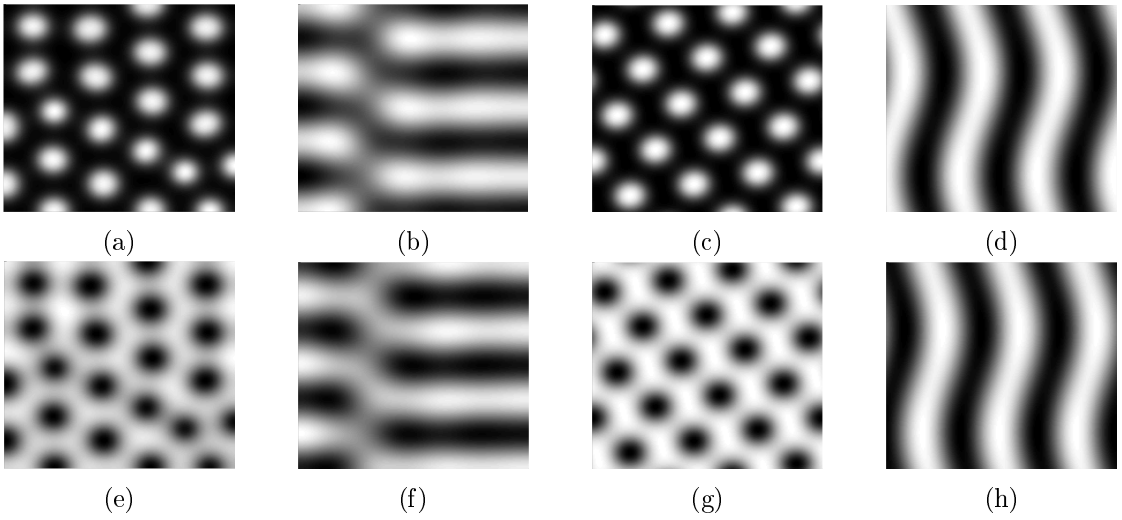

Figure 3.2: Examples of typical patterns in the classical case without unilateral terms. (a) sol. u, spots, Neumann b.c. (b) sol. u, stripes, Neumann b.c. (c) sol. u, spots, periodic b.c. (d) sol. u, stripes, periodic b.c. (e) sol. v, spots, Neumann b.c. (f) sol. v, stripes, Neumann b.c. (g) sol. v, spots, periodic b.c. (h) sol. v, stripes, periodic b.c.

method of lines, i.e., we discretize the spatial variable to get a system of ordinary differential equations, where the evolution in time can be realized by one of *ode solvers* implemented in MATLAB. We use five-point finite difference scheme to approximate Laplace operator

together with the idea of a ghost point to deal with either Neumann or periodic boundary conditions. For the evolution in time we chose the solver *ode15s*, which is in our experience most suitable for this kind of problems. Also if the system contains an integral of the type

$$\int_K u \, dx,$$

with $K \subset \Omega$ being a square, which happens in cases of unilateral integral terms in Section 3.4, then we use trapezoidal rule to approximate this integral. This type of approximation has the same error as five-point scheme, hence, it will not worsen the overall error of the method.

Typical patterns produced by numerical experiments on reaction-diffusion system with Schnakenberg kinetics without any unilateral terms and coupled either with periodic or with Neumann boundary conditions can be seen in Figure 3.2. The pattern with spots typically appears for some $[d_1, d_2]$ deep in the domain of instability, while stripe patterns are produced for $[d_1, d_2]$ close to the envelope C_E. One can see that the shape of patterns in solution u and v are the same, there is just inverted coloring (maximums and minimums). We will always show the solution v so that spots are always black.

3.3 | Reaction-diffusion problem with unilateral sources and sinks

In this section we present new results concerning the reaction-diffusion system supplemented by unilateral sources and sinks in the activator equation. The unilateral source or the sink is based on the negative part $\psi^- = \max\{-\psi, 0\}$ or the positive part $-\psi^+ = -\max\{\psi, 0\}$ of the function ψ, respectively, where ψ represents the variable of the activator. The unilateral source ψ^- turns on only if the value of the component ψ drops under zero, otherwise it is switched off. The unilateral sink $-\psi^+$ behaves in the opposite way. We show that if terms of this type are present in the activator equation of the system and certain conditions are satisfied, then the set of points $[d_1, d_2] \in \mathbb{R}^2_+$, for which bifurcation from the trivial solution can occur, is smaller than in the classical case, i.e., the problem without unilateral terms. The main motivation for this study was the paper [Kuč97], where was studied a system with unilateral conditions related to the activator equation instead of unilateral terms and similar results were achieved. The dual problem, where unilateral terms were present in the inhibitor equation, was studied in the paper [KN18]. Firstly, we present analytical results from our paper [FK19]. We follow with results of numerical experiments for specific reaction kinetics, which were presented in [Fen20]. The dual problem was also studied numerically, e.g., in [VJKR17] and [RV15]. For more information about the history of problems with unilateral conditions or terms in reaction-diffusion systems see, e.g., [FK19],[Fen20] and references therein.

Let us consider the system (3.1) supplemented by a unilateral source $\tilde{f}_-$ and a sink $-\tilde{f}_+$

$$\begin{aligned} \frac{\partial u}{\partial t} &= d_1 \Delta u + f(u, v) + \tilde{f}_-(\mathbf{x}, u^-) - \tilde{f}_+(\mathbf{x}, u^+), \\ \frac{\partial v}{\partial t} &= d_2 \Delta v + g(u, v) \quad \text{in } \Omega \times [0, +\infty) \end{aligned} \tag{3.23}$$

where $\tilde{f}_-, \tilde{f}_+ : \Omega \times \mathbb{R} \to \mathbb{R}$ are functions satisfying Carathéodory conditions and such that there exist

$$s_-(\mathbf{x}) := \frac{\partial \tilde{f}_-}{\partial \xi}(\mathbf{x}, \xi)|_{\xi=0} \geq 0, \; s_+(\mathbf{x}) := \frac{\partial \tilde{f}_+}{\partial \xi}(\mathbf{x}, \xi)|_{\xi=0} \geq 0 \text{ for a.a. } \mathbf{x} \in \Omega, s_\pm \in L_\infty(\Omega). \tag{3.24}$$

Moreover we assume that

$$\tilde{f}_-(\mathbf{x}, 0) = \tilde{f}_+(\mathbf{x}, 0) = 0, \tag{3.25}$$

which together with (3.2) implies that $[\overline{u}, \overline{v}] = [0, 0]$ is the constant steady state of the problem (3.23), (3.3).

We will consider two distinctive cases based the choice of Γ_D in boundary conditions (3.3), i.e., the case $\Gamma_D \neq \emptyset$ (Dirichlet or mixed boundary conditions) and the case $\Gamma_D = \emptyset$ (pure Neumann boundary conditions). The main reason is that in the former case, we can significantly simplify our analysis, while the latter case is technically more demanding. We do not distinguish the case of pure Dirichlet boundary conditions, because it is already included in the case of mixed boundary conditions and it does not bring anything new. If we consider $\tilde{f}_- \equiv \tilde{f}_+ \equiv 0$, then the system (3.23) reduces to the classical system without unilateral terms (3.1).

Now we introduce system

$$\begin{aligned} d_1 \Delta u + b_{1,1} u + b_{1,2} v + n_1(u, v) + \tilde{f}_-(\mathbf{x}, u^-) - \tilde{f}_+(\mathbf{x}, u^+) = 0, \\ d_2 \Delta v + b_{2,1} u + b_{2,2} v + n_2(u, v) = 0, \end{aligned} \tag{3.26}$$

which is the stationary problem of (3.23) with expanded functions f, g around the origin and

$$\begin{aligned} d_1 \Delta u + b_{1,1} u + b_{1,2} v + s_-(\mathbf{x}) u^- - s_+(\mathbf{x}) u^+ = 0, \\ d_2 \Delta v + b_{2,1} u + b_{2,2} v = 0, \end{aligned} \tag{3.27}$$

which is the homogenized system of (3.26). These two systems are closely related to systems (3.4) and (3.6), respectively. While in the classical case without unilateral terms we could simply linearize the system (3.4), in this case it is not possible, because the system (3.26) is non-smooth at the origin. Hence, we can only have the homogenized system (3.27). As far as we know, this homogenized system does not say anything about dynamics of the nonlinear system (3.26). However, the same relation between bifurcation points of (3.26), (3.3) and critical points of (3.27), (3.3), which we presented in Lemma 3.8 in the classical case, holds here too (see, e.g., [FK19, Lemma A.2]), i.e., every bifurcation point of (3.26), (3.3) is a critical point of (3.27), (3.3).

In the next notation we define two subsets of the part $\mathbb{R}^2_+$ of the plane of points $[d_1, d_2]$, which are crucial for the formulation of our analytical results.

Notation 3.11.
Let us assume constants $r, R, \varepsilon \in \mathbb{R}_+$, which satisfy $r < R$. We define two sets $C_r^R, C_r^R(\varepsilon)$ by

$$C_r^R := \{d = [d_1, d_2] \in C_E : d_2 \in [r, R]\}, \tag{3.28}$$

$$C_r^R(\varepsilon) := \{d = [d_1, d_2] \in C_E \cup D_U : d_2 \in [r, R] \wedge dist(d, C_E) < \varepsilon\}. \tag{3.29}$$

The following theorem is the main result of [FK19] for the case of general mixed boundary conditions (3.3). The proof of the following theorem and technical details can be found in Sections 4, 5 and 6 of [FK19].

Theorem 3.12 (see also Theorem 3.1 of [FK19] in Appendix A).

(i) The domain of stability D_S contains neither critical points of (3.27),(3.3) *nor bifurcation points of* (3.26),(3.3).

(ii) Let $0 < r < R$. Let $C_k, \dots, C_{k+l-1}$ be all hyperbolas which have a non-empty intersection with C_r^R. Let any linear combination e of the eigenfunctions of (3.12) *corresponding to $\kappa_k, \dots, \kappa_{k+l-1}$ satisfy*

$$s_- e^- - s_+ e^+ \not\equiv 0. \tag{3.30}$$

Then there exists $\varepsilon > 0$ such that there are neither critical points of (3.27),(3.3) *nor bifurcation points of* (3.26),(3.3) *in $C_r^R(\varepsilon)$.*

Remark 3.13.
If the condition (3.30) *is not satisfied for some e, then* (3.27) *becomes* (3.6) *and every point $[d_1, d_2] \in C_r^R$ is a critical point of* (3.27),(3.3) *due to Observation 3.5 and Remark 3.6. Let, e.g., C_r^R has non-empty intersection with exactly two non-coinciding hyperbolas C_1 and C_2. Now it is possible that both e_1 and e_2 satisfy the condition* (3.30)*, hence, there are no critical points on C_1 and C_2 excluding their intersection. In the same time this intersection can be a critical point due to the fact that a linear combination of e_1 and e_2 does not have to satisfy this condition. However, the opposite case that there would be critical points on C_1 and C_2, but not in their intersection, is not possible. In the scenario in which $C_1 = C_2$ all linear combinations of e_1 and e_2 must satisfy* (3.30) *so that there would not be any critical points on C_1 or C_2.*

The illustration of the main result is in Figure 3.3. While Theorem 3.12 states that there are no bifurcation points in some neighbourhood $C_r^R(\varepsilon)$ under some conditions, it does not say anything about nontrivial solutions themselves. The following corollary provide us with nonexistence of, at least, small non-trivial solutions.

Corollary 3.14 (see also Corollary 3.1 of [FK19] in Appendix A).

(i) For any compact part M of D_S there exists $\delta > 0$ such that for any $[d_1, d_2] \in M$ there are no non-trivial solutions of (3.26),(3.3) *with $0 < \|u\|_{H_D^1} + \|v\|_{H_D^1} < \delta$.*

(ii) Under the assumptions (ii) of Theorem 3.12, for any compact part M of $D_S \cup C_r^R(\varepsilon)$ there exists $\delta > 0$ such that for any $[d_1, d_2] \in M$ there are no non-trivial solutions of (3.26),(3.3) *with $0 < \|u\|_{H_D^1} + \|v\|_{H_D^1} < \delta$.*

Here follow two results in special cases of Dirichlet–Neumann and pure Neumann boundary conditions in the case that only sources or sinks are present in the system.

Theorem 3.15 (see also Theorem 3.2 of [FK19] in Appendix A).
Let $\Gamma_D \neq \emptyset$. Let one of the functions s_+, s_- be identically zero and the other positive almost everywhere on Ω (that means only sources or sinks are present in the system). Let d_2^I be the second coordinate of the intersection point of C_1 and C_2.

(i) Any $d \in C_1$, in particular any $d \in C_r^R$ with $d_2^I \leq r < R$, is a critical point of (3.27),(3.3).

(ii) If $0 < r < R < d_2^I$, then there exists $\varepsilon > 0$ such that there are neither critical points of (3.27),(3.3) *nor bifurcation points of* (3.26),(3.3) *in $C_r^R(\varepsilon)$.*

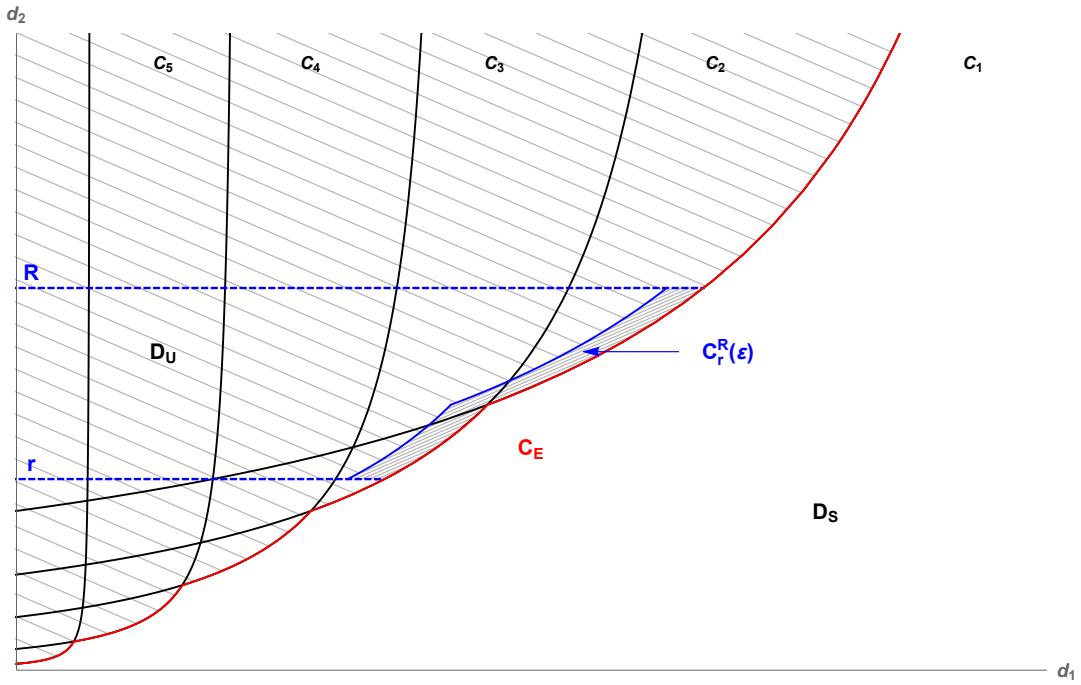

Figure 3.3: The illustration of the main result and $C_r^R(\varepsilon)$ neighbourhood. The case when all eigenvalues κ_k are simple.

Theorem 3.16 (see also Theorem 3.3 of [FK19] in Appendix A).
Let $\Gamma_D = \emptyset$. Let one of the functions s_+, s_- be identically zero and the other positive almost everywhere on Ω (that means only sources or sinks are present in the system). Then for any $0 < r < R$ there exists $\varepsilon > 0$ such that there are neither critical points of (3.27),(3.3) *nor bifurcation points of* (3.26),(3.3) *in $C_r^R(\varepsilon)$.*

The following theorem is a modification of Theorem 3.12 for the case of unilateral terms in boundary conditions, namely for systems (3.6) and (3.4) with boundary conditions

$$\begin{aligned} u = v = 0 \quad &\text{on} \quad \Gamma_D, \\ \frac{\partial u}{\partial n} = s_-(\mathbf{x})u^- - s_+(\mathbf{x})u^+ \quad &\text{on} \quad \Gamma_N, \\ \frac{\partial v}{\partial n} = 0 \quad &\text{on} \quad \Gamma_N. \end{aligned} \tag{3.31}$$

Theorem 3.17 (see also Theorem 3.5 of [FK19] in Appendix A).

(i) The domain of stability D_S contains neither critical points of (3.6),(3.31) *nor bifurcation points of* (3.4),(3.31).

(ii) Let $0 < r < R$. Let $C_k, \dots, C_{k+l-1}$ be all hyperbolas which have a non-empty intersection with C_r^R. Let any linear combination e of the eigenfunctions of (3.12) *corresponding to $\kappa_k, \dots, \kappa_{k+l-1}$ satisfy*

$$s_- e^- - s_+ e^+ \not\equiv 0 \quad \text{on } \Gamma_N. \tag{3.32}$$

Then there exists $\varepsilon > 0$ such that there are neither critical points of (3.6),(3.31) *nor bifurcation points of* (3.4),(3.31) *in $C_r^R(\varepsilon)$.*

Since we did not consider periodic boundary conditions in [FK19], the following theorem is not included in there, but it is hinted in Remark 3.4 of [Fen20]. The proof is the same as the proof of Theorem 3.12 in the case of pure Neumann boundary conditions.

Theorem 3.18.
Let us suppose that the domain Ω satisfies (3.16).

(i) The domain of stability D_S contains neither critical points of (3.27),(3.17) *nor bifurcation points of* (3.26),(3.17).

(ii) Let $0 < r < R$. Let $C_k, \dots, C_{k+l-1}$ be all hyperbolas which have a non-empty intersection with C_r^R. Let any linear combination e of the eigenfunctions of (3.19),(3.17) *corresponding to $\kappa_k, \dots, \kappa_{k+l-1}$ satisfy* (3.30). *Then there exists $\varepsilon > 0$ such that there are neither critical points of* (3.27),(3.17) *nor bifurcation points of* (3.26),(3.17) *in $C_r^R(\varepsilon)$.*

The following theorem provide us with sufficient conditions for the existence of, at least, one critical point $[d_1, d_2]$ of the problem (3.27),(3.3). The opposite question, whether for sufficiently strong unilateral source or sink there are no critical points of the problem (3.27),(3.3) in the positive part $\mathbb{R}^2_+$ of the plane of points $[d_1, d_2]$, is an open problem.

Theorem 3.19 (see also Theorem 3.4 of [FK19] in Appendix A).
Let $d_2 > 0$ be arbitrary fixed. Let k_0 be such that $\left[\frac{1}{\kappa_{k_0}}\left(\frac{b_{1,2}b_{2,1}}{d_2\kappa_{k_0}-b_{2,2}}+b_{1,1}\right), d_2\right] \in C_E$ *(see* (3.13),(3.14)*). If* $\max\{\|s_-\|_\infty, \|s_+\|_\infty\} < b_{1,1} + \frac{b_{1,2}b_{2,1}}{d_2\kappa_{k_0}-b_{2,2}}$, *then there exists at least one d_1 such that $[d_1, d_2] \in D_U \cup C_E$ is a critical point of the problem* (3.27),(3.3).

In our numerical experiments of this section we consider the unilateral source

$$\tau\chi^{\Omega_S}(\mathbf{x})(u-\overline{u})^- \tag{3.33}$$

added to the activator equation of the reaction-diffusion system with Schnakenberg kinetics (3.20). The parameter τ is real non-negative, $\Omega_S \subseteq \Omega$ is a square with the center in the center of the square Ω and χ^{Ω_S} is the characteristic function of this set. The number $\overline{u} = a+b$ is the first component of the constant steady state $\left[a+b, \frac{b}{(a+b)^2}\right]$ of the reaction-diffusion problem with Schnakenberg reaction kinetics. We chose this simple unilateral source, because we can expect the existence of $C_r^R(\varepsilon)$ for any choice of C_r^R according to Theorem 3.16 (for $\tau > 0$ and $\Omega_S = \Omega$).

First, let us focus on the case of Neumann boundary conditions and the case $\Omega_S = \Omega$, hence, the source acts on the whole domain Ω. We experimentally found the critical interval I_{crit} for several values of d_2 and three values of τ. A sample of these experiments for $d_2 = 600$ can be found in Table 3.1, the full table for several values of d_2 can be found in the appendix of [Fen20] (see Table 7). One can see that as we increase τ, the critical interval shifts to the left. It would be interesting to find a large enough value of τ, such that the critical interval reaches zero, but numerical methods we used are not very reliable for d_1 close to zero. Hence, this remains an open problem. The case $\tau = 0$ corresponds to the classical case without unilateral sources. Of course, we could just use d_1 computed exactly using the definition of C_E (in the second column). However, since everything is just approximate here, we should compare I_{crit} for positive τ with I_{crit} for $\tau = 0$. The patterns have usually the same shape when we use

the unilateral source (3.33) on the whole domain Ω as in the classical case (meaning in the problem without any unilateral terms).

d_2	d_1	I_{crit} for $\tau = 0$	I_{crit} for $\tau = 0.1$	I_{crit} for $\tau = 0.5$	I_{crit} for $\tau = 1$
600	14.73	(14.6149,14.6221)	(12.8456,12.8528)	(9.8967,9.9039)	(8.6452,8.6524)

Table 3.1: Critical intervals I_{crit} for different values of τ and $\Omega_S = \Omega$. The case of the unilateral source (3.33) and Neumann boundary conditions. The value of d_1 in the second column is exactly computed value of d_1 such that $[d_1, d_2] \in C_E$.

In the next series of experiments we investigate the influence of the unilateral source depending on the size of $\Omega_S \subseteq \Omega$. The goal is once again to find the critical interval for different sizes of Ω_S. We can see in the sample in Table 3.2, that as we increase the size of Ω_S, the unilateral term has bigger influence and the critical interval is closer to zero (see Table 8 in the appendix of [Fen20] for more values of d_2). This is the expected result, but it is interesting that even for $|\Omega_S| = 30^2$, which is quite large square, the shift is very small. This suggests that using unilateral terms on small subset is not very effective in this sense.

d_2	I_{crit} for $\|\Omega_S\| = 50^2$	I_{crit} for $\|\Omega_S\| = 40^2$	I_{crit} for $\|\Omega_S\| = 30^2$	I_{crit} for $\|\Omega_S\| = 10^2$
600	(9.8967,9.9039)	(12.637,12.6442)	(14.1258,14.133)	(14.6005,14.6077)

Table 3.2: Critical intervals I_{crit} for $\tau = 0.5$ on square support Ω_S in the middle of Ω. The case of the unilateral source (3.33) and Neumann boundary conditions.

The shape of patterns is more interesting in the case that the unilateral source is acting only on the part of the domain Ω. In Figure 3.4 we illustrate the dependence of the shape of patterns on the size of Ω_S and the value of d_1. One can see that for the higher value of d_1 or the larger Ω_S, the pattern is not produced.

In the case of periodic boundary conditions, the situation considering the critical interval and the shape of patterns is very similar to the case of Neumann boundary conditions. The shift of the critical interval I_{crit} for $d_2 = 600$ and three values of τ is in Table 3.3, for the several values of d_2 see full Table 9 in the appendix of [Fen20]. The patterns are more of less the same as typical patterns in Figure 3.2g, 3.2h.

d_2	I_{crit} for $\tau = 0$	I_{crit} for $\tau = 0.1$	I_{crit} for $\tau = 0.5$	I_{crit} for $\tau = 1$
600	(14.1258,14.133)	(12.6946,12.7017)	(9.7169,9.7241)	(8.6596,8.6668)

Table 3.3: Critical intervals I_{crit} for different values of τ and $\Omega_S = \Omega$. The case of the unilateral source (3.33) and periodic boundary conditions.

In the case that the unilateral source is active only on Ω_S, the shift of the critical interval I_{crit} for $d_2 = 600$ and four sizes of Ω_S is in Table 3.4, for the several values of d_2 see again full Table 10 in the appendix of [Fen20]. The shape of patterns is again in this case more interesting than in the case that the unilateral source is active on the whole domain Ω (see

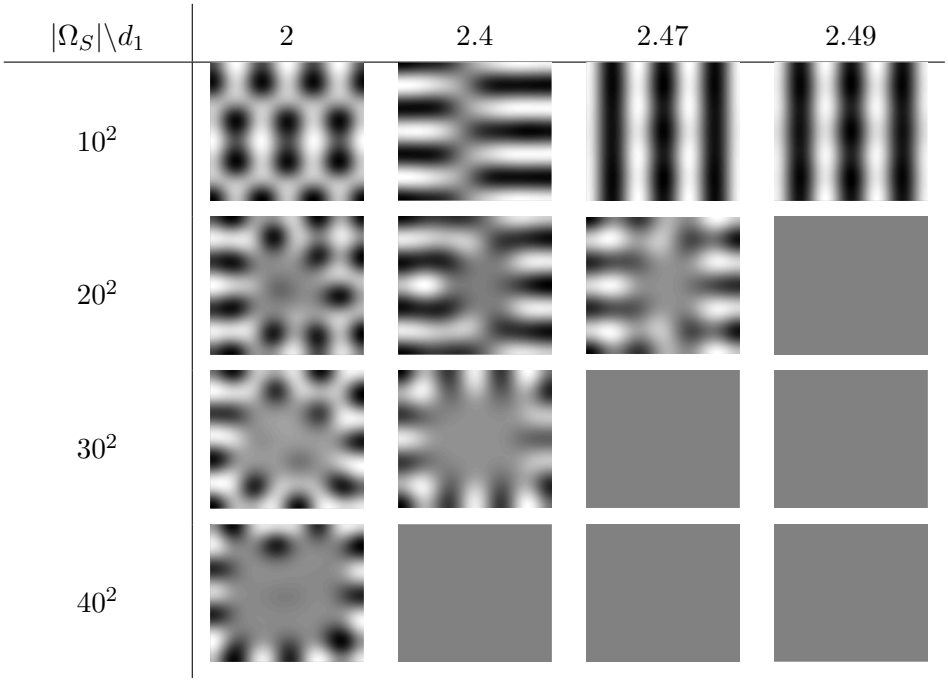

Figure 3.4: The dependence of the shape of patterns on the size of Ω_S and the diffusion parameter d_1- the case of Neumann boundary conditions and fixed $d_2 = 100$.

Figure 3.5).

d_2	I_{crit} for $\lvert\Omega_S\rvert = 40^2$	I_{crit} for $\lvert\Omega_S\rvert = 30^2$	I_{crit} for $\lvert\Omega_S\rvert = 20^2$	I_{crit} for $\lvert\Omega_S\rvert = 10^2$
600	(12.1881,12.1934)	(14.0108,14.018)	(14.1412,14.148)	(14.1345,14.1412)

Table 3.4: Critical intervals I_{crit} for $\tau = 0.5$ on square support Ω_S in the middle of Ω. The case of the unilateral source (3.33) and periodic boundary conditions.

The unilateral source (3.33) can be of course replaced with more complicated sources or we could use both the source and the sink. We repeated some of experiments for the unilateral source with saturation $\tau\chi^{\Omega_S}\frac{(u-\overline{u})^-}{1+(u-\overline{u})^-}$ and got similar results, which we do not present here.

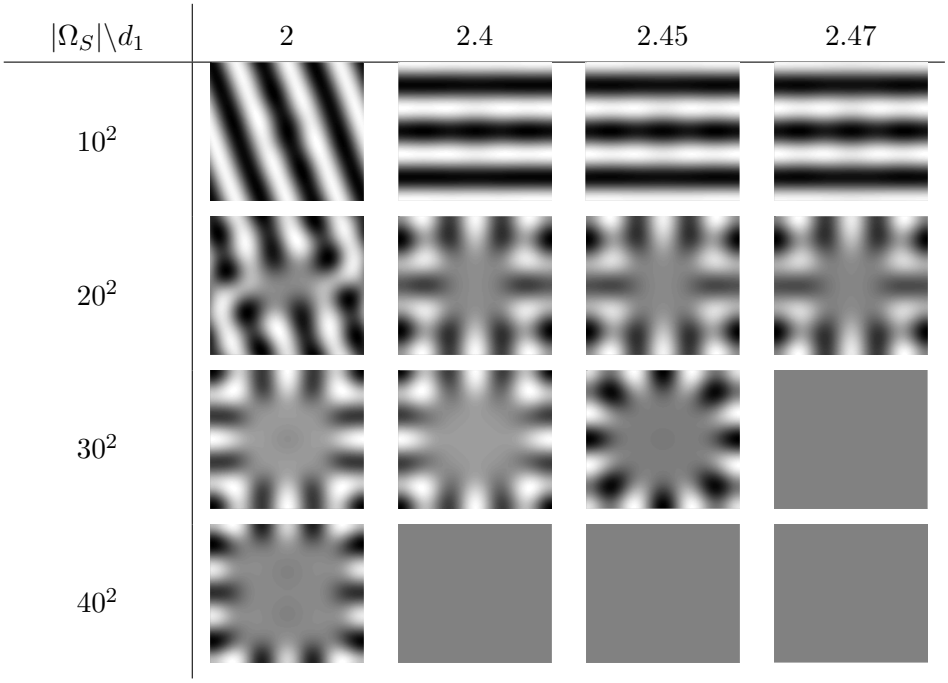

Figure 3.5: The dependence of the shape of patterns on the size of Ω_S and the diffusion parameter d_1- the case of periodic boundary conditions and fixed $d_2 = 100$.

3.4 | Reaction-diffusion problem with unilateral sources and sinks containing an integral average

In the previous section we have considered reaction-diffusion problems with unilateral terms of the type ψ^-, ψ^+ in the activator equation. The behaviour of these terms is local in the sense that, e.g., the unilateral source $\psi^-(x)$ switches on in a point x of Ω if the value $\psi(x)$ drops under zero. We propose here a different type of unilateral terms, which we call unilateral integral terms. One simple example of such a term is

$$\chi^M(x) \left(\int_K \frac{\psi(x)}{|K|}\, dK \right)^-,$$

where K, M are subsets of the domain Ω, χ^M is the characteristic function of the set M and $|K|$ denotes the Lebesgue measure of the set K. This type of a unilateral term measures the average of $\psi(x)$ on the set K and if this average drops under the threshold value (in this case the zero), the source switches on and is active on the set M. It seems more natural to measure the average of concentrations in some area as this term propose, rather than measure the concentration in every single point. For our analytical results we will always consider $K = M$, but we also investigate the option $K \neq M$ in our numerical experiments.

We will show that if unilateral integral sources and sinks are present in the reaction-diffusion system and a condition similar to (3.30) is satisfied, then again the set of points $[d_1, d_2] \in \mathbb{R}^2_+$, for which the bifurcation can occur, is smaller than in the classical case. We also complete analytical results by numerical experiments, similarly as in the previous section. All results were published in the paper [Fen20], which is motivated by our previous paper [FK19] and the paper [KRE03], where unilateral integral terms were presented in boundary

conditions.

We supplement the activator equation of the system (3.1) by unilateral integral terms and get

$$\begin{aligned}\frac{\partial u}{\partial t} &= d_1\Delta u + f(u,v)\\ &\quad + \sum_{i=1}^{n}\chi^{K_i^-}(x) f_-^i\left(\left(\int_{K_i^-}\frac{u}{|K_i^-|}\,dK_i^-\right)^-\right) - \sum_{j=1}^{m}\chi^{K_j^+}(x) f_+^j\left(\left(\int_{K_j^+}\frac{u}{|K_j^+|}\,dK_j^+\right)^+\right),\\ \frac{\partial v}{\partial t} &= d_2\Delta v + g(u,v) \quad \text{in } \Omega\times[0,+\infty)\end{aligned} \tag{3.34}$$

where $f_-^i, f_+^j : \mathbb{R}\to\mathbb{R}$ are real functions such that

$$f_-^i(0) = f_+^j(0) = 0 \quad \text{for every } i = 1,\dots n, j = 1,\dots,m, \tag{3.35}$$

and there exist

$$\tau_-^i := \frac{\partial f_-^i}{\partial\xi}(\xi)|_{\xi=0}\in\mathbb{R}_0^+, \quad \tau_+^j := \frac{\partial f_+^j}{\partial\xi}(\xi)|_{\xi=0}\in\mathbb{R}_0^+ \quad \text{for all } i=1,\dots,n, j=1,\dots,m. \tag{3.36}$$

Once again we can see that $[\overline{u},\overline{v}] = [0,0]$ is the constant steady state of the problem (3.34),(3.3). We suppose that $K_i^-, K_j^+ \subseteq \Omega$ and functions $\chi^{K_i^-}(x)$ and $\chi^{K_j^+}(x)$ are characteristic functions of sets K_i^- and K_j^+, respectively. We will assume that sets K_i^- are connected and disjoint. The same is assumed for sets K_j^+. Hence, there is n unilateral integral sources and m unilateral integral sinks in the system (3.34). Source terms are always active in the area, where the integral average is measured. The same applies to sink terms. The area where the source and the sink is active can of course overlap.

Let us define the functional $T_X^{\mp} : H_D^1\to\mathbb{R}_0^+$ by

$$T_X^{\mp}(\psi) = \left(\int_X\frac{\psi}{|X|}\,dX\right)^{\mp}, \tag{3.37}$$

where X is some subset of Ω. It will allow us to write upcoming systems with unilateral integral terms in more compact form.

Similarly as in the previous section we introduce stationary system of (3.34)

$$\begin{aligned}0 &= d_1\Delta u + b_{1,1}u + b_{1,2}v + n_1(u,v) + \sum_{i=1}^{n}\chi^{K_i^-}(x) f_-^i\left(T_{K_i^-}^-(u)\right) - \sum_{j=1}^{m}\chi^{K_j^+}(x) f_+^j\left(T_{K_j^+}^+(u)\right),\\ 0 &= d_2\Delta v + b_{2,1}u + b_{2,2}v + n_2(u,v),\end{aligned} \tag{3.38}$$

and its homogenization

$$\begin{aligned}0 &= d_1\Delta u + b_{1,1}u + b_{1,2}v + \sum_{i=1}^{n}\chi^{K_i^-}(x)\tau_-^i T_{K_i^-}^-(u) - \sum_{j=1}^{m}\chi^{K_j^+}(x)\tau_+^j T_{K_j^+}^+(u),\\ 0 &= d_2\Delta v + b_{2,1}u + b_{2,2}v.\end{aligned} \tag{3.39}$$

The next theorem is the main theoretical result of [Fen20] and it has the same role in the case of unilateral integral terms as Theorem 3.12 in the case of unilateral terms.

Theorem 3.20 (see also Theorem 3.1 of [Fen20] in Appendix B)**.**

(i) *The domain of stability D_S contains neither critical points of* (3.39),(3.3) *nor bifurcation points of* (3.38),(3.3).

(ii) *Let $0 < r < R$. Let $C_k, \dots, C_{k+l-1}$ be all hyperbolas which have a non-empty intersection with C_r^R. Let any linear combination e of the eigenfunctions of* (3.12) *corresponding to $\kappa_k, \dots, \kappa_{k+l-1}$ satisfy*

$$\sum_{i=1}^{n} \chi^{K_i^-}(x)\tau_-^i T_{K_i^-}^-(e) - \sum_{j=1}^{m} \chi^{K_j^+}(x)\tau_+^j T_{K_j^+}^+(e) \not\equiv 0. \tag{3.40}$$

Then there exists $\varepsilon > 0$ such that there are neither critical points of (3.39),(3.3) *nor bifurcation points of* (3.38),(3.3) *in $C_r^R(\varepsilon)$.*

While in the case of unilateral terms we had Theorem 3.15, which ensured existence of $C_r^R(\varepsilon)$ along the part of C_E without satisfying condition (3.30) in the special case, it is not possible to get the same result here in the case of unilateral integral terms. We can only show that there are critical points of (3.39),(3.3) on the hyperbola C_1. Similarly, we cannot achieve the same results as we did in Theorem 3.16 in the case of pure Neumann boundary conditions.

Theorem 3.21 (see also Theorem 3.2 of [Fen20] in Appendix B).
Let $\Gamma_D \neq \emptyset$. Let either $\tau_-^i = 0$ and $\tau_+^j > 0$ or $\tau_-^i > 0$ and $\tau_+^j = 0$ for all $i = 1, \dots, n$ and $j = 1, \dots, m$ (that means we have either sources or sinks in the system). Let d_2^I be the second coordinate of the intersection point of C_1 and C_2. Any $d \in C_1$, in particular any $d \in C_r^R$ with $d_2^I \leq r < R$, is a critical point of (3.39),(3.3).

Theorem 3.22 (see also Theorem 3.3 of [Fen20] in Appendix B).
Let $\Gamma_D = \emptyset$ and $K_i^- = K_j^+ = \Omega$ for all $i = 1, \dots, n$ and $j = 1, \dots, m$. The condition (3.40) *from Theorem 3.20 can never be satisfied and any point $[d_1, d_2] \in C_E$ is a critical point of* (3.39),(3.3).

Let us assume that $K_i^-, K_j^+ \subset \Gamma_N$ and let us consider boundary conditions

$$\begin{aligned} u = v = 0 \quad &\text{on} \quad \Gamma_D, \\ \frac{\partial u}{\partial n} = \sum_{i=1}^{n} \chi^{K_i^-}(x)\tau_-^i T_{K_i^-}^-(u) - \sum_{j=1}^{m} \chi^{K_j^+}(x)\tau_+^j T_{K_j^+}^+(u) \quad &\text{on} \quad \Gamma_N, \\ \frac{\partial v}{\partial n} = 0 \quad &\text{on} \quad \Gamma_N. \end{aligned} \tag{3.41}$$

We have considered a problem with unilateral terms in boundary conditions in the previous section. The same can be done here in the case unilateral integral terms.

Theorem 3.23 (see also Theorem 3.4 of [Fen20] in Appendix B).
Let $K_i^-, K_j^+ \subseteq \Gamma_N$ for all $i = 1, \dots, n$ and $j = 1, \dots, m$.

(i) *The domain of stability D_S contains neither critical points of* (3.6),(3.41) *nor bifurcation points of* (3.4),(3.41).

(ii) *Let $0 < r < R$. Let $C_k, \dots, C_{k+l-1}$ be all hyperbolas which have a non-empty intersection with C_r^R. Let any linear combination e of the eigenfunctions of* (3.12) *corresponding to $\kappa_k, \dots, \kappa_{k+l-1}$ satisfy*

$$\sum_{i=1}^{n} \chi^{K_i^-}(x)\tau_-^i T^-_{K_i^-}(e) - \sum_{j=1}^{m} \chi^{K_j^+}(x)\tau_+^j T^+_{K_j^+}(e) \not\equiv 0 \quad \text{on } \Gamma_N. \tag{3.42}$$

Then there exists $\varepsilon > 0$ such that there are neither critical points of (3.6),(3.41) *nor bifurcation points of* (3.4),(3.41) *in $C_r^R(\varepsilon)$.*

Theorem 3.24 (see also Theorem 3.5 of [Fen20] in Appendix B).
Let us suppose that the domain Ω satisfies (3.16).

(i) *The domain of stability D_S contains neither critical points of* (3.39),(3.17) *nor bifurcation points of* (3.38),(3.17).

(ii) *Let $0 < r < R$. Let $C_k, \dots, C_{k+l-1}$ be all hyperbolas which have a non-empty intersection with C_r^R. Let any linear combination e of the eigenfunctions of* (3.19),(3.17) *corresponding to $\kappa_k, \dots, \kappa_{k+l-1}$ satisfy* (3.40). *Then there exists $\varepsilon > 0$ such that there are neither critical points of* (3.39),(3.17) *nor bifurcation points of* (3.38),(3.17) *in $C_r^R(\varepsilon)$.*

Remark 3.25.
We could repeat here Corollary 3.14 for Theorem 3.20 and other theorems as well. Also Theorem 3.22 holds even in the case of periodic boundary conditions (3.17) *and it is also possible to combine Neumann and periodic boundary conditions on the boundary $\partial\Omega$.*

For our numerical experiments we consider one unilateral integral source and one sink

$$\tau\chi^M(\mathbf{x})\left(\int_K \frac{u-\overline{u}}{|K|}\,dK\right)^- - \varepsilon\chi^M(\mathbf{x})\left(\int_K \frac{u-\overline{u}}{|K|}\,dK\right)^+ \tag{3.43}$$

where $\tau, \varepsilon > 0$ and $\overline{u} = a+b$ is the first component of the constant steady state $\left[a+b, \frac{b}{(a+b)^2}\right]$ of the reaction-diffusion problem with Schnakenberg kinetics. In the analytical part of the paper we always supposed $K = M$. Here, we will make some experiments even in the case that $K \neq M$. The convergence to the stationary solution takes much more time for unilateral integral terms. Hence, we look for I_{crit} for fewer values of d_2. Also we found out that the shift of I_{crit} to the left is much smaller than in the case of unilateral terms, therefore we require that $|d_1^U - d_1^S| < 0.001$ in the definition of the critical interval I_{crit} instead of the value 0.01 we used before, to be able to recognise this shift.

In the case of Neumann boundary conditions, we tested several settings of parameters τ, ε and sets K, M. In Tables 3.5 and 3.6 we summarize computed critical intervals I_{crit} for two different values of d_2. Let us mention here that Table 3.6 with columns (v) and (vi) expands Table 3.5. One can see here that the shift of the critical interval is very small. Looking at the case (ii) (only the source) and (iii) (both the source and the sink), we can see that the shift is bigger, when we use both the source and the sink, not just the source. On the other hand taking small sets K, M does not necessarily result in smaller shift (compare (iii) and

(iv)). This make sense, because the integral does not need to be larger if we take larger sets K, M. The same apparently is true, when we increase values of τ and ε (compare (iii) and (v)). The last case (vi) is the case, where the sets K and M are different, which is the case excluded in the analytic part of this section. We can observe here the shift to the right, which is something new.

d_2	(i)	(ii)	(iii)	(iv)
600	(14.6218,14.6224)	(14.6166,14.6172)	(14.6218,14.6224)	(14.6189,14.6195)
500	(12.3099,12.3109)	(12.213,12.214)	(12.246,12.2469)	(11.9368,11.9377)

Table 3.5: Critical intervals I_{crit} in different cases for two values of d_2. (i)- the classical case (no unilateral integral terms), (ii)- the case $\tau = 0.8$, $\varepsilon = 0$, $K = M = [-20, 20]^2$, (iii)- the case $\tau = 0.8$, $\varepsilon = 0.7$, $K = M = [-20, 20]^2$, (iv)- the case $\tau = 0.8$, $\varepsilon = 0.7$, $K = M = [-10, 10]^2$.

d_2	(i)	(v)	(vi)
600	(14.6218,14.6224)	(14.6103,14.6109)	(15.5855,15.5862)
500	(12.3099,12.3109)	(12.0921,12.0931)	(13.6883,13.6891)

Table 3.6: Critical intervals I_{crit} in different cases for two values of d_2 (extension of Table 3.5). (i)- the classical case (no unilateral integral terms), (v)- the case $\tau = 1.5$, $\varepsilon = 1.2$, $K = M = [-20, 20]^2$ (vi)- the case $\tau = 0.8$, $\varepsilon = 0.7$, $K = [0, 20]^2$, $M = [-20, 0]^2$ (i.e., the case $K \neq M$).

The shape of patterns does not seem to be very influenced by unilateral integral terms. One could say that patterns are in some cases more blurry than in the classical case, but the difference is quite small. Also the case of periodic boundary conditions gives the same results as the case of Neumann boundary conditions.

3.5 | Discussion of numerical results

- Adding the unilateral source (3.33) with some non-zero τ to the activator equation of the reaction-diffusion problem results in the shift of the critical interval I_{crit} to the left (see tables in Section 5.1 and in the appendix of [Fen20]). Hence, the set of pairs $[d_1, d_2]$, for which the perturbation of the constant steady state evolves into some heterogeneous state and we can observe pattern formation, is smaller than in the classical case. The bigger is the parameter τ, the bigger is the shift to the left. Increasing the size of the set Ω_S, where the source works, has the same effect.

- If we have $\Omega_S = \Omega$ in (3.33), we do not observe any qualitatively different patterns from the classical case without any unilateral terms. However, if there is $\Omega_S \subset \Omega$, then we can observe breaking of the pattern formation on Ω_S in some cases (see, e.g., Figure 3.4).

- Adding the unilateral integral source and the sink (3.43) to the activator equation of the reaction-diffusion problem has similar effect as the unilateral source (3.33). However, this shift of I_{crit} is quite small in all studied cases and increasing the size of sets K, M and parameters τ, ε does not give significant improvement. In some cases it is even unrecognisable. Moreover, the computation is very slow in all these cases and results can be unreliable for high values of τ and ε. Hence, we conclude that in the effort to decrease the size of the set of points $[d_1, d_2]$, for which we observe instability and pattern formation, unilateral integral terms are not very suitable. Especially, considering very reliable behaviour of unilateral terms of the type ψ^-, ψ^+.

- If we consider the special case $K \neq M$ in (3.43), which does not fall under theoretical results of Section 3.4, it is possible to observe the shift of the critical interval I_{crit} to the right. This behaviour is new and was not observed in any other case of unilateral terms or unilateral integral terms in the activator equation.

- Lastly, we have observed that the problem with periodic boundary conditions gives similar results as the problem with Neumann boundary conditions. Since we consider periodic boundary conditions more natural for the pattern formation, it is suggested to use them instead of Neumann boundary conditions in future experiments.

References

[AG03] E. L. Allgower and K. Georg. *Introduction to numerical continuation methods.* SIAM Classics in Applied Mathematics, Vol. 45, Philadelphia, 2003.

[CR71] M. G. Crandall and P. H. Rabinowitz. *Bifurcation from simple eigenvalues.* J. Functional Analysis, 8:321–340, 1971.

[CR73] M. G. Crandall and P. H. Rabinowitz. *Bifurcation, perturbation of simple eigenvalues and linearized stability.* Arch. Rational Mech. Anal., 52:161–180, 1973.

[Eil86] J. C. Eilbeck. *The pseudospectral method and path following in reaction-diffusion bifurcation studies.* SIAM J. Sci. Statist. Comput., 7(2):599–610, 1986.

[EK97] J. Eisner and M. Kučera. *Spatial patterns for reaction-diffusion systems with conditions described by inclusions.* Appl. Math., 42(6):421–449, 1997.

[Fen20] M. Fencl. *An influence of unilateral sources and sinks in reaction-diffusion systems exhibiting Turing's instability on bifurcation and pattern formation.* Nonlinear Anal., 196:111815, 2020, doi:10.1016/j.na.2020.111815

[FK19] M. Fencl and M. Kučera. *Unilateral sources and sinks of an activator in reaction-diffusion systems exhibiting diffusion-driven instability.* Nonlinear Anal., 187:71–92, 2019, doi:10.1016/j.na.2019.04.001

[FLG20] M. Fencl and J. López-Gómez. *Nodal solutions of weighted indefinite problems.* Journal of Evolution Equations, 2020, published on-line at doi:10.1007/s00028-020-00625–7

[FLG21] M. Fencl and J. López-Gómez. *Global bifurcation diagrams of positive solutions for a class of 1-d superlinear indefinite problems.* arXiv:2005.09369v3 [math.AP]7Mar2021, Submitted to Nonlinearity. superlinear indefinite problems, 2021.

[GM72] A. Gierer and H. Meinhardt. *A theory of biological pattern formation.* Kybernetik, 12(1):30–39, Dec 1972.

[GRnLG00] R. Gómez-Reñasco and J. López-Gómez. *The effect of varying coefficients on the dynamics of a class of superlinear indefinite reaction-diffusion equations.* J. Differential Equations, 167(1):36–72, 2000.

[Kel86] H. B. Keller. *Lectures on Numerical Methods in Bifurcation Problems.* Tata Institute of Fundamental Research, Springer, Berlin, Germany, 1986.

[KN18] M. Kučera and J. Navrátil. *Eigenvalues and bifurcation for problems with positively homogeneous operators and reaction-diffusion systems with unilateral terms.* Nonlinear Anal., 166:154–180, 2018.

[KRE03] M. Kučera, L. Recke, and J. Eisner. *Smooth bifurcation for variational inequalities and reaction-diffusion systems.* Progress in analysis, Vol. I, II (Berlin, 2001), 1125–1133. World Sci. Publ., River Edge, NJ, 2003.

[Kuč97] M. Kučera. *Reaction-diffusion systems: stabilizing effect of conditions described by quasivariational inequalities.* Czechoslovak Math. J., 47(122)(3):469–486, 1997.

[LG88] J. López-Gómez. *Estabilidad y Bifurcación Estática. Aplicaciones y Méthodos Numéricos.* Cuadernos de Mathematica y Mechanica, Serie Cursos y Seminaros 4, Santa Fe, R. Argentina, 1988.

[LG13] J. López-Gómez. *Linear second order elliptic operators.* World Scientific Publishing Co. Pte. Ltd., Hackensack, NJ, 2013.

[LGMM05] J. López-Gómez and M. Molina-Meyer. *Bounded components of positive solutions of abstract fixed point equations: mushrooms, loops and isolas.* J. Differential Equations, 209(2):416–441, 2005.

[Mei00] Z. Mei. *Numerical bifurcation analysis for reaction-diffusion equations.* Springer Series in Computational Mathematics, Vol. 28, Springer-Verlag, Berlin, 2000.

[MNY79] M. Mimura, Y. Nishiura, and M. Yamaguti. *Some diffusive prey and predator systems and their bifurcation problems.* Ann. New York Acad. Sci., Vol. 316, 490–510, New York Acad. Sci., New York, 1979.

[Mur03] J. D. Murray. *Mathematical biology II: Spatial models and biomedical applications.* Interdisciplinary Applied Mathematics, Vol. 18, third edition, Springer-Verlag, New York, 2003.

[Nis82] Y. Nishiura. *Global structure of bifurcating solutions of some reaction-diffusion systems.* SIAM J. Math. Anal., 13(4):555–593, 1982.

[RV15] V. Rybář and T. Vejchodský. *Irregularity of Turing patterns in the Thomas model with a unilateral term.* In Programs and algorithms of numerical mathematics 17, 188–193, Acad. Sci. Czech Repub. Inst. Math., Prague, 2015.

[Sch79] J. Schnakenberg. *Simple chemical reaction systems with limit cycle behaviour.* J. Theoret. Biol., 81(3):389–400, 1979.

[Tur52] A. M. Turing. *The chemical basis of morphogenesis.* Philos. Trans. Roy. Soc. London Ser. B, 237(641):37–72, 1952.

[VJKR17] T. Vejchodský, F. Jaroš, M. Kučera, and V. Rybář. *Unilateral regulation breaks regularity of turing patterns.* Phys. Rev. E, 96:022212, Aug 2017.

Author's list of publications

- Baustian, F., Fencl, M., Pospíšil, J., Švígler, V., *A note on a PDE approach to option pricing under xVA.* arXiv:2105.00051[math.NA]30Apr2021, Submitted to Wilmott.
- Fencl, M., López-Gómez, J., *Global bifurcation diagrams of positive solutions for a class of 1-D superlinear indefinite problems.* arXiv:2005.09369v3[math.AP]7Mar2021, Submitted to Nonlinearity.
- Fencl, M., López-Gómez, J., *Nodal solutions of weighted indefinite problems.* Journal of Evolution Equations, 2020, published on-line at doi:10.1007/s00028-020-00625-7
- Fencl, M., *An influence of unilateral sources and sinks in reaction–diffusion systems exhibiting Turing's instability on bifurcation and pattern formation.* Nonlinear Analysis, Theory, Methods and Applications, 196:111815, 2020, doi:10.1016/j.na.2020.111815
- Fencl, M., Kučera, M., *Unilateral sources and sinks of an activator in reaction–diffusion systems exhibiting diffusion-driven instability.* Nonlinear Analysis, Theory, Methods and Applications, 187:71-92, 2019, doi:10.1016/j.na.2019.04.001
- Fencl, M., *Biological reaction–diffusion models.* University of West Bohemia, Faculty of Applied Sciences, Pilsen, 2016. Master thesis (supervisors Milan Kučera, Petr Tomiczek, in English).
- Fencl, M., *Populační modely v biologii a epidemiologii.* University of West Bohemia, Faculty of Applied Sciences, Pilsen, 2014. Bachelor thesis (supervisor Petr Tomiczek, in Czech).

Author's talks at conferences and seminars

- Studentská vědecká konference, Západočeská univerzita, Fakulta Aplikovaných Věd, Plzeň, 25.5.2017, *Numerical experiments in spatial patterning.*
- Matematicko–biologický seminář, Matematický Ústav Akademie Věd, Praha, 11.4.2017, *On the influence of unilateral sources on the creation of spatial patterns.*
- Matematicko–biologický seminář, Matematický Ústav Akademie Věd, Praha, 27.2.2018, *About time periodic Turing patterns.*
- Seminář matematické analýzy, Západočeská univerzita, Fakulta Aplikovaných Věd, Plzeň, 4.5.2018, *Unilateral sources of an activator in reaction-diffusion systems describing Turing's patterns.*
- XXXI. Seminar in Differential Equations, Velehrad, 2018, *Unilateral sources of an activator in reaction-diffusion systems describing Turing´s patterns.*
- Emerging Trends in Applied Mathematics and Mechanics, Krakow, 2018, *Unilateral sources of an activator in reaction-diffusion systems describing Turing´s patterns.*
- Joint meeting of the Italian Mathematical Union, the Italian Society of Industrial and Applied Mathematics and the Polish Mathematical Society, Wroclaw, 2018, *Unilateral sources and sinks of an activator in reaction-diffusion systems exhibiting Turing's diffusion-driven instability.*
- Seminář parciálních diferenciálních rovnic, Matematický Ústav Akademie Věd, Praha, 4.12.2018, *Unilateral sources and sinks of an activator in reaction–diffusion systems describing Turing's patterns.*
- Equadiff, Leiden, 2019, *Reaction-diffusion systems: an influence of unilateral terms on Turing's patterns.*

Co–author's statements

Vyjádření ke spoluautorství článku

M. Fencl, M. Kučera: Unilateral sources and sinks of an activator in reaction-diffusion systems exhibiting diffusion-driven instability, Nonlinear Analysis 187 (2019), 71-92 .

K uvedenému článku jsem předložil základní ideje a M. Fencl pak na něm pracoval samostatně s pomocí pravidelných konzultací. Můj celkový podíl nepřekročil 50%.

V Praze 12.5.2021

Milan Kučera

Análisis Matemático y
Matemática Aplicada

As the co-author of the papers

- M. Fencl, J. López-Gómez, Nodal solutions of weighted indefinite problems, Journal of Evolution Equations, published on line at https://doi.org/10.1007/s00028-020-00625-7

- M. Fencl, J. López-Gómez, Global bifurcation diagrams of positive solutions for a class of 1-D superlinear indefinite problems arXiv:2005.09369v2[math.AP]18Jan2021

I certify that Mr. Martin Fencl has done personally all numerical computations of these two papers and has collaborated, at the same level as me, in all the theoretical developments carried over in them, being imposible to know who got any particular advance.

Madrid, May 8th 2021.

Julián López-Gómez
Professor of Applied Mathematics
Associated Professor of Mathematical Analysis

A | Appendix

[FK19] M. Fencl and M. Kučera. *Unilateral sources and sinks of an activator in reaction-diffusion systems exhibiting diffusion-driven instability.* Nonlinear Anal., 187:71–92, 2019, doi:10.1016/j.na.2019.04.001

Nonlinear Analysis 187 (2019) 71–92

Contents lists available at ScienceDirect

Nonlinear Analysis

www.elsevier.com/locate/na

Unilateral sources and sinks of an activator in reaction–diffusion systems exhibiting diffusion-driven instability

Martin Fencl [a,b,*], Milan Kučera [a,c]

[a] Department of Mathematics, Faculty of Applied Sciences, University of West Bohemia, Univerzitní 8, 30100 Pilsen, Czech Republic
[b] NTIS, Faculty of Applied Sciences, University of West Bohemia, Univerzitní 8, 30100 Pilsen, Czech Republic
[c] Institute of Mathematics, Czech Academy of Sciences, Žitná 25, 11567 Prague 1, Czech Republic

ARTICLE INFO

Article history:
Received 17 July 2018
Accepted 1 April 2019
Communicated by S. Carl

MSC:
35K57
35B32
35J57
35J50
92C15

Keywords:
Reaction–diffusion systems
Unilateral terms
Turing's patterns
Positively homogeneous operators
Maximal eigenvalue

ABSTRACT

A reaction–diffusion system exhibiting Turing's diffusion driven instability is considered. The equation for an activator is supplemented by unilateral terms of the type $s_-(\mathbf{x})u^-$, $s_+(\mathbf{x})u^+$ describing sources and sinks active only if the concentration decreases below and increases above, respectively, the value of the basic spatially constant solution which is shifted to zero. We show that the domain of diffusion parameters in which spatially non-homogeneous stationary solutions can bifurcate from that constant solution is smaller than in the classical case without unilateral terms. It is a dual information to previous results stating that analogous terms in the equation for an inhibitor imply the existence of bifurcation points even in diffusion parameters for which bifurcation is excluded without unilateral sources. The case of mixed (Dirichlet–Neumann) boundary conditions as well as that of pure Neumann conditions is described.

1. Introduction

Let us consider a reaction–diffusion system

$$\begin{aligned} \frac{\partial u}{\partial t} &= d_1 \Delta u + f(u,v) + \tilde{f}_-(\mathbf{x},u^-) - \tilde{f}_+(\mathbf{x},u^+), \\ \frac{\partial v}{\partial t} &= d_2 \Delta v + g(u,v) \quad \text{in } \Omega \times [0,+\infty) \end{aligned} \tag{1}$$

where $\Omega \subset \mathbb{R}^N$ is a bounded domain with Lipschitz boundary, d_1 and d_2 are positive parameters (diffusion coefficients), $f, g : \mathbb{R} \times \mathbb{R} \to \mathbb{R}$ are real differentiable functions, $\tilde{f}_-, \tilde{f}_+ : \Omega \times \mathbb{R} \to \mathbb{R}$ are functions satisfying

* Corresponding author at: NTIS, Faculty of Applied Sciences, University of West Bohemia, Univerzitní 8, 30100 Pilsen, Czech Republic.
E-mail addresses: fenclm37@kma.zcu.cz (M. Fencl), kucera@math.cas.cz (M. Kučera).

https://doi.org/10.1016/j.na.2019.04.001
0362-546X/

Carathéodory conditions and such that there exist

$$s_-(\mathbf{x}) := \frac{\partial \tilde{f}_-}{\partial \xi}(\mathbf{x},\xi)|_{\xi=0} \geq 0, \quad s_+(\mathbf{x}) := \frac{\partial \tilde{f}_+}{\partial \xi}(\mathbf{x},\xi)|_{\xi=0} \geq 0 \quad \text{for a.a. } \mathbf{x} \in \Omega, s_\pm \in L_\infty(\Omega). \tag{2}$$

As usually, $u^+ = \max\{u,0\}$ and $u^- = \max\{-u,0\}$ denotes the positive and negative, respectively, part of u. We will always assume that

$$f(0,0) = g(0,0) = \tilde{f}_-(\mathbf{x},0) = \tilde{f}_+(\mathbf{x},0) = 0 \quad \text{for a.a. } \mathbf{x} \in \Omega. \tag{3}$$

Our system will be supplemented by boundary conditions

$$\begin{aligned} &u = v = 0 \quad \text{on } \Gamma_D, \\ &\frac{\partial u}{\partial n} = \frac{\partial v}{\partial n} = 0 \quad \text{on } \Gamma_N, \end{aligned} \tag{4}$$

where n is the unit outward-pointing normal vector of the boundary $\partial\Omega$ and Γ_N, Γ_D are open disjoint subsets of $\partial\Omega$, $\partial\Omega = \overline{\Gamma_D} \cup \overline{\Gamma_N}$.

Apparently the problem (1),(4) has always the trivial solution $[0,0]$. Our system should describe a reaction of two chemicals, e.g. morphogens, having a basic positive spatially constant steady state $[\overline{u},\overline{v}]$, that means we should assume in fact $f(\overline{u},\overline{v}) = g(\overline{v},\overline{v}) = \tilde{f}_-(\mathbf{x},\overline{u}) = \tilde{f}_+(\mathbf{x},\overline{u}) = 0$ instead of (3), but as usually, we can shift the positive steady state to zero and we obtain our system satisfying (3). Let us emphasize that then the functions u, v do not describe concentrations of the reactants, but their differences from the basic constant stationary state $[\overline{u},\overline{v}]$.

We will consider assumptions under which the problem (1),(4) with $\tilde{f}_- \equiv \tilde{f}_+ \equiv 0$ exhibits diffusion driven instability discovered in the famous Turing's paper [11]. That means if $\tilde{f}_- \equiv \tilde{f}_+ \equiv 0$ then the trivial solution $[0,0]$ is stable as a solution of the corresponding problem without diffusion (ODE's obtained for $d_1 = d_2 = 0$), but as a solution of the whole system it is unstable for $[d_1,d_2]$ from a certain subdomain D_U of the positive quadrant $\mathbb{R}^2_+$ (domain of instability), and stable only for $[d_1,d_2] \in D_S = \mathbb{R}^2_+ \setminus \overline{D_U}$ (domain of stability). Spatially non-homogeneous steady states bifurcate from the basic constant equilibrium in some points of $\overline{D_U}$, but such a bifurcation is excluded in D_S. Let us note that spatially non-homogeneous steady states can describe spatial patterns in some models in biology.

Our goal is to prove that if we add unilateral terms $\tilde{f}_-(\mathbf{x},u^-)$, $\tilde{f}_+(\mathbf{x},u^+)$, then the domain of diffusion coefficients where spatially non-homogeneous steady states can bifurcate is smaller than $\overline{D_U}$. In fact we will prove more, see below. An example of unilateral terms can be

$$\tilde{f}_-(\mathbf{x},u^-) = s_-(\mathbf{x})\frac{u^-}{1+\varepsilon u^-}, \quad \tilde{f}_+(\mathbf{x},u^+) = s_+(\mathbf{x})\frac{u^+}{1+\varepsilon u^+}.$$

The stationary system corresponding to (1) can be written in the form

$$\begin{aligned} d_1\Delta u + b_{1,1}u + b_{1,2}v + n_1(u,v) + \tilde{f}_-(\mathbf{x},u^-) - \tilde{f}_+(\mathbf{x},u^+) = 0, \\ d_2\Delta v + b_{2,1}u + b_{2,2}v + n_2(u,v) = 0, \end{aligned} \tag{5}$$

where $\mathbf{B} := (b_{i,j})_{i,j=1,2}$ is the Jacobi matrix of the mappings f, g at $[0,0]$ and the functions n_1, n_2 are higher order terms, i.e.

$$n_{1,2}(u,v) = o(|u| + |v|) \text{ as } |u| + |v| \to 0. \tag{6}$$

(The nonlinear part in the first equation could be written also in the form $s_-(\mathbf{x})u^- - s_+(\mathbf{x})u^+ + \tilde{n}_1(\mathbf{x},u,v)$, that means a homogenization + higher order terms dependent on $\mathbf{x}$).

We will always assume that the following conditions necessary for Turing's diffusion driven instability mentioned above are fulfilled:

$$b_{1,1} > 0, b_{2,2} < 0, b_{1,2}b_{2,1} < 0, tr(\mathbf{B}) < 0, det(\mathbf{B}) > 0. \tag{7}$$

The first three conditions in (7) correspond to an activator–inhibitor system (for $b_{1,2} < 0, b_{2,1} > 0$), or to a substrate depletion system (for $b_{1,2} > 0, b_{2,1} < 0$), see e.g. [9]. The last two conditions ensure the stability of $[0,0]$ as a solution of the system without any diffusion.

We will work mainly with the homogenized system

$$\begin{aligned} d_1 \Delta u + b_{1,1} u + b_{1,2} v + s_-(\mathbf{x}) u^- - s_+(\mathbf{x}) u^+ = 0, \\ d_2 \Delta v + b_{2,1} u + b_{2,2} v = 0. \end{aligned} \tag{8}$$

We will show more than what is mentioned above, namely that critical points, i.e. couples $[d_1, d_2]$ for which the homogenized problem (8), (4) has a non-trivial solution, can exist only in a smaller domain than in the classical case $\tilde{s}_- = \tilde{s}_+ \equiv 0$. Since any bifurcation point is simultaneously a critical point, the main goal mentioned above will follow. A similar result was proved in [5] for the case of unilateral sources on the boundary described by quasi-variational inequalities, but we consider the description of unilateral sources and sinks by the terms $\tilde{f}_-(\mathbf{x}, u^-)$, $\tilde{f}_+(\mathbf{x}, u^+)$ more natural. We will briefly discuss also problems with unilateral terms of the type $s_-(x)u^-$, $s_+(x)u^+$ on the boundary.

Main ideas are similar to those from [5]. Considering a weak formulation, we will write our problem as a system of operator equations in Sobolev space and we will consider an arbitrary fixed d_2. Expressing the variable v from the second equation and substituting it to the first equation, we reduce the originally non-symmetric problem to a single equation with a positively homogeneous operator having a potential. A variational characterization of its largest eigenvalue enables us to compare the largest eigenvalue corresponding to the problem with and without unilateral terms, which is simultaneously the largest d_1 for which $[d_1, d_2]$ is a critical point of the original system with and without unilateral terms.

Let us note that if unilateral sources of the second variable v (inhibitor) are supplemented in the second equation then bifurcation of spatial patterns occurs even in the domain D_S, where it is excluded for the classical case without unilateral sources. See e.g. [7] and references therein for the case of sources described by variational inequalities, [4] for unilateral sources described by multivalued maps and [3,6] for the case of unilateral terms similar to the current paper. These results motivated numerical experiments [12] showing that for a concrete model also spatial patterns arise from small initial perturbations for diffusion parameters from D_S, where it is not the case without unilateral sources. The sense of these results is positive because one of the problems of Turing's theory is that the set of diffusion parameters for which diffusion-driven instability occurs is too small, so unilateral sources for v improve this situation. The result of the current paper is opposite, unilateral sources for u make larger the set of diffusion parameters for which bifurcation of spatial patterns is excluded, i.e. for which no small spatial patterns can exist. We believe that, at least in some cases, it is a signal that the same is true for the set of parameters for which spatial patterns evolve from small perturbations of the basic spatially constant steady state. It agrees with numerical experiments which will be published in a forthcoming paper. This seems to be a negative result, but perhaps there are situations when it would be valuable to understand how to prevent evolution of spatial patterns. For instance, patterns play a role in models of tumors, see e.g. [1] and references therein. In spite of that the paper [1] has completely different goals, it can be perhaps motivating from the point of view mentioned, in particular its Section 5.

We present the basic general assumptions and definitions in Section 2. Main results of this paper are formulated and discussed in Section 3. In Section 4 we formulate our problem as a system of operator equations in Sobolev space and we describe properties of the corresponding operators. Section 5 concerns a reduction of our system to a single equation with a positively homogeneous operator and a variational characterization of its largest eigenvalue. A comparison of largest eigenvalues and consequently also critical points with and without unilateral terms by using this variational characterization is given. The proofs of the main results are done in Section 6.

2. Basic assumptions and definitions

We will always suppose that there exists $c \in \mathbb{R}$ such that

$$|n_j(\chi,\xi)| \le c(1+|\chi|^{q-1}+|\xi|^{q-1}) \quad \text{for all } \chi,\xi\in\mathbb{R}, j=1,2, \tag{9}$$

$$|\tilde{f}_{\mp}(\mathbf{x},\xi)| \le c(1+|\xi|^{q-1}) \quad \text{for all } \xi\in\mathbb{R} \text{ and a.a. } \mathbf{x}\in\Omega, \tag{10}$$

with some $q>2$ if $N=2$ or $2<q<\frac{2N}{N-2}$ if $N>2$. In the dimension $N=1$ no growth assumptions are necessary.

Besides systems (5) and (8) we will discuss systems

$$\begin{aligned} d_1\Delta u + b_{1,1}u + b_{1,2}v &= 0,\\ d_2\Delta v + b_{2,1}u + b_{2,2}v &= 0 \end{aligned} \tag{11}$$

and

$$\begin{aligned} d_1\Delta u + b_{1,1}u + b_{1,2}v + n_1(u,v) &= 0,\\ d_2\Delta v + b_{2,1}u + b_{2,2}v + n_2(u,v) &= 0. \end{aligned} \tag{12}$$

By solutions we will always mean weak solutions in the space

$$H^1_D(\Omega) := \{\phi\in W^{1,2}(\Omega) : \phi = 0 \text{ on } \Gamma_D \text{ in the sense of traces}\}. \tag{13}$$

If $\Gamma_D=\emptyset$, then the space H^1_D is actually the whole Sobolev space $W^{1,2}$ equipped with the standard inner product

$$(u,\varphi)_{H^1_D} = (u,\varphi)_{W^{1,2}} = \int_\Omega (\nabla u\nabla\varphi + u\varphi)\ d\Omega \tag{14}$$

and the Sobolev norm $\|u\|_{W^{1,2}} = \left(\int_\Omega (\nabla u)^2 + u^2\ d\Omega\right)^{\frac{1}{2}}$. If $\Gamma_D\neq\emptyset$, then we will use the inner product

$$(u,\varphi)_{H^1_D} = \int_\Omega \nabla u\nabla\varphi\ d\Omega \tag{15}$$

and the norm $\|u\|_{H^1_D} = \left(\int_\Omega (\nabla u)^2\ d\Omega\right)^{\frac{1}{2}}$ equivalent to the classical Sobolev norm.

Definition 2.1 (*Critical Point*)**.** A parameter $d=[d_1,d_2]\in\mathbb{R}^2_+$ will be called a critical point of (11),(4) or (8),(4) if there exists a non-trivial (weak) solution of (11),(4) or (8),(4), respectively.

Definition 2.2 (*Bifurcation Point*)**.** A parameter $d^0=[d^0_1,d^0_2]\in\mathbb{R}^2_+$ will be called a bifurcation point of (12),(4) or (5),(4) if in any neighborhood of $[d^0,0,0]\in\mathbb{R}^2_+\times H^1_D\times H^1_D$ there exists $[d,W]=[d,u,v]$, $\|W\|\neq 0$ satisfying (12),(4) or (5),(4), respectively.

Remark 2.1. Let us consider the problem

$$\begin{aligned} -\Delta u &= \kappa u,\\ u &= 0 \text{ on } \Gamma_D,\\ \frac{\partial u}{\partial n} &= 0 \text{ on } \Gamma_N. \end{aligned} \tag{16}$$

The eigenvalues of (16) form a non-negative non-decreasing sequence κ_j with $j=1,2,\dots$ (for $\Gamma_D\neq\emptyset$) or $j=0,1,2,\dots$ (for $\Gamma_D=\emptyset$). The first eigenvalue is always simple. In the case $\Gamma_D\neq\emptyset$, the eigenfunction e_1 corresponding to the first eigenvalue κ_1 does not change the sign on the domain Ω. In the case $\Gamma_D=\emptyset$, the eigenfunction e_0 corresponding to the first eigenvalue $\kappa_0=0$ is constant. Other eigenfunctions change the sign in both cases. We can choose an orthonormal basis e_j in H^1_D, $j=1,2,\dots$ (for $\Gamma_D\neq\emptyset$) or $j=0,1,2,\dots$ (for $\Gamma_D=\emptyset$) composed of the eigenfunctions of (16).

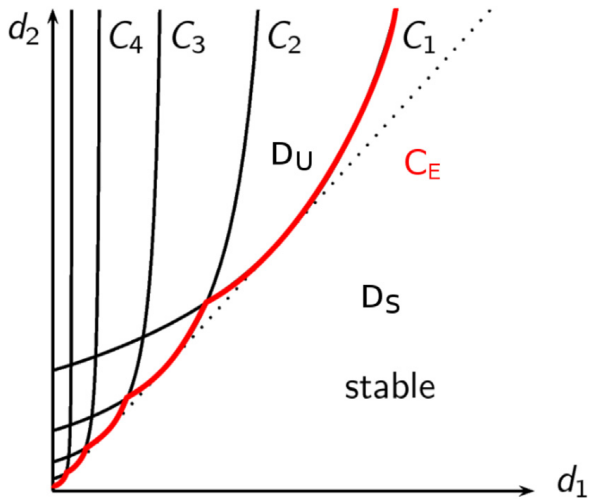

Fig. 1. Illustration of the hyperbolas C_j and the envelope C_E. The case when all eigenvalues κ_j are simple.

Let us remind that the conditions (7) are always considered. The sets

$$C_j := \left\{ [d_1, d_2] \in \mathbb{R}^2_+ : \ d_1 = \frac{1}{\kappa_j} \left(\frac{b_{1,2} b_{2,1}}{d_2 \kappa_j - b_{2,2}} + b_{1,1} \right) \right\}, \ j = 1, 2, \dots \tag{17}$$

are hyperbolas (or more specifically their parts) in the positive quadrant $\mathbb{R}^2_+$. Let us note that we present hyperbolas in the different form than usually, namely with respect to d_1. It is of course equivalent to the standard form derived from the relation

$$(\kappa_j d_1 - b_{1,1})(\kappa_j d_2 - b_{2,2}) - b_{1,2} b_{2,1} = 0$$

(see e.g. [9]). If $\Gamma_D = \emptyset$, for $j = 0$ the last equality is never satisfied, because $det(B)$ is positive by (7). The envelope

$$C_E := \left\{ d = [d_1, d_2] \in \mathbb{R}^2_+ : \ d_1 = \max_{\tilde{d}_1 \in \mathbb{R}_+} \left\{ \tilde{d}_1 : [\tilde{d}_1, d_2] \in \bigcup_{j=1}^{\infty} C_j \right\} \right\} \tag{18}$$

divides the positive quadrant $\mathbb{R}^2_+$ onto two sets D_U and D_S (see Fig. 1).

Remark 2.2. If all eigenvalues of (16) are simple, i.e. $\kappa_j < \kappa_{j+1}$ for all $j \in \mathbb{N}$, then $C_j \neq C_{j+1}$ for all $j > 0$. If an eigenvalue κ_j has a multiplicity k, then $\kappa_{j-1} < \kappa_j = \dots = \kappa_{j+k-1} < \kappa_{j+k}$ and $C_{j-1} \neq C_j = \dots = C_{j+k-1} \neq C_{j+k}$. The sets

$$D_U := \{ d = [d_1, d_2] \in \mathbb{R}^2_+ : d \text{ is on the left of } C_E \},$$
$$D_S := \{ d = [d_1, d_2] \in \mathbb{R}^2_+ : d \text{ is on the right of } C_E \}$$

are called the domain of instability and the domain of stability. It is known that if $[d_1, d_2] \in D_S$, then all eigenvalues λ of the problem deciding about stability of the trivial solution of the evolution system corresponding to (12),(4) have negative real parts and if $[d_1, d_2] \in D_U$, then there is an eigenvalue λ with positive real part (for a particular case see [8,10] and for a general case [2]). In particular, the trivial solution of (12),(4) is linearly stable for $[d_1, d_2] \in D_S$ and unstable for $[d_1, d_2] \in D_U$.

Remark 2.3. The following properties of the curves C_j are known, see e.g. [8,10] for a particular case, or [2] for the general case.

- A point $d = [d_1, d_2]$ is a critical point of (11),(4) if and only if there exists j such that $d \in C_j$. In particular, the domain of stability D_S does not contain any critical point of (11),(4) or bifurcation point of (12),(4). Under some additional assumptions, e.g. if the eigenvalue κ_j is simple or of odd multiplicity, the points on C_j are simultaneously bifurcation points (see e.g. [10]).
- If $d \in C_n$ for $n = j, \dots, j+k-1$ (either k is the multiplicity of the eigenvalue κ_j or d is in the intersection of two hyperbolas C_j, C_m and k is the sum of multiplicities of κ_j, κ_m, see Remark 2.2), then $\operatorname{span}\left(\left[\frac{d_2\kappa_j - b_{2,2}}{b_{2,1}} e_j, e_j\right]_{n=j}^{j+k-1}\right)$ is the set of the solutions of (11),(4).

3. Main results

Let us recall that the assumptions (9),(10) are automatically supposed. Besides the notions introduced in Section 2 we will use the following symbols.

Notation 3.1. Let $r, R, \varepsilon \in \mathbb{R}_+$ and $r < R$. We define
$C_r^R := \{d = [d_1, d_2] \in C_E : d_2 \in [r, R]\}$,
$C_r^R(\varepsilon) := \{d = [d_1, d_2] \in C_E \cup D_U : d_2 \in [r, R] \wedge dist(d, C_E) < \varepsilon\}$.

The following theorem is the main result of this paper.

Theorem 3.1.

(i) The domain of stability D_S contains neither critical points of (8),(4) nor bifurcation points of (5),(4).

(ii) Let $0 < r < R$. Let $C_j, \dots, C_{j+k-1}$ be all hyperbolas which have a non-empty intersection with C_r^R. Let any linear combination e of the eigenfunctions of (16) corresponding to $\kappa_j, \dots, \kappa_{j+k-1}$ satisfy

$$s_- e^- - s_+ e^+ \not\equiv 0. \tag{19}$$

Then there exists $\varepsilon > 0$ such that there are neither critical points of (8),(4) nor bifurcation points of (5),(4) in $C_r^R(\varepsilon)$.

We emphasize that if the condition (19) is not satisfied for some linear combination e mentioned, then there are critical points of (8), (4) directly on C_r^R due to Remark 2.3. Let us note that if all hyperbolas $C_j, \dots, C_{j+k-1}$ do not coincide, i.e. it is not $\kappa_j = \kappa_{j+1} = \dots = \kappa_{j+k-1}$, then the eigenfunctions $e_j, \dots, e_{j+k-1}$ do not correspond to the same eigenvalue and their linear combination need not be an eigenfunction. We discuss possible situations in the following two examples:

- First let us assume that C_r^R has a non-empty intersection with exactly two non-coinciding hyperbolas C_k and C_{k+1}. If both $e = e_k$ and $e = e_{k+1}$ satisfy (19), then there are no critical points of (8),(4) on $C_r^R \setminus (C_k \cap C_{k+1})$. However, it can happen that there is a linear combination e of e_k, e_{k+1} such that $s_- e^- - s_+ e^+ \equiv 0$, and in this case the intersection point $C_k \cap C_{k+1}$ is a critical point of (8), (4) (see also Remark 2.3).
- In another scenario we take C_r^R which consists of a part of two coinciding hyperbolas $C_k = C_{k+1}$, i.e. $\kappa_k = \kappa_{k+1}$. In this case the assumption of Theorem 3.1 (ii) means that every eigenfunction corresponding to $\kappa_k = \kappa_{k+1}$ must satisfy (19). Otherwise the critical points of (8), (4) are on the whole C_k, in particular on C_r^R (see Remark 2.3).

The result is illustrated on Fig. 2.

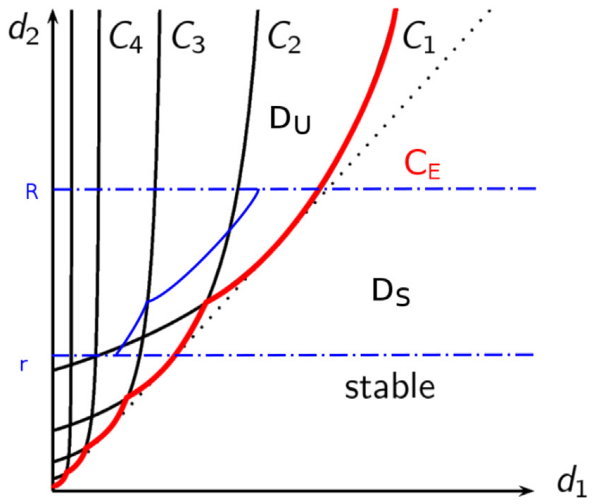

Fig. 2. Illustration of the result of Theorem 3.1. The critical points are no longer in the region between C_E (red curve) and blue curve. Assuming the case when all eigenvalues κ_j are simple, i.e. $C_j \neq C_k$ for all $k \neq j$, and any linear combination of eigenfunctions e_1, e_2 corresponding to κ_1, κ_2 satisfy (19). (For interpretation of the references to color in this figure legend, the reader is referred to the web version of this article.)

Corollary 3.1.

(i) For any compact part M of D_S there exists $\delta > 0$ such that for any $[d_1, d_2] \in M$ there are no non-trivial solutions of (5),(4) with $0 < \|u\|_{H^1_D} + \|v\|_{H^1_D} < \delta$.

(ii) Under the assumption from Theorem 3.1 (ii), for any compact part M of $D_S \cup C_r^R(\varepsilon)$ there exists $\delta > 0$ such that for any $[d_1, d_2] \in M$ there are no non-trivial solutions of (5),(4) with $0 < \|u\|_{H^1_D} + \|v\|_{H^1_D} < \delta$.

Proof. Indeed, it is easy to see that if this were not true, then a bifurcation point of (5),(4) would exist in M, which would contradict Theorem 3.1. □

There are two important particular cases for $\Gamma_D \neq \emptyset$ and $\Gamma_D = \emptyset$:

Theorem 3.2. *Let $\Gamma_D \neq \emptyset$. Let one of the functions s_+, s_- be identically zero and the other positive a.e. on Ω. Let d_2^I be the second coordinate of the intersection point of C_1 and C_2.*

(i) Any $d \in C_1$, in particular any $d \in C_r^R$ with $d_2^I \leq r < R$, is a critical point of (8),(4).

(ii) If $0 < r < R < d_2^I$, then there exists $\varepsilon > 0$ such that there are neither critical points of (8),(4) nor bifurcation points of (5),(4) in $C_r^R(\varepsilon)$.

Theorem 3.3. *Let $\Gamma_D = \emptyset$. Let one of the functions s_+, s_- be identically zero and the other positive a.e. on Ω. Then for any $0 < r < R$ there exists $\varepsilon > 0$ such that there are neither critical points of (8),(4) nor bifurcation points of (5),(4) in $C_r^R(\varepsilon)$.*

Remark 3.1. The size of ε in Theorem 3.1–3.3 depends on r and R. Actually $\varepsilon \to 0$ as $R \to d_2^I$ or $r \to 0$ in Theorem 3.2 and $\varepsilon \to 0$ as $r \to 0$ in Theorem 3.3. The following theorem states that if the source and sink are in some sense small enough, then there exists at least one critical point $[d_1, d_2] \in D_U \cup C_E$ with a given d_2. A question if sometimes (for a strong source or sink) no critical point with a given d_2 exists remains an open problem. Cf. Remark 5.5 in Section 5.

Theorem 3.4. *Let $d_2 > 0$ be arbitrary fixed. Let j_0 be such that $\left[\frac{1}{\kappa_{j_0}}\left(\frac{b_{1,2}b_{2,1}}{d_2\kappa_{j_0}-b_{2,2}}+b_{1,1}\right), d_2\right] \in C_E$ (see (17) and (18)). If $\max\{\|s_-\|_\infty, \|s_+\|_\infty\} < b_{1,1} + \frac{b_{1,2}b_{2,1}}{d_2\kappa_{j_0}-b_{2,2}}$, then there exists at least one d_1 such that $[d_1, d_2] \in D_U \cup C_E$ is a critical point of the problem (8),(4).*

The last theorem of this section is a modification of Theorem 3.1 for the case of unilateral terms in boundary conditions, namely for systems (11) and (12) with boundary conditions

$$\begin{aligned} u = v = 0 \quad &\text{on} \quad \Gamma_D, \\ \frac{\partial u}{\partial n} = s_-(\mathbf{x})u^- - s_+(\mathbf{x})u^+ \quad &\text{on} \quad \Gamma_N, \\ \frac{\partial v}{\partial n} = 0 \quad &\text{on} \quad \Gamma_N. \end{aligned} \tag{20}$$

Let us note that we consider only positively homogeneous boundary conditions because introducing more general boundary terms as $\tilde{f}_\mp$ in the case of sources and sinks in the interior of the domain would mean additional technical complications.

Theorem 3.5.

(i) The domain of stability D_S contains neither critical points of (11),(20) nor bifurcation points of (12),(20).

(ii) Let $0 < r < R$. Let $C_j, \dots, C_{j+k-1}$ be all hyperbolas which have a non-empty intersection with C_r^R. Let any linear combination e of the eigenfunctions of (16) corresponding to $\kappa_j, \dots, \kappa_{j+k-1}$ satisfy

$$s_-e^- - s_+e^+ \not\equiv 0 \quad \text{on } \Gamma_N. \tag{21}$$

Then there exists $\varepsilon > 0$ such that there are neither critical points of (11),(20) nor bifurcation points of (12),(20) in $C_r^R(\varepsilon)$.

Analogous consequence as in Corollary 3.1 can be formulated for Theorems 3.2, 3.3 and 3.5.

4. Abstract formulation

We define the operator $A : H_D^1 \mapsto H_D^1$ as

$$(Au, \varphi) = \int_\Omega u\varphi \, d\Omega \quad \text{for all } u, \varphi \in H_D^1(\Omega). \tag{22}$$

Remark 4.1. The operator A defined by (22) is linear, bounded, symmetric and compact due to compact embedding $W^{1,2} \hookrightarrow\hookrightarrow L^2$. Simple calculation gives that the eigenvalues of the operator A are $\mu_j = \frac{1}{\kappa_j}, j = 1, 2, \dots$ for $\Gamma_D \neq \emptyset$ and $\mu_j = \frac{1}{\kappa_{j+1}}, j = 0, 1, 2, \dots$ for $\Gamma_D = \emptyset$, and the corresponding eigenvectors of A coincide with the eigenfunctions e_j of (16). In particular, the maximal eigenvalue of A is always one and therefore $(Au, u) \leq \|u\|^2_{H_D^1}$, where the equality holds only for all multiples u of e_1 or e_0 if $\Gamma_D \neq \emptyset$ or $\Gamma_D = \emptyset$, respectively, see also Remark 2.1. Hence, $((I - A)u, u) > 0$ for all $u \notin span\{e_1\}$ in the case $\Gamma_D \neq \emptyset$ and for all $u \notin span\{e_0\}$ in the case $\Gamma_D = \emptyset$.

We define two non-linear operators $N_1, N_2 : H_D^1 \times H_D^1 \mapsto H_D^1$ as

$$(N_i(u, v), \varphi) = \int_\Omega n_i(u, v)\varphi \, d\Omega \quad \text{for all } u, v, \varphi \in H_D^1, \ i = 1, 2. \tag{23}$$

These two operators are well-defined and continuous due to the theorem about Nemytskii operators and the assumptions (9).

Remark 4.2. It is known that under the assumptions (6) and (9) we have

$$\lim_{\|u\|_{H^1_D}+\|v\|_{H^1_D}\to 0} \frac{N_i(u,v)}{\|u\|_{H^1_D}+\|v\|_{H^1_D}} = 0, \quad i=1,2. \tag{24}$$

For details see e.g. Appendix A.1 of [5].

Furthermore we define operators $\beta^-, \beta^+ : H^1_D \mapsto H^1_D$ by

$$(\beta^{\mp}(u),\varphi) = \mp \int_\Omega s_{\mp} u^{\mp}\varphi \, d\Omega \quad \text{for all } u,\varphi \in H^1_D \tag{25}$$

and $\beta : H^1_D \mapsto H^1_D$ as

$$\beta := \beta^+ + \beta^-. \tag{26}$$

Due to the theorem about Nemytskii operators and (10) we can also define operators $\tilde{F}_-, \tilde{F}_+ : H^1_D \mapsto H^1_D$ by

$$(\tilde{F}_{\mp}(u),\varphi) = \mp \int_\Omega \tilde{f}_{\mp}(\mathbf{x}, u^{\mp})\varphi \, d\Omega \quad \text{for all } u,\varphi \in H^1_D \tag{27}$$

and $\tilde{F} : H^1_D \mapsto H^1_D$ as

$$\tilde{F} := \tilde{F}_+ + \tilde{F}_-. \tag{28}$$

Lemma 4.1. *The operator β is positively homogeneous (i.e. $\beta(tu) = t\beta(u)$ for all $t>0, u \in H^1_D$) and*

$$\textit{(i)} \quad \exists c \in \mathbb{R} : \|\beta(u)\|_{H^1_D} \le c\|s_-\|_\infty \|u^-\|_{H^1_D} + c\|s_+\|_\infty \|u^+\|_{H^1_D} \quad \forall u \in H^1_D, \tag{29}$$

$$\textit{(ii)} \quad u_n \rightharpoonup u \implies \beta(u_n) \to \beta(u), \tag{30}$$

$$\textit{(iii)} \quad (\beta(u), u) \ge 0 \quad \forall u \in H^1_D, \tag{31}$$

$$\textit{(iv)} \quad u_n \to 0, \frac{u_n}{\|u_n\|_{H^1_D}} \rightharpoonup w \implies \frac{\tilde{F}(u_n)}{\|u_n\|_{H^1_D}} \to \beta(w). \tag{32}$$

Proof. The positive homogeneity is apparent.

(i) Using the continuous embedding $H^1_D \hookrightarrow L^2$ and Hölder's inequality we get

$$\begin{aligned}
\|\beta(u)\| &= \sup_{\|\varphi\|_{H^1_D}\le 1} |(\beta(u),\varphi)| = \sup_{\|\varphi\|_{H^1_D}\le 1} \left| \int_\Omega s_+ u^+ \varphi \, d\Omega - \int_\Omega s_- u^- \varphi \, d\Omega \right| \le \\
&\le \|s_+\|_\infty \sup_{\|\varphi\|_{H^1_D}\le 1} \left\{ \|u^+\|_{L^2} \cdot \|\varphi\|_{L^2} \right\} + \|s_-\|_\infty \sup_{\|\varphi\|_{H^1_D}\le 1} \left\{ \|u^-\|_{L^2} \cdot \|\varphi\|_{L^2} \right\} \le \\
&\le c\|s_+\|_\infty \sup_{\|\varphi\|_{H^1_D}\le 1} \left\{ \|u^+\|_{H^1_D} \cdot \|\varphi\|_{H^1_D} \right\} + c\|s_-\|_\infty \sup_{\|\varphi\|_{H^1_D}\le 1} \left\{ \|u^-\|_{H^1_D} \cdot \|\varphi\|_{H^1_D} \right\} \le \\
&\le c\|s_+\|_\infty \|u^+\|_{H^1_D} + c\|s_-\|_\infty \|u^-\|_{H^1_D}.
\end{aligned}$$

(ii) Let us have a sequence $(u_n) \subset H^1_D$ such that $u_n \rightharpoonup u \in H^1_D$. Then by the compact embedding $W^{1,2} \hookrightarrow\hookrightarrow L^2$, we get $u_n \to u$ in L^2. It is easy to see that $|u_n^- - u^-| \le |u_n - u|$ holds almost everywhere on Ω. Hence,

$$\begin{aligned}
\|\beta^-(u_n) - \beta^-(u)\|_{H^1_D} &= \sup_{\|\varphi\|_{H^1_D}\le 1} |(\beta^-(u_n) - \beta^-(u),\varphi)| \le \sup_{\|\varphi\|_{H^1_D}\le 1} \int_\Omega |u_n^- - u^-| \cdot |\varphi| \, d\Omega \le \\
&\le C\|u_n - u\|_{L^2} \to 0.
\end{aligned}$$

The same can be shown for β^+ and the assertion follows.

(iii) Let $u \in H^1_D$ be arbitrary and Ω_+, Ω_- subsets of the domain Ω such that $\Omega = \Omega_+ \cup \Omega_-$, $u \geq 0$ a.e. on Ω_+ and $u < 0$ a.e. on Ω_-. Hence

$$(\beta(u), u) = \int_\Omega s_+ u^+ u \, d\Omega - \int_\Omega s_- u^- u \, d\Omega = \int_{\Omega_+} s_+ u^2 d\Omega_+ + \int_{\Omega_-} s_- u^2 d\Omega_-$$

and our assertion follows.

(iv) Now we will define a new auxiliary operator $F : H^1_D \mapsto H^1_D$ by

$$(F(u), \varphi) = -\int_\Omega (\tilde{f}_-(\mathbf{x}, u) - s_- u)\varphi \, d\Omega \quad \text{for all } u, \varphi \in H^1_D.$$

We have

$$\lim_{\xi \to 0} \frac{\tilde{f}_-(\mathbf{x}, \xi) - s_- \xi}{\xi} = 0 \quad \text{for a.a. } \mathbf{x} \in \Omega$$

by assumption (2). The growth conditions (10) and Proposition 3.2 of [4] give

$$\lim_{u \to 0} \frac{F(u)}{\|u\|_{H^1_D}} = 0. \tag{33}$$

If $u_n \to 0$, then $u_n^- \to 0$ (see [13]) and using (33) we get

$$\lim_{n \to +\infty} \frac{\|\tilde{F}_-(u_n) - \beta^-(u_n)\|_{H^1_D}}{\|u_n\|_{H^1_D}} = \lim_{n \to +\infty} \frac{\|F(u_n^-)\|_{H^1_D}}{\|u_n\|_{H^1_D}} \leq \lim_{n \to +\infty} \frac{\|F(u_n^-)\|_{H^1_D}}{\|u_n^-\|_{H^1_D}} = 0.$$

If $u_n \to 0$, $\frac{u_n}{\|u_n\|_{H^1_D}} \rightharpoonup w$ then

$$\frac{\tilde{F}_-(u_n)}{\|u_n\|_{H^1_D}} \to \beta^-(w)$$

due to positive homogeneity of β^- and (30).

The same can be shown for $\tilde{F}_+$ and β^+ and the assertion is proved. □

In order to give an operator formulation of the problem (11) or (12) with unilateral sources and sinks on the boundary (20), we define operators $\beta_N^\pm : H^1_D \mapsto H^1_D$ as

$$(\beta_N^\mp(u), \varphi) = \mp \int_{\Gamma_N} s_\mp u^\mp \varphi \, d\Gamma_N \quad \text{for all } u, \varphi \in H^1_D \tag{34}$$

and $\beta_N : H^1_D \mapsto H^1_D$ as

$$\beta_N = \beta_N^+ + \beta_N^-. \tag{35}$$

Remark 4.3. The operator β_N possess the same properties as the operator β (see Lemma 4.1).

Let us emphasize that for cases $\Gamma_D = \emptyset$ and $\Gamma_D \neq \emptyset$ we have two different inner products and therefore operators defined above are in these two cases also different. In the case $\Gamma_D \neq \emptyset$ we consider the function space H^1_D equipped with the inner product $(u, \varphi) = \int_\Omega \nabla u \nabla \varphi \, d\Omega$. A weak solution of the problem (8),(4) or (5),(4) is then a pair of functions $u, v \in H^1_D$ satisfying

$$\begin{aligned} d_1 u - b_{1,1} A u - b_{1,2} A v + \beta(u) &= 0, \\ d_2 v - b_{2,1} A u - b_{2,2} A v &= 0 \end{aligned} \tag{36}$$

or

$$\begin{aligned} d_1u - b_{1,1}Au - b_{1,2}Av - N_1(u,v) + \tilde{F}(u) = 0,\\ d_2v - b_{2,1}Au - b_{2,2}Av - N_2(u,v) = 0, \end{aligned} \tag{37}$$

respectively.

If $\Gamma_D = \emptyset$, the function space H^1_D is identical with $W^{1,2}$ and is equipped with the inner product $(u,\varphi) = \int_\Omega (\nabla u \nabla\varphi + u\varphi)\ d\Omega$. A weak solution of (8),(4) or (5),(4) is then a pair of functions $u, v \in W^{1,2}$ satisfying

$$\begin{aligned} d_1(I-A)u - b_{1,1}Au - b_{1,2}Av + \beta(u) = \quad 0,\\ d_2(I-A)v - b_{2,1}Au - b_{2,2}Av = \quad 0 \end{aligned} \tag{38}$$

or

$$\begin{aligned} d_1(I-A)u - b_{1,1}Au - b_{1,2}Av - N_1(u,v) + \tilde{F}(u) = \quad 0,\\ d_2(I-A)v - b_{2,1}Au - b_{2,2}Av - N_2(u,v) = \quad 0, \end{aligned} \tag{39}$$

respectively.

For the problem (11),(20) or (12),(20) we will get analogous systems, we just replace operators β and $\tilde{F}$ with β_N.

5. Critical points for fixed d_2

In this section we will assume that $d_2 > 0$ is fixed and we will use the notation from Sections 2 and 4. As usually, by an eigenvalue of a positively homogeneous operator P we mean a number λ such that the equation $P(u) = \lambda u$ has a non-trivial solution. More generally, by an eigenvalue of a problem with a positively homogeneous operator we mean a parameter for which the problem under consideration has a non-trivial solution.

5.1. Reduction to one operator equation for the case $\Gamma_D \neq \emptyset$

Let us suppose $\Gamma_D \neq \emptyset$. Since the operator A is positive by Remark 4.1 and $b_{2,2} < 0$ by the assumption (7), the number $\frac{d_2}{b_{2,2}}$ is not its eigenvalue. Therefore the operator $d_2I - b_{2,2}A$ is invertible and surjective. Hence, we can express v from the second equation in (36), substitute it into the first one and get

$$d_1u - b_{1,1}Au - b_{1,2}A(d_2I - b_{2,2}A)^{-1}b_{2,1}Au + \beta(u) = 0.$$

Introducing the operator $S_{d_2} : H^1_D \mapsto H^1_D$ as

$$S_{d_2} := b_{1,1}A + b_{1,2}A(d_2I - b_{2,2}A)^{-1}b_{2,1}A, \tag{40}$$

we can write the system (36) as

$$d_1u - S_{d_2}u + \beta(u) = 0, \tag{41a}$$

$$v = (d_2I - b_{2,2}A)^{-1}b_{2,1}Au. \tag{41b}$$

In particular, the system of the operator equations

$$d_1u - S_{d_2}u = 0, \tag{42a}$$

$$v = (d_2I - b_{2,2}A)^{-1}b_{2,1}Au \tag{42b}$$

is equivalent with the system

$$\begin{aligned} d_1u - b_{1,1}Au - b_{1,2}Av = 0,\\ d_2v - b_{2,1}Au - b_{2,2}Av = 0. \end{aligned} \tag{43}$$

Remark 5.1. The operator $S_{d_2} : H^1_D \mapsto H^1_D$ defined by (40) is linear, bounded, symmetric and compact. It follows from simple calculations and Remark 4.1 that the eigenvalues of the operator S_{d_2} are

$$d_1^j = \frac{1}{\kappa_j}\left(\frac{b_{1,2}b_{2,1}}{d_2\kappa_j - b_{2,2}} + b_{1,1}\right),\ j = 1, 2, \dots \tag{44}$$

and since $\kappa_j \to \infty$ as $j \to \infty$, we get $d_1^j \to 0$ as $j \to \infty$. The eigenvectors of S_{d_2} corresponding to d_1^j coincide with those of the operator A corresponding to μ_j, i.e. with the eigenfunctions of (16) corresponding to κ_j.

5.2. Reduction to one operator equation for the case $\Gamma_D = \emptyset$

Let us consider the case $\Gamma_D = \emptyset$. It follows from Remark 4.1 that the number d_2 is not an eigenvalue of the operator $d_2A + b_{2,2}A$. Indeed, we have $d_2 \neq \frac{d_2+b_{2,2}}{\kappa_j+1}$, because $d_2\kappa_j \neq b_{2,2}$ ($b_{2,2}$ is negative by (7)). Hence, the operator $d_2I - d_2A - b_{2,2}A$ (in (38)) is surjective and invertible. Similarly as in Section 5.1 we can transform the system (38) to the system

$$d_1(I - A)u - S_{d_2}u + \beta(u) = 0, \tag{45a}$$
$$v = (d_2I - d_2A - b_{2,2}A)^{-1}b_{2,1}Au, \tag{45b}$$

with the new operator

$$S_{d_2} := b_{1,1}A + b_{1,2}A(d_2I - d_2A - b_{2,2}A)^{-1}b_{2,1}A. \tag{46}$$

In particular, the system of the operator equations

$$d_1(I - A)u - S_{d_2}u = 0, \tag{47a}$$
$$v = (d_2I - d_2A - b_{2,2}A)^{-1}b_{2,1}Au \tag{47b}$$

is equivalent with the system

$$\begin{aligned} d_1(I - A)u - b_{1,1}Au - b_{1,2}Av = 0,\\ d_2(I - A)v - b_{2,1}Au - b_{2,2}Av = 0. \end{aligned} \tag{48}$$

Remark 5.2. The operator S_{d_2} defined by (46) is linear, continuous, symmetric and compact. Simple calculations and Remark 4.1 imply that the eigenvalues of the operator S_{d_2} are

$$\lambda^j = \frac{1}{\kappa_j + 1}\left(\frac{b_{1,2}b_{2,1}}{d_2\kappa_j - b_{2,2}} + b_{1,1}\right),\ j = 0, 1, 2, \dots \tag{49}$$

and the eigenvectors of S_{d_2} corresponding to λ^j coincide with those of A corresponding to μ_j, i.e. with the eigenfunctions of (16) corresponding to κ_j. However, the eigenvalues d_1^j of the problem (47a) are the same as those of the operator S_{d_2} defined by (40) in the case $\Gamma_D \neq \emptyset$, i.e. they are given by (44). (There is no eigenvalue with $j = 0$.)

5.3. Maximal eigenvalues and critical points

Notation 5.1. We will denote by d_1^{MAX} the maximal eigenvalue of the operator S_{d_2} or of the problem (47a) in the case $\Gamma_D \neq \emptyset$ or $\Gamma_D = \emptyset$, respectively. We will also denote by $d_1^{MAX,\beta}$ the maximal eigenvalue of the operator $S_{d_2} - \beta$ or of the problem (45a) in the case $\Gamma_D \neq \emptyset$ or $\Gamma_D = \emptyset$, respectively, if it exists.

Observation 5.1. *We can see from the form (44) of the eigenvalues d_1^j (see Remarks 5.1 and 5.2) and from (17), that a point $[d_1, d_2]$ lies on a hyperbola C_j for some $j \in \mathbb{N}$ if and only if d_1 is an eigenvalue of S_{d_2} in the*

case $\Gamma_D \neq \emptyset$ or an eigenvalue of (47a) in the case $\Gamma_D = \emptyset$. For the maximal eigenvalue d_1^{MAX} of S_{d_2} in the case $\Gamma_D \neq \emptyset$ and of (47a) in the case $\Gamma_D = \emptyset$ we have $[d_1^{MAX}, d_2] \in C_E$. It follows from (44) and Remark 5.2 that the operator S_{d_2} in the case $\Gamma_D \neq \emptyset$ and the problem (47a) in the case $\Gamma_D = \emptyset$ have infinitely many positive eigenvalues and maximally finite number of negative eigenvalues. See also Fig. 1.

Lemma 5.1. *If $\Gamma_D \neq \emptyset$, then a point $[d_1, d_2] \in \mathbb{R}^2_+$ is a critical point of the system (11),(4) or (8),(4) if and only if d_1 is an eigenvalue of the operator S_{d_2} or $S_{d_2} - \beta$, respectively.*

If $\Gamma_D = \emptyset$, then a point $[d_1, d_2] \in \mathbb{R}^2_+$ is a critical point of the system (11),(4) or (8),(4) if and only if d_1 is an eigenvalue of the problem (47a) or (45a), respectively.

Proof. Let $\Gamma_D \neq \emptyset$. A point $[d_1, d_2] \in \mathbb{R}^2_+$ is a critical point of the system (11),(4) or (8),(4) if and only if there exists a non-trivial solution $[u, v]$ of (43) or (36), respectively. This is true if and only if there exists a non-trivial solution $u \in H^1_D$ of (42a) or (41a), i.e. d_1 is an eigenvalue of the operator S_{d_2} or $S_{d_2} - \beta$, respectively (see Section 5.1). The proof for the case $\Gamma_D = \emptyset$ is analogous, we only use (48), (38), (45a) and (47a) and the result of Section 5.2. □

We will use a variational characterization of the largest eigenvalue of an eigenvalue problem with a positively homogeneous operator to a study of critical points of the problem (8),(4). The following abstract theorem is a slight modification of the result proved for the particular case $L \equiv 0$ in [6] and for the general case in a forthcoming paper of J. Navrátil. Let us remind that $Ker(I-L)$ is the kernel of the operator $I-L$.

Theorem 5.1. *Let H be a Hilbert space, $P : H \mapsto H$ a positively homogeneous, continuous operator such that*

$$u_n \rightharpoonup u \implies P(u_n) \to P(u)$$

and $L : H \mapsto H$ a linear, continuous, symmetric and compact operator. In the case $L \not\equiv 0$ we suppose that the maximal eigenvalue of L is in the interval $(0, 1]$. Let there exist $u_0 \in H, u_0 \notin Ker(I - L)$ such that

$$\lambda_0 := \max_{\substack{u \in H \\ u \notin Ker(I-L)}} \frac{(P(u), u)}{((I-L)u, u)} = \frac{(P(u_0), u_0)}{((I-L)u_0, u_0)} > 0 \tag{50}$$

and

$$\lim_{t \to 0} \frac{1}{t}(P(u_0 + th) - P(u_0), u_0) = (P(u_0), h) \quad \forall h \in H. \tag{51}$$

Then λ_0 is the maximal eigenvalue of the problem

$$\lambda(I - L)u - P(u) = 0 \tag{52}$$

and u_0 is a corresponding eigenvector. If $u_1 \notin Ker(I - L)$ is an arbitrary eigenvector of (52) corresponding to λ_0 then it satisfies (50) with u_0 replaced by u_1.

Let us note that the problem (52) has an eigenvector in $Ker(I - L)$ only if there is $u \in Ker(I - L)$ such that $P(u) = 0$. In this case any λ is an eigenvalue.

Proof. We will assume that $L \not\equiv 0$, the case $L \equiv 0$ is simpler. Let us denote by μ_L^{MAX} the maximal eigenvalue of L. Since $\mu_L^{MAX} \in (0, 1]$, we have $\max_{\substack{u \neq 0 \\ \|u\|_{H^1_D} = 1}} (Lu, u) = \mu_L^{MAX} \leq 1$. If $\mu_L^{MAX} < 1$, then $(Lu, u) < 1$ and therefore $((I - L)u, u) > 0$ for all u. If $\mu_L^{MAX} = 1$, then $\max_{\substack{u \neq 0 \\ \|u\|_{H^1_D} = 1}} (Lu, u) = 1$, but the maximum is attained only in the elements of $Ker(I - A)$. Hence, $((I - L)u, u) > 0$ for all $u \notin Ker(I - L)$ and the expression in (50) makes sense.

Let $u_0 \notin Ker(I-L)$ be arbitrary such that (50) and (51) are fulfilled, and let $h \in H^1_D$ be arbitrary fixed. Then for $t \in \mathbb{R}$ small such that $(u_0+th) \notin Ker(I-L)$ we have

$$\frac{(P(u_0+th),u_0+th)}{((I-L)(u_0+th),u_0+th)} \leq \frac{(P(u_0),u_0)}{((I-L)u_0,u_0)} =: \lambda_0.$$

We can rewrite this inequality as

$$(P(u_0+th),u_0)+t(P(u_0+th),h) \leq \frac{(P(u_0),u_0)}{((I-L)u_0,u_0)}\left[((I-L)u_0,u_0)+2t((I-L)u_0,h)\right.$$
$$\left.+t^2((I-L)h,h)\right]$$

and eventually as

$$(P(u_0+th),u_0)-(P(u_0),u_0)+t(P(u_0+th),h) \leq \lambda_0\left[2t((I-L)u_0,h)+t^2((I-L)h,h)\right].$$

We divide it by $2t$ and get

$$\frac{1}{2t}\left[(P(u_0+th),u_0)-(P(u_0),u_0)\right]+\frac{1}{2}(P(u_0+th),h) \leq \lambda_0\left[((I-L)u_0,h)+\frac{t}{2}((I-L)h,h)\right], \quad t>0,$$
$$\frac{1}{2t}\left[(P(u_0+th),u_0)-(P(u_0),u_0)\right]+\frac{1}{2}(P(u_0+th),h) \geq \lambda_0\left[((I-L)u_0,h)+\frac{t}{2}((I-L)h,h)\right], \quad t<0.$$

Let $t \to 0$. We use the condition (51) and continuity of P to get

$$(P(u_0),h) \leq \lambda_0((I-L)u_0,h),$$
$$(P(u_0),h) \geq \lambda_0((I-L)u_0,h).$$

Since h was arbitrary, we have

$$(P(u_0),h) = \lambda_0((I-L)u_0,h) \quad \text{for all } h \in H^1_D,$$

that means

$$P(u_0) = \lambda_0(I-L)u_0.$$

Hence, the number λ_0 is an eigenvalue of the problem (52) and u_0 is a corresponding eigenvector.

Let λ_1 be another eigenvalue of the problem (52) and let $u_1 \notin Ker(I-L)$ be a corresponding eigenvector. Then we have

$$P(u_1) = \lambda_1(I-L)u_1$$

and if we multiply it by u_1 and divide by $((I-L)u_1,u_1)$, we get

$$\lambda_1 = \frac{(P(u_1),u_1)}{((I-L)u_1,u_1)} \leq \frac{(P(u_0),u_0)}{((I-L)u_0,u_0)} = \lambda_0.$$

Hence, λ_0 is the maximal eigenvalue. If $\lambda_1 = \lambda_0$, then we have equality in the last estimate, that means u_1 is a maximizer of the expression (50). That means an arbitrary eigenvector corresponding to λ_0 not lying in $Ker(I-L)$ satisfies (50) with u_0 replaced by u_1. □

If the condition (51) is fulfilled for any u_0, then it actually means that P has a potential $\Phi = \frac{1}{2}(Pu,u)$.

Remark 5.3. In the particular case $L \equiv 0$, $\lambda_0 := \max_{\substack{u \in H \\ u \neq o}} \frac{(P(u),u)}{\|u\|^2_H}$ is the maximal eigenvalue of P.

Theorem 5.2. *Let $\Gamma_D \neq \emptyset$ and let S_{d_2} be the operator from (40). If there exists a function $\varphi \in H^1_D$ such that*

$$(S_{d_2}\varphi, \varphi) - (\beta(\varphi), \varphi) > 0, \tag{53}$$

then the maximal eigenvalue of the operator $S_{d_2} - \beta$ is

$$d_1^{MAX,\beta} := \max_{\substack{u \in H^1_D \\ u \neq o}} \frac{(S_{d_2}u, u) - (\beta(u), u)}{\|u\|^2_{H^1_D}} = \max_{\substack{u \in H^1_D \\ \|u\|_{H^1_D} = 1}} (S_{d_2}u, u) - (\beta(u), u) > 0. \tag{54}$$

Maximizers of the expression in (54) are exactly all eigenvectors of $S_{d_2} - \beta$ corresponding to $d_1^{MAX,\beta}$.

Proof. Let us prove that the maximum in (54) exists. Let

$$M := \sup_{\substack{u \in H^1_D \\ \|u\|_{H^1_D} = 1}} (S_{d_2}u, u) - (\beta(u), u).$$

The existence of φ satisfying (53) implies $M > 0$. We can choose a sequence $(u_n) \subset H^1_D$ with $\|u_n\|_{H^1_D} = 1$ such that

$$\lim_{n\to\infty} (S_{d_2}u_n, u_n) - (\beta(u_n), u_n) = M. \tag{55}$$

We can assume $u_n \rightharpoonup u_0 \in H^1_D$. Since S_{d_2} is linear and compact and β satisfies (30), we get

$$(S_{d_2}u_n, u_n) - (\beta(u_n), u_n) \to (S_{d_2}u_0, u_0) - (\beta(u_0), u_0) = M. \tag{56}$$

Now we will show that $\|u_0\|_{H^1_D} = 1$. We know that $\|u_0\|_{H^1_D} \leq 1$. If $0 < \|u_0\|_{H^1_D} < 1$, then $\left(S_{d_2}\frac{u_0}{\|u_0\|_{H^1_D}}, \frac{u_0}{\|u_0\|_{H^1_D}}\right) - \left(\beta\left(\frac{u_0}{\|u_0\|_{H^1_D}}\right), \frac{u_0}{\|u_0\|_{H^1_D}}\right) = \frac{M}{\|u_0\|^2_{H^1_D}} > M$ due to positive homogeneity of β (see Lemma 4.1), which contradicts the fact that M is supremum. If $u_0 = 0$, then $M = 0$, which is not the case. Therefore the last maximum in (54) exists and it is attained at u_0 with $\|u_0\|_{H^1_D} = 1$. The equality between two maxima in (54) follows from the positive homogeneity of β.

It is known that $P = \beta$ and therefore also $P = S_{d_2} - \beta$ satisfies (51) for any u_0 (see Lemma A.3 in Appendix). The operator $P = S_{d_2} - \beta$ satisfies also the other assumptions of Theorem 5.1 (see Remark 5.1 and Lemma 4.1). Hence, the assertions of Theorem 5.2 follow from Theorem 5.1, where we choose $L = 0$, that means we have $Ker(I - L) = \{0\}$. □

Remark 5.4. Let us consider the case $\Gamma_D = \emptyset$. The definition of the inner product and of the operator A (Section 4) give $((I - A)u, \varphi) = \int_\Omega (\nabla u, \nabla\varphi)\, d\Omega$ for all u, φ. It follows that $(I - A)u = 0$ is equivalent to $((I - A)u, u) = 0$, and this holds if and only if u is a constant function. In other words, $Ker(I - A) = span\{e_0\}$, e_0 being the eigenfunction of (16) corresponding to κ_0. Due to Remark 5.2, any non-trivial $u_0 \in Ker(I - A)$ is simultaneously an eigenvector of S_{d_2} from (46) corresponding to λ^0. Hence, by using (7) we get

$$(S_{d_2}u_0, u_0) = (\lambda^0 u_0, u_0) = \left(b_{1,1} + \frac{b_{1,2}b_{2,1}}{-b_{2,2}}\right)\|u_0\|^2_{W^{1,2}} = \frac{-det(\mathbf{B})}{-b_{2,2}}\|u_0\|^2_{W^{1,2}} < 0. \tag{57}$$

Theorem 5.3. *Let $\Gamma_D = \emptyset$ and let S_{d_2} be the operator from (46). If there exists a function $\varphi \in W^{1,2}$ satisfying (53), then the maximal eigenvalue of the problem (45a) is*

$$d_1^{MAX,\beta} := \max_{\substack{u \in W^{1,2} \\ u \notin Ker(I-A)}} \frac{(S_{d_2}u, u) - (\beta(u), u)}{((I - A)u, u)} > 0. \tag{58}$$

Maximizers of the expression in (58) are exactly all eigenvectors of the problem (45a) corresponding to $d_1^{MAX,\beta}$.

Proof. Let us denote

$$M := \sup_{\substack{u\in W^{1,2}\\ u\notin Ker(I-A)}} \frac{(S_{d_2}u,u)-(\beta(u),u)}{((I-A)u,u)}.$$

Since $((I-A)u,u)=\int_\Omega (\nabla u)^2\ d\Omega \geq 0$ for every u and we assume that there exists a function φ satisfying (53), we have $M>0$.

We can choose a sequence $u_n \notin Ker(I-A)$ with $\|u_n\|_{W^{1,2}}=1$ such that

$$\lim_{n\to\infty} \frac{(S_{d_2}u_n,u_n)-(\beta(u_n),u_n)}{((I-A)u_n,u_n)} = M.$$

We can assume that $u_n \rightharpoonup u_0$. If $u_0=0$, then we have

$$((I-A)u_n,u_n)=1-(Au_n,u_n)\to 1-(Au_0,u_0)=1$$

due to the compactness of A, and

$$(S_{d_2}u_n,u_n)-(\beta(u_n),u_n)\to (S_{d_2}u_0,u_0)-(\beta(u_0),u_0)=0$$

by the compactness of S_{d_2} and (30). This means that $M=0$, which contradicts the positivity of M.

Further, let us show that $u_0 \notin Ker(I-A)\setminus\{0\}$, i.e. u_0 is not a constant function. Let u_0 be a non-zero constant function. Then $(S_{d_2}u_0,u_0)<0$ by Remark 5.4. Since we have $-(\beta(u),u)\leq 0$ for every u by (31), we get $(S_{d_2}u_0,u_0)-(\beta(u_0),u_0)<0$ and consequently

$$\lim_{n\to\infty} \frac{(S_{d_2}u_n,u_n)-(\beta(u_n),u_n)}{((I-A)u_n,u_n)} \leq 0.$$

That contradicts the fact that u_n is a maximizing sequence and the supremum M is positive. Hence, we have $u_0 \notin Ker(I-L)$.

We need to show that $\|u_0\|_{W^{1,2}}=1$. We already know that $0<\|u_0\|_{W^{1,2}}\leq 1$. Now let $0<\|u_0\|_{W^{1,2}}<1$. We have $1-(Au_0,u_0)>0$ (see Remark 4.1) and

$$\frac{(S_{d_2}u_n,u_n)-(\beta(u_n),u_n)}{((I-A)u_n,u_n)} \to \frac{(S_{d_2}u_0,u_0)-(\beta(u_0),u_0)}{1-(Au_0,u_0)} = M$$

by the compactness of S_{d_2}, A and the condition (30). Simultaneously $\|u_0\|^2_{W^{1,2}}-(Au_0,u_0)>0$ because of $u_0\notin Ker(I-A)$ (see Remarks 4.1 and 5.4). It follows that

$$\frac{(S_{d_2}u_0,u_0)-(\beta(u_0),u_0)}{\|u_0\|^2_{W^{1,2}}-(Au_0,u_0)} > \frac{(S_{d_2}u_0,u_0)-(\beta(u_0),u_0)}{1-(Au_0,u_0)} = M>0,$$

which contradicts that fact that M is a supremum. Hence, we have $\|u_0\|_{W^{1,2}}=1$.

We use compactness of S_{d_2}, A, the property (30) of β and the fact that $\|u_n\|_{W^{1,2}}=1=\|u_0\|_{W^{1,2}}$ to get

$$\frac{(S_{d_2}u_n,u_n)-(\beta(u_n),u_n)}{((I-A)u_n,u_n)} \to \frac{(S_{d_2}u_0,u_0)-(\beta(u_0),u_0)}{((I-A)u_0,u_0)}. \tag{59}$$

Hence, the maximum exists and it is attained at the function $u_0\notin Ker(I-A)$ with $\|u_0\|_{W^{1,2}}=1$.

It is known that $P=S_{d_2}-\beta$ satisfies (51) for any u_0 (see Lemma A.3 in Appendix). The operators $P=S_{d_2}-\beta$ and $L=A$ also satisfy the other assumptions of Theorem 5.1 (see Remark 4.1, Remark 5.2 and Lemma 4.1). Hence, $d_1^{MAX,\beta}$ is the maximal eigenvalue and u_0 is a corresponding eigenvector of the problem (45a) by Theorem 5.1.

Let us show that if u_1 is an arbitrary eigenvector of (45a) corresponding to $d_1^{MAX,\beta}$ then $u_1\notin Ker(I-A)$. If $u_1\in Ker(I-A)\setminus\{0\}$, then we have $-(S_{d_2}u_1,u_1)+(\beta(u_1),u_1)>0$ (see (57)) and Lemma 4.1 and $d_1^{MAX,\beta}((I-A)u_1,u_1)=0$, which contradicts Eq. (45a) with $u=u_1$ multiplied by u_1. Hence, $u_1\notin Ker(I-A)$, and the last assertion of Theorem 5.3 follows also from Theorem 5.1. □

Remark 5.5. The assumption (53) is clearly satisfied if there exists φ such that $(\beta(\varphi),\varphi) = 0$ and $(S_{d_2}\varphi,\varphi) > 0$, which is easier to verify. If there is no φ satisfying (53) then the supremum in proofs of Theorems 5.2 and 5.3 is not positive. It follows that there is no positive eigenvalue of the operator $S_{d_2} - \beta$ in the case $\Gamma_D \neq \emptyset$ or of the problem (45a) in the case $\Gamma_D = \emptyset$. Indeed:

- in the case $\Gamma_D \neq \emptyset$, if $d_1 > 0$ were an eigenvalue, then we would have $(S_{d_2}u,u) - (\beta(u),u) = d_1(u,u) > 0$ for the corresponding eigenvector u, which would contradict the non-positivity of the supremum.
- in the case $\Gamma_D = \emptyset$, an eigenvector u cannot be constant (see the end of the proof of Theorem 5.3), and if u were non-constant, then we would have $(S_{d_2}u,u) - (\beta(u),u) = d_1((I-A)u,u) > 0$ by the last assertion of Remark 4.1, which would be a contradiction again.

It follows that in the situation of Theorem 3.4 there exists φ satisfying (53) because that theorem guarantees the existence of a critical point in $D_U \cup C_E$ and consequently also existence of a positive eigenvalue of the operator $S_{d_2} - \beta$ in the case $\Gamma_D \neq \emptyset$ or of the problem (45a) in the case $\Gamma_D = \emptyset$ (see Sections 5.1, 5.2).

The following theorem is formulated for both cases $\Gamma_D \neq \emptyset$ and $\Gamma_D = \emptyset$.

Theorem 5.4. *If $[d_1,d_2]$ is a critical point of (8),(4), then always $d_1 \le d_1^{MAX}$. If $[d_1^{MAX},d_2] \in C_i$ exactly for $i = j,\dots,j+k-1$, all linear combinations e of $e_j,\dots,e_{j+k-1}$ satisfy (19) and $[d_1,d_2]$ is a critical point of (8),(4), then $d_1 < d_1^{MAX}$. Moreover, if the assumption (53) is satisfied, then $d_1 \le d_1^{MAX,\beta} < d_1^{MAX}$.*

The assumption concerning a position of $[d_1^{MAX},d_2]$ is fulfilled either if $[d_1^{MAX},d_2]$ lies in fact only on one hyperbola $C_j = \cdots C_{j+k-1}$ (the eigenvalue κ_j has the multiplicity k) or in the intersection of two different hyperbolas $C_j = \cdots C_{j+l-1} \neq C_{j+l} = \cdots C_{j+k-1}$ (κ_j has the multiplicity l, κ_{j+l} has the multiplicity $k-l$). See also Remark 2.2. Cf. also comments after Theorem 3.1, where the assumptions are related to a set C_r^R, while in Theorem 5.4 they concern only one point $[d_1^{MAX},d_2]$ with a given fixed d_2.

Proof. First let us consider the case $\Gamma_D \neq \emptyset$.

Let us show that if (53) were fulfilled with no φ then no critical point of (8),(4) with d_2 under consideration would exist. If $[d_1,d_2]$ were a critical point with $d_1 > 0$, then d_1 would be an eigenvalue of $S_{d_2} - \beta$ (see Lemma 5.1). Hence, we would have u with $\|u\|_{H_D^1} = 1$ satisfying (41a). It would follow that $(S_{d_2}u,u) - (\beta(u),u) = d_1\|u\|_{H_D^1} > 0$ and the condition (53) would be satisfied with $\varphi = u$, which is a contradiction.

Hence, in the following we can assume that (53) is fulfilled with some φ. Due to Theorem 5.2 and Lemma 4.1 we get

$$d_1^{MAX,\beta} = \max_{\substack{u\in H_D^1\\ u\neq o}} \frac{(S_{d_2}u,u) - (\beta(u),u)}{\|u\|^2_{H_D^1}} \le \max_{\substack{u\in H_D^1\\ u\neq o}} \frac{(S_{d_2}u,u)}{\|u\|^2_{H_D^1}} = d_1^{MAX}.$$

As above, if $[d_1,d_2]$ is a critical point (8),(4), then d_1 is an eigenvalue of $S_{d_2} - \beta$ (see Lemma 5.1). Hence, the first assertion of Theorem 5.4 is true.

There exists $u_0 \in H_D^1$ such that

$$d_1^{MAX,\beta} = \frac{(S_{d_2}u_0,u_0) - (\beta(u_0),u_0)}{\|u_0\|^2_{H_D^1}}.$$

Due to Lemma 4.1 we have

$$d_1^{MAX,\beta} \le \frac{(S_{d_2}u_0,u_0)}{\|u_0\|^2_{H_D^1}} \le d_1^{MAX}. \tag{60}$$

Let $(\beta(u_0),u_0) = 0$. Let us show that then the last inequality is strict. Indeed, if we had equality in (60), then u_0 would be an eigenvector of S_{d_2} corresponding to d_1^{MAX}, that means a linear combination

of $e_j, \dots, e_{j+k-1}$ (see Remark 5.1). Hence, (19) with e replaced by u would be fulfilled by our assumptions and we would get $(\beta(u_0), u_0) > 0$. This contradiction implies that the inequality in (60) must be strict and we get $d_1^{MAX,\beta} < d_1^{MAX}$.
If $(\beta(u_0), u_0) > 0$, then the first inequality in (60) is strict and consequently $d_1^{MAX,\beta} < d_1^{MAX}$ again.

If $[d_1, d_2]$ is a critical point of the problem (8),(4), then d_1 is an eigenvalue of $S_{d_2} - \beta$ by Lemma 5.1 and therefore

$$d_1 \le d_1^{MAX,\beta} < d_1^{MAX}.$$

The proof for $\Gamma_D = \emptyset$ is analogous, but we must use Remark 5.2 and Theorem 5.3, in particular formula (58) instead of (54). □

6. Proofs of main results

We will use notation from the previous sections.

Proof of Theorem 3.1.

(i) Since $d_2 > 0$ was arbitrary in Section 5 and $[d_1^{MAX}, d_2] \in C_E$ (see Observation 5.1), it follows from Theorem 5.4 that there are no critical points of (8),(4) in D_S (see also Fig. 1). Consequently there are also no bifurcation points of (5),(4) in D_S (see Lemma A.2 in Appendix).

(ii) Let us consider the case $\Gamma_D \neq \emptyset$. Let us suppose the opposite, i.e. the assumptions of the second part of Theorem 3.1 are satisfied and there are critical points of (8),(4) in $C_r^R(\varepsilon)$ for every $\varepsilon > 0$. We can choose a sequence $d^n = [d_1^n, d_2^n] \in D_U$ and $W_n = [u_n, v_n]$ such that $d^n \to d^0 \in C_r^R$, $\|W_n\| = \|u\|_{H_D^1} + \|v\|_{H_D^1} \neq 0$ and d^n, W_n satisfy (36). We can assume that $\frac{W_n}{\|W_n\|} \rightharpoonup W = [w, z]$. Let us divide (36) by $\|W_n\|$ to get

$$\begin{aligned} d_1^n \frac{u_n}{\|W_n\|} - b_{1,1} A \frac{u_n}{\|W_n\|} - b_{1,2} A \frac{v_n}{\|W_n\|} + \beta\left(\frac{u_n}{\|W_n\|}\right) &= 0, \\ d_2^n \frac{v_n}{\|W_n\|} - b_{2,1} A \frac{u_n}{\|W_n\|} - b_{2,2} A \frac{v_n}{\|W_n\|} &= 0. \end{aligned} \tag{61}$$

By the compactness of A and (30), we get $A\frac{u_n}{\|W_n\|} \to Aw$ and $\beta\left(\frac{u_n}{\|W_n\|}\right) \to \beta(w)$, analogously for v_n and z. Hence, it follows easily from (61) that $\frac{u_n}{\|W_n\|} \to w$, $\frac{v_n}{\|W_n\|} \to z$ and

$$\begin{aligned} d_1^0 w - b_{1,1} A w - b_{1,2} A z - \beta(w) &= 0, \\ d_2^0 z - b_{2,1} A w - b_{2,2} A z &= 0. \end{aligned}$$

Therefore the point $d^0 = [d_1^0, d_2^0] \in C_r^R$ is a critical point of the system (8),(4), which contradicts Theorem 5.4 for $d_2 = d_2^0$. Hence, there exists $\varepsilon > 0$ such that there are no critical points of (8),(4) and consequently no bifurcation points of (5),(4) in $C_r^R(\varepsilon)$ (see Lemma A.2 in Appendix).

The proof for $\Gamma_D = \emptyset$ is analogous, we only use the system (38) instead of the system (36). □

Proof of Theorem 3.2.

(i) Under the assumptions about $s_\pm$, either $e = e_1$ or $e = -e_1$ satisfies $s_- e^- - s_+ e^+ \equiv 0$. Since any point $d \in C_1$ is a critical point of the problem (11),(4) with a non-trivial solution $\left[\frac{d_2\kappa_1 - b_{2,2}}{b_{2,1}} e_1, e_1\right]$ due to Remark 2.3, it is also a critical point of the problem (8),(4).

(ii) Due to the definition of d_2^I, for $d_2 < d_2^I$ we have $[d_1^{MAX}, d_2] \in C_j$ for a finite number of indices $j > 1$ (see Section 2 and also Observation 5.1). Any linear combination e of the eigenfunctions $e_j, j > 1$ changes the sign (see Lemma A.1 in Appendix). Hence, under the assumptions of Theorem 3.2 we have $s_- e^- - s_+ e^+ \not\equiv 0$. Therefore any critical point $[d_1, d_2]$ with $d_2 < d_2^I$ of the problem (8),(4) satisfies $d_1 < d_1^{MAX}$ by Theorem 5.4. Now, it is possible to repeat the part (ii) of the proof of Theorem 3.1. □

Proof of Theorem 3.3. For any $d_2 > 0$ we have $[d_1^{MAX}, d_2] \in C_j$ for a finite number of indices $j > 0$ (see Section 2 and also Observation 5.1). Any linear combination e of the eigenfunctions $e_j, j > 0$ changes the sign (see Lemma A.1 for details), therefore the relation $s_- e^- - s_+ e^+ \not\equiv 0$ is always satisfied. Hence, any critical point $[d_1, d_2]$ of the problem (8),(4) satisfies $d_1 < d_1^{MAX}$ by Theorem 5.4. Now, it is possible to repeat the part (ii) of the proof of Theorem 3.1. □

Proof of Theorem 3.4. The assumption on j_0 directly implies that the j_0-th eigenvalue of the operator S_{d_2} in the case $\Gamma_D \neq \emptyset$ or of the problem (47a) in the case $\Gamma_D = \emptyset$ is positive (see Remarks 5.1 and 5.2 and (17),(18)). Hence, we have $(S_{d_2} e_{j_0}, e_{j_0}) > 0$, where e_{j_0} is the corresponding eigenvector. Let us denote $\tau := \max\{\|s_-\|_\infty, \|s_+\|_\infty\}$. We get

$$\begin{aligned}(S_{d_2} e_{j_0}, e_{j_0}) - (\beta(e_{j_0}), e_{j_0}) &= (S_{d_2} e_{j_0}, e_{j_0}) - \int_\Omega s_+ e_{j_0} e_{j_0}^+ \, d\Omega - \int_\Omega -s_- e_{j_0} e_{j_0}^- \, d\Omega \geq \\ &\geq (S_{d_2} e_{j_0}, e_{j_0}) - \|s_+\|_\infty \int_\Omega (e_{j_0}^+)^2 \, d\Omega - \|s_-\|_\infty \int_\Omega (e_{j_0}^-)^2 \, d\Omega \\ &\geq (S_{d_2} e_{j_0}, e_{j_0}) - \tau \left(\int_\Omega (e_{j_0}^+)^2 \, d\Omega + \int_\Omega (e_{j_0}^-)^2 \, d\Omega \right) \geq \\ &\geq (S_{d_2} e_{j_0}, e_{j_0}) - \tau (A e_{j_0}, e_{j_0}).\end{aligned}$$

Since e_{j_0} is non-trivial, we have $(A e_{j_0}, e_{j_0}) > 0$. Hence, if $\tau < \frac{(S_{d_2} e_{j_0}, e_{j_0})}{(A e_{j_0}, e_{j_0})}$, then $(S_{d_2} e_{j_0}, e_{j_0}) - (\beta(e_{j_0}), e_{j_0}) > 0$.

If $\Gamma_D \neq \emptyset$ then we get

$$\frac{(S_{d_2} e_{j_0}, e_{j_0})}{(A e_{j_0}, e_{j_0})} = \frac{\frac{1}{\kappa_{j_0}} \left(\frac{b_{1,2} b_{2,1}}{d_2 \kappa_{j_0} - b_{2,2}} + b_{1,1} \right) \|e_{j_0}\|_{H_D^1}^2}{\frac{1}{\kappa_{j_0}} \|e_{j_0}\|_{H_D^1}^2} = \frac{b_{1,2} b_{2,1}}{d_2 \kappa_{j_0} - b_{2,2}} + b_{1,1} \tag{62}$$

(see Remarks 4.1 and 5.1) and if $\Gamma_D = \emptyset$ we get

$$\frac{(S_{d_2} e_{j_0}, e_{j_0})}{(A e_{j_0}, e_{j_0})} = \frac{\frac{1}{\kappa_{j_0}+1} \left(\frac{b_{1,2} b_{2,1}}{d_2 \kappa_{j_0} - b_{2,2}} + b_{1,1} \right) \|e_{j_0}\|_{H_D^1}^2}{\frac{1}{\kappa_{j_0}+1} \|e_{j_0}\|_{H_D^1}^2} = \frac{b_{1,2} b_{2,1}}{d_2 \kappa_{j_0} - b_{2,2}} + b_{1,1}. \tag{63}$$

(see Remarks 4.1 and 5.2). Hence, if $\tau < \frac{b_{1,2} b_{2,1}}{d_2 \kappa_{j_0} - b_{2,2}} + b_{1,1}$, then the assumption (53) of Theorems 5.2 and 5.3 is satisfied with $\varphi = e_{j_0}$ and therefore $d_1^{MAX,\beta} > 0$ exists. A point $[d_1^{MAX,\beta}, d_2]$ is a critical point of (8),(4) by Lemma 5.1 and it lies in $D_U \cup C_E$ by Theorem 5.4 and because $[d_1^{MAX}, d_2] \in C_E$ (see Observation 5.1). □

Proof of Theorem 3.5. If unilateral terms in boundary conditions are considered, we replace the operators $\tilde{F}$ and β in (36)–(39) by the operator β_N, which has the same properties as β. Then it is necessary to repeat whole Section 5 for this operator. The actual proof of Theorem 3.5 is then the same as the proof of Theorem 3.1.

Acknowledgment

M.Fencl has been supported by the project SGS-2016-003 of University of West Bohemia and the project LO1506 of the Czech Ministry of Education, Youth and Sport. M. Kučera has been supported by RVO:67985840.

Appendix

For a completeness we give here proofs of two standard assertions used in the text (Lemmas A.1 and A.2), and a slightly simplified proof of a result given already in [6] (Lemma A.3).

Lemma A.1. *Any linear combination* $\sum_{k=j_0}^{n} a_k e_k, n \in \mathbb{N}$ *of eigenfunctions of* (16)*, where* $j_0 = 2$ *for* $\Gamma_D \neq \emptyset$ *and* $j_0 = 1$ *for* $\Gamma_D = \emptyset$*, changes the sign on the domain* Ω*.*

Proof.
Case $\Gamma_D = \emptyset$:

Since e_k is an orthonormal basis (see Remark 4.1) and e_0 is constant, we have

$$\int_\Omega e_0 \sum_{k=j_0}^{n} a_k e_k \, d\Omega = \sum_{k=j_0}^{n} a_k \int_\Omega e_0 e_k \, d\Omega = \sum_{k=j_0}^{n} a_k \int_\Omega (\nabla e_0 \nabla e_k + e_0 e_k) \, d\Omega = \sum_{k=j_0}^{n} a_k (e_0, e_k)_{W^{1,2}} = 0.$$

Hence, the function $e_0 \sum_{k=j_0}^{n} a_k e_k$ changes the sign on the domain Ω. Since e_0 is constant, also the function $\sum_{k=j_0}^{n} a_k e_k$ changes the sign on Ω.
Case $\Gamma_D \neq \emptyset$:

We will use the eigenfunction e_1 instead of e_0. Again since e_k is the orthonormal basis, we have

$$\int_\Omega e_1 e_k \, d\Omega = \int_\Omega -\frac{1}{\kappa_1} \Delta e_1 e_k \, d\Omega = \frac{1}{\kappa_1} \int_\Omega \nabla e_1 \nabla e_k \, d\Omega = \frac{1}{\kappa_1} (e_1, e_k)_{H^1_D} = 0 \quad \text{for any } k > 1.$$

The rest is the same as in the case $\Gamma_D = \emptyset$. □

Lemma A.2. *Every bifurcation point* $[d_1, d_2]$ *of* (5),(4) *is also a critical point of* (8),(4)*.*

Proof. We will show the proof for $\Gamma_D \neq \emptyset$. The proof for $\Gamma_D = \emptyset$ is the same, we only use the system (39) instead of the system (37).

Let $d^0 = [d_1, d_2] \in \mathbb{R}^2_+$ be a bifurcation point of (5),(4). Then there exists a sequence $d^n = [d_1^n, d_2^n]$ such that $d^n \to d^0$ and $W_n = [u_n, v_n] \to 0$ with $\|W_n\| = \|u\|_{H^1_D} + \|v\|_{H^1_D} \neq 0$ and d^n, W_n satisfy (5),(4), i.e. (37). We can assume $\frac{W_n}{\|W_n\|} \rightharpoonup W = [w, z]$. Let us divide the system (37) by $\|W_n\|$. We get

$$\begin{aligned} d_1^n \frac{u_n}{\|W_n\|} - b_{1,1} A \frac{u_n}{\|W_n\|} - b_{1,2} A \frac{v_n}{\|W_n\|} - \frac{N_1(u_n, v_n)}{\|W_n\|} + \frac{\tilde{F}(u_n)}{\|W_n\|} &= 0, \\ d_2^n \frac{v_n}{\|W_n\|} - b_{2,1} A \frac{u_n}{\|W_n\|} - b_{2,2} A \frac{v_n}{\|W_n\|} - \frac{N_2(u_n, v_n)}{\|W_n\|} &= 0 \end{aligned} \tag{64}$$

due to linearity of A. Due to (24) we have $\frac{N_j(u_n, v_n)}{\|W_n\|} \to 0$ as $n \to +\infty$ for $j = 1, 2$. Since $\frac{u_n}{\|W_n\|} \rightharpoonup w$ and $\frac{v_n}{\|W_n\|} \rightharpoonup z$, using compactness of A and (32) we get $A\frac{u_n}{\|W_n\|} \to Aw$ and $\frac{\tilde{F}(u_n)}{\|W_n\|} \to \beta(w)$, analogously for v_n and z. We have $d_1, d_2 > 0$, therefore it follows from (64) that $\frac{u_n}{\|W_n\|} \to w$, $\frac{v_n}{\|W_n\|} \to z$, $\|W\| = 1$ and

$$\begin{aligned} d_1^0 w - b_{1,1} A w - b_{1,2} A z + \beta(w) &= 0, \\ d_2^0 z - b_{2,1} A w - b_{2,2} A z &= 0. \end{aligned}$$

Therefore the point d^0 is a critical point of the system (8),(4). □

Lemma A.3 (*See [6]*)**.** *For any* $d_2 > 0$ *and* $u_0 \in H^1_D$ *the operators* $P \equiv \beta$ *and* $P \equiv S_{d_2} - \beta$ *satisfy the condition* (51)*.*

Proof.

We will prove (51) for $P = \beta^-$. The proof for β^+ is analogous and for $P \equiv S_{d_2} - \beta$ it will follow by using the definition of β and linearity of S_{d_2}.

Let $u_0, h \in H^1_D$. We will introduce two sets Ω_0 and Ω_{th} such that

$$u_0(\mathbf{x}) < 0 \text{ a.e. on } \Omega_0, \quad u_0(\mathbf{x}) \geq 0 \text{ a.e. on } \Omega \setminus \Omega_0,$$
$$u_0(\mathbf{x}) + th(\mathbf{x}) < 0 \text{ a.e. on } \Omega_{th}, \quad u_0(\mathbf{x}) + th(\mathbf{x}) \geq 0 \text{ a.e. on } \Omega \setminus \Omega_{th}.$$

Then

$$\begin{aligned}\frac{1}{t}(\beta^-(u_0 + th) - \beta^-(u_0), u_0) - (\beta^-(u_0), h) = \\ = \frac{1}{t}\left[\int_\Omega -(u_0 + th)^- u_0 + u_0 u_0^- \, d\Omega\right] - \int_\Omega -u_0^- h \, d\Omega = \\ = \frac{1}{t}\left[\int_{\Omega_{th}} (u_0 + th) u_0 \, d\Omega_{th} - \int_{\Omega_0} u_0^2 \, d\Omega_0\right] - \int_{\Omega_0} u_0 h \, d\Omega_0 = \\ = \frac{1}{t}\left[\int_{\Omega_{th}} u_0^2 \, d\Omega_{th} - \int_{\Omega_0} u_0^2 \, d\Omega_0\right] + \int_{\Omega_{th}} u_0 h \, d\Omega_{th} - \int_{\Omega_0} u_0 h \, d\Omega_0.\end{aligned}$$

We can afford to work with the definition of β^- without s_-, because it is non-negative, i.e. it does not affect the sign of terms under integration.

Let χ_{th} and χ_0 be the characteristic function of Ω_{th} and Ω_0, respectively. We have

$$\lim_{t\to 0} \int_{\Omega_{th}} u_0 h \, d\Omega_{th} = \lim_{t\to 0} \int_\Omega u_0 h \chi_{th} \, d\Omega = \int_\Omega u_0 h \chi_0 \, d\Omega = \int_{\Omega_0} u_0 h \, d\Omega_0$$

by Dominated Convergence theorem. Let us introduce sets $\Omega_{th1}, \Omega_{th2}, \Omega_{th3}$ such that

$$u_0(\mathbf{x}) < -th(\mathbf{x}) \text{ and } u_0(\mathbf{x}) < 0 \text{ almost everywhere on } \Omega_{th1},$$
$$u_0(\mathbf{x}) < -th(\mathbf{x}) \text{ and } u_0(\mathbf{x}) \geq 0 \text{ almost everywhere on } \Omega_{th2},$$
$$u_0(\mathbf{x}) \geq -th(\mathbf{x}) \text{ and } u_0(\mathbf{x}) < 0 \text{ almost everywhere on } \Omega_{th3},$$

with $\Omega_{th} = \Omega_{th1} \cup \Omega_{th2}$ and $\Omega_0 = \Omega_{th1} \cup \Omega_{th3}$. This way we get

$$\begin{aligned}\int_{\Omega_{th}} u_0^2 \, d\Omega_{th} - \int_{\Omega_0} u_0^2 \, d\Omega_0 = \int_{\Omega_{th1}} u_0^2 \, d\Omega_{th1} + \int_{\Omega_{th2}} u_0^2 \, d\Omega_{th2} - \int_{\Omega_{th1}} u_0^2 \, d\Omega_{th1} - \int_{\Omega_{th3}} u_0^2 \, d\Omega_{th3} = \\ = \int_{\Omega_{th2}} u_0^2 \, d\Omega_{th2} - \int_{\Omega_{th3}} u_0^2 \, d\Omega_{th3}.\end{aligned}$$

Since $0 \leq u_0 < -th$ a.e. on Ω_{th2} and $0 > u_0 \geq -th$ a.e. on Ω_{th3}, we get

$$\lim_{t\to 0} \frac{1}{t}\left(\int_{\Omega_{th2}} u_0^2 \, d\Omega_{th2} - \int_{\Omega_{th3}} u_0^2 \, d\Omega_{th3}\right) \leq \lim_{t\to 0} \frac{1}{t}\left(\int_{\Omega_{th2}} (th)^2 \, d\Omega_{th2} - \int_{\Omega_{th3}} (th)^2 \, d\Omega_{th3}\right) = 0.$$

Hence, it follows from the discussion above that

$$\lim_{t\to 0} \frac{1}{t}(\beta^-(u_0 + th) - \beta^-(u_0), u_0) - (\beta^-(u_0), h) = 0$$

which proves (51) for β^-. □

References

[1] M.A.J. Chaplain, M. Ganesh, I.G. Graham, Spatio-temporal pattern formation on spherical surfaces: numerical simulation and application to solid tumour growth, J. Math. Biol. 42 (2001) 387–423.
[2] J. Eisner, M. Kučera, Spatial patterns for reaction–diffusion systems with conditions described by inclusions, Appl. Math. 42 (6) (1997) 421–449.
[3] J. Eisner, M. Kučera, Bifurcation of solutions to reaction–diffusion systems with jumping nonlinearities, in: A. Sequeira, H. Beirao da Veiga, J.H. Videman (Eds.), Applied Nonlinear Analysis, Kluwer Academic/Plenum Publishers, New York, 1999, pp. 79–96.
[4] J. Eisner, M. Kučera, M. Väth, Degree and global bifurcation for elliptic equations with multivalued unilateral conditions, Nonlinear Anal. 64 (2006) 1710–1736.
[5] M. Kučera, Reaction–diffusion systems: stabilizing effect of conditions described by quasivariational inequalities, Czechoslovak Math. J. 47 (122) (1997) 469–486.
[6] M. Kučera, J. Navrátil, Eigenvalues and bifurcation for problems with positively homogeneous operators and reaction–diffusion systems with unilateral terms, Nonlinear Anal. 166 (2018) 154–180.
[7] M. Kučera, M. Väth, Bifurcation for a reaction–diffusion system with unilateral and Neumann boundary conditions, J. Differential Equations 252 (2012) 2951–2982.
[8] M. Mimura, Y. Nishiura, M. Yamaguti, Some diffusive prey and predator systems and their bifurcation problems, Ann. New York Acad. Sci. 316 (1979) 490–510.
[9] J.D. Murray, Mathematical Biology II: Spatial Models and Biomedical Applications, Interdisciplinary Applied Mathematics, Vol. 18, third ed., Springer-Verlag, New York, 2003.
[10] Y. Nishiura, Global structure of bifurcating solutions of some reaction–diffusion systems, SIAM J. Math. Anal. 13 (1982) 555–593.
[11] A.M. Turing, The chemical basis of morphogenesis, Phil. Trans. R. Soc. B 237 (1952) 37–72.
[12] T. Vejchodský, F. Jaroš, M. Kučera, V. Rybář, Unilateral regulation breaks regularity of turing patterns, Phys. Rev. E 96 (2017) 022212.
[13] W.P. Ziemer, Weakly Differentiable Functions: Sobolev Spaces and Functions of Bounded Variation, Graduate Texts in Mathematics, Vol. 120, Springer-Verlag, New York, 1989.

B | Appendix

[Fen20] M. Fencl. *An influence of unilateral sources and sinks in reaction-diffusion systems exhibiting Turing's instability on bifurcation and pattern formation.* Nonlinear Anal., 196:111815, 2020, doi:10.1016/j.na.2020.111815

Nonlinear Analysis 196 (2020) 111815

Contents lists available at ScienceDirect

Nonlinear Analysis

www.elsevier.com/locate/na

An influence of unilateral sources and sinks in reaction–diffusion systems exhibiting Turing's instability on bifurcation and pattern formation

Martin Fencl

Department of Mathematics and NTIS, Faculty of Applied Sciences, University of West Bohemia, Pilsen, Univerzitní 8, 30100 Plzeň, Czech Republic

ARTICLE INFO

Article history:
Received 4 September 2019
Accepted 12 February 2020
Communicated by Vicentiu D. Radulescu

MSC:
35B32, 35B36, 35J57, 35K57, 65M99

Keywords:
Reaction–diffusion systems
Pattern formation
Turing's instability
Unilateral integral terms
Numerical experiments

ABSTRACT

We consider a general reaction–diffusion system exhibiting Turing's diffusion-driven instability. In the first part of the paper, we supplement the activator equation by unilateral integral sources and sinks of the type $\left(\int_K \frac{u(x)}{|K|}\,dK\right)^-$ and $\left(\int_K \frac{u(x)}{|K|}\,dK\right)^+$. These terms measure an average of the concentration over the set K and are active only when this average decreases below or increases above the value of the reference spatially homogeneous steady state, which is shifted to the origin. We show that the set of diffusion parameters in which spatially heterogeneous stationary solutions can bifurcate from the reference state is smaller than in the classical case without any unilateral integral terms. This problem is studied for the case of mixed, pure Neumann and periodic boundary conditions. In the second part of the paper, we investigate the effect of both unilateral terms of the type u^-, u^+ and unilateral integral terms on the pattern formation using numerical experiments on the system with well-known Schnakenberg kinetics.

1. Introduction

In 1952 Alan M. Turing wrote his paper "*The Chemical Basis of Morphogenesis*" [23] on biological pattern formation, in which he described that a reaction of two chemicals and diffusion in the space can lead to the production of a spatially heterogeneous structure. That means, the spatially homogeneous steady state of the system, that is stable in the absence of diffusion, could be destabilized by diffusion and produce a spatially heterogeneous state, in other words a "pattern". This behaviour is quite counter-intuitive since diffusion is usually perceived as a stabilization effect. Twenty years later, Gierer and Meinhardt published their paper [6], in which they analysed this problem in more detail and introduced so called "short range activation-long range inhibition" mechanism. Their research was completely independent, because they did not know about Turing's paper. A lot of work has been done in this area in past few decades. This effect

E-mail address: fenclm37@kma.zcu.cz.

https://doi.org/10.1016/j.na.2020.111815
0362-546X/

is usually called Turing's instability, Turing's effect or diffusion-driven instability (diffusion "drives" stable homogeneous state unstable). The theory is very thoroughly summarized e.g., in the second instalment of J.D. Murray's "*Mathematical biology*" [16].

A pattern formation is not a process exclusive to reaction–diffusion equations, but they are one of the most common models for pattern formation problems. We consider a classical system of two reaction–diffusion equations

$$\begin{aligned} \frac{\partial u}{\partial t} &= d_1 \Delta u + f(u,v), \\ \frac{\partial v}{\partial t} &= d_2 \Delta v + g(u,v), \end{aligned} \tag{1}$$

with functions $u = u(x,t), v = v(x,t)$ describing concentrations of some chemicals and f, g being reaction kinetics as our starting point.

The idea of Turing's instability is not perfect and one of problems it suffers is the strict requirement that diffusion coefficients must be different. Actually, for the most usual reaction kinetics this difference must be significant. The fact that one chemical diffuses with very different intensity than the other is not very realistic in many problems. There were efforts to modify or generalize the idea of Turing's instability. For example Rovinsky and Menzinger presented so called differential-flow-induced chemical instability [14] in the system, in which one of the chemicals is immobilized and the other diffuses and flows. This idea leads to a similar destabilization as by Turing's DDI. This mechanism was experimentally verified on Belousov–Zhabotinsky reaction (see [19]). Their work later inspired Klika et al. [7] to add advection to the complete reaction–diffusion system (no immobilized chemical). They were able to show that, even if diffusion coefficients are equal, the homogeneous steady state can be destabilized utilizing relatively small amount of advection.

Several authors focused on the analysis of the bifurcation during the destabilization of the spatially homogeneous steady state and bifurcating patterns. The set of couples of diffusion parameters, such that the reference steady state is stable or unstable, is usually denoted D_S or D_U, respectively, in following papers. Kučera et al. studied unilateral conditions related to the inhibitor equation (the equation for the chemical that is inhibiting its production) and some of these results were first mentioned in [9]. The abstract result for variational inequalities concerning destabilization of the reference spatially homogeneous steady state was shown in [2] and the influence of unilateral conditions on bifurcation of patterns was revealed in [3]. There were also other papers concerning similar problems e.g., [1,4,12,18]. It is known that in the classical case the bifurcation from the reference steady state is excluded in D_S. However, if unilateral conditions are present in boundary conditions for the inhibitor equation, this bifurcation exists under some conditions. Hence, the set of couples of diffusion parameters, for which the bifurcation occurs and a bifurcating pattern exists, is larger than in the classical case without unilateral conditions. It was natural to ask, what effect will have unilateral conditions related to the activator equation (the equation for the chemical that is activating its production). The problem was explored in [8] and it was shown that the effect is exactly opposite, i.e., the set of couples of diffusion parameters, for which the bifurcation occurs and a bifurcating pattern exists, is smaller than in the classical case without unilateral conditions.

Later, the idea of unilateral conditions and variational inequalities was replaced by the idea of adding unilateral sources and sinks to the activator equation (see [5]) or to the inhibitor equation (see [10]), respectively. The unilateral source or sink is based on the negative part $\psi^- = \max\{-\psi, 0\}$ or the positive part $-\psi^+ = -\max\{\psi, 0\}$ of the function ψ, respectively (ψ represents the variable of an activator or an inhibitor). These terms act in the interior of the domain and they seem to be more natural than unilateral conditions given by variational inequalities. Unilateral terms cannot be linearized and the study of the stability is difficult and so far an open problem. Therefore only bifurcations were studied in these papers. It was again shown that if there are unilateral terms in the inhibitor equation, then the set of couples of diffusion parameters, for which the bifurcation occurs and a bifurcating pattern exists, is larger than in the classical case without unilateral terms. The case with unilateral terms in the activator equation again

brings opposite results. There were performed many numerical experiments in [24] and [20] for the case of the unilateral source τv^- (and its modifications) in the inhibitor equation for the specific reaction kinetics.

In our paper we will investigate the impact of unilateral terms involving the integral average over some subset of the domain Ω, where we will work. To put it in the context with the previous work mentioned above, for example we had the unilateral source $s_-(x)\frac{\psi^-}{1+\psi^-}$ in our paper [5]. This term measures exactly the value of ψ in each point x of Ω and if the value drops under certain threshold (in this case the zero), then the production of ψ is switched on locally on the support of $s_-(x)$. One simple example of unilateral terms we introduce in this paper is

$$\chi^K(x)\left(\int_K \frac{\psi(x)}{|K|}\,dK\right)^-,$$

where K is a subset of the domain Ω and $\chi^K(x)$ is the characteristic function of the set K. We denote by $|K|$ the Lebesgue measure of the set K. This term measures the average of ψ over the set K and if this average drops below the threshold (again in this case the zero), then the source is switched on and is acting again on the set K.

We will work with more general terms e.g., several sources (and sinks) and we will correctly describe properties of K, Ω etc. later. Our inspiration is partially papers about unilateral terms mentioned above and also [11], in which integral terms are used in some sense in boundary conditions.

We consider the reaction–diffusion system

$$\begin{aligned}
\frac{\partial u}{\partial t} &= d_1\Delta u + f(u,v) + \sum_{i=1}^{n}\chi^{M_i^-}(x)f_-^i\left(\left(\int_{K_i^-}\frac{u-\overline{u}}{|K_i^-|}\,dK_i^-\right)^-\right) - \sum_{j=1}^{m}\chi^{M_j^+}(x)f_+^j\left(\left(\int_{K_j^+}\frac{u-\overline{u}}{|K_j^+|}\,dK_j^+\right)^+\right),\\
\frac{\partial v}{\partial t} &= d_2\Delta v + g(u,v) \quad \text{in } \Omega\times[0,+\infty)
\end{aligned} \tag{2}$$

where $\Omega\subset\mathbb{R}^N$ is a bounded domain with Lipschitz boundary, d_1 and d_2 are positive diffusion parameters, $f,g:\mathbb{R}\times\mathbb{R}\to\mathbb{R}$ are real differentiable functions and there exist constants $\overline{u},\overline{v}>0$ such that

$$f(\overline{u},\overline{v}) = g(\overline{u},\overline{v}) = 0, \tag{3}$$

i.e., $[\overline{u},\overline{v}]$ is a spatially homogeneous steady state. Furthermore we assume that $f_-^i, f_+^j : \mathbb{R}\to\mathbb{R}$ are real functions such that

$$f_-^i(0) = f_+^j(0) = 0 \quad \text{for every } i=1,\dots,n, j=1,\dots,m, \tag{4}$$

and there exist

$$\tau_-^i := \frac{\partial f_-^i}{\partial\xi}(\xi)|_{\xi=0}\in\mathbb{R}_0^+, \quad \tau_+^j := \frac{\partial f_+^j}{\partial\xi}(\xi)|_{\xi=0}\in\mathbb{R}_0^+ \quad \text{for all } i=1,\dots,n, j=1,\dots,m. \tag{5}$$

We suppose that $K_i^-, K_j^+\subseteq\Omega$ and functions $\chi^{K_i^-}(x)$ and $\chi^{K_j^+}(x)$ are characteristic functions of sets K_i^- and K_j^+, respectively. We will assume that sets K_i^- are connected and disjoint. The same is assumed for sets K_j^+.

The system (2) will be completed by boundary conditions

$$\begin{aligned}
u = \overline{u}, v = \overline{v} \quad &\text{on } \Gamma_D,\\
\frac{\partial u}{\partial n} = \frac{\partial v}{\partial n} = 0 \quad &\text{on } \Gamma_N,
\end{aligned} \tag{6}$$

where n is a unit out-ward pointing normal vector of the boundary $\partial\Omega$ and Γ_D, Γ_N are open disjoint subsets of $\partial\Omega$ such that $\partial\Omega = \overline{\Gamma_D}\cup\overline{\Gamma_N}$. We will distinguish two cases $\Gamma_D\neq\emptyset$, i.e., mixed boundary conditions, and $\Gamma_D=\emptyset$, i.e., pure Neumann boundary conditions. The case of pure Dirichlet boundary conditions is included in the case $\Gamma_D\neq\emptyset$ and we do not treat it separately, because the analysis and the results are the

same. We will also discuss problems with unilateral integral terms in boundary conditions as well as the case of periodic boundary conditions

$$\begin{aligned} u(\mathbf{x}) &= u(\mathbf{x}_P), \\ -\frac{\partial u}{\partial n}(\mathbf{x}) &= \frac{\partial u}{\partial n}(\mathbf{x}_P), \end{aligned} \tag{7}$$

on special domains. We will describe this case in more detail in the next section.

Our goal is to show that we can get similar results concerning bifurcations for reaction–diffusion systems with unilateral integral terms as we did for unilateral terms without integral in the activator equation in [5]. Hence, the set of couples of diffusion parameters, for which the bifurcation occurs and a bifurcating pattern exists, is smaller than in the classical case. In the second part of the paper we use numerical experiments to investigate the influence of unilateral terms from [5] and unilateral integral terms presented in this paper on the pattern formation. We study the case of Neumann and periodic boundary conditions on the square domain Ω and we use well-known Schnakenberg kinetics as functions f and g. The goal is to study the shape of patterns, to compare Neumann and periodic boundary conditions and to show that with increasing strength of unilateral (integral) terms the set of $[d_1, d_2]$ such that patterns are produced and the spatially homogeneous steady state seems to be unstable is getting smaller.

Main ideas are in some sense similar to those in [5] and [8]. We will take the stationary problem of the reaction–diffusion system (2), (6) and rewrite it into the weak formulation in Sobolev space and further to the system of operator equations. Then we will extract the variable v from the second equation and substitute it to the first one. This way the system of operator equation will be reduced to a single operator equation. In the paper [5] we used a variational characterization of the maximal eigenvalue. However, in this case it is not possible. Therefore, we will use different, maybe more simple, approach to get our results, similar to the one in [8]. The numerical experiments are inspired by analytical results from [5] and this paper in some sense follows the paper [24].

The text is divided in the following manner. Section 2 consists of essential definitions, general assumptions and the summary of important known facts. We formulate our main results in Section 3. In Section 4 we define operators and prove their properties and in Section 5 we reduce our system to a single operator equation and present proofs of theorems from Section 3. Section 6 concerns numerical experiments.

2. Turing's instability, basic assumptions and periodic boundary conditions

It is possible without the loss of generality to shift the reference spatially homogeneous steady state $[\overline{u}, \overline{v}]$ to the origin for the sake of simpler analysis. Therefore we will assume from the start that $[\overline{u}, \overline{v}] = [0, 0]$. In such case, functions u and v do not describe concentrations of the chemicals, but rather the difference of these concentrations from the original positive reference steady state $[\overline{u}, \overline{v}]$. Hence, our boundary conditions (6) are transformed to

$$\begin{aligned} u = v &= 0 \quad \text{on } \Gamma_D, \\ \frac{\partial u}{\partial n} = \frac{\partial v}{\partial n} &= 0 \quad \text{on } \Gamma_N. \end{aligned} \tag{8}$$

Remark 2.1. By solutions we will mean weak solutions usually in the space

$$H^1_D(\Omega) := \{\phi \in W^{1,2}(\Omega) : \phi = 0 \text{ on } \Gamma_D \text{ in the sense of traces}\}. \tag{9}$$

If $\Gamma_D = \emptyset$, then the space H^1_D is actually the whole Sobolev space $W^{1,2}$ equipped with the standard inner product

$$(u, \varphi)_{H^1_D} = (u, \varphi)_{W^{1,2}} = \int_\Omega (\nabla u \nabla \varphi + u\varphi) \ d\Omega \tag{10}$$

and the Sobolev norm $\|u\|_{W^{1,2}} = \left(\int_\Omega (\nabla u)^2 + u^2 \ d\Omega\right)^{\frac{1}{2}}$. If $\Gamma_D \neq \emptyset$, then we will use the inner product

$$(u, \varphi)_{H^1_D} = \int_\Omega \nabla u \nabla \varphi \ d\Omega \tag{11}$$

and the norm $\|u\|_{H^1_D} = \left(\int_\Omega (\nabla u)^2 \ d\Omega\right)^{\frac{1}{2}}$ equivalent to the classical Sobolev norm.

We will now define the functional $T_X^{\mp} : H_D^1 \to \mathbb{R}_0^+$ by

$$T_X^{\mp}(\psi) = \left(\int_X \frac{\psi}{|X|}\, dX \right)^{\mp}, \tag{12}$$

where X is some subset of Ω. It will allow us to write many upcoming formulas in more compact way.

We can write stationary system corresponding to the system (2) and to the classical system without unilateral integral terms (1) as

$$\begin{aligned} 0 &= d_1 \Delta u + b_{1,1} u + b_{1,2} v + n_1(u,v) + \sum_{i=1}^{n} \chi^{K_i^-}(x) f_-^i \left(T^-_{K_i^-}(u) \right) - \sum_{j=1}^{m} \chi^{K_j^+}(x) f_+^j \left(T^+_{K_j^+}(u) \right), \\ 0 &= d_2 \Delta v + b_{2,1} u + b_{2,2} v + n_2(u,v), \end{aligned} \tag{13}$$

and

$$\begin{aligned} 0 &= d_1 \Delta u + b_{1,1} u + b_{1,2} v + n_1(u,v), \\ 0 &= d_2 \Delta v + b_{2,1} u + b_{2,2} v + n_2(u,v), \end{aligned} \tag{14}$$

respectively, where $b_{i,j}, i,j = 1,2$ are elements of Jacobi matrix of mappings f, g at $[0,0]$ and n_1, n_2 are higher order terms, i.e.,

$$n_{1,2}(u,v) = o(|u| + |v|) \text{ as } |u| + |v| \to 0. \tag{15}$$

We will always assume that the following set of inequalities is satisfied:

$$b_{1,1} + b_{2,2} < 0,\ b_{1,1} b_{2,2} - b_{1,2} b_{2,1} > 0,\ b_{1,1} > 0,\ b_{2,2} < 0,\ b_{1,2} b_{2,1} < 0. \tag{16}$$

The first two conditions of (16) guarantee that the reference steady state is stable as a solution of the classical system in the absence of diffusion. The third and fourth conditions correspond to the fact that we expect that the first equation of the system (2) is the activator equation while the second one is the inhibitor equation. The last condition decides whether the system is in activator–inhibitor form (for $b_{1,2} < 0$, $b_{2,1} > 0$) or substrate-depletion form (for $b_{1,2} > 0$, $b_{2,1} < 0$) as was specified in [6].

Further we will suppose that there exists $c \in \mathbb{R}$ such that

$$|n_j(\chi, \xi)| \le c(1 + |\chi|^{q-1} + |\xi|^{q-1}) \quad \text{for all } \chi, \xi \in \mathbb{R},\ j = 1,2, \tag{17}$$

with some $q > 2$ if $N = 2$ or $2 < q < \frac{2N}{N-2}$ if $N > 2$. In the dimension $N = 1$ no growth assumptions are necessary.

We can homogenize the system (13) and linearize the classical system (14) to get

$$\begin{aligned} 0 &= d_1 \Delta u + b_{1,1} u + b_{1,2} v + \sum_{i=1}^{n} \chi^{K_i^-}(x) \tau_-^i T^-_{K_i^-}(u) - \sum_{j=1}^{m} \chi^{K_j^+}(x) \tau_+^j T^+_{K_j^+}(u), \\ 0 &= d_2 \Delta v + b_{2,1} u + b_{2,2} v, \end{aligned} \tag{18}$$

and

$$\begin{aligned} 0 &= d_1 \Delta u + b_{1,1} u + b_{1,2} v, \\ 0 &= d_2 \Delta v + b_{2,1} u + b_{2,2} v. \end{aligned} \tag{19}$$

Definition 2.1 (*Critical Point*)**.** A parameter $d = [d_1, d_2] \in \mathbb{R}_+^2$ will be called a critical point of (19), (8) or (18), (8) if there exists a non-trivial (weak) solution of (19), (8) or (18), (8), respectively.

Definition 2.2 (*Bifurcation Point*)**.** A parameter $d^0 = [d_1^0, d_2^0] \in \mathbb{R}_+^2$ will be called a bifurcation point of (14), (8) or (13), (8) if in any neighbourhood of $[d^0, 0, 0] \in \mathbb{R}_+^2 \times H_D^1 \times H_D^1$ there exists $[d, W] = [d, u, v]$, $\|W\| \neq 0$ satisfying (14), (8) or (13), (8), respectively.

Remark 2.2. Let us consider the problem

$$\begin{aligned} -\Delta u &= \kappa u, \\ u &= 0 \text{ on } \Gamma_D, \\ \frac{\partial u}{\partial n} &= 0 \text{ on } \Gamma_N. \end{aligned} \tag{20}$$

The eigenvalues of (20) form a non-negative non-decreasing sequence κ_k with $k = 1, 2, \dots$ (for $\Gamma_D \neq \emptyset$) or $k = 0, 1, 2, \dots$ (for $\Gamma_D = \emptyset$). The first eigenvalue is always simple. In the case $\Gamma_D \neq \emptyset$, the eigenfunction e_1 corresponding to the first eigenvalue κ_1 does not change the sign on the domain Ω. In the case $\Gamma_D = \emptyset$, the eigenfunction e_0 corresponding to the first eigenvalue $\kappa_0 = 0$ is constant. Other eigenfunctions change the sign in both cases. We can choose an orthonormal basis e_k in H^1_D, $k = 1, 2, \dots$ (for $\Gamma_D \neq \emptyset$) or $k = 0, 1, 2, \dots$ (for $\Gamma_D = \emptyset$) composed of the eigenfunctions of (20).

The eigenvalue problem

$$\begin{aligned} \lambda u &= d_1 \Delta u + b_{1,1} u + b_{1,2} v, \\ \lambda v &= d_2 \Delta v + b_{2,1} u + b_{2,2} v. \end{aligned} \tag{21}$$

with boundary conditions (8) determines the stability of the reference stationary solution $[0, 0]$ of the evolutionary problem corresponding to (14), (8). From the dispersion relation

$$b_{1,1} b_{2,2} - b_{1,2} b_{2,1} + \kappa^2 d_1 d_2 - \kappa (b_{1,1} d_2 + b_{2,2} d_1) = 0 \tag{22}$$

we can derive sets of points $[d_1, d_2]$ for which λ from the system (21) is zero. These sets can be written with respect to d_1 as

$$C_k := \left\{ [d_1, d_2] \in \mathbb{R}^2_+ : \ d_1 = \frac{1}{\kappa_k} \left(\frac{b_{1,2} b_{2,1}}{d_2 \kappa_k - b_{2,2}} + b_{1,1} \right) \right\}, \ k = 1, 2, \dots \tag{23}$$

where κ_k are the eigenvalues of the problem (20). These sets are actually hyperbolas, but since we consider only positive d_1, d_2, we have only parts of these hyperbolas (see Fig. 1). There is no hyperbola for the zero eigenvalue κ_0 (see (22) and (16)). Let us define the envelope

$$C_E := \left\{ d = [d_1, d_2] \in \mathbb{R}^2_+ : \ d_1 = \max_{\tilde{d}_1 \in \mathbb{R}_+} \left\{ \tilde{d}_1 : [\tilde{d}_1, d_2] \in \bigcup_{k=1}^{\infty} C_k \right\} \right\}, \tag{24}$$

which divides the positive quadrant $\mathbb{R}^2_+$ on two sets D_U and D_S (see Fig. 1). Moreover, we define two sets, which will be important in the formulation of our main results. Let $r, R, \varepsilon \in \mathbb{R}_+$ and $r < R$. We define

$$C_r^R := \{ d = [d_1, d_2] \in C_E : d_2 \in [r, R] \}, \tag{25}$$

$$C_r^R(\varepsilon) := \{ d = [d_1, d_2] \in C_E \cup D_U : d_2 \in [r, R] \wedge \operatorname{dist}(d, C_E) < \varepsilon \}. \tag{26}$$

Remark 2.3. If all eigenvalues of (20) are simple, i.e., $\kappa_k < \kappa_{k+1}$ for all $k \in \mathbb{N}$, then $C_k \neq C_{k+1}$ for all $k \in \mathbb{N}$. If an eigenvalue κ_k has a multiplicity l, then $\kappa_{k-1} < \kappa_k = \dots = \kappa_{k+l-1} < \kappa_{k+l}$ and $C_{k-1} \neq C_k = \dots = C_{k+l-1} \neq C_{k+l}$. The sets

$$\begin{aligned} D_U &:= \{ d = [d_1, d_2] \in \mathbb{R}^2_+ : d \text{ is on the left of } C_E \}, \\ D_S &:= \{ d = [d_1, d_2] \in \mathbb{R}^2_+ : d \text{ is on the right of } C_E \} \end{aligned}$$

are called the domain of instability and the domain of stability. It is known that if $[d_1, d_2] \in D_S$, then all eigenvalues λ of the problem (21), (8) have negative real parts and if $[d_1, d_2] \in D_U$, then there is a positive eigenvalue λ (for the particular case see [15,17] and for the general case [4]). In particular, the trivial solution of (14), (8) is linearly stable for $[d_1, d_2] \in D_S$ and unstable for $[d_1, d_2] \in D_U$ (see e.g., Chapter 11 in [22]).

Remark 2.4. The following properties of the curves C_k are known, see e.g., [15,17] for the particular case, or [4] for the general case.

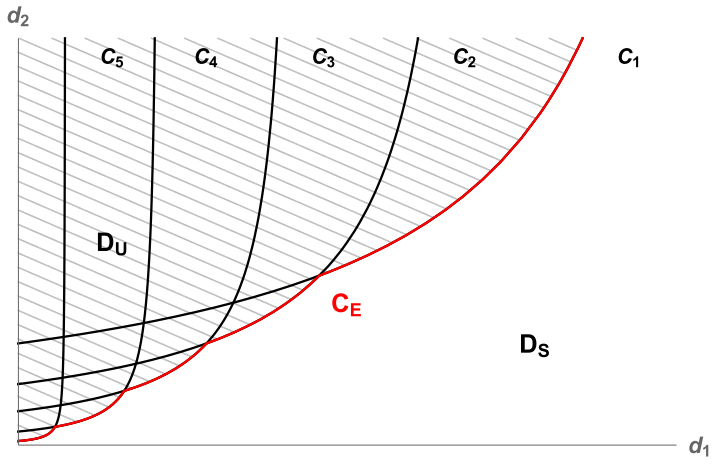

Fig. 1. The illustration of hyperbolas C_k and the envelope C_E. The case when all eigenvalues κ_k are simple. The hatched region is the domain of instability D_U.

- A point $d = [d_1, d_2]$ is a critical point of (19), (8) if and only if there exists k such that $d \in C_k$. In particular, the domain of stability D_S does not contain any critical point of (19), (8) or bifurcation point of (14), (8). Under some additional assumptions, e.g., if the eigenvalue κ_k is simple or of odd multiplicity, the points on C_k are simultaneously bifurcation points (see e.g., [17]).
- If $d \in C_n$ for $n = k, \dots, k+l-1$ (either l is the multiplicity of the eigenvalue κ_k or d is in the intersection of two hyperbolas C_k, C_m and l is the sum of multiplicities of κ_k, κ_m, see Remark 2.3), then $\operatorname{span}\left(\left[\frac{d_2\kappa_k - b_{2,2}}{b_{2,1}} e_k, e_k\right]_{n=k}^{k+l-1}\right)$ is the set of the solutions of (19), (8).

Now let us assume that $K_i^-, K_j^+ \subseteq \Gamma_N$. We will also consider a problem with unilateral integral terms in boundary conditions, i.e., systems (14) and (19) with boundary conditions

$$\begin{aligned} u = v = 0 \quad &\text{on} \quad \Gamma_D, \\ \frac{\partial u}{\partial n} = \sum_{i=1}^{n} \chi^{K_i^-}(x) \tau_-^i T_{K_i^-}^-(u) - \sum_{j=1}^{m} \chi^{K_j^+}(x) \tau_+^j T_{K_j^+}^+(u) \quad &\text{on} \quad \Gamma_N, \\ \frac{\partial v}{\partial n} = 0 \quad &\text{on} \quad \Gamma_N. \end{aligned} \tag{27}$$

2.1. Periodic boundary conditions

Probably the most common boundary conditions considered in the theory of Turing's DDI and pattern formation are homogeneous Neumann boundary conditions. While they are more natural for these kinds of problems than Dirichlet boundary conditions, they are not always the best option. Let us for example study the pattern formation on the skin of some animal (e.g., cheetah). We would like to assume that our domain Ω is actually a cut out part of its fur and we could construct his fur by repeating this domain Ω. For such case periodic boundary conditions are better option than Neumann.

The basic idea of periodic boundary conditions is that in paired points the solution has the same value and the same derivative in the corresponding direction (see below). The definition is simple in dimension $N = 1$, let us assume i.e., $\Omega = (a, b)$ with $a < b$. In this case periodic boundary conditions are

$$\begin{aligned} u(a) &= u(b), \\ -\frac{\partial u}{\partial n}(a) &= \frac{\partial u}{\partial n}(b), \end{aligned} \tag{28}$$

and the same for v.

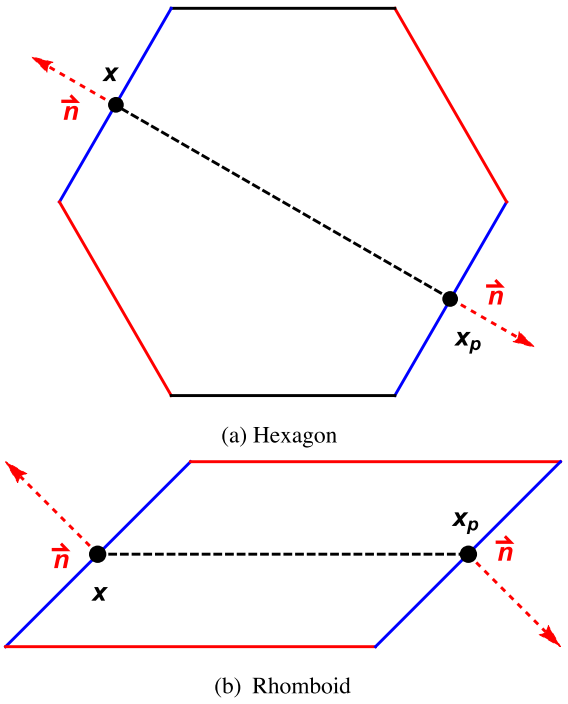

Fig. 2. Illustration of periodic boundary conditions. Every two edges, where we define periodic boundary conditions, have the same colour. (For interpretation of the references to colour in this figure legend, the reader is referred to the web version of this article.)

The setting of periodic boundary conditions in the higher dimension is not so easy. We will suppose here that the domain Ω satisfies the following properties:

$$\begin{gathered} \text{for } N=2: \Omega \text{ is convex and its boundary is composed of } n \text{ pairs of edges } \Gamma^i \text{ and } \Gamma_P^i \\ \text{with } i=1,\dots,n, \text{ which are parallel and of the same length.} \\ \text{for } N\neq 2: \Omega \text{ is a hypercube with } N \text{ pairs of parallel facets } \Gamma^i \text{ and } \Gamma_P^i \text{ with } i=1,\dots,N. \end{gathered} \tag{29}$$

The dimension $N = 2$ is the most interesting for us, because patterns are often studied by numerical experiments in this dimension and it is probably the most important one for applications. That is why we assume more general Ω in (29) despite the fact that we could just settle here with a hypercube (square) too. We mention that periodic boundary conditions could be defined on even more general domains.

Now in general, we denote $\overrightarrow{p_i}$ the vector of the line connecting the centre of Γ^i and the centre of Γ_P^i. For every point $\mathbf{x} \in \Gamma^i$ there exists a point $\mathbf{x}_P \in \Gamma_P^i$ such that $\mathbf{x}_P$ lies in the intersection of Γ_P^i and the line given by $\overrightarrow{p_i}$ and $\mathbf{x}$. By periodic boundary conditions we will mean boundary conditions of the type

$$u(\mathbf{x}) = u(\mathbf{x}_P), \tag{30a}$$

$$-\frac{\partial u}{\partial n}(\mathbf{x}) = \frac{\partial u}{\partial n}(\mathbf{x}_P), \tag{30b}$$

for every pair of $\mathbf{x} \in \Gamma^i, \mathbf{x}_P \in \Gamma_P^i$ (and the same for v). The illustration of periodic boundary conditions on hexagon and rhomboid is in Fig. 2.

In the following remark, we discuss a special type of the shape of Ω in the dimension $N = 2$ suitable for construction of the animal skin.

Remark 2.5. As we mentioned above, the motivation for periodic boundary conditions is to simulate pattern formation on Ω and we aim to construct something larger by repeatedly folding Ω ("as a puzzle"). This leads to the tesselation (or tilling) of the plane, in particular the tesselation by a single geometrical object, i.e., we cannot combine e.g., squares and octagons. The plane can be tesselated by equilateral triangles, squares and hexagons (and their distorted variants). Since triangles do not satisfy the condition

(29), we exclude them. Hence, we can use only convex parallelogons (e.g., square, rhomboid, hexagon etc.) for these purposes.

Remark 2.6. When we consider reaction–diffusion system with periodic boundary conditions described in Remark 2.5, by solution we will always mean weak solution in the space of periodic functions

$$H^1_{per}(\Omega) := \left\{\varphi \in W^{1,2}(\Omega) : \varphi \text{ satisfies (30a)}\right\}. \tag{31}$$

The space is equipped with the same norm and inner product as $W^{1,2}$ (see Remark 2.1).

The Laplace eigenvalue problem

$$-\Delta u = \kappa u \tag{32}$$

with periodic boundary conditions has similar structure of eigenvalues and eigenfunctions as if pure Neumann boundary conditions were considered. Hence, there is the eigenvalue $\kappa_0 = 0$ and the corresponding eigenfunction e_0 is constant. Other eigenvalues are positive. Let us note that hyperbolas and their properties are the same.

3. Main results

We will use notation from previous sections and we assume that conditions (4), (5), (15), (16), (17) are satisfied. Proofs of results presented here are postponed to the end of Section 5.

Theorem 3.1.

(i) The domain of stability D_S contains neither critical points of (18), (8) nor bifurcation points of (13), (8).

(ii) Let $0 < r < R$. Let $C_k, \dots, C_{k+l-1}$ be all hyperbolas which have a non-empty intersection with C_r^R. Let any linear combination e of the eigenfunctions of (20) corresponding to $\kappa_k, \dots, \kappa_{k+l-1}$ satisfy

$$\sum_{i=1}^{n} \chi^{K_i^-}(x)\tau_-^i T^-_{K_i^-}(e) - \sum_{j=1}^{m} \chi^{K_j^+}(x)\tau_+^j T^+_{K_j^+}(e) \not\equiv 0. \tag{33}$$

Then there exists $\varepsilon > 0$ such that there are neither critical points of (18), (8) nor bifurcation points of (13), (8) in $C_r^R(\varepsilon)$.

Remark 3.1. If the condition (33) is not satisfied, then (18) becomes (19) and every point $[d_1, d_2] \in C_r^R$ is a critical point of (18), (8) due to Remark 2.4. Let e.g., C_r^R have non-empty intersection with exactly two non-coinciding hyperbolas C_1 and C_2. Now it is possible that both e_1 and e_2 satisfy the condition (33), hence there are no critical points on C_1 and C_2 excluding their intersection. At the same time this intersection can be a critical point due to the fact that a linear combination of e_1 and e_2 does not have to satisfy this condition. However, the opposite case that there would be critical points on C_1 and C_2, but not in their intersection, is not possible. In the scenario in which $C_1 = C_2$ all linear combinations of e_1 and e_2 must satisfy (33) so that there would not be any critical points on C_1 or C_2.

For the case of unilateral terms of the type u^-, u^+, if only sources or sinks were present in the system, it was possible to show the existence of the ε-neighbourhood along the whole envelope C_E (excluding C_1 in the mixed boundary conditions case) free of critical points of (18), (8) without satisfying the condition similar to (33) (see [5, Theorems 3.2, 3.3]). It was based on the fact that the eigenfunctions e_k of (20) for $k > 1$ change the sign. This is not enough in the case of unilateral integral terms and it is necessary to satisfy condition (33). The result of Theorem 3.1 is illustrated in Fig. 3.

Theorem 3.2. *Let $\Gamma_D \neq \emptyset$. Let either $\tau_-^i = 0$ and $\tau_+^j > 0$ or $\tau_-^i > 0$ and $\tau_+^j = 0$ for all $i = 1, \dots, n$ and $j = 1, \dots, m$ (that means we have either sources or sinks in the system). Let d_2^I be the second coordinate of the intersection point of C_1 and C_2. Any $d \in C_1$, in particular any $d \in C_r^R$ with $d_2^I \leq r < R$, is a critical point of (18), (8).*

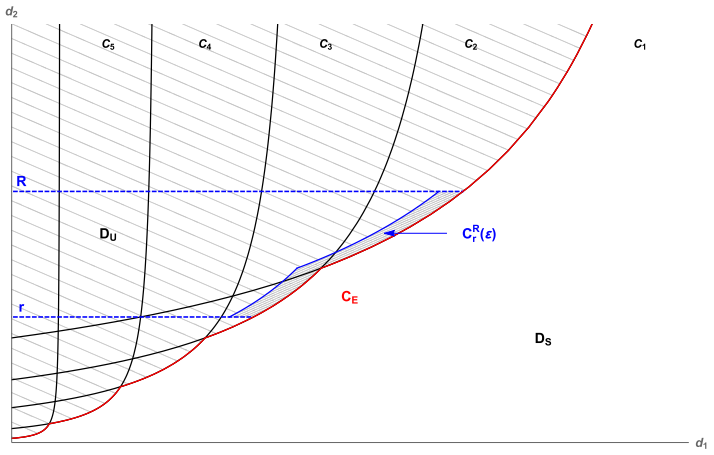

Fig. 3. The illustration of the main result and $C_r^R(\varepsilon)$ neighbourhood. The case when all eigenvalues κ_k are simple.

Theorem 3.3. *Let $\Gamma_D = \emptyset$ and $K_i^- = K_j^+ = \Omega$ for all $i = 1, \dots, n$ and $j = 1, \dots, m$. The condition (33) from Theorem 3.1 can never be satisfied and any point $[d_1, d_2] \in C_E$ is a critical point of (18), (8).*

Remark 3.2. The same formulation of Theorem 3.3 holds in the case that we consider Ω with property (29) and systems with periodic boundary conditions instead of Neumann.

Theorem 3.4. *Let $K_i^-, K_j^+ \subseteq \Gamma_N$ for all $i = 1, \dots, n$ and $j = 1, \dots, m$.*

(i) The domain of stability D_S contains neither critical points of (19), (27) nor bifurcation points of (14), (27).

(ii) Let $0 < r < R$. Let $C_k, \dots, C_{k+l-1}$ be all hyperbolas which have a non-empty intersection with C_r^R. Let any linear combination e of the eigenfunctions of (20) corresponding to $\kappa_k, \dots, \kappa_{k+l-1}$ satisfy

$$\sum_{i=1}^{n} \chi^{K_i^-}(x) \tau_-^i T_{K_i^-}^-(e) - \sum_{j=1}^{m} \chi^{K_j^+}(x) \tau_+^j T_{K_j^+}^+(e) \not\equiv 0 \quad \text{on } \Gamma_N. \tag{34}$$

Then there exists $\varepsilon > 0$ such that there are neither critical points of (19), (27) nor bifurcation points of (14), (27) in $C_r^R(\varepsilon)$.

Remark 3.3. The fact that there are no bifurcation points in D_S or even in $C_r^R(\varepsilon) \cup D_S$ implies that for any compact part M of D_S or $C_r^R(\varepsilon) \cup D_S$, respectively, there exists $\delta > 0$ such that for any $[d_1, d_2] \in M$ there are no non-trivial solutions of (18), (8) (or (19), (27)) with $0 < \|u\|_{H_D^1}^1 + \|v\|_{H_D^1}^1 < \delta$.

Theorem 3.5. *Let us suppose that the domain Ω satisfies (29).*

(i) The domain of stability D_S contains neither critical points of (18), (30) nor bifurcation points of (13), (30).

(ii) Let $0 < r < R$. Let $C_k, \dots, C_{k+l-1}$ be all hyperbolas which have a non-empty intersection with C_r^R. Let any linear combination e of the eigenfunctions of (32), (30) corresponding to $\kappa_k, \dots, \kappa_{k+l-1}$ satisfy (33). Then there exists $\varepsilon > 0$ such that there are neither critical points of (18), (30) nor bifurcation points of (13), (30) in $C_r^R(\varepsilon)$.

Remark 3.4. The same assertion considering periodic boundary conditions as in Theorem 3.5 could be stated for the case of unilateral sources and sinks studied in [5]. Also one could assume a combination of periodic and Neumann boundary conditions, e.g., periodic boundary conditions on two parallel edges of the square and Neumann boundary conditions on the rest of the boundary.

4. Abstract setting

We define the operator $A : H^1_D \to H^1_D$ as

$$(A\psi, \varphi) = \int_\Omega \psi\varphi \, d\Omega \quad \text{for all } \psi, \varphi \in H^1_D(\Omega). \tag{35}$$

Remark 4.1. The operator A defined by (35) is linear, bounded, symmetric and compact due to compact embedding $W^{1,2} \hookrightarrow\hookrightarrow L^2$. Simple calculation gives that the eigenvalues of the operator A are $\mu_k = \frac{1}{\kappa_k}, k = 1, 2, \dots$ for $\Gamma_D \neq \emptyset$ and $\mu_k = \frac{1}{\kappa_k + 1}, k = 0, 1, 2, \dots$ for $\Gamma_D = \emptyset$, and the corresponding eigenvectors of A coincide with the eigenfunctions of (20). Also in the case $\Gamma_D = \emptyset$ we have $((I - A)u, u) \geq 0$ for all u and the equality holds only for $u \in span\{e_0\}$, i.e., u constant.

We define operators $\beta^-, \beta^+ : H^1_D \to H^1_D$ by

$$\begin{aligned} (\beta^-(\psi), \varphi) &= -\int_\Omega \left(\sum_{i=1}^{n} \chi^{K_i^-}(x) \tau_-^i T^-_{K_i^-}(\psi) \right) \varphi \, d\Omega \quad \text{for all } \psi,\ \varphi \in H^1_D, \\ (\beta^+(\psi), \varphi) &= \int_\Omega \left(\sum_{j=1}^{m} \chi^{K_j^+}(x) \tau_+^j T^+_{K_j^+}(\psi) \right) \varphi \, d\Omega \quad \text{for all } \psi,\ \varphi \in H^1_D \end{aligned} \tag{36}$$

and the operator $\beta : H^1_D \to H^1_D$ as

$$\beta = \beta^- + \beta^+. \tag{37}$$

We also define operators $F^-, F^+ : H^1_D \to H^1_D$ by

$$\begin{aligned} (F^-(\psi), \varphi) &= -\int_\Omega \left(\sum_{i=1}^{n} \chi^{K_i^-}(x) f_-^i \left(T^-_{K_i^-}(\psi) \right) \right) \varphi \, d\Omega \quad \text{for all } \psi, \varphi \in H^1_D, \\ (F^+(\psi), \varphi) &= \int_\Omega \left(\sum_{j=1}^{m} \chi^{K_j^+}(x) f_+^j \left(T^+_{K_j^+}(\psi) \right) \right) \varphi \, d\Omega \quad \text{for all } \psi, \varphi \in H^1_D \end{aligned} \tag{38}$$

and $F : H^1_D \to H^1_D$ as

$$F := F^- + F^+. \tag{39}$$

Lemma 4.1. *Functionals $T_X^\mp$ and operators β, F have the following properties:*

$$\textit{(i)} \quad \beta(t\psi) = t\beta(\psi) \text{ for all } t > 0,\ \psi \in H^1_D, \tag{40}$$

$$\textit{(ii)} \quad (\beta(\psi), \psi) \geq 0, \tag{41}$$

$$\textit{(iii)} \quad \psi_k \rightharpoonup \psi \implies T_X^\mp(\psi_k) \to T_X^\mp(\psi), \tag{42}$$

$$\textit{(iv)} \quad \psi_k \rightharpoonup \psi \implies \beta(\psi_k) \to \beta(\psi), \tag{43}$$

$$\textit{(v)} \quad \psi_k \to 0, \frac{\psi_k}{\|\psi_k\|_{H^1_D}} \rightharpoonup w \implies \frac{F(\psi_k)}{\|\psi_k\|_{H^1_D}} \to \beta(w). \tag{44}$$

Proof.

(i) The property described in *(i)* is positive homogeneity and it is apparent.

(ii) For any $\psi \in H^1_D$ we have

$$\begin{aligned}(\beta(\psi),\psi) &= -\int_\Omega \left(\sum_{i=1}^n \chi^{K_-^i}(x)\tau_-^i T^-_{K_i^-}(\psi)\right)\psi\, d\Omega + \int_\Omega \left(\sum_{j=1}^m \chi^{K_j^+}(x)\tau_+^j T^+_{K_j^+}(\psi)\right)\psi\, d\Omega = \\ &= -\sum_{i=1}^n \tau_-^i T^-_{K_i^-}(\psi)\int_{K_i^-}\psi\, dK_i^- + \sum_{j=1}^m \tau_+^j T^+_{K_j^+}(\psi)\int_{K_j^+}\psi\, dK_j^+ = \\ &= \sum_{i=1}^n \tau_-^i \left(T^-_{K_i^-}(\psi)\right)^2 |K_i^-| + \sum_{j=1}^m \tau_+^j \left(T^+_{K_j^+}(\psi)\right)^2 |K_j^+| \geq 0.\end{aligned}$$

(iii) We will prove the assertion for T_X^-, the proof for T_X^+ is the same. Let us have a sequence $(\psi_k) \subset H^1_D$ such that $\psi_k \rightharpoonup \psi \in H^1_D$. Then by the compact embedding $W^{1,2} \hookrightarrow\hookrightarrow L^2$, we get $\psi_k \to \psi$ in L^2. One can see that

$$\begin{aligned}\left|T_X^-(\psi_k) - T_X^-(\psi)\right| &= \left|\left(\int_X \frac{\psi_k}{|X|}\, dX\right)^- - \left(\int_X \frac{\psi}{|X|}\, dX\right)^-\right| \leq \frac{1}{|X|}\int_X |\psi_k - \psi|\, dX \leq \\ &\leq \frac{1}{|X|}\int_\Omega |\psi_k - \psi|\, d\Omega \leq \frac{c}{|X|}\|\psi_k - \psi\|_{L^2} \to 0.\end{aligned}$$

(iv) We will show this property for β^-. Let us have a sequence $(\psi_k) \subset H^1_D$ such that $\psi_k \rightharpoonup \psi \in H^1_D$. Then by the compact embedding $W^{1,2} \hookrightarrow\hookrightarrow L^2$, we get $\psi_k \to \psi$ in L^2. We use the property (ii) of this lemma, the continuous embedding $W^{1,2} \hookrightarrow L^2$ and Hölder's inequality to get

$$\begin{aligned}\|\beta^-(\psi_k) - \beta^-(\psi)\|_{H^1_D} &= \sup_{\|\varphi\|_{H^1_D}\leq 1} |(\beta^-(\psi_k) - \beta^-(\psi),\varphi)| \leq \\ &\leq \sup_{\|\varphi\|_{H^1_D}\leq 1}\int_\Omega |\varphi| \cdot \sum_{i=1}^n \chi^{K_i^-}(x)\tau_i^- \left|T^-_{K_i^-}(\psi_k) - T^-_{K_i^-}(\psi)\right|\, d\Omega \leq \\ &\leq C\|\psi_k - \psi\|_{L^2} \to 0.\end{aligned}$$

The same can be shown for β^+ and the assertion follows.

(v) We will prove this property for F^- and β^-. We again use the continuous embedding $W^{1,2} \hookrightarrow L^2$ with some embedding constant c_{emb} and Hölder's inequality to get

$$\begin{aligned}\left\|\frac{F^-(\psi_k)}{\|\psi_k\|_{H^1_D}} - \beta^-(w)\right\|_{H^1_D} &\leq \sup_{\|\varphi\|_{H^1_D}\leq 1}\sum_{i=1}^n \left|\frac{f_-^i\left(T^-_{K_i^-}(\psi_k)\right)}{\|\psi_k\|_{H^1_D}} - \tau_-^i T^-_{K_i^-}(w)\right| \cdot \int_\Omega \left|\chi^{K_i^-}(x)\cdot\varphi\right|\, d\Omega \leq \\ &\leq c_{emb}\sum_{i=1}^n \left|\frac{f_-^i\left(T^-_{K_i^-}(\psi_k)\right)}{T^-_{K_i^-}(\psi_k)} \cdot \frac{T^-_{K_i^-}(\psi_k)}{\|\psi_k\|_{H^1_D}} - \tau_-^i T^-_{K_i^-}(w)\right| \cdot \left\|\chi^{K_i^-}(x)\right\|_{L^2}\end{aligned}$$

Since $\frac{\psi_k}{\|\psi_k\|_{H^1_D}} \rightharpoonup w$, we get $\frac{T^-_{K_i^-}(\psi_k)}{\|\psi_k\|_{H^1_D}} \to T^-_{K_i^-}(w)$ by properties (i) and (iii). From the assumption (5) we have

$$\lim_{\xi\to 0}\frac{f_-^i(\xi)}{\xi} = \tau_-^i, \tag{45}$$

and due to the fact that $\psi_k \to 0 \implies T^-_{K_i^-}(\psi_k) \to 0$ we have

$$\frac{f^i_-\left(T^-_{K_i^-}(\psi_k)\right)}{T^-_{K_i^-}(\psi_k)} \to \tau^i_- \quad \text{for every } i = 1, \dots, n. \tag{46}$$

All of this together yields

$$\left| \frac{f^i_-\left(T^-_{K_i^-}(\psi_k)\right)}{T^-_{K_i^-}(\psi_k)} \cdot \frac{T^-_{K_i^-}(\psi_k)}{\|\psi_k\|_{H^1_D}} - \tau^i_- T^-_{K_i^-}(w) \right| \to 0, \quad \text{for every } i = 1, \dots, n, \tag{47}$$

which means $\frac{F^-(\psi_k)}{\|\psi_k\|_{H^1_D}} \to \beta^-(w)$. The proof for F^+ and β^+ is analogous and the assertion is proved. □

Remark 4.2. One could consider more general type of unilateral integral terms, e.g., $\chi^M(\mathbf{x})\left(\int_K \frac{u(\mathbf{x})}{|K|}\, dK\right)^-$ with $M \neq K$. While these terms could be interesting for applications, the crucial non-negativity condition (41) is not satisfied in such cases and therefore we exclude them.

5. Reduction to a single operator equation and proofs of main results

Let us remind that we have two different inner products in two different cases $\Gamma_D = \emptyset$ and $\Gamma_D \neq \emptyset$. The system of operator equations is slightly different in these two cases, but the approach is the same. We will focus here on technically more difficult case $\Gamma_D = \emptyset$, i.e., pure zero Neumann boundary conditions. Hence, the space H^1_D is the identical with the space $W^{1,2}$ and we use the inner product $(u, \varphi) = \int_\Omega (\nabla u \nabla \varphi + u\varphi)\, d\Omega$. Now, a weak solution of the problem (18), (8) or (19), (8) is a pair of functions $u, v \in H^1_D$ satisfying

$$\begin{aligned} d_1(I - A)u - b_{1,1}Au - b_{1,2}Av + \beta(u) &= 0, \\ d_2(I - A)v - b_{2,1}Au - b_{2,2}Av &= 0 \end{aligned} \tag{48}$$

or

$$\begin{aligned} d_1(I - A)u - b_{1,1}Au - b_{1,2}Av &= 0, \\ d_2(I - A)v - b_{2,1}Au - b_{2,2}Av &= 0, \end{aligned} \tag{49}$$

respectively.

Let us suppose $d_2 > 0$ fixed. Now we can reduce each of these systems of operator equations to one operator equation by expressing the variable v from the second equation and substituting it to the first one. This way we can transform systems (48) and (49) to

$$d_1(I - A)u - S_{d_2}u + \beta(u) = 0, \tag{50a}$$
$$v = (d_2 I - d_2 A - b_{2,2}A)^{-1} b_{2,1} Au \tag{50b}$$

and

$$d_1(I - A)u - S_{d_2}u = 0, \tag{51a}$$
$$v = (d_2 I - d_2 A - b_{2,2}A)^{-1} b_{2,1} Au \tag{51b}$$

with the new operator

$$S_{d_2} := b_{1,1}A + b_{1,2}A(d_2 I - d_2 A - b_{2,2}A)^{-1} b_{2,1} A. \tag{52}$$

The inverse in equations above always exists and the reduction is very similar in the case $\Gamma_D \neq \emptyset$ (see Section 5.1 and 5.2 in [5]). This idea of reduction can be found e.g., in [5] or [8]. In the next remark we will summarize known properties of S_{d_2}, present the form of eigenvalues d_1 of the problem (51a) and the connection of hyperbolas, critical points of (19), (8) and bifurcation points of (14), (8).

Remark 5.1. The operator S_{d_2} defined by (52) is linear, continuous, symmetric and compact. The eigenvalues of the operator S_{d_2} are

$$\lambda^k = \frac{1}{\kappa_k + 1}\left(\frac{b_{1,2}b_{2,1}}{d_2\kappa_k - b_{2,2}} + b_{1,1}\right),\ k = 0, 1, 2, \dots \tag{53}$$

and the eigenvectors of S_{d_2} corresponding to λ^k coincide with those of A corresponding to μ_k, i.e., with the eigenfunctions of (20) corresponding to κ_k. Also for u_0 constant we have

$$(S_{d_2}u_0, u_0) = (\lambda^0 u_0, u_0) = \left(b_{1,1} + \frac{b_{1,2}b_{2,1}}{-b_{2,2}}\right)\|u_0\|^2_{H^1_D} = \frac{-det(\mathbf{B})}{-b_{2,2}}\|u_0\|^2_{H^1_D} < 0. \tag{54}$$

The eigenvalues d_1^k of the problem (51a) are given by

$$d_1^k = \frac{1}{\kappa_k}\left(\frac{b_{1,2}b_{2,1}}{d_2\kappa_k - b_{2,2}} + b_{1,1}\right),\ k = 1, 2, \dots \tag{55}$$

There is no eigenvalue with $k = 0$ (c.f. (22)).

We will denote by d_1^{MAX} the maximal eigenvalue of the problem (51a). It is well known that we can characterize this maximal eigenvalue of (51a) as

$$d_1^{MAX} = \max_{\substack{u\notin Ker(I-A)\\ u\in H^1_D}} \frac{(S_{d_2}u, u)}{((I-A)u, u)}. \tag{56}$$

We can see from the form of eigenvalues d_1^k that $[d_1^k, d_2] \in C_k$, $[d_1^{MAX}, d_2] \in C_E$ and there are infinitely many positive eigenvalues d_1^k and only finite number of negative ones.

It can be shown that d_1 is an eigenvalue of (51a) or (50a) if and only if $[d_1, d_2]$ is a critical point of (19), (8) or (18), (8), respectively (see Remark 2.4 for the classical case or Lemma 5.1 of [5]). Also every bifurcation point $[d_1, d_2]$ of (14), (8) or (13), (8) is a critical point of (19), (8) or (18), (8), respectively. To prove this implication, one needs properties of β and F we proved in Lemma 4.1 and definition of nonlinear operators corresponding to higher order terms n_1, n_2 for which the growth conditions (17) are necessary. The proof is the same as the proof in the case of problems with unilateral terms and it can be found in appendix of [5] (see Lemma A.2).

In our previous paper [5], we used the variational characterization of the maximal eigenvalue d_1 of problems (50a) (with different β) and (51a) and compared them. The eigenvalue problem (50a) is non-linear, therefore we used [5, Theorem 5.1] (originally from [10]) to get the existence of the maximal eigenvalue and its variational characterization. In the case of unilateral integral terms this is not possible, because we are not able to verify the crucial potentiality condition (51) of [5, Theorem 5.1]. Hence, we use a different approach that does not guarantee the existence of critical points of (18), (8), but considering the fact that we aim to prove the non-existence of critical points on C_E, this is not an issue.

Theorem 5.1. *Let $d_2 > 0$ be arbitrary fixed. If $[d_1, d_2]$ is a critical point of (18), (8), then we always have $d_1 \le d_1^{MAX}$. If $[d_1^{MAX}, d_2] \in C_n$ exactly for $n = k, \dots, k + l - 1$, all linear combinations e of $e_k, \dots, e_{k+l-1}$ satisfy (33) and $[d_1, d_2]$ is a critical point of (18), (8), then $d_1 < d_1^{MAX}$.*

Proof. Let $[d_1, d_2]$ be a critical point of (18), (8), i.e., d_1 is an eigenvalue of the problem (50a) with some eigenfunction u_0. The eigenfunction u_0 cannot be constant, i.e., it cannot be $u_0 \in Ker(I - A)$. If it were, we would have $-(S_{d_2}u_0, u_0) + (\beta(u_0), u_0) > 0$ due to (41) and (54). However, this is not possible, because an eigenfunction u_0 satisfies

$$((I-A)u_0, u_0) - (S_{d_2}u_0, u_0) + (\beta(u_0), u_0) = 0.$$

For any eigenfunction $u_0 \notin Ker(I - A)$ corresponding to the eigenvalue d_1 we have

$$d_1 = \frac{(S_{d_2}u_0, u_0) - (\beta(u_0), u_0)}{((I-A)u_0, u_0)} \le \frac{(S_{d_2}u_0, u_0)}{((I-A)u_0, u_0)} \le \max_{\substack{u\notin Ker(I-A)\\ u\in H^1_D}} \frac{(S_{d_2}u, u)}{((I-A)u, u)} = d_1^{MAX}$$

due to non-negativity of $(\beta(u), u)$ (see Lemma 4.1). Hence, the first assertion is proved.

Let e be as in the assumptions of the theorem and let us suppose that $[d_1^{MAX}, d_2] \in C_E$ is a critical point of (18), (8), i.e., d_1^{MAX} is an eigenvalue of (50a) with corresponding eigenfunction u_0. It means that

$$d_1^{MAX} = \frac{(S_{d_2}u_0, u_0) - (\beta(u_0), u_0)}{((I-A)u_0, u_0)} \leq \frac{(S_{d_2}u_0, u_0)}{((I-A)u_0, u_0)} \leq d_1^{MAX}$$

due to (41) and the fact that d_1^{MAX} is the maximal eigenvalue of (51a). Hence, the inequality is not possible, but in the same moment e is an eigenfunction corresponding to the maximal eigenvalue d_1^{MAX} too and $(\beta(e), e) > 0$ because of (33), which leads to the contradiction. Hence, $[d_1^{MAX}, d_2] \in C_E$ cannot be a critical point of (18), (8) and together with already proven first assertion of the theorem we get that every critical point $[d_1, d_2]$ of (18), (8) satisfies $d_1 < d_1^{MAX}$. □

Proof of Theorem 3.1

(i) By Theorem 5.1, any critical point $[d_1, d_2]$ of (18), (8) satisfies $d_1 \leq d_1^{MAX}$ for a fixed $d_2 > 0$. By Remark 5.1 there is $[d_1^{MAX}, d_2] \in C_E$. Hence, there are no critical points in D_S (see Fig. 1 and Remark 2.4). Since any bifurcation point of (13), (8) is also a critical point of (18), (8) (see Remark 5.1), there are no bifurcation points of (13), (8) in D_S.

(ii) The idea of the following proof is the same as in our paper [5]. We will make the proof for the case $\Gamma_D = \emptyset$. The case $\Gamma_D \neq \emptyset$ is analogous.
Let us suppose the opposite, i.e., the assumptions of the second part of Theorem 3.1 are satisfied and there are critical points of (13), (8) in $C_r^R(\varepsilon)$ for every $\varepsilon > 0$. We can choose a sequence $d^n = [d_1^n, d_2^n] \in D_U$ and $W_n = [u_n, v_n]$ such that $d^n \to d^0 \in C_r^R$, $\|W_n\| = \|u\|_{H_D^1} + \|v\|_{H_D^1} \neq 0$ and d^n, W_n satisfy (48). We can assume that $\frac{W_n}{\|W_n\|} \rightharpoonup W = [w, z]$. Let us divide (48) by $\|W_n\|$ to get

$$\begin{aligned} d_1^n(I-A)\frac{u_n}{\|W_n\|} - b_{1,1}A\frac{u_n}{\|W_n\|} - b_{1,2}A\frac{v_n}{\|W_n\|} + \beta\left(\frac{u_n}{\|W_n\|}\right) &= 0, \\ d_2^n(I-A)\frac{v_n}{\|W_n\|} - b_{2,1}A\frac{u_n}{\|W_n\|} - b_{2,2}A\frac{v_n}{\|W_n\|} &= 0. \end{aligned} \tag{57}$$

By the compactness of A and (43), we get $A\frac{u_n}{\|W_n\|} \to Aw$ and $\beta\left(\frac{u_n}{\|W_n\|}\right) \to \beta(w)$, analogously for v_n and z. Hence, it follows easily from (57) that $\frac{u_n}{\|W_n\|} \to w$, $\frac{v_n}{\|W_n\|} \to z$ and

$$\begin{aligned} d_1^0(I-A)w - b_{1,1}Aw - b_{1,2}Az - \beta(w) &= 0, \\ d_2^0(I-A)z - b_{2,1}Aw - b_{2,2}Az &= 0. \end{aligned}$$

Therefore the point $d^0 = [d_1^0, d_2^0] \in C_r^R$ is a critical point of the problem (18), (8), which contradicts Theorem 5.1 for $d_2 = d_2^0$. Hence, there exists $\varepsilon > 0$ such that there are no critical points of (18), (8) and consequently no bifurcation points of (13), (8) in $C_r^R(\varepsilon)$, because every bifurcation point is also a critical point (see Remark 5.1). □

Proof of Theorem 3.2

Since we assume $\Gamma_D \neq \emptyset$, the first eigenfunction e_1 of (20) does not change the sign by Remark 2.2. Hence, for either $e = e_1$ or $e = -e_1$ we have $\sum_{i=1}^n \chi^{K_i^-}(x)\tau_-^i T_{K_i^-}^-(e) - \sum_{j=1}^m \chi^{K_j^+}(x)\tau_+^j T_{K_j^+}^+(e) = 0$. Since any point $[d_1, d_2] \in C_1$ is a critical point of (19), (8) with the solution $\left[\frac{d_2\kappa_1 - b_{2,2}}{b_{2,1}}e_1, e_1\right]$ (see Remark 2.4), it is also a critical point of (18), (8). □

Proof of Theorem 3.3

In the case $\Gamma_D = \emptyset$ any linear combination e of eigenfunctions e_k for $k > 0$ satisfies $\int_\Omega e \, d\Omega = 0$. Indeed, using Green's formula and zero Neumann boundary conditions we have

$$\kappa_k \int_\Omega e_k \, d\Omega = \int_\Omega -\Delta e_k \, d\Omega = -\int_{\partial\Omega} \frac{\partial e_k}{\partial n} \, d\partial\Omega = 0 \quad \text{for every } k > 0.$$

Since all κ_k for $k > 0$ are positive, we immediately get $\int_\Omega e \, d\Omega = 0$. This means that $T_\Omega^{\mp}(e) = 0$ and by the similar argumentation as in the proof of Theorem 3.2 the assertion follows. □

Proof of Theorem 3.4

First let us define operators $\beta_N^-, \beta_N^+ : H_D^1 \to H_D^1$ as

$$\begin{aligned}(\beta_N^-(\psi), \varphi) &= -\int_{\Gamma_N} \left(\sum_{i=1}^{n} \chi^{K_i^-}(x) \tau_-^i T_{K_i^-}^-(\psi) \right) \varphi \, d\Gamma_N \quad \text{for all } \psi,\ \varphi \in H_D^1, \\ (\beta_N^+(\psi), \varphi) &= \int_{\Gamma_N} \left(\sum_{j=1}^{m} \chi^{K_j^+}(x) \tau_+^j T_{K_j^+}^+(\psi) \right) \varphi \, d\Gamma_N \quad \text{for all } \psi,\ \varphi \in H_D^1\end{aligned} \tag{58}$$

and then the operator $\beta_N : H_D^1 \to H_D^1$ as

$$\beta_N = \beta_N^+ + \beta_N^-. \tag{59}$$

The operator β_N has the same properties as β (see Lemma 4.1). Now we can rewrite problem (19), (27) as

$$\begin{aligned} d_1(I - A)u - b_{1,1}Au - b_{1,2}Av + \beta_N(u) = 0, \\ d_2(I - A)v - b_{2,1}Au - b_{2,2}Av = 0. \end{aligned} \tag{60}$$

Then it is necessary to repeat the process of the reduction to one operator equation from the beginning of this section. Theorem 5.1 applies to this problem as well and the rest of the proof of Theorem 3.4 is the same as the proof of Theorem 3.1 presented above. □

Proof of Theorem 3.5

In the case of periodic boundary conditions, we use the function space H_{per}^1 from Remark 2.6 and by solution we mean a weak solution from this space. We can define the same operators A, β etc. from Section 4 using the inner product of H_{per}^1 (let us remind that it is the same inner product as the inner product of $W^{1,2}$). These operators have again the properties described in Lemma 4.1. Eventually, we get the same systems of operator equations (48), (49) as we had in the case of Neumann boundary conditions. Then we can apply again the reduction to one operator equation. Theorem 5.1 still applies in this case and the proof of Theorem 3.5 is then exactly the same as the proof of Theorem 3.1. □

6. Numerical experiments

In this section we will present a collection of results of our numerical experiments with specific reaction kinetics. In some sense we take inspiration in the paper [24], where Vejchodský et al. investigated the influence of unilateral sources of the type τv^- (and its modifications) in the inhibitor equation of the reaction–diffusion system on pattern formation. Analytical results for systems with unilateral terms suggest that the domain of instability could be bigger than in the classical case. Vejchodský et al. were looking for a critical value of the portion of diffusion parameters $D = \frac{d_1}{d_2}$ where Turing's instability occurs. Of course, one cannot talk here about true stability (or instability), because everything is just based on numerical experiments and one can only observe whether the solution evolving from initial perturbations of the homogeneous steady state converges to this state or not (i.e., it is evolving into something significantly bigger). We are investigating here the dual problem, i.e., unilateral terms in the activator equation. We focus both on numerical experiments considering unilateral terms of the type u^-, u^+ (analytical results were presented in [5]) and also unilateral integral terms presented in the analytic part of this paper. One goal is to investigate the influence of these terms on the "change of stability" of the reference steady state in the similar way as Vejchodský et al. did. Also we are interested in the shape of resulting patterns in different scenarios. We use here two types of boundary conditions, i.e., pure Neumann boundary conditions and periodic boundary conditions. Since we most commonly used Neumann boundary conditions before and

we deem periodic boundary conditions more realistic, we want to compare results and shapes of patterns for these two types of boundary conditions and conclude that periodic boundary conditions are the better option for future experiments.

We use the well-known Schnakenberg reaction kinetics (see [21])

$$\begin{aligned} f(u,v) &= a - u + u^2 v, \\ g(u,v) &= b - u^2 v, \end{aligned} \tag{61}$$

where a, b are positive coefficients. The reaction–diffusion system with this kinetics and either Neumann or periodic boundary conditions has only one constant steady state $[\overline{u}, \overline{v}] = \left[a+b, \frac{b}{(a+b)^2}\right]$. We will assume values of coefficients

$$a = 0.2, \quad b = 2. \tag{62}$$

One can easily verify in such case that conditions (16) are satisfied and the kinetics is of the substrate-depletion type. The spatial domain is always the square $\Omega = [-25, 25]^2$.

The overall approach of numerical solving of our reaction–diffusion system is made in the sense of the method of lines. We use finite difference method for the spatial approximation, in particular the five-point scheme to approximate the Laplace operator. The evolution in time is managed by *ode15s* solver in the software MATLAB. We should mention that we use the idea of the ghost-point and the central difference to deal with Neumann boundary condition and periodic boundary conditions (see e.g., [13]). We adopt the trapezoidal rule to compute integral terms in the activator equation.

We use the random noise around $[\overline{u}, \overline{v}]$ as an initial condition with range $[-10^{-2}, 10^{-2}]$. We label the solution stationary, when it does not change too much, i.e., the difference of solutions in the maximum norm in two consecutive times is smaller than 10^{-3}. We say that $[\overline{u}, \overline{v}]$ is unstable if the solution $u(\mathbf{x})$ that evolved from perturbations of the reference homogeneous steady state satisfy

$$\frac{\max_{\mathbf{x}\in\Omega} |u(\mathbf{x}) - \overline{u}|}{\overline{u}} > 0.1. \tag{63}$$

The value 0.1 is ten times bigger than the range of initial perturbation, hence we assume that the solution has evolved enough and it suggests instability of $[\overline{u}, \overline{v}]$. We use the relative difference from $\overline{u}$ here, because the constant $\overline{u}$ is quite bigger that $\overline{v}$ and the stationary solution u is in general much bigger than v. It does not seem to be the best idea to look for some exact value of d_1, where the stability changes. We will rather look for a critical interval $I_{crit} := (d_1^U, d_1^S)$ such that $|d_1^U - d_1^S| < 0.01$ and $[\overline{u}, \overline{v}]$ is unstable for $[d_1^U, d_2]$ and stable for $[d_1^S, d_2]$ (in the sense of (63)).

The typical patterns produced by reaction–diffusion system with Schnakenberg kinetics and either periodic of Neumann boundary conditions can be seen in Fig. 4. The pattern with spots typically appears for some $[d_1, d_2]$ deep in the domain of instability, while stripe patterns are produced for $[d_1, d_2]$ close to the envelope C_E (the eigenfunctions corresponding to the smaller eigenvalues have probably bigger influence here). One can see that the shape of patterns in solutions u and v is the same, there is just inverted colouring (maximums and minimums). In [24], Vejchodský et al. always showed the solution u, but they also used inverted colourmap in Matlab. Since we use standard colourmap (grey), we will always show the solution u so that spots are always black.

6.1. Experiments with unilateral terms

We will consider the unilateral source

$$\tau(\mathbf{x})(u - \overline{u})^- \tag{64}$$

in the activator equation with $\tau(\mathbf{x}) \geq 0$ for every $\mathbf{x} \in \Omega$. We chose this simple unilateral source, because we can expect the existence of $C_r^R(\varepsilon)$ along the whole envelope C_E according to analytical results from [5] (for $\tau > 0$).

First, let us focus on the case of Neumann boundary conditions and τ constant on the whole domain Ω. We experimentally found the critical interval I_{crit} for several values of d_2 and three values of τ. A sample of

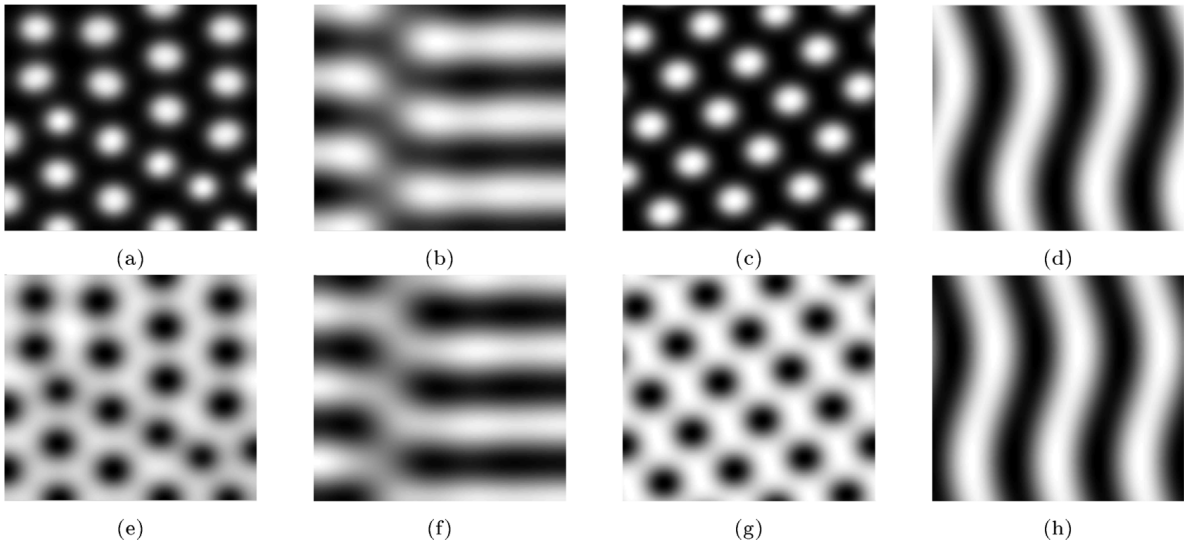

Fig. 4. Examples of typical patterns in the classical case without unilateral terms. (a) sol. u, spots, Neumann b.c. (b) sol. u, stripes, Neumann b.c. (c) sol. u, spots, periodic b.c. (d) sol. u, stripes, periodic b.c. (e) sol. v, spots, Neumann b.c. (f) sol. v, stripes, Neumann b.c. (g) sol. v, spots, periodic b.c. (h) sol. v, stripes, periodic b.c.

Table 1
Critical intervals I_{crit} for different values of τ. The case of the unilateral source $\tau(u-\overline{u})^-$ and Neumann boundary conditions. The value of d_1 in the second column is analytically computed value of d_1 such that $[d_1, d_2] \in C_E$.

d_2	d_1	I_{crit} for $\tau = 0$	I_{crit} for $\tau = 0.1$	I_{crit} for $\tau = 0.5$	I_{crit} for $\tau = 1$
600	14.73	(14.6149, 14.6221)	(12.8456, 12.8528)	(9.8967, 9.9039)	(8.6452, 8.6524)

Table 2
Critical intervals I_{crit} for $\tau(\mathbf{x}) = 0.5$ on square support Ω_S in the middle of Ω. The case of the unilateral source $\tau(\mathbf{x})(u-\overline{u})^-$ and Neumann boundary conditions.

d_2	I_{crit} for $\lvert\Omega_S\rvert = 50^2$	I_{crit} for $\lvert\Omega_S\rvert = 40^2$	I_{crit} for $\lvert\Omega_S\rvert = 30^2$	I_{crit} for $\lvert\Omega_S\rvert = 10^2$
600	(9.8967, 9.9039)	(12.637, 12.6442)	(14.1258, 14.133)	(14.6005, 14.6077)

these experiments for $d_2 = 600$ can be found in Table 1, the full table for several values of d_2 is Table 7 in the appendix. One can see that as we increase τ, the critical interval shifts to zero. It would be interesting to find large enough value of τ, such that the critical interval reaches zero, but the numerical methods we used are not very reliable for d_1 close to zero. Hence, this remains open problem. The case $\tau = 0$ corresponds to the classical case without unilateral sources. Of course, we could just use d_1 computed analytically using the definition of C_E (in the second column). However, since everything is just approximate here, we should compare I_{crit} for positive τ with I_{crit} for $\tau = 0$. The patterns have usually the same shape when we use τu^- on the whole domain Ω as in the classical case (meaning in the problem without any unilateral terms).

In the next series of experiments we investigate the influence of the unilateral source acting only on some subset of the domain Ω. We assume

$$\tau(\mathbf{x}) = \begin{cases} 0.5 & \dots \quad \mathbf{x} \in \Omega_S, \\ 0 & \dots \quad \text{otherwise}, \end{cases} \tag{65}$$

where Ω_S is a square with centre in the centre of the square Ω. The goal is once again to find the critical interval for different sizes of Ω_S. We can see in the sample in Table 2, that as we increase the size of Ω_S, the unilateral term has bigger influence and the critical interval is closer to zero (see full Table 8 in the appendix). This is the expected result, but it is interesting that even for $|\Omega_S| = 30^2$, which is quite large square, the shift is very small. This suggests that using unilateral terms on small subset is not very effective in this sense.

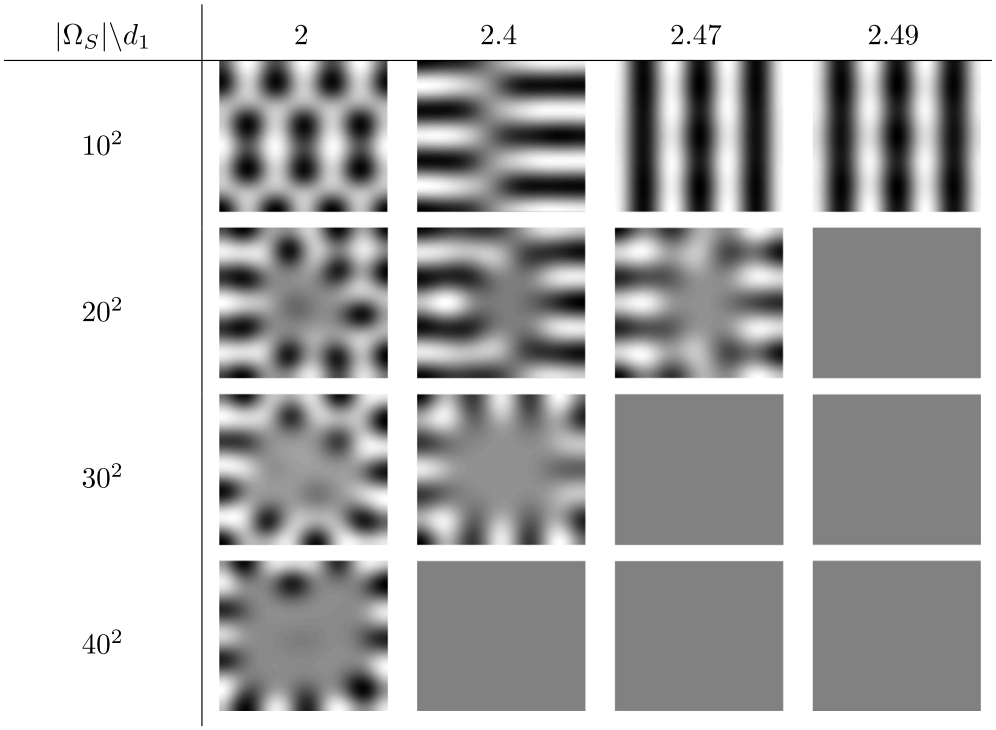

Fig. 5. The dependence of the shape of patterns on the size of Ω_S and the diffusion parameter d_1- the case of Neumann boundary conditions and fixed $d_2 = 100$.

Table 3
Critical intervals I_{crit} for different values of τ. The case of the unilateral source $\tau(u-\overline{u})^-$ and periodic boundary conditions.

d_2	I_{crit} for $\tau = 0$	I_{crit} for $\tau = 0.1$	I_{crit} for $\tau = 0.5$	I_{crit} for $\tau = 1$
600	(14.1258, 14.133)	(12.6946, 12.7017)	(9.7169, 9.7241)	(8.6596, 8.6668)

Table 4
Critical intervals I_{crit} for $\tau(\mathbf{x}) = 0.5$ on square support Ω_S in the middle of Ω. The case of the unilateral source $\tau(\mathbf{x})(u-\overline{u})^-$ and periodic boundary conditions.

d_2	I_{crit} for $\lvert\Omega_S\rvert = 40^2$	I_{crit} for $\lvert\Omega_S\rvert = 30^2$	I_{crit} for $\lvert\Omega_S\rvert = 20^2$	I_{crit} for $\lvert\Omega_S\rvert = 10^2$
600	(12.1881, 12.1934)	(14.0108, 14.018)	(14.1412, 14.148)	(14.1345, 14.1412)

The shape of patterns is more interesting in the case that the unilateral source is acting only on the part of the domain Ω. In Fig. 5 we illustrate the dependence of the shape of patterns on the size of Ω_S and the value of d_1. One can see that for the higher value of d_1 or the larger Ω_S the pattern is not produced.

In the case of periodic boundary conditions, the situation considering the critical interval and the shape of patterns is very similar to the case of Neumann boundary conditions. The shift of the critical interval I_{crit} for $d_2 = 600$ and three values of τ is in Table 3, for the several values of d_2 see full Table 9. The patterns are more of less the same as typical patterns in Figs. 4(g), 4(h).

In the case that the unilateral source is active only on Ω_S the shift of the critical interval I_{crit} for $d_2 = 600$ and four sizes of Ω_S is in Table 4, for the several values of d_2 see full Table 10. The shape of patterns is again in this case more interesting than in the case that the unilateral source is active on the whole domain Ω (see Fig. 6).

The unilateral source $\tau(u-\overline{u})^-$ can be of course replaced with more complicated sources or we could use both the source and the sink. We repeated some of experiments for the unilateral source with saturation $\frac{\tau(u-\overline{u})^-}{1+(u-\overline{u})^-}$ and we got similar results. We should mention that this term is more natural due to the fact that it is bounded, while $\tau(u-\overline{u})^-$ is not.

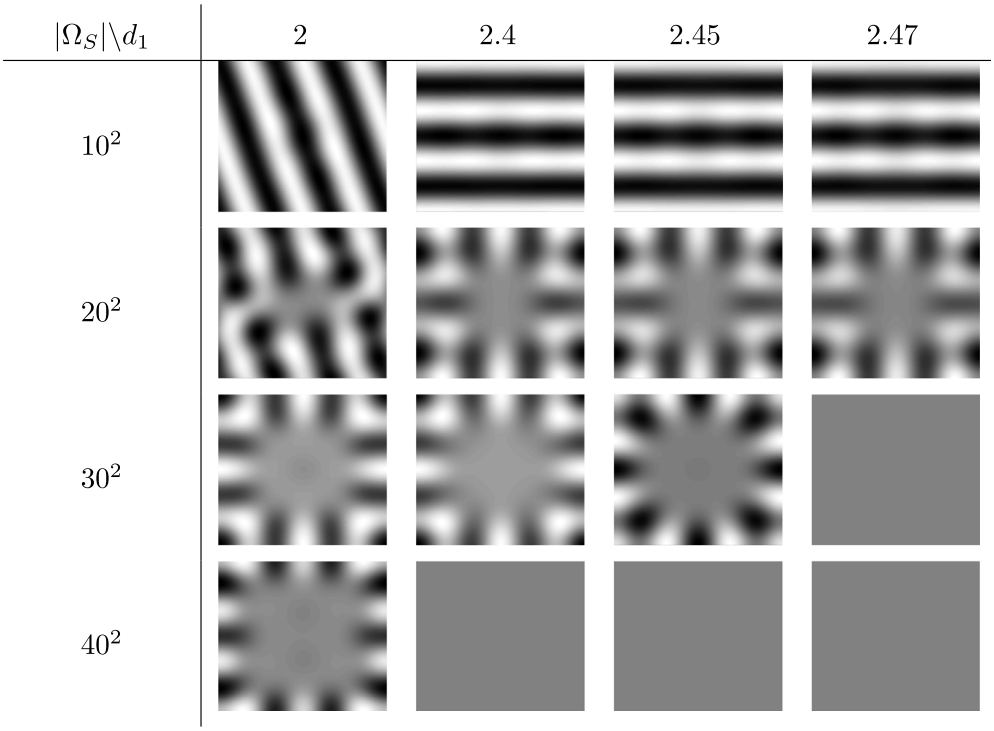

Fig. 6. The dependence of the shape of patterns on the size of Ω_S and the diffusion parameter d_1- the case of periodic boundary conditions and fixed $d_2 = 100$.

6.2. Experiments with unilateral integral terms

We consider one unilateral integral source and one sink

$$\tau\chi_M(\mathbf{x})\left(\int_K \frac{u-\overline{u}}{|K|}\,dK\right)^- - \varepsilon\chi_M(\mathbf{x})\left(\int_K \frac{u-\overline{u}}{|K|}\,dK\right)^+ \tag{66}$$

with $\tau, \varepsilon > 0$. In the analytical part of the paper we always suppose $K = M$. Here, we will make some experiments even in the case that $K \neq M$. The convergence to the stationary solution takes much more time for unilateral integral terms. Hence, we look for I_{crit} for fewer values of d_2. Also we discovered that the shift of I_{crit} to the left is much smaller than in the case of unilateral terms, therefore we require that $|d_1^U - d_1^S| < 0.001$ in the definition of the critical interval I_{crit} instead of the value 0.01 we used before.

In the case of Neumann boundary conditions, we tested several settings of parameters τ, ε and sets K, M. In Tables 5 and 6 we summarize computed critical intervals I_{crit} for two different values of d_2. One can see here that the shift of the critical interval is very small. We note here that columns (v) and (vi) are in Table 6. Looking at the case (ii) (only source) and (iii) (both source and sink), we can see that the shift is bigger, when we use both source and sink, not just the source. On the other hand taking small sets K, M does not necessarily result in smaller shift (compare (iii) and (iv)). This makes sense, because the integral does not need to be larger if we take larger sets K, M. The same apparently is true, when we increase values of τ and ε (compare (iii) and (v)). The last case (vi) is the case, where the sets K and M are different, which is the case excluded in the analytic part of this paper. We can observe here the shift to the right, which is something new.

The shape of patterns does not seem to be very influenced by unilateral integral terms. One could say that patterns are in some cases more blurry than in the classical case, but the difference is quite small. Also the case of periodic boundary conditions gives the same results as the case of Neumann boundary conditions.

Table 5
Critical intervals I_{crit} in different cases for two values of d_2. (i) — The classical case (no unilateral integral terms), (ii) — the case $\tau = 0.8$, $\varepsilon = 0$, $K = M = [-20, 20]^2$, (iii) — the case $\tau = 0.8$, $\varepsilon = 0.7$, $K = M = [-20, 20]^2$, (iv) — the case $\tau = 0.8$, $\varepsilon = 0.7$, $K = M = [-10, 10]^2$.

d_2	(i)	(ii)	(iii)	(iv)
600	(14.6218, 14.6224)	(14.6166, 14.6172)	(14.6218, 14.6224)	(14.6189, 14.6195)
500	(12.3099, 12.3109)	(12.213, 12.214)	(12.246, 12.2469)	(11.9368, 11.9377)

Table 6
Critical intervals I_{crit} in different cases for two values of d_2 (extension of Table 5). (i) — the classical case (no unilateral integral terms), (v) — the case $\tau = 1.5$, $\varepsilon = 1.2$, $K = M = [-20, 20]^2$ (vi) — the case $\tau = 0.8$, $\varepsilon = 0.7$, $K = [0, 20]^2$, $M = [-20, 0]^2$ (i.e., the case $K \neq M$).

d_2	(i)	(v)	(vi)
600	(14.6218, 14.6224)	(14.6103, 14.6109)	(15.5855, 15.5862)
500	(12.3099, 12.3109)	(12.0921, 12.0931)	(13.6883, 13.6891)

Table 7
Critical intervals I_{crit} for several values of d_2. The case of the unilateral source $\tau(u - \overline{u})^-$ and Neumann boundary conditions.

d_2	d_1	I_{crit} for $\tau = 0$	I_{crit} for $\tau = 0.1$	I_{crit} for $\tau = 0.5$	I_{crit} for $\tau = 1$
600	14.73	(14.6149, 14.6221)	(12.8456, 12.8528)	(9.8967, 9.9039)	(8.6452, 8.6524)
400	9.96	(9.9503, 9.96)	(8.8706, 8.8804)	(6.7211, 6.7308)	(5.7776, 5.7873)
300	7.47	(7.4262, 7.4335)	(6.6821, 6.6894)	(5.0919, 5.0992)	(4.3332, 4.3405)
200	5.01	(4.9904, 5.0002)	(4.4718, 4.4816)	(3.3661, 3.3759)	(2.8866, 2.8964)
150	3.75	(3.7207, 3.728)	(3.3398, 3.3472)	(2.5342, 2.5415)	(2.168, 2.1753)
100	2.51	(2.4806, 2.4904)	(2.2257, 2.2355)	(1.6962, 1.706)	(1.4511, 1.4609)
70	1.76	(1.7462, 1.7531)	(1.5675, 1.5744)	(1.1894, 1.1963)	(1.0106, 1.0175)
80	2.01	(1.9943, 2.0021)	(1.798, 1.8059)	(1.3583, 1.3662)	(1.1542, 1.162)
60	1.5	(1.4941, 1.5)	(1.3359, 1.3418)	(1.0195, 1.0254)	(0.86719, 0.87305)
50	1.25	(1.2402, 1.25)	(1.1133, 1.123)	(0.83984, 0.84961)	(0.72266, 0.73242)

6.3. Conclusion

The numerical investigation of unilateral and unilateral integral terms yielded several observations. Should we compare the influence of unilateral terms and unilateral integral terms, former ones have much bigger impact on the pattern formation. First we have seen that with the increasing strength of unilateral terms, the shift of the critical interval I_{crit} to the left is getting bigger and the same is true, when we increase the set, where these terms are active. We have observed that the pattern formation can be locally broken on the set, where unilateral terms are active and it leads to quite interesting patterns. This behaviour can be detected for the case of Neumann boundary conditions and also periodic boundary conditions. Hence, we conclude that we should focus more on periodic boundary conditions in the future, because they give qualitatively similar results as Neumann boundary conditions and we deem them more natural. On the other hand, in the case of unilateral integral terms, we observed that the shift of I_{crit} is small in several scenarios. The shift is especially small in comparison to the shift in the case of unilateral terms. Also the shape of patterns usually remains unchanged. The most interesting observation here is the fact that when $K \neq M$ (the set where we compute integral and the set where these terms are active is different), the critical interval can truly shift to the right. This is something new, which was not possible in the case of unilateral terms.

Acknowledgements

M. Fencl has been supported by the project SGS-2019-010 of University of West Bohemia, Czech Republic, the project 18-03253S of the Grant Agency of Czech Republic and the project LO1506 of the Czech Ministry of Education, Youth and Sport.

Table 8
Critical intervals I_{crit} for $\tau(\mathbf{x}) = 0.5$ on square support Ω_S in the middle of Ω. The case of the unilateral source $\tau(\mathbf{x})(u - \overline{u})^-$ and Neumann boundary conditions.

d_2	I_{crit} for $\lvert\Omega_S\rvert = 50^2$	I_{crit} for $\lvert\Omega_S\rvert = 40^2$	I_{crit} for $\lvert\Omega_S\rvert = 30^2$	I_{crit} for $\lvert\Omega_S\rvert = 10^2$
600	(9.8967, 9.9039)	(12.637, 12.6442)	(14.1258, 14.133)	(14.6005, 14.6077)
400	(6.7211, 6.7308)	(8.7053, 8.715)	(9.7266, 9.7363)	(9.9308, 9.9405)
300	(5.0919, 5.0992)	(6.6092, 6.6165)	(7.2074, 7.2147)	(7.3606, 7.3679)
200	(3.3661, 3.3759)	(4.6088, 4.6186)	(4.9121, 4.9219)	(4.9806, 4.9904)
150	(2.5342, 2.5415)	(3.457, 3.4644)	(3.6401, 3.6475)	(3.728, 3.7354)
100	(1.6962, 1.706)	(2.3727, 2.3825)	(2.4512, 2.461)	(2.4904, 2.5002)
80	(1.3583, 1.3662)	(1.9079, 1.9158)	(1.9629, 1.9707)	(1.9864, 1.9943)
70	(1.1894, 1.1963)	(1.7325, 1.7394)	(1.7462, 1.7531)	(1.6775, 1.6844)
60	(1.0195, 1.0254)	(1.4473, 1.4531)	(1.4766, 1.4824)	(1.4941, 1.5)
50	(0.83984, 0.84961)	(1.2109, 1.2207)	(1.2305, 1.2402)	(1.2402, 1.25)

Table 9
Critical intervals I_{crit} for several values of d_2. The case of the unilateral source $\tau(u - \overline{u})^-$ and periodic boundary conditions.

d_2	I_{crit} for $\tau = 0$	I_{crit} for $\tau = 0.1$	I_{crit} for $\tau = 0.5$	I_{crit} for $\tau = 1$
600	(14.1258, 14.133)	(12.6946, 12.7017)	(9.7169, 9.7241)	(8.6596, 8.6668)
400	(9.8919, 9.9016)	(8.608, 8.6177)	(6.6432, 6.653)	(5.7484, 5.7581)
300	(7.0615, 7.0688)	(6.3466, 6.3539)	(4.8949, 4.9022)	(4.3259, 4.3332)
200	(4.9415, 4.9513)	(4.4718, 4.4816)	(3.3661, 3.3759)	(2.8866, 2.8964)
150	(3.6548, 3.6621)	(3.2153, 3.2227)	(2.4829, 2.4902)	(2.168, 2.1753)
100	(2.4806, 2.4904)	(2.2355, 2.2453)	(1.6864, 1.6962)	(1.4413, 1.4511)
80	(1.9786, 1.9864)	(1.7745, 1.7823)	(1.3583, 1.3662)	(1.1542, 1.162)
70	(1.7394, 1.7462)	(1.5675, 1.5744)	(1.1825, 1.1894)	(1.0106, 1.0175)
60	(1.4824, 1.4883)	(1.3184, 1.3242)	(1.0195, 1.0254)	(0.86719, 0.87305)
50	(1.2402, 1.25)	(1.1133, 1.123)	(0.83984, 0.84961)	(0.72266, 0.73242)

Table 10
Critical intervals I_{crit} for $\tau(\mathbf{x}) = 0.5$ on square support Ω_S in the middle of Ω. The case of the unilateral source $\tau(\mathbf{x})(u - \overline{u})^-$ and periodic boundary conditions.

d_2	I_{crit} for $\lvert\Omega_S\rvert = 40^2$	I_{crit} for $\lvert\Omega_S\rvert = 30^2$	I_{crit} for $\lvert\Omega_S\rvert = 20^2$	I_{crit} for $\lvert\Omega_S\rvert = 10^2$
600	(12.1881, 12.1934)	(14.0108, 14.018)	(14.1412, 14.148)	(14.1345, 14.1412)
400	(8.2662, 8.2733)	(9.7849, 9.7946)	(9.8978, 9.904)	(9.8915, 9.8978)
300	(6.508, 6.5157)	(6.9375, 6.9448)	(6.9626, 6.9716)	(7.0582, 7.065)
200	(4.6114, 4.6189)	(4.9062, 4.9125)	(4.9286, 4.9348)	(4.9411, 4.9474)
150	(3.3953, 3.401)	(3.5375, 3.5438)	(3.6201, 3.6293)	(3.6572, 3.6665)
100	(2.3624, 2.3716)	(2.4563, 2.4625)	(2.4786, 2.4849)	(2.4849, 2.4912)
80	(1.8992, 1.9066)	(1.9563, 1.9625)	(1.9698, 1.9748)	(1.9798, 1.9849)
70	(1.6404, 1.649)	(1.7062, 1.7125)	(1.7248, 1.7336)	(1.7424, 1.7512)
60	(1.4394, 1.4449)	(1.4688, 1.475)	(1.4775, 1.485)	(1.485, 1.4925)
50	(1.2129, 1.2191)	(1.2375, 1.2437)	(1.2375, 1.2437)	(1.2437, 1.25)

Appendix

A.1. Tables

See Tables 7–10.

References

[1] J.I. Baltaev, M. Kučera, M. Väth, A variational approach to bifurcation in reaction-diffusion systems with Signorini type boundary conditions, Appl. Math. 57 (2) (2012) 143–165.
[2] P. Drábek, M. Kučera, Reaction-diffusion systems: destabilizing effect of unilateral conditions, Nonlinear Anal. 12 (11) (1988) 1173–1192.
[3] P. Drábek, M. Kučera, M. Míková, Bifurcation points of reaction-diffusion systems with unilateral conditions, Czechoslovak Math. J. 35(110) (4) (1985) 639–660.
[4] J. Eisner, M. Kučera, Spatial patterns for reaction-diffusion systems with conditions described by inclusions, Appl. Math. 42 (6) (1997) 421–449.

[5] M. Fencl, M. Kučera, Unilateral sources and sinks of an activator in reaction-diffusion systems exhibiting diffusion-driven instability, Nonlinear Anal. 187 (2019) 71–92.
[6] A. Gierer, H. Meinhardt, A theory of biological pattern formation, Kybernetik 12 (1) (1972) 30–39.
[7] V. Klika, M. Kozák, E.A. Gaffney, Domain size driven instability: self-organization in systems with advection, SIAM J. Appl. Math. 78 (5) (2018) 2298–2322.
[8] M. Kučera, Reaction-diffusion systems: stabilizing effect of conditions described by quasivariational inequalities, Czechoslovak Math. J. 47(122) (3) (1997) 469–486.
[9] M. Kučera, Stability and bifurcation problems for reaction-diffusion systems with unilateral conditions, in: Equadiff 6 (Brno, 1985), in: Lecture Notes in Math., vol. 1192, Springer, Berlin, 1986, pp. 227–234.
[10] M. Kučera, J. Navrátil, Eigenvalues and bifurcation for problems with positively homogeneous operators and reaction-diffusion systems with unilateral terms, Nonlinear Anal. 166 (2018) 154–180.
[11] M. Kučera, L. Recke, J. Eisner, Smooth bifurcation for variational inequalities and reaction-diffusion systems, in: Progress in Analysis, Vols. I, II (Berlin, 2001), World Sci. Publ., River Edge, NJ, 2003, pp. 1125–1133.
[12] M. Kučera, M. Väth, Bifurcation for a reaction-diffusion system with unilateral and Neumann boundary conditions, J. Differential Equations 252 (4) (2012) 2951–2982.
[13] R.J. LeVeque, Finite Difference Methods for Ordinary and Partial Differential Equations: Steady-State and Time-Dependent Problems, Society for Industrial and Applied Mathematics, SIAM, Philadelphia, PA, 2007, p. xvi+341.
[14] M. Menzinger, A.B. Rovinsky, Instabilities induced by differential flows, in: Pattern Formation: Symmetry Methods and Applications (Waterloo, On, 1993), in: Fields Inst. Commun., vol. 5, Amer. Math. Soc., Providence, RI, 1996, pp. 297–320.
[15] M. Mimura, Y. Nishiura, M. Yamaguti, Some diffusive prey and predator systems and their bifurcation problems, in: Bifurcation Theory and Applications in Scientific Disciplines (Papers, Conf., New York, 1977), in: Ann. New York Acad. Sci., vol. 316, New York Acad. Sci., New York, 1979, pp. 490–510.
[16] J.D. Murray, Mathematical Biology II: Spatial Models and Biomedical Applications, third ed., in: Interdisciplinary Applied Mathematics, vol. 18, Springer-Verlag, New York, 2003, p. xxvi+811.
[17] Y. Nishiura, Global structure of bifurcating solutions of some reaction-diffusion systems, SIAM J. Math. Anal. 13 (4) (1982) 555–593.
[18] P. Quittner, Bifurcation points and eigenvalues of inequalities of reaction-diffusion type, J. Reine Angew. Math. 380 (1987) 1–13.
[19] A.B. Rovinsky, M. Menzinger, Self-organization induced by the differential flow of activator and inhibitor, Phys. Rev. Lett. 70 (1993) 778–781.
[20] V. Rybář, T. Vejchodský, Irregularity of Turing patterns in the Thomas model with a unilateral term, in: Programs and Algorithms of Numerical Mathematics, Vol. 17, Acad. Sci. Czech Repub. Inst. Math., Prague, 2015, pp. 188–193.
[21] J. Schnakenberg, Simple chemical reaction systems with limit cycle behaviour, J. Theoret. Biol. 81 (3) (1979) 389–400.
[22] J. Smoller, Shock Waves and Reaction-Diffusion Equations, in: Fundamental Principles of Mathematical Science, vol. 258, Springer-Verlag, New York-Berlin, 1983, p. xxi+581.
[23] A.M. Turing, The chemical basis of morphogenesis, Philos. Trans. R. Soc. Lond. Ser. B 237 (641) (1952) 37–72.
[24] T. Vejchodský, F. Jaroš, M. Kučera, V. Rybář, Unilateral regulation breaks regularity of Turing patterns, Phys. Rev. E 96 (2017) 022212.

C | Appendix

[FLG20] M. Fencl and J. López-Gómez. *Nodal solutions of weighted indefinite problems.* Journal of Evolution Equations, 2020, published on-line at doi:10.1007/s00028-020-00625–7

J. Evol. Equ.

https://doi.org/10.1007/s00028-020-00625-7

Journal of Evolution Equations

Nodal solutions of weighted indefinite problems

M. FENCL AND J. LÓPEZ-GÓMEZ

This paper is dedicated to M. Hieber at the occasion of his 60th birthday mit Wertschätzung und Freundschaft

Abstract. This paper analyzes the structure of the set of nodal solutions, i.e., solutions changing sign, of a class of one-dimensional superlinear indefinite boundary value problems with indefinite weight functions in front of the spectral parameter. Quite surprisingly, the associated high-order eigenvalues may not be concave as is the case for the lowest one. As a consequence, in many circumstances, the nodal solutions can bifurcate from three or even four bifurcation points from the trivial solution. This paper combines analytical and numerical tools. The analysis carried out is a paradigm of how mathematical analysis aids the numerical study of a problem, whereas simultaneously the numerical study confirms and illuminates the analysis.

1. Introduction

In this paper, we analyze the nodal solutions of the one-dimensional nonlinear weighted boundary value problem

$$\begin{cases} -u'' - \mu u = \lambda m(x)u - a(x)u^2 & \text{in } (0,1), \\ u(0) = u(1) = 0, \end{cases} \tag{1.1}$$

where $a, m \in \mathcal{C}[0,1]$ are functions that change sign in $(0,1)$ and $\lambda, \mu \in \mathbb{R}$ are regarded as bifurcation parameters. More precisely, λ is the primary parameter and μ the secondary one. All the numerical experiments carried out in this paper have been implemented in the special case when

$$a(x) := \begin{cases} -0.2 \sin\left(\frac{\pi}{0.2}(0.2 - x)\right) & \text{if } 0 \le x \le 0.2, \\ \sin\left(\frac{\pi}{0.6}(x - 0.2)\right) & \text{if } 0.2 < x \le 0.8, \\ -0.2 \sin\left(\frac{\pi}{0.2}(x - 0.8)\right) & \text{if } 0.8 < x \le 1, \end{cases} \tag{1.2}$$

Mathematics Subject Classification: 34B15, 34B08, 34L16

Keywords: Superlinear indefinite problems, Weighted problems, Positive solutions, Nodal solutions, Eigencurves, Concavity, Bifurcation, Global components, Path-following, Pseudo-spectral methods, Finite-difference scheme.

Partially supported by the Research Grant PGC2018-097104-B-I00 of the Spanish Ministry of Science, Innovation and Universities, and the Institute of Inter-disciplinary Mathematics (IMI) of Complutense University. M. Fencl has been supported by the Project SGS-2019-010 of the University of West Bohemia, the Project 18-03253S of the Grant Agency of the Czech Republic and the Project LO1506 of the Czech Ministry of Education, Youth and Sport.

Published online: 06 October 2020

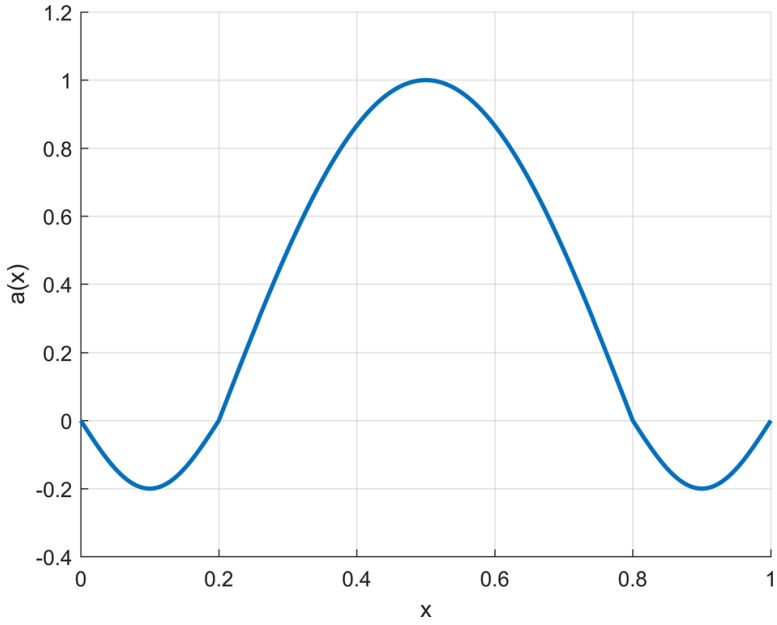

Figure 1. Graph of the weight function $a(x)$

because this is the weight function $a(x)$ considered by López-Gómez and Molina-Meyer [29] to compute the global bifurcation diagrams of positive solutions. Figure 1 shows a plot of this function. In this paper, we pay a very special attention to the particular, but very interesting, case when

$$m(x) = \sin(j\pi x)$$

for some integer $j \geq 2$.

To the best of our knowledge, this is the first paper where the problem of the existence and the structure of nodal solutions of a weighted superlinear indefinite problem is addressed when $m(x)$ changes sign. The existence results for large solutions of Mawhin et al. [40] required $m \equiv 1$, as well as the results of López-Gómez et al. [36], where the attention was focused on the problem of ascertaining the structure of the set of positive solutions. Most available results on nodal solutions deal with the special cases when $m \equiv 1$, $\mu = 0$ and $a(x)$ is a positive function with $\min_{[0,1]} a > 0$ (see Rabinowitz [41–43]), or with the degenerate case when $a(x)$ is a continuous positive function such that $a^{-1}(0) = [\alpha, \beta] \subset (0, 1)$ (see López-Gómez and Rabinowitz [37–39] and López-Gómez et al. [34]). In strong contrast to the classical cases when $\min_{[0,1]} a > 0$, in the degenerate case when $a \geq 0$ with $a^{-1}(0) = [\alpha, \beta] \subset (0, 1)$, the set of nodal solutions might consist of two, or even more, components, depending on the nature of the weight function $a(x)$ (see [34,39] for further details). Nevertheless, as for the special choice $a(x)$ given by (1.2), $a(x)$ is negative in the intervals $(0, 0.2)$ and $(0.8, 1)$, while it is positive in the central interval $(0.2, 0.8)$, this is the first time that the problem of analyzing the structure of the nodal solutions in this type of superlinear indefinite problems is addressed.

A natural strategy for constructing the solutions of (1.1) with $n \geq 0$ interior zeroes, or nodes, consists in linearizing (1.1) at the trivial solution, $u = 0$, and then searching for the eigenvalues of the linearization having an associated eigenfunction with exactly n interior nodes in $(0, 1)$, for as these values of the parameters will provide us, through the local bifurcation theorem of Crandall and Rabinowitz [12], with all the small nodal solutions of (1.1) bifurcating from $u = 0$. This strategy leads us, in a rather natural way, to the linear weighted eigenvalue problem

$$\begin{cases} -\varphi'' - \mu\varphi - \lambda m(x)\varphi = \sigma\varphi & \text{in } (0, 1), \\ \varphi(0) = \varphi(1) = 0. \end{cases} \tag{1.3}$$

By Sturm–Liouville theory, Problem (1.3) has a sequence of eigenvalues

$$\Sigma_n(\lambda, \mu) := \sigma_n[-D^2 - \mu - \lambda m(x); (0, 1)], \qquad n \geq 1,$$

which are algebraically simple. Moreover, associated with each of them, there is an eigenfunction, φ_n, with $\varphi_n'(0) > 0$, unique up to a multiplicative constant, with exactly $n - 1$ interior nodes, necessarily simple, in $(0, 1)$. By uniqueness,

$$\Sigma_n(\lambda, \mu) := \sigma_n[-D^2 - \lambda m(x); (0, 1)] - \mu, \qquad n \geq 1. \tag{1.4}$$

It turns out that the set of all the possible bifurcation points from $u = 0$ to solutions of (1.1) with $n - 1$ interior zeroes corresponds to values of λ and μ for which

$$\Sigma_n(\lambda, \mu) = 0.$$

This motivates the analysis of these curves. Throughout this paper, we will denote

$$\Sigma_n(\lambda) := \Sigma(\lambda, 0) = \sigma_n[-D^2 - \lambda m(x); (0, 1)], \qquad n \geq 1. \tag{1.5}$$

Then,

$$\Sigma_n(\lambda, \mu) = \Sigma_n(\lambda) - \mu$$

and $\Sigma_n(0) = (n\pi)^2$ for all $n \geq 1$. Based on a classical result of Kato [22] on perturbation of simple eigenvalues, for every $n \geq 1$, $\Sigma_n(\lambda)$ is analytic in $\lambda \in \mathbb{R}$. A proof of this can be obtained by means of [27, Ch. 9] and Section 5 of Antón and López-Gómez [2], where the result was established when $n = 1$. An extremely important property of $\Sigma_1(\lambda)$ is its strict concavity with respect to the parameter λ (see Berestycki et al. [5], Cano-Casanova and López-Gómez [10] and Chapter 9 of [27]). It holds that $\Sigma_1'(\lambda) > 0$ for all $\lambda < 0$, $\Sigma_1'(0) = 0$, $\Sigma_1'(\lambda) < 0$ for all $\lambda > 0$, and

$$\Sigma_1''(\lambda) < 0 \quad \text{for all } \lambda \in \mathbb{R}. \tag{1.6}$$

Since $\Sigma_1(0) = \pi^2$, this property entails that, for every $\mu < \pi^2$, $\Sigma_1^{-1}(\mu)$ consists of two values of λ,

$$\lambda_- \equiv \lambda_-(\mu) < 0 < \lambda_+ \equiv \lambda_+(\mu),$$

which are the unique bifurcation values to positive solutions from $u = 0$ of (1.1) (see López-Gómez and Molina-Meyer [29]). Even dealing with general second order elliptic operators under general mixed boundary conditions of non-classical type, the strict concavity of $\Sigma_1(\lambda)$ relies on the strong ellipticity of the operator (see, e.g., Chapter 8 of [27]).

For analytic semigroups, the spectral mapping theorem holds (see, e.g., [3,4]), i.e.,

$$\sigma(e^{D^2+\lambda m})\backslash\{0\} = e^{-\sigma(-D^2-\lambda m)} = \left\{e^{-\sigma_n(-D^2-\lambda m;(0,1))} \ : \ n \geq 1\right\}.$$

Thus, the spectral radius of the associated semigroup is given through the formula

$$\varrho(\lambda) := \mathrm{spr}\,(e^{D^2+\lambda m}) = e^{-\sigma_1(-D^2-\lambda m;(0,1))} = e^{-\Sigma_1(\lambda)}, \qquad \lambda \in \mathbb{R}.$$

Hence, $\varrho(\lambda)$ is logarithmically convex, which is a classical property observed by Kato [21], and equivalent to the concavity of $\Sigma_1(\lambda)$.

According to Propositions 1.10 and 1.11 of Figueiredo [17], for every $\mu \leq 0$, the eigenvalue problem

$$\begin{cases} -\varphi'' - \mu\varphi = \lambda m(x)\varphi & \text{in } (0,1), \\ \varphi(0) = \varphi(1) = 0, \end{cases}$$

has a double sequence of eigenvalues

$$\cdots \leq \lambda_{-2}(\mu) \leq \lambda_{-1}(\mu) < 0 < \lambda_1(\mu) \leq \lambda_2(\mu) \leq \cdots$$

such that $\lim_{n\to\infty} \lambda_n(\mu) = +\infty$ and $\lim_{n\to\infty} \lambda_{-n}(\mu) = -\infty$. Actually, by a result of Hess and Kato [20], $\lambda_{-2}(\mu) < \lambda_{-1}(\mu) < 0 < \lambda_1(\mu) < \lambda_2(\mu)$. Thus, it is rather natural to believe that in the one-dimensional setting $\lambda_{-(n+1)}(\mu) < \lambda_{-n}(\mu)$ and $\lambda_n(\mu) < \lambda_{n+1}(\mu)$ for all $n \geq 1$ and that for every $n \in \mathbb{Z}$, associated with $\lambda_n(\mu)$ there is a unique eigenfunction, up to a multiplicative constant, φ_n, with $n-1$ interior nodes in $(0,1)$, as it occurs in the setting of the Sturm–Liouville theory. Rather surprisingly, this is not true for sufficiently large $\mu > 0$ because $\Sigma_n(\lambda)$ is not necessarily concave for all $n \geq 2$. Actually, there are examples of weight functions $m(x)$ for which none of the remaining eigenvalues $\Sigma_n(\lambda)$, $n \geq 2$, is concave with respect to λ. Figure 2 shows one of these examples for the special choice $m(x) = \sin(2\pi x)$.

In this case, $\Sigma_1(\lambda)$ is the unique eigencurve which is concave. All other curves are symmetric functions of λ, with a quadratic local minimum at $\lambda = 0$, as illustrated by Fig. 2. This fact has dramatic implications from the point of view of the structure of the set of nodal solutions of the problem (1.1). Indeed, setting

$$\mu_n = \max_{\lambda\in\mathbb{R}} \Sigma_n(\lambda), \qquad n \geq 1, \tag{1.7}$$

it is easily seen that $\mu_n > \Sigma_n(0) = (n\pi)^2$ for all $n \geq 1$ and, hence, for every $n \geq 2$ and any $\mu \in ((n\pi)^2, \mu_n)$, $\Sigma_n^{-1}(\mu)$ consists of two negative eigenvalues, $\lambda_{-[1,n]}(\mu) < \lambda_{-[2,n]}(\mu) < 0$, and two positive eigenvalues $0 < \lambda_{+[2,n]}(\mu) < \lambda_{+[1,n]}(\mu)$ such that

$$0 < \lambda_{+[2,n]}(\mu) = -\lambda_{-[2,n]}(\mu) < \lambda_{+[1,n]}(\mu) = -\lambda_{-[1,n]}(\mu).$$

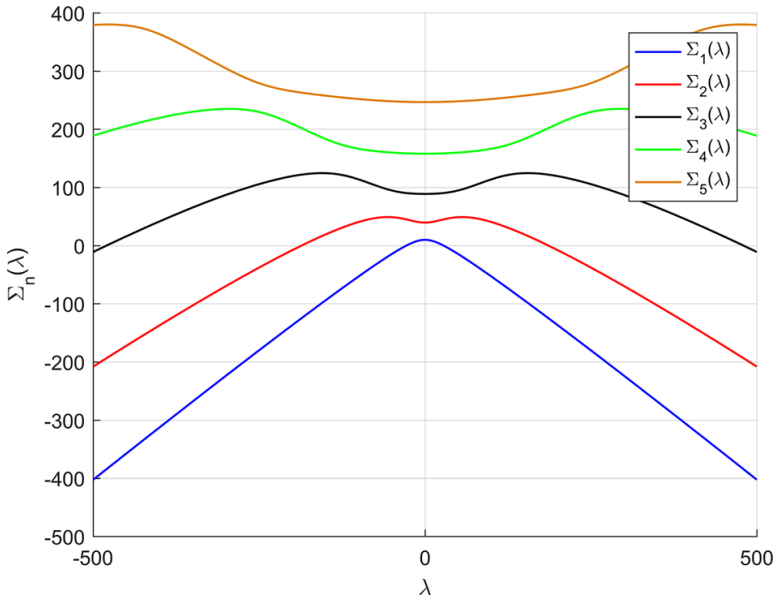

Figure 2. Curves $\Sigma_n(\lambda)$ for $1 \leq n \leq 5$ and $m(x) = \sin(2\pi x)$

Therefore, for this range of μ, we expect that the solutions with $n-1$ interior nodes of (1.1) will bifurcate from the trivial solution at each of the four values

$$\lambda = \lambda_{\pm[i,n]}, \quad i = 1, 2.$$

By construction, letting $\mu \downarrow (n\pi)^2$, it follows that

$$\lambda_{\pm[2,n]}((n\pi)^2) = 0.$$

Moreover,

$$\lambda_{-[1,n]}(\mu_n) = \lambda_{-[2,n]}(\mu_n) < 0 < \lambda_{+[2,n]}(\mu_n) = \lambda_{+[1,n]}(\mu_n),$$

at least for $n \in \{2, 3, 4, 5\}$.

As illustrated in Fig. 3, the number of eigencurves, $\Sigma_n(\lambda)$, $n \geq 2$, which are concave in λ might vary with the weight function $m(x)$. Indeed, when $m(x) = \sin(4\pi x)$, it turns out that not only $\Sigma_1(\lambda)$ but also $\Sigma_2(\lambda)$ is strictly concave, while the remaining eigencurves, $\Sigma_n(\lambda)$, with $n \geq 3$, are not concave. Similarly, when $m(x) = \sin(6\pi x)$, then $\Sigma_j(\lambda)$ are concave for $j \in \{1, 2, 3\}$, while they are not concave for $j \geq 4$.

As suggested by our numerical computations, the more wiggled $m(x)$ is, the higher the number of modes is for which $\Sigma_n(\lambda)$ is concave.

The structure of this paper is as follows. Section 2 studies some global properties of the eigencurves $\Sigma_n(\lambda)$ for all $n \geq 2$ and analyzes their concavities in the special case when, for some $k \geq 1$,

$$m(x) = \sin(2k\pi x), \qquad x \in [0, 1]. \tag{1.8}$$

In Sect. 3, some global bifurcation diagrams of nodal solutions of (1.1) with one and two interior nodes are derived; they complement the global bifurcation diagrams of positive solutions of López-Gómez and Molina-Meyer [29]. Finally, in Sect. 4, we describe the numerical schemes used to get the global bifurcation diagrams of Sect. 3.

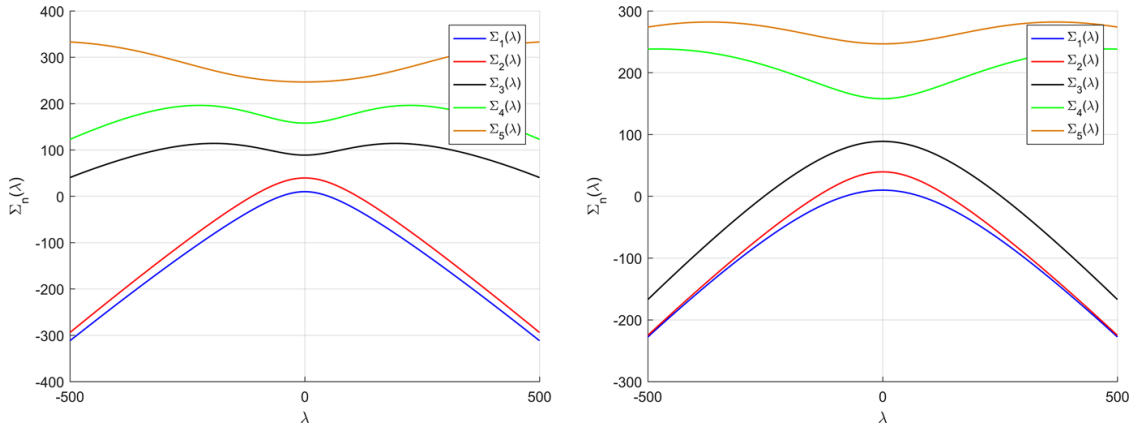

Figure 3. Curves $\Sigma_n(\lambda)$ for $1 \leq n \leq 5$ with $m(x) = \sin(j\pi x)$, $j = 4, 6$

2. Some global properties of the nodal eigencurves $\Sigma_n(\lambda)$

Throughout this paper, for any given $r, s \in \mathbb{R}$ with $r < s$ and every continuous function $q \in \mathcal{C}[r, s]$, we denote by $\sigma_n[-D^2 + q(x); (r, s)]$, $n \geq 1$, the nth eigenvalue of the eigenvalue problem

$$\begin{cases} -\varphi'' + q(x)\varphi = \sigma\varphi & \text{in } (r, s), \\ \varphi(r) = \varphi(s) = 0. \end{cases} \tag{2.1}$$

The next properties are well known (see, e.g., [9]):

(i) *Monotonicity of σ_n with respect to $q(x)$:* If $q, \tilde{q} \in \mathcal{C}[r, s]$ satisfy $q \lneq \tilde{q}$, then

$$\sigma_n[-D^2 + q(x); (r, s)] < \sigma_n[-D^2 + \tilde{q}; (r, s)] \quad \text{for all } n \geq 1.$$

(ii) *Monotonicity of σ_n with respect to the interval:* If $[\alpha, \beta] \subset (r, s)$, then

$$\sigma_n[-D^2 + q; (r, s)] < \sigma_n[-D^2 + q; (\alpha, \beta)] \quad \text{for all } n \geq 1.$$

Based on these properties, as suggested by Figs. 2 and 3, the next result holds.

Proposition 2.1. *Suppose that there exist $x_\pm \in (0, 1)$ such that $\pm m(x_\pm) > 0$, i.e., $m(x)$ changes the sign in $(0, 1)$. Then, for every $n \geq 1$,*

$$\lim_{\lambda \downarrow -\infty} \Sigma_n(\lambda) = -\infty, \qquad \lim_{\lambda \uparrow \infty} \Sigma_n(\lambda) = -\infty. \tag{2.2}$$

Proof. Consider a sufficiently small $\varepsilon > 0$ such that

$$J_\varepsilon := [x_+ - \varepsilon, x_+ + \varepsilon] \subset (0, 1), \qquad \min_{J_\varepsilon} m = m_L > 0.$$

Then, by the monotonicity properties of Σ_n, for every $\lambda > 0$ and $n \geq 1$, we have that

$$\begin{aligned} \Sigma_n(\lambda) &= \sigma_n[-D^2 - \lambda m(x); (0, 1)] < \sigma_n[-D^2 - \lambda m(x); J_\varepsilon] \\ &< \sigma_n[-D^2 - \lambda m_L; J_\varepsilon] = \sigma_n[-D^2; J_\varepsilon] - \lambda m_L = \left(\frac{n\pi}{2\varepsilon}\right)^2 - \lambda m_L. \end{aligned}$$

Thus, letting $\lambda \uparrow \infty$, the second relation of (2.2) holds. The first one follows by applying this result to the weight function $-m(x)$. □

The fact that all the eigencurves plotted in Figs. 2 and 3 are symmetric about the y-axis is a direct consequence of the next general result, because

$$\sin(2k\pi(1-x)) = -\sin(2k\pi x),$$

for all integer $k \geq 1$ and $x \in [0,1]$.

Proposition 2.2. *Suppose that $m \neq 0$ is a continuous function in $[0,1]$ such that*

$$m(1-x) = -m(x) \quad \text{for all} \quad x \in [0,1]; \tag{2.3}$$

this holds assuming (1.8). Then, $\Sigma_n(-\lambda) = \Sigma_n(\lambda)$ for all $\lambda \in \mathbb{R}$ and any integer $n \geq 1$. In particular,

$$\dot{\Sigma}_n(0) = 0 \quad \text{for all} \quad n \geq 1, \tag{2.4}$$

where we are denoting $\dot{\Sigma}_n = \frac{d\Sigma_n}{d\lambda}$.

Proof. Since $m \neq 0$, either there exists $x_+ \in (0,1)$ such that $m(x_+) > 0$, or $m(x_-) < 0$ for some $x_- \in (0,1)$. Suppose the first alternative occurs. Then, by (2.3), we also have that

$$m(1-x_+) = -m(x_+) < 0$$

and hence, $m(x)$ changes the sign in $(0,1)$. In particular, (2.2) holds.

Pick an integer $n \geq 1$, a real number λ, and let ϕ_n be an eigenfunction associated with $\Sigma_n(\lambda)$. Then, ϕ_n possesses $n-1$ zeros in $(0,1)$, $\phi_n(0) = \phi_n(1) = 0$, and

$$-\phi_n''(x) = \lambda m(x)\phi_n(x) + \Sigma_n(\lambda)\phi_n(x)$$

for all $x \in (0,1)$. Thus, setting

$$\psi_n(x) := \phi_n(1-x), \qquad x \in [0,1],$$

it is easily seen that

$$\psi_n'(x) := -\phi_n'(1-x), \quad \psi_n''(x) = \phi_n''(1-x), \qquad x \in [0,1],$$

and hence, for every $x \in (0,1)$,

$$\begin{aligned} -\psi_n''(x) = -\phi_n''(1-x) &= \lambda m(1-x)\phi_n(1-x) + \Sigma_n(\lambda)\phi_n(1-x) \\ &= \lambda m(1-x)\psi_n(x) + \Sigma_n(\lambda)\psi_n(x) \\ &= -\lambda m(x)\psi_n(x) + \Sigma_n(\lambda)\psi_n(x). \end{aligned}$$

Consequently, $\psi_n(x)$ is an eigenfunction associated with $-D^2 + \lambda m(x)$ with $n-1$ interior zeros. Therefore, by the uniqueness of Σ_n, it becomes apparent that

$$\Sigma_n(-\lambda) = \Sigma_n(\lambda) \quad \text{for all} \quad \lambda \in \mathbb{R}.$$

Since $\Sigma_n(\lambda)$ is an analytic function of λ, necessarily $\dot{\Sigma}_n(0) = 0$. □

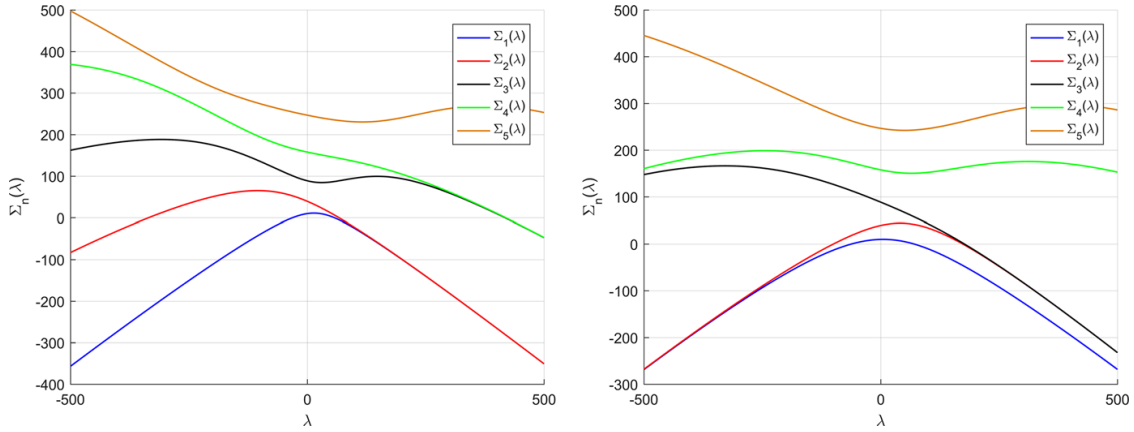

Figure 4. Curves $\Sigma_n(\lambda)$ for $1 \leq n \leq 5$ with $m(x) = \sin(j\pi x)$, $j = 3, 5$

Figure 4 shows that the function $\Sigma_n(\lambda)$ may not be an even function of λ if condition (2.3) fails.

The next result establishes that, as already suggested by Figs. 2 and 3, the nodal eigencurves, $\Sigma_n(\lambda)$, cannot be concave for the choice (1.8) if $n \geq k+1$. We conjecture that, in general, for that particular choice, Σ_n is concave if $n \leq k$. Therefore, Σ_n should be concave if, and only if, $n \leq k$. The analysis of the concavity when $n \leq k$ for the choice (1.8) remains outside the general scope of this paper.

Theorem 2.1. *Assume* (1.8) *for some integer* $k \geq 1$. *Then, as soon as* $n \geq k+1$,

$$\ddot{\Sigma}_n(0) > 0 \quad \textit{for all} \quad n \geq k+1. \tag{2.5}$$

Therefore, by (2.4), $\lambda = 0$ *is a local minimum of* $\Sigma_n(\lambda)$ *and, in particular,* $\Sigma_n(\lambda)$ *cannot be concave.*

Proof. Since $\Sigma_n(\lambda)$ is algebraically simple for all $n \geq 1$, we already know that $\Sigma_n(\lambda)$ is analytic, by well-known perturbation results of Kato [21]. Moreover, the eigenfunction associated with $\Sigma_n(\lambda)$, denoted by $\varphi_{[n,\lambda]}$, can be chosen to be analytic in λ by normalizing it so that

$$\int_0^1 \varphi^2_{[n,\lambda]}(x)\,\mathrm{d}x = \frac{1}{2}. \tag{2.6}$$

By definition, $\varphi_{[n,\lambda]}(0) = \varphi_{[n,\lambda]}(1) = 0$ and

$$-\varphi''_{[n,\lambda]}(x) = \lambda m(x)\varphi_{[n,\lambda]}(x) + \Sigma_n(\lambda)\varphi_{[n,\lambda]}(x) \quad \text{for all} \quad x \in (0,1). \tag{2.7}$$

Thus, since $\Sigma_n(0) = (n\pi)^2$, evaluating (2.7) at $\lambda = 0$ and taking (2.6) into account, it becomes apparent that $\varphi_{[n,\lambda]}$ is an analytic perturbation of the eigenfunction

$$\varphi_{[n,0]}(x) = \sin(n\pi x), \qquad x \in [0,1].$$

Moreover, differentiating (2.7) with respect to λ yields

$$-\dot{\varphi}''_{[n,\lambda]}(x) = \lambda m\dot{\varphi}_{[n,\lambda]} + m\varphi_{[n,\lambda]} + \dot{\Sigma}_n(\lambda)\varphi_{[n,\lambda]} + \Sigma_n(\lambda)\dot{\varphi}_{[n,\lambda]} \quad \text{in} \quad (0,1). \tag{2.8}$$

Thus, since $\Sigma_n(0) = (n\pi)^2$ and $\dot{\Sigma}_n(0) = 0$, evaluating (2.8) at $\lambda = 0$ shows that $\dot{\varphi}_{[n,0]}$ solves the problem

$$\begin{cases} [-D^2 - (n\pi)^2]u = m\varphi_{[n,0]} & \text{in } (0,1), \\ u(0) = u(1) = 0. \end{cases} \tag{2.9}$$

In order to find $\dot{\varphi}_{[n,0]}$, we first determine the general solution of the linear inhomogeneous equation

$$[-D^2 - (n\pi)^2]u = m(x)\sin(n\pi x). \tag{2.10}$$

Set $v := u'$ in order to vary coefficients in the first-order system associated with (2.10),

$$\begin{pmatrix} u' \\ v' \end{pmatrix} = \begin{pmatrix} 0 & 1 \\ -(n\pi)^2 & 0 \end{pmatrix} \begin{pmatrix} u \\ v \end{pmatrix} + \begin{pmatrix} 0 \\ -m(x)\sin(n\pi x) \end{pmatrix}. \tag{2.11}$$

Since

$$W(x) := \begin{pmatrix} \cos(n\pi x) & \sin(n\pi x) \\ -n\pi\sin(n\pi x) & n\pi\cos(n\pi x) \end{pmatrix}$$

is a fundamental matrix of solutions for the homogeneous linear system associated with (2.11), the change of variable

$$\begin{pmatrix} u \\ v \end{pmatrix} = W(x) \begin{pmatrix} c_1(x) \\ c_2(x) \end{pmatrix}$$

transforms (2.11) into the equivalent system

$$W(x) \begin{pmatrix} c_1'(x) \\ c_2'(x) \end{pmatrix} = \begin{pmatrix} 0 \\ -m(x)\sin(n\pi x) \end{pmatrix},$$

whose solution, according to Cramer's rule, is given through

$$c_1'(x) = \frac{1}{n\pi} m(x)\sin^2(n\pi x), \qquad c_2'(x) = \frac{-1}{n\pi} m(x)\sin(n\pi x)\cos(n\pi x).$$

Thus,

$$\begin{aligned} c_1(x) &= \frac{1}{n\pi}\int_0^x m(s)\sin^2(n\pi s)\,\mathrm{d}s + A, \\ c_2(x) &= -\frac{1}{n\pi}\int_0^x m(s)\sin(n\pi s)\cos(n\pi s)\,\mathrm{d}s + B, \end{aligned}$$

for some constants $A, B \in \mathbb{R}$. Therefore, the general solution of (2.10) is given by

$$\begin{aligned} u(x) &= \cos(n\pi x)c_1(x) + \sin(n\pi x)c_2(x) \\ &= \cos(n\pi x)\left(A + \frac{1}{n\pi}\int_0^x m(s)\sin^2(n\pi s)\,\mathrm{d}s\right) \end{aligned}$$

$$+\sin(n\pi x)\left(B-\frac{1}{n\pi}\int_0^x m(s)\sin(n\pi s)\cos(n\pi s)\,\mathrm{d}s\right)$$
$$=A\cos(n\pi x)+B\sin(n\pi x)+p(x),$$

where

$$p(x):=\frac{1}{n\pi}\int_0^x m(s)\sin(n\pi s)\sin[n\pi(s-x)]\,\mathrm{d}s,\qquad x\in[0,1],\tag{2.12}$$

is a particular solution of (2.10). It is the solution obtained by making the choice $A=B=0$. Obviously, $p(0)=0$. Moreover, by (1.8),

$$p(1)=\int_0^1 m(s)\sin(n\pi s)\sin[n\pi(s-1)]\,\mathrm{d}s$$
$$=(-1)^n\int_0^1\sin(2k\pi s)\sin^2(n\pi s)\,\mathrm{d}s=0,$$

because the integrand,

$$\theta(s):=\sin(2k\pi s)\sin^2(n\pi s),\qquad s\in[0,1],$$

satisfies $\theta(1-s)=-\theta(s)$ for all $s\in[0,1]$ and hence, it is odd about 0.5. As we are interested in solving (2.9), we should make the choice

$$0=u(0)=A+p(0)=A.$$

Thus,

$$\dot\varphi_{[n,0]}(x)=B\sin(n\pi x)+p(x),\qquad x\in[0,1],$$

for some constant $B\in\mathbb{R}$. To determine B, we can proceed as follows. Differentiating (2.6) with respect to λ and evaluating the resulting identity at $\lambda=0$ yield

$$0=\int_0^1\varphi_{[n,0]}(x)\dot\varphi_{[n,0]}(x)\,\mathrm{d}x=B\int_0^1\sin^2(n\pi x)\,\mathrm{d}x+\int_0^1\sin(n\pi x)p(x)\,\mathrm{d}x.$$

Consequently,

$$B=-2\int_0^1\sin(n\pi x)p(x)\,\mathrm{d}x$$

and therefore,

$$\dot\varphi_{[n,0]}(x)=-2\left(\int_0^1\sin(n\pi s)p(s)\,\mathrm{d}s\right)\sin(n\pi x)+p(x),\qquad x\in[0,1].\tag{2.13}$$

To find $\ddot\Sigma_n(0)$, we can differentiate identity (2.8) with respect to λ. After rearranging terms, this gives

$$[-D^2-\lambda m-\Sigma_n(\lambda)]\ddot\varphi_{[n,\lambda]}=2m\dot\varphi_{[n,\lambda]}+2\dot\Sigma_n(\lambda)\dot\varphi_{[n,\lambda]}+\ddot\Sigma_n(\lambda)\varphi_{[n,\lambda]}.$$

Thus, evaluating at $\lambda = 0$ yields

$$[-D^2 - (n\pi)^2]\ddot{\varphi}_{[n,0]} = 2m\dot{\varphi}_{[n,0]} + \ddot{\Sigma}_n(0)\varphi_{[n,0]} \tag{2.14}$$

and hence, multiplying (2.14) by $\varphi_{[n,0]}$ and integrating over $(0, 1)$, it is apparent that

$$\ddot{\Sigma}_n(0) = -4\int_0^1 m(x)\dot{\varphi}_{[n,0]}(x)\varphi_{[n,0]}(x)\,\mathrm{d}x. \tag{2.15}$$

Therefore, substituting (2.13) into (2.15) and using (1.8) yield

$$\begin{aligned}\ddot{\Sigma}_n(0) &= -4\int_0^1 m(x)\varphi_{[n,0]}(x)p(x)\,\mathrm{d}x \\ &= -4\int_0^1 \sin(2k\pi x)\sin(n\pi x)\left[\frac{1}{n\pi}\int_0^x \sin(2k\pi s)\sin(n\pi s)\sin(n\pi(s-x))\,\mathrm{d}s\right]\mathrm{d}x.\end{aligned}$$

Finally, we need the trigonometric formulas

$$\sin x \sin y = \tfrac{1}{2}\left[\cos(x-y) - \cos(x+y)\right], \tag{2.16}$$

$$\sin x \cos y = \tfrac{1}{2}\left[\sin(x-y) + \sin(x+y)\right], \tag{2.17}$$

to simplify the integrands in $\ddot{\Sigma}_n(0)$. First, we will determine the function $p(x)$. For this, we use formula (2.16) on $\sin(2k\pi s)\sin(n\pi s)$ and then formula (2.17) to simplify the integrand in $p(x)$. Then, integrating yields

$$p(x) = -\frac{1}{8\pi^2}\left[\frac{\cos(\pi x(2k-n))}{k(n-k)} + \frac{\cos(\pi x(2k+n))}{k(n+k)} - \frac{n\cos(n\pi x)}{k(n^2-k^2)}\right]. \tag{2.18}$$

After substituting (2.18) into the formula for $\ddot{\Sigma}_n(0)$, we can again use formulae (2.16) and (2.17) to simplify the underlying integrands, which can then be directly integrated. The result can be simplified to get the final formula

$$\ddot{\Sigma}_n(0) = \frac{1}{4\pi^2(n^2-k^2)}.$$

Obviously, $n^2 - k^2 > 0$ if $n \geq k+1$, and therefore $\ddot{\Sigma}_n(0) > 0$. Hence, the eigencurves $\Sigma_n(\lambda)$ are convex in a neighborhood of $\lambda = 0$ for $n \geq k+1$. Thus, they cannot be globally concave.

3. Global bifurcation of nodal solutions

Since $\Sigma_1(0) = \pi^2$, for every $\mu < \pi^2$ the set $\Sigma_1^{-1}(\mu)$ consists of two points,

$$\lambda_-(\mu) < 0 < \lambda_+(\mu),$$

such that

$$\lim_{\mu\uparrow\pi^2} \lambda_\pm(\mu) = 0.$$

Moreover, owing to Theorem 9.4 of [27],

$$\dot{\Sigma}_1(\lambda_-(\mu)) > 0 \quad \text{and} \quad \dot{\Sigma}_1(\lambda_+(\mu)) < 0.$$

Thus, by the main theorem of Crandall and Rabinowitz [12] (one can see also Chapter 2 of [26]), $\lambda = \lambda_\pm(\mu)$ are the unique bifurcation values of λ to positive solutions of (1.1) from $u = 0$. The first plot of Fig. 1 of López-Gómez and Molina-Meyer [29] shows one of those bifurcation diagrams for the special choice (1.2) of $a(x)$ with

$$m(x) = \sin(2\pi x), \qquad x \in [0, 1]. \tag{3.1}$$

In order to complement the numerical experiments of [29] with our new findings here, all the numerical experiments of this section have been carried out for this special choice of $m(x)$. As μ increases to reach the critical value $\mu = \pi^2$, the set of positive solutions of (1.1) bifurcating from $u = 0$ consists of one single closed loop bifurcating from $u = 0$ at the single point $\lambda = 0$. These loops, separated from $u = 0$, are persistent for a large range of values of $\mu > \pi^2$, until they shrink to a single point before disappearing at some critical value of the parameter μ (see [29, Fig. 1]).

According to Theorem 2.1, $\Sigma_2(\lambda)$ is not concave if (3.1) holds, which is clearly illustrated by simply looking at the plot of $\Sigma_2(\lambda)$ in Fig. 2. This feature has important implications concerning the structure of the set of 1-node solutions of (1.1). Indeed, according to the plot of $\Sigma_2(\lambda)$, for every $\mu < (2\pi)^2$, the set $\Sigma_2^{-1}(\mu)$ consists of two single values $\lambda_-(\mu) < 0 < \lambda_+(\mu)$ with $\dot{\Sigma}_2(\lambda_-(\mu)) > 0$ and $\dot{\Sigma}_2(\lambda_+(\mu)) < 0$. Thus, according to [27, Th. 9.4], the transversality condition of Crandall and Rabinowitz [12] holds at $(\lambda, u) = (\lambda_\pm(\mu), 0)$. Hence, an analytic curve of one-node solutions of (1.1) emanates from $u = 0$ at each of these values of λ, $\lambda_\pm(\mu)$. Figure 5a shows the plots of these two curves for the value of the parameter $\mu = 35$. Our numerical experiments suggest that they are separated from each other. In this bifurcation diagram, as well as in all the remaining ones, we are plotting the values of λ versus the L^2-norm of the solutions. So, each point on the curves of the bifurcation diagrams, (λ, u), represents a value of λ and a nodal solution u of (1.1) for that particular value of λ.

When μ grows to reach the critical value $(2\pi)^2$, the two components become closer and closer until they meet at $\lambda = 0$ at $\mu = (2\pi)^2$, where the set of bifurcation points to one-node solutions from $u = 0$ consists of the points $(\lambda_\pm((2\pi)^2), 0)$ plus $(0, 0)$. This is the situation sketched by Fig. 5b, where we have plotted the global bifurcation diagram computed for

$$\mu = 39.6 > 39.4786 \sim (2\pi)^2.$$

When $\mu \in ((2\pi)^2, \mu_2)$, where μ_2 is given by (1.7), the set $\Sigma_2^{-1}(\mu)$ consists of four values: two negative, $\lambda_{-[1,2]}(\mu) < \lambda_{-[2,2]}(\mu) < 0$, plus two positive, $0 < \lambda_{+[2,2]}(\mu) < \lambda_{+[1,2]}(\mu)$. Moreover, by Proposition 2.2, it is apparent that

$$0 < \lambda_{+[2,2]}(\mu) = -\lambda_{-[2,2]}(\mu) < \lambda_{+[1,2]}(\mu) = -\lambda_{-[1,2]}(\mu).$$

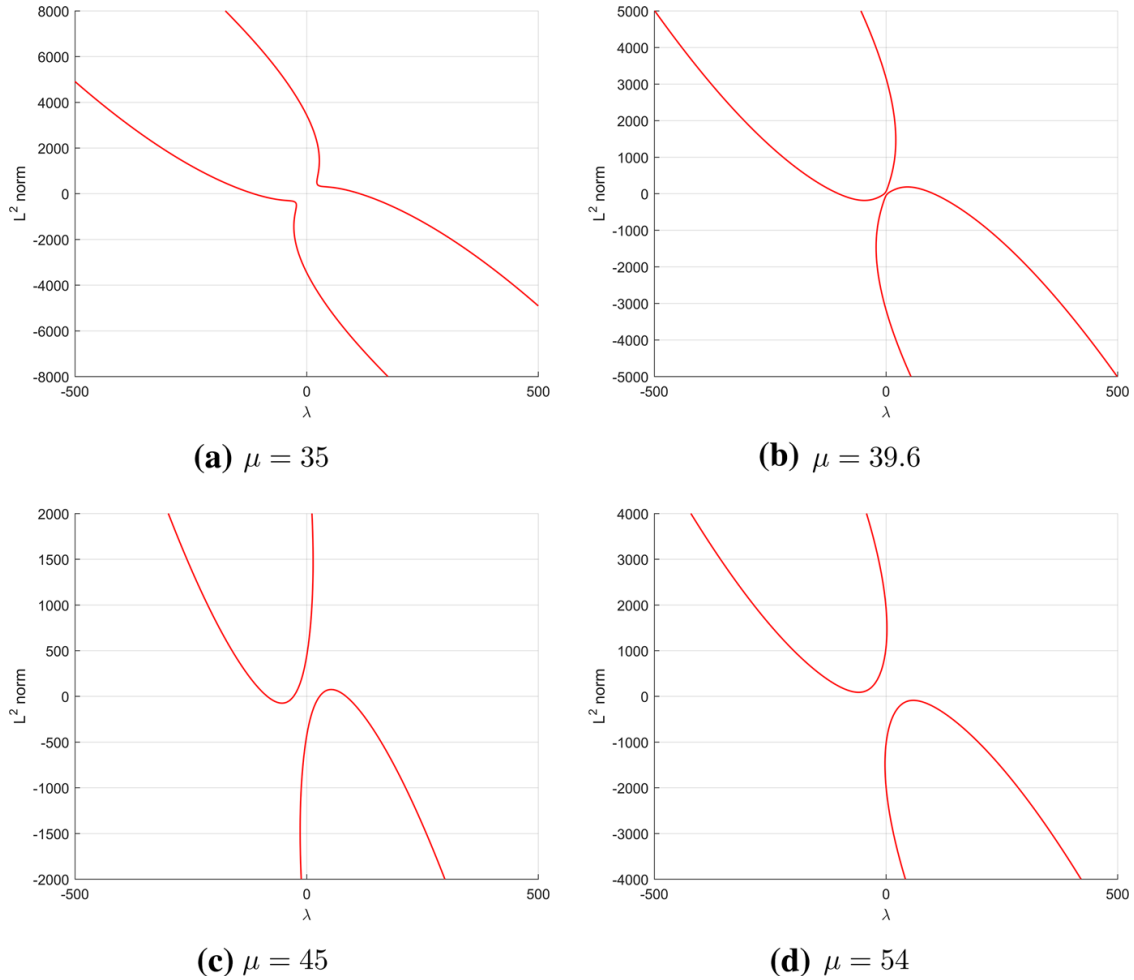

(a) $\mu = 35$ **(b)** $\mu = 39.6$

(c) $\mu = 45$ **(d)** $\mu = 54$

Figure 5. Four representative bifurcation diagrams of one-node solutions

Furthermore, as suggested by our numerical experiments,

$$\dot{\Sigma}_2(\lambda_{-[1,2]}(\mu)) > 0, \quad \dot{\Sigma}_2(\lambda_{-[2,2]}(\mu)) < 0,$$
$$\dot{\Sigma}_2(\lambda_{+[2,2]}(\mu)) > 0, \quad \dot{\Sigma}_2(\lambda_{+[1,2]}(\mu)) < 0.$$

Thus, again the transversality condition of [12] holds at each of these critical values of the parameter λ. Therefore, (1.1) should possess four analytic curves filled in by one-node solutions bifurcating from $u = 0$ at each of these critical values of the parameter λ. Figure 5c shows the global bifurcation diagram of one-node solutions bifurcating from these four bifurcation points that we have computed for $\mu = 45$. Once again, the set of one-node solutions consists of two components.

As soon as the transversality condition of Crandall and Rabinowitz [12] holds, the generalized algebraic multiplicity of Esquinas and López-Gómez [15,26], χ, equals 1 and hence, thanks to Theorem 5.6.2 of López-Gómez [26], the Leray–Schauder index of $u = 0$, as a solution of (1.1), changes as λ crosses each of these values. Therefore, each component of the set of nontrivial solutions of (1.1) emanating from $u = 0$ at each of these critical values of the primary parameter λ satisfies the global alternative

of Rabinowitz [41], i.e., either it is unbounded in $\mathbb{R} \times \mathcal{C}[0, 1]$, or it meets the trivial solution in, at least, two of these singular values.

Each of the two components plotted in Fig. 5c bifurcates from two different points of $(\lambda, 0)$, and according to our numerical experiments, both seem to be unbounded. The problem of ascertaining their precise global behavior remains open. As μ increases and crosses the critical value μ_2, these two components disconnect from the trivial solution and stay separated from it, becoming *isolas*, i.e., components separated from the trivial branch. Figure 5d shows the plots of these components for $\mu = 54$. In Fig. 6, we plot some distinguished solutions with one node along some of the pieces of the global bifurcation diagrams of Fig. 5. Namely, Fig. 6b shows a series of solutions with one node along the same-colored branches of Fig. 6a, which is a magnification of a part of the left component of Fig. 5a, and Fig. 6d shows a series of solutions with one node along the bifurcation diagram plotted in Fig. 6c, which is a magnification of a part of the left component plotted in Fig. 5d. The colors of each of these one-node solutions correspond to the color of the part of the bifurcation diagram on the left where they are coming from.

Similarly, according to Theorem 2.1, for the special choice (3.1), the third eigencurve, $\Sigma_3(\lambda)$, is not concave if (3.1) holds. This can be seen in the plot of $\Sigma_3(\lambda)$ in Fig. 2. For every $\mu \in ((3\pi)^2, \mu_3)$, the set $\Sigma_3^{-1}(\mu)$ consists of two negative eigenvalues, $\lambda_{-[1,3]}(\mu) < \lambda_{-[2,3]}(\mu) < 0$, and two positive eigenvalues, $0 < \lambda_{+[2,3]}(\mu) < \lambda_{+[1,3]}(\mu)$. Moreover, by Proposition 2.2,

$$0 < \lambda_{+[2,3]}(\mu) = -\lambda_{-[2,3]}(\mu) < \lambda_{+[1,3]}(\mu) = -\lambda_{-[1,3]}(\mu)$$

and, according to our numerical experiments,

$$\dot{\Sigma}_2(\lambda_{-[1,3]}(\mu)) > 0, \quad \dot{\Sigma}_2(\lambda_{-[2,3]}(\mu)) < 0, \quad \dot{\Sigma}_2(\lambda_{+[2,3]}(\mu)) > 0,$$
$$\dot{\Sigma}_2(\lambda_{+[1,3]}(\mu)) < 0.$$

Thus, the transversality condition of [12] holds at each of these critical values and the local bifurcation theorem of [12] implies that an analytic curve of two-node solutions emanates from $u = 0$ at each of these four singular values of λ. The first three plots of Fig. 7 show these curves for three different values of the secondary parameter μ. Namely, $\mu = 105$, $\mu = 108.1$ and $\mu = 110$, respectively. All these values satisfy $\mu < \mu_3$. The last plot of Fig. 7 is computed for $\mu = 140 > \mu_3$ and shows three components of two-node solutions separated from $u = 0$. For this value of μ, no solution with two interior nodes can bifurcate from $u = 0$.

More precisely, at $\mu = 105$, problem (1.1) possesses three components of solutions with two interior nodes: two of them bifurcating from $u = 0$ at $\lambda_{-[1,3]}(105)$ and $\lambda_{+[1,3]}(105)$, respectively, and the third one linking $(\lambda_{-[2,3]}(105), 0)$ with $(\lambda_{+[2,3]}(105), 0)$. According to our numerical experiments, these components are unbounded in $\mathbb{R} \times \mathcal{C}[0, 1]$ and are persistent for all further value of μ below some critical value, $\mu_c < 108.1$, where the three components meet. Thus, for $\mu = \mu_c$, there is a component of the set of nontrivial solutions of (1.1) bifurcating from $u = 0$ at four

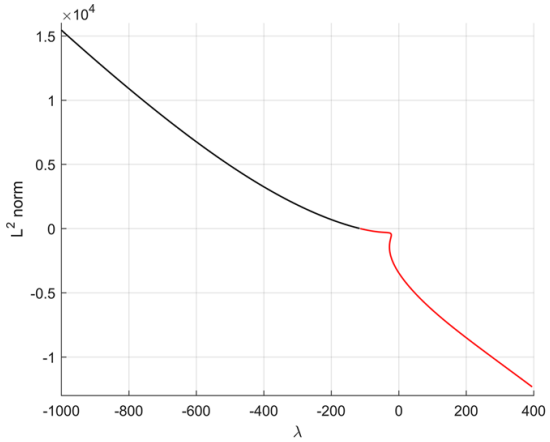

(a) A part of the left branch of Figure 5a for $\mu = 35$

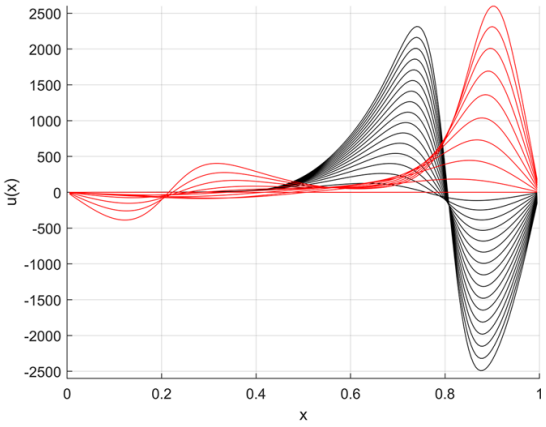

(b) A series of same-colored solutions on the left branches

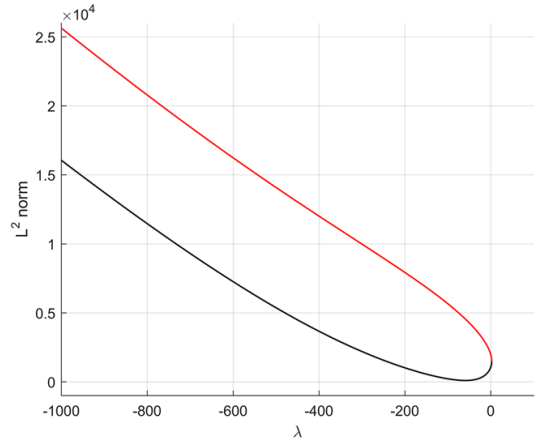

(c) A part of the left branch of Figure 5d for $\mu = 54$

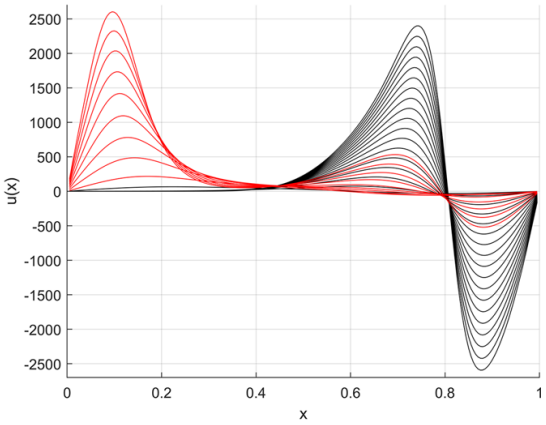

(d) A series of same-colored solutions on the left branches

Figure 6. A series of plots of one-node solutions (right) along some of the same-colored components of Fig. 5 (left) (Color figure online)

different values of λ: $\lambda_{\pm[1,3]}(\mu_c)$ and $\lambda_{\pm[2,3]}(\mu_c)$. The plot in Fig. 7b shows the corresponding global bifurcation diagram for $\mu = 108.1$, a value of μ slightly greater than μ_c, where the three components of nontrivial solutions are very close. Comparing to the global bifurcation diagram for $\mu = 105$, it becomes apparent that a *global imperfect bifurcation* has happened at the critical value μ_c. As a consequence, one of the components bifurcating from $u = 0$ links $(\lambda_{-[1,3]}(108.1), 0)$ with $(\lambda_{-[2,3]}(108.1), 0)$, another links $(\lambda_{+[2,3]}(108.1), 0)$ with $(\lambda_{+[1,3]}(108.1), 0)$, while the third one remains separated from $u = 0$. The latter remains separated from zero for any further value of μ. Therefore, a reorganization of the components of the set of two-node solutions occurs as μ crosses μ_c. The pictures in Fig. 7c, d show the plots of the corresponding components for $\mu = 110 < \mu_3$ and $\mu = 140 > \mu_3$, where the previous bifurcations from $u = 0$ of these components are lost. For larger values of μ, the solutions along these three components become larger and larger and it remains an open problem to

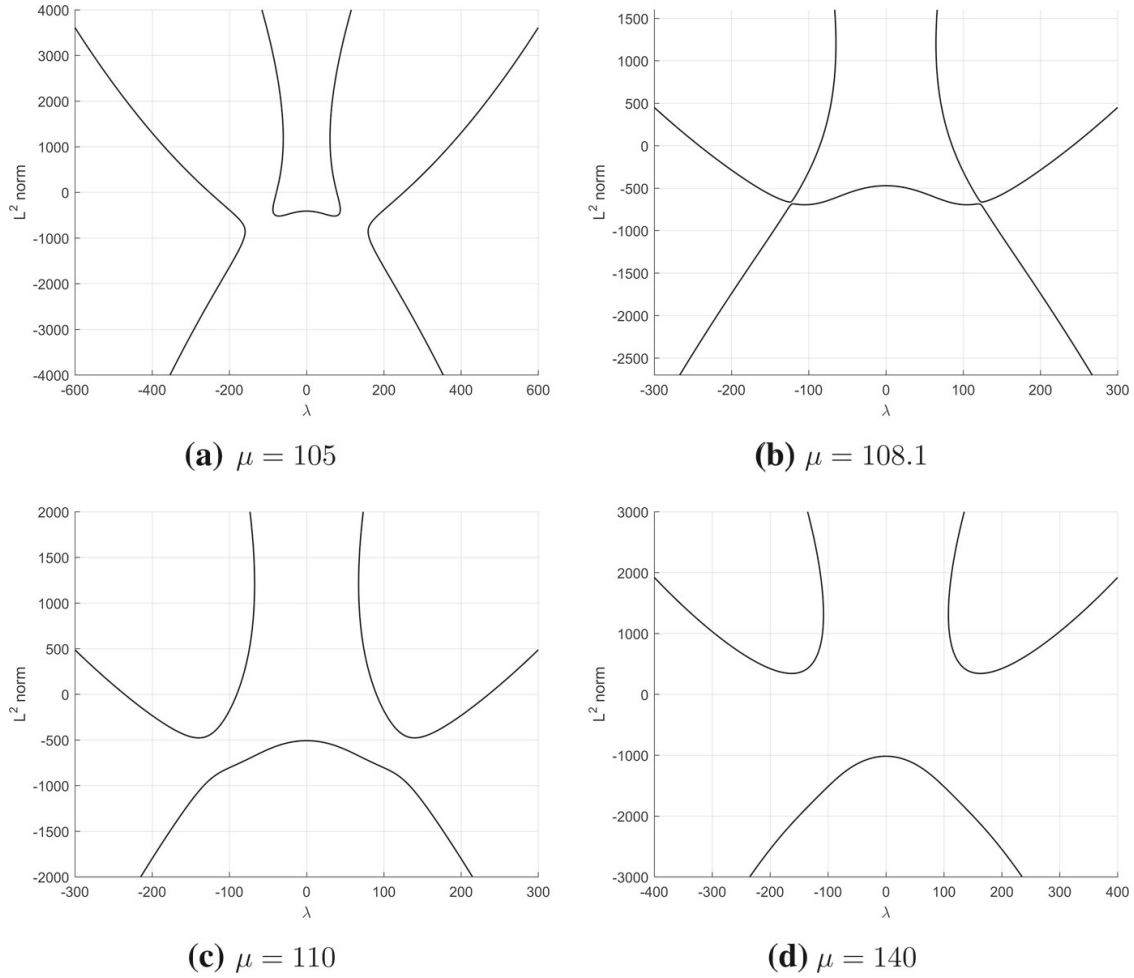

(a) $\mu = 105$ **(b)** $\mu = 108.1$

(c) $\mu = 110$ **(d)** $\mu = 140$

Figure 7. Four representative bifurcation diagrams of two-node solutions

ascertain whether, or not, (1.1) can admit some two-node solution for sufficiently large μ. Figure 8 shows the plots of some distinguished two-node solutions of (1.1) along some of the curves of the bifurcation diagrams plotted in Fig. 7.

Finally, Fig. 9 contains the global bifurcation diagrams of positive solutions found in [29] (in blue) together with the global bifurcation diagrams of nodal solutions with one node (in red) and two nodes (in black) computed in this paper for four different values of μ: 0, 54, 70 and 100. Although all the components of nodal solutions persist for these values of μ, the component of positive solutions shrinks to a single point and disappears at a value of μ above 54 but very close to it. In Fig. 9b, one can still see an small piece of blue trace component shortly before disappearing for an slightly greater value of μ.

4. Numerical methods and their implementation

To discretize (1.1), we have used two methods. To compute the small solutions bifurcating from $u = 0$, we implemented a pseudo-spectral method combining a

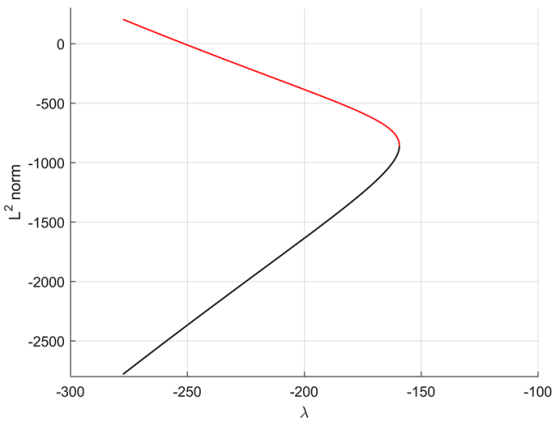

(a) Left branch of Figure 7a ($\mu = 105$)

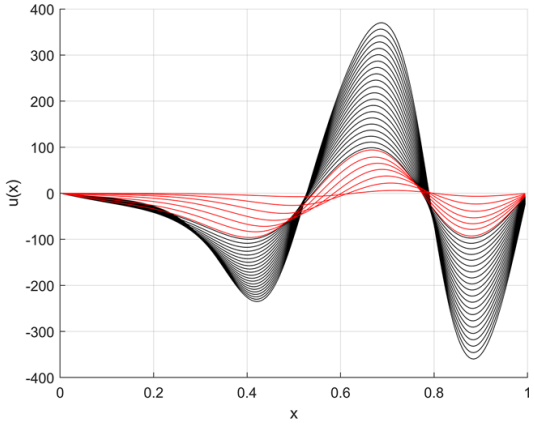

(b) Corresponding profiles of solutions.

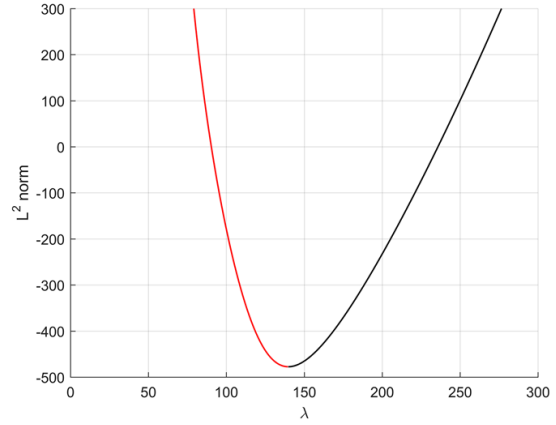

(c) Right branch of Figure 7c ($\mu = 110$)

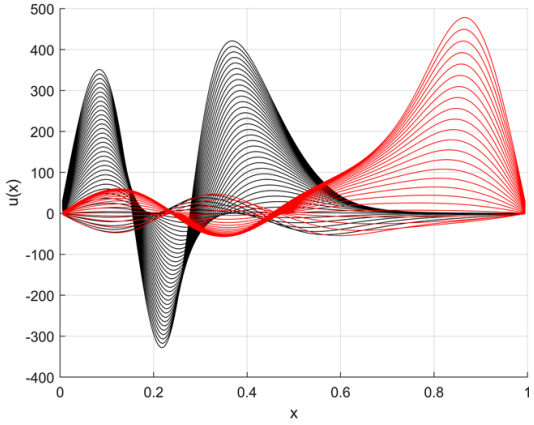

(d) Corresponding profiles of solutions

Figure 8. Some plots of two-node solutions (right) along the bifurcation diagrams of Fig. 7 (left)

trigonometric spectral method with collocation at equidistant points, as in most of the previous numerical experiments of the second author and coworkers (see, e.g., [18,19,28,30–33]). This gives high accuracy (see, e.g., Canuto et al. [11]). However, to compute the large solutions, we have used a centered finite difference scheme, which gives high accuracy at a lower computational cost. This provides us with a much faster code to compute global solution curves.

The pseudo-spectral method is easier to use and more efficient for choosing the shooting direction from the trivial solution in order to compute the small nodal solutions of (1.1), as well as to detect bifurcation points along the bifurcation diagrams. This is due to the fact that it provides us with the true bifurcation values from $u = 0$, while the schemes in differences only approximate them.

For general Galerkin approximations, the local convergence of the solution paths at regular, turning and simple bifurcation points was proven by Brezzi et al. [6–8] and by López-Gómez et al. [28,35] at codimension two singularities in the context of systems. In these situations, the local structures of the solution sets for the continuous and the discrete models are known to be equivalent. The global continuation solvers

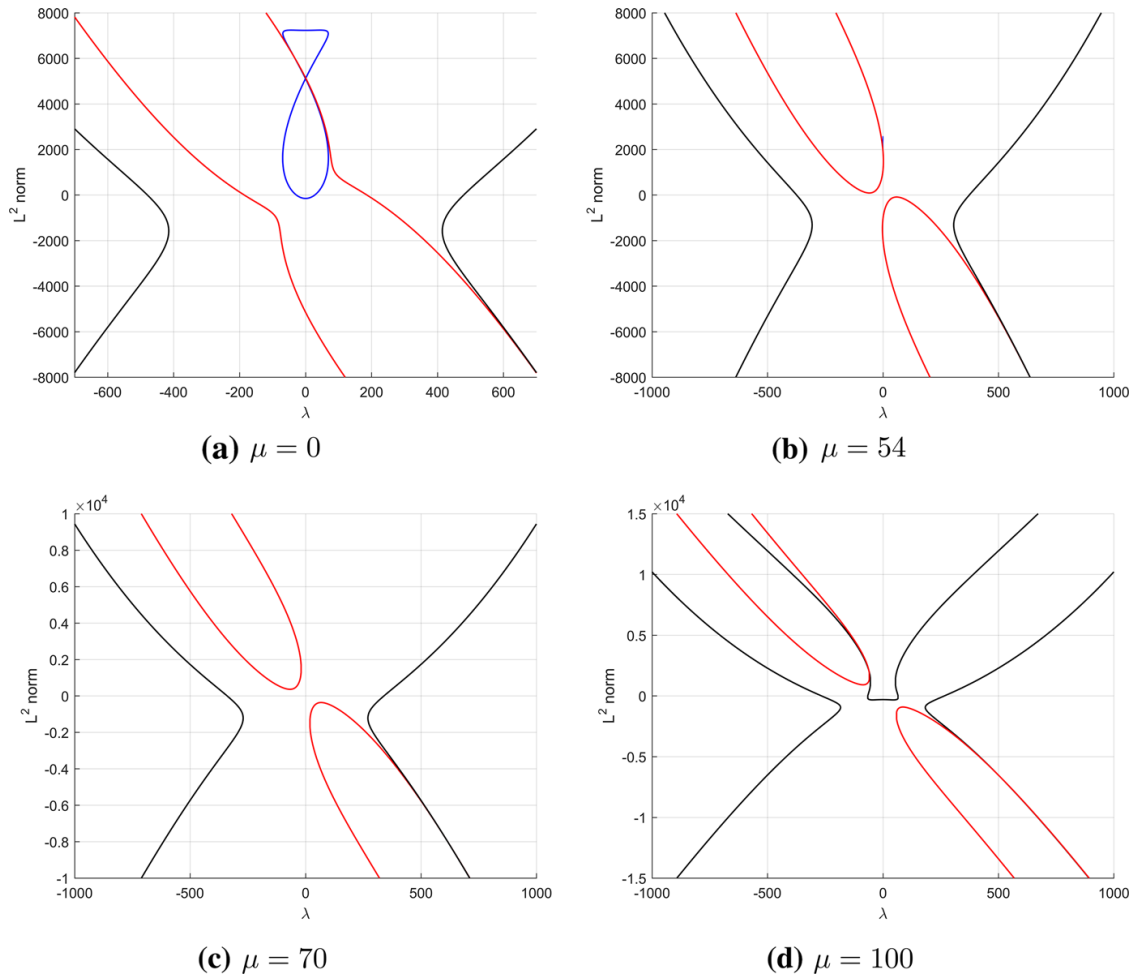

Figure 9. Some bifurcation diagrams with superimposed branches of positive (blue), one-node (red) and two-node (black) solutions (Color figure online)

used to compute the solution curves of this papers, as well as the dimensions of the unstable manifolds of all the solutions along them, have been built from the theory on continuation methods of Allgower and Georg [1], Crouzeix and Rappaz [13], Eilbeck [16], Keller [23], Keller and Yang [24], López-Gómez [25] and López-Gómez et al. [28].

The complexity of the bifurcation diagrams, as well as their quantitative features, required an extremely careful control of all the steps in subroutines. This explains why the available commercial bifurcation packages such as AUTO-07P are not useful to deal with differential equations with heterogeneous coefficients. As a matter of fact, Doedel and Oldeman admitted in [14, p.18] that

"Note that, given the non-adaptive spatial discretization, the computational procedure here is not appropriate for PDEs with solutions that rapidly vary in space, and care must be taken to recognize spurious solutions and bifurcations."

This is just one of the main problems that we found in our numerical experiments, as the number of critical points of the solutions increases according to the dimensions of unstable manifolds, and the turning and bifurcation points might be very close.

Acknowledgements

We thank the, anonymous, reviewer for his/her extremely careful reading of the paper, which has greatly improved it.

REFERENCES

[1] E. L. Allgower and K. Georg, *Introduction to Numerical Continuation Methods*, SIAM Classics in Applied Mathematics 45, SIAM, Philadelphia, 2003.

[2] I. Antón and J. López-Gómez, Principal eigenvalues of weighted periodic-parabolic problems, *Rend. Istit. Mat. Univ. Trieste* **49** (2017), 287–318.

[3] W. Arendt, C. J. K. Batty, M. Hieber and F. Neubrander, *Vector-valued Laplace transforms and Cauchy problems*, Monographs in Mathematics vol. 96, Birkhäuser/Springer, Basel, 2011.

[4] W. Arendt, A. Grabosch, G. Greiner, U. Groh, H. P. Lotz, U. Moustakas, R. Nagel, F. Neubrander and U. Schlotterbeck, *One Parameter Semigroups of Positive Operators*, Lectures Notes in Mathematics 1184, Berlin, Springer, 1986.

[5] H. Berestycki, L. Nirenberg and S. R. S. Varadhan, The principal eigenvalue and maximum principle for second order elliptic operator sin general domains, *Comm. Pure Appl. Math.* **47** (1994), 47–92.

[6] F. Brezzi, J. Rappaz and P. A. Raviart, Finite dimensional approximation of nonlinear problems, part I: Branches of nonsingular solutions, *Numer. Math.* **36** (1980), 1–25.

[7] F. Brezzi, J. Rappaz and P. A. Raviart, Finite dimensional approximation of nonlinear problems, part II: Limit points, *Numer. Math.* **37** (1981), 1–28.

[8] F. Brezzi, J. Rappaz and P. A. Raviart, Finite dimensional approximation of nonlinear problems, part III: Simple bifurcation points, *Numer. Math.* **38** (1981), 1–30.

[9] G. Buttazzo, M. Giaquinta and S. Hildebrandt, *One-dimensional Variational Problems*, Clarendon Press, Oxford, 1998.

[10] S. Cano-Casanova and J. López-Gómez, Properties of the principal eigenvalues of a general class of nonclassical mixed boundary value problems, *J. Dif. Eqns.* **178** (2002), 123–211.

[11] C. Canuto, M. Y. Hussaini, A. Quarteroni and T. A. Zang, *Spectral Methods in Fluid Mechanics*, Springer, Berlin, Germany, 1988.

[12] M. G. Crandall and P. H. Rabinowitz, Bifurcation from simple eigenvalues, *J. Funct. Anal.* **8** (1971), 321–340.

[13] M. Crouzeix and J. Rappaz, *On Numerical Approximation in Bifurcation Theory*, Recherches en Mathématiques Appliquées 13, Masson, Paris, 1990.

[14] E. J. Doedel and B. E. Oldeman, AUTO-07P: Continuation and bifurcation software for ODEs, 2012, http://www.dam.brown.edu/people/sandsted/auto/auto07p.pdf.

[15] J. Esquinas and J. López-Gómez, Optimal multiplicity in local bifurcation theory: Generalized generic eigenvalues, *J. Diff. Eqns.* **71** (1988), 72–92.

[16] J. C. Eilbeck, The pseudo-spectral method and path-following in reaction-diffusion bifurcation studies, *SIAM J. Sci. Stat. Comput.* **7** (1986), 599–610.

[17] D. G. de Figueiredo, *Positive Solutions of Semilinear Elliptic Problems*, Lectures Notes of a Latin-American School on Differential Equations, Sao Paolo 1981, Lectures Notes in Mathematics 957 (pp. 34–87), Springer, 1982.

[18] R. Gómez-Reñasco and J. López-Gómez, The effect of varying coefficients on the dynamics of a class of superlinear indefinite reaction diffusion equations, *J. Diff. Eqns.* **167** (2000), 36–72.

[19] R. Gómez-Reñasco and J. López-Gómez, On the existence and numerical computation of classical and non-classical solutions for a family of elliptic boundary value problems, *Nonl. Anal. TMA* **48** (2002), 567–605.
[20] P. Hess and T. Kato, On some linear and nonlinear eigenvalue problems with an indefinite weight function, *Comm. Part. Dif. Eqns.* **5** (1980), 999–1030.
[21] T. Kato, Superconvexity of the spectral radius and convexity of the spectral bound and the type, *Math. Z.* **180** (1982), 265–273.
[22] T. Kato, *Perturbation Theory for Linear Operators*, Springer, 1995.
[23] H. B. Keller, *Lectures on Numerical Methods in Bifurcation Problems*, Tata Insitute of Fundamental Research, Springer, Berlin, Germany, 1986.
[24] H. B. Keller and Z. H. Yang, A direct method for computing higher order folds, *SIAM J. Sci. Stat.* **7** (1986), 351–361.
[25] J. López-Gómez *Estabilidad y Bifurcación Estática. Aplicaciones y Métodos Numéericos*, Cuadernos de Matemática y Mecánica, Serie Cursos y Seminarios 4, Santa Fe, R. Argentina, 1988.
[26] J. López-Gómez, *Spectral Theory and Nonlinear Functional Analysis*, CRC Press, Boca Raton, 2001.
[27] J. López-Gómez, *Linear Second Order Elliptic Operators*, World Scientific Publishing, 2013.
[28] J. López-Gómez, J. C. Eilbeck, K. Duncan and M. Molina-Meyer, Structure of solution manifolds in a strongly coupled elliptic system, *IMA J. Numer. Anal.* **12** (1992), 405–428.
[29] J. López-Gómez and M. Molina-Meyer, Bounded components of positive solutions of abstract fized point equations: mushrooms, loops and isolas, *J. Diff. Eqns.* **209** (2005), 416–441.
[30] J. López-Gómez and M. Molina-Meyer, Superlinear indefinite systems: Beyond Lotka Volterra models, *J. Differ. Eqns.* **221** (2006), 343–411.
[31] J. López-Gómez and M. Molina-Meyer, The competitive exclusion principle versus biodiversity through segregation and further adaptation to spatial heterogeneities, *Theor. Popul. Biol.* **69** (2006), 94–109.
[32] J. López-Gómez and M. Molina-Meyer, Modeling coopetition, *Math. Comput. Simul.* **76** (2007), 132–140.
[33] J. López-Gómez, M. Molina-Meyer and A. Tellini, Intricate dynamics caused by facilitation in competitive environments within polluted habitat patches, *Eur. J. Appl. Maths.* https://doi.org/10.1017/S0956792513000429(2014), 1–17.
[34] J. López-Gómez, M. Molina-Meyer and P. H. Rabinowitz, Global bifurcation diagrams of one node solutions in a class of degenerate bundary value problems, *Disc. Cont. Dyn. Sys. B* **22** (2017), 923–946.
[35] J. López-Gómez, M. Molina-Meyer and M. Villareal, Numerical coexistence of coexistence states, *SIAM J. Numer. Anal.* **29** (1992), 1074–1092.
[36] J. López-Gómez, A. Tellini and F. Zanolin, High multiplicity and complexity of the bifurcation diagrams of large solutions for a class of superlinear indefinite problems, *Commun. Pure Appl. Anal.* **13** (2014), 1–73.
[37] J. López-Gómez and P. H. Rabinowitz, Nodal solutions for a class of degenerate boundary value problems, *Adv. Nonl. Studies* **15** (2015), 253–288.
[38] J. López-Gómez and P. H. Rabinowitz, Nodal solutions for a class of degenerate one dimensional BVPs, *Top. Meth. Nonl. Anal.* **49** (2017), 359–376.
[39] J. López-Gómez and P. H. Rabinowitz, The structure of the set of 1-node solutions of a class of degenerate BVP's, *J. Diff. Eqns.* 268 (2020), 4691–4732.
[40] J. Mawhin, D. Papini and F. Zanolin, Boundary blow-up for differential equations with indefinite weight, *J. Diff. Eqns.* **188** (2003), 33–51.
[41] P. H. Rabinowitz, Some global results for nonlinear eigenvalue problems, *J. Funct. Anal.* **7** (1971), 487–513.
[42] P. H. Rabinowitz, A note on a nonlinear eigenvalue problem for a class of differential equations, *J. Diff. Eqns.* **9** (1971), 536–548.
[43] P. H. Rabinowitz, A note on a pair of solutions of a nonlinear Sturm–Liouville problem, *Manuscr. Math.* **11** (1974), 273–282.

Nodal solutions of weighted indefinite problems

M. Fencl
Department of Mathematics and NTIS, Faculty of Applied Sciences
University of West Bohemia
Univerzitní 8
30100 Plzeň
Czech Republic
E-mail: fenclm37@ntis.zcu.cz

J. López-Gómez
Department of Analysis and Applied Mathematics,
Institute of Inter-disciplinary Mathematics (IMI)
Complutense University of Madrid
28040 Madrid
Spain
E-mail: Lopez_Gomez@mat.ucm.es

Accepted: 10 September 2020

D | Appendix

[FLG21] M. Fencl and J. López-Gómez. *Global bifurcation diagrams of positive solutions for a class of 1-d superlinear indefinite problems.* arXiv:2005.09369v3[math.AP] 7Mar2021, Submitted to Nonlinearity.

GLOBAL BIFURCATION DIAGRAMS OF POSITIVE SOLUTIONS FOR A CLASS OF 1-D SUPERLINEAR INDEFINITE PROBLEMS

M. FENCL AND J. LÓPEZ-GÓMEZ

Abstract. This paper analyzes the structure of the set of positive solutions of a class of one-dimensional superlinear indefinite bvp's. It is a paradigm of how mathematical analysis aids the numerical study of a problem, whereas simultaneously its numerical study confirms and illuminates the analysis. On the analytical side, we establish the fast decay of the positive solutions as $\lambda \downarrow -\infty$ in the region where $a(x) < 0$ (see (1.1)), as well as the decay of the solutions of the parabolic counterpart of the model (see (1.2)) as $\lambda \downarrow -\infty$ on any subinterval of $[0,1]$ where $u_0 = 0$, provided u_0 is a subsolution of (1.1). This result provides us with a proof of a conjecture of [29] under an additional condition of a dynamical nature. On the numerical side, this paper ascertains the global structure of the set of positive solutions on some paradigmatic prototypes whose intricate behavior is far from predictable from existing analytical results.

2010 MSC: 34B15, 34B08, 65N35, 65P30

Keywords and phrases: superlinear indefinite problems, positive solutions, bifurcation, uniqueness, multiplicity, global components, path-following, pseudo-spectral methods, finite-differences schemes.

Partially supported by the Research Grant PGC2018-097104-B-IOO of the Spanish Ministry of Science, Innovation and Universities, and the Institute of Inter-disciplinar Mathematics (IMI) of Complutense University. M. Fencl has been supported by the project SGS-2019-010 of the University of West Bohemia, the project 18-03253S of the Grant Agency of the Czech Republic and the project LO1506 of the Czech Ministry of Education, Youth and Sport.

1. Introduction

In this paper we study, both analytically and numerically, the global structure of the bifurcation diagram of positive solutions of the semilinear boundary value problem

$$\begin{cases} -u'' = \lambda u + a(x)u^2 & \text{in } (0,1), \\ u(0) = u(1) = 0, \end{cases} \tag{1.1}$$

where $a \in C[0,1]$ is a real function that changes the sign in $(0,1)$ and $\lambda \in \mathbb{R}$ is regarded as a bifurcation parameter. Moreover, we analyze the dynamics of its parabolic counterpart

$$\begin{cases} \frac{\partial u}{\partial t} - \frac{\partial^2 u}{\partial x^2} = \lambda u + a(x)u^2, & t > 0, \ \ x \in (0,1), \\ u(0,t) = u(1,t) = 0, & t > 0, \\ u(x,0) = u_0(x), & x \in [0,1], \end{cases} \tag{1.2}$$

for some significative choices of the initial data $u_0 \gneq 0$, i.e., $u_0 \geq 0$, $u_0 \neq 0$.

In our numerical experiments we have used the special choices

$$a(x) := \sin[(2n+1)\pi x], \qquad n \in \{1,2,3\}, \tag{1.3}$$

and

$$a(x) := \begin{cases} \mu \sin(5\pi x) & \text{if } \ x \in [0, 0.2) \cup (0.8, 1], \\ \sin(5\pi x) & \text{if } \ x \in [0.2, 0.8], \end{cases} \tag{1.4}$$

where $\mu \geq 1$ is regarded as a secondary bifurcation parameter. In these examples, the graph of $a(x)$ has $n+1$ positive and n negative bumps.

Since $a(x)$ changes the sign, (1.1) is a superlinear indefinite problem. These problems have attracted a lot of attention during the last three decades. Some significant monographs dealing with them are those of Berestycki, Capuzzo-Dolcetta and Nirenberg [5, 6], Alama and Tarantello [1], Amann and López-Gómez [3], Gómez-Reñasco and López-Gómez [29, 30], Mawhin, Papini and Zanolin [59], López-Gómez, Tellini and Zanolin [57], López-Gómez and Tellini [56], Feltrin and Zanolin, as well as Chapter 9 of López-Gómez [42], the recent monograph of Feltrin [24], and the list of references there in. Superlinear indefinite problems have been recently introduced in the context of quasilinear elliptic equations by López-Gómez, Omari and Rivetti [54, 55], and López-Gómez and Omari [51, 52, 53].

Thanks to Amann and López-Gómez [3], it is already known that (1.1) possesses a component of positive solutions, $\mathscr{C}^+ \subset \mathbb{R}\times\mathcal{C}[0,1]$, such that $(\pi^2, 0) \in \overline{\mathscr{C}^+}$, i.e., $\mathscr{C}^+$ bifurcates from $u = 0$ at $\lambda = \pi^2$. Moreover, $\mathscr{C}^+$ is unbounded in $\mathbb{R} \times \mathcal{C}[0,1]$, and (1.1) cannot admit a positive solution for sufficiently large $\lambda > \pi^2$. Furthermore, by the existence of universal a priori bounds uniform on compact subintervals of $\lambda \in \mathbb{R}$ for the positive solutions of (1.1), $(-\infty, \pi^2) \subset \mathcal{P}_\lambda(\mathscr{C}^+)$, where $\mathcal{P}_\lambda$ stands for the λ-projection operator defined by

$$\mathcal{P}_\lambda(\lambda, u) = \lambda, \qquad (\lambda, u) \in \mathbb{R} \times \mathcal{C}[0,1].$$

Actually, according to Gómez-Reñasco and López-Gómez [29, 30], either $\mathcal{P}_\lambda(\mathscr{C}^+) = (-\infty, \pi^2)$, or there exists $\lambda_t > \pi^2$ such that $\mathcal{P}_\lambda(\mathscr{C}^+) = (-\infty, \lambda_t]$. Moreover, (1.1) admits some stable positive solution if, and only if, $\lambda \in (\pi^2, \lambda_t]$, and, in such case, the stable solution is unique, and it equals the minimal positive solution of (1.1). The fact that λ_t is turning point is emphasized by its subindex.

Besides the (optimal) multiplicity result of Amann and López-Gómez [3], establishing that (1.1) has, at least, two positive solutions for every $\lambda \in (\pi^2, \lambda_t)$ if $\lambda_t > \pi^2$, there are some others multiplicity results by Gaudenzi, Habets and Zanolin [28] later generalized by Feltrin and Zanolin [25] and Feltrin [24]. Precisely, according to Corollary 1.4.2 of Feltrin [24], which extends [28, Th.2.1], setting $a = a^+ - \mu a^-$, there exists $\mu_c > 0$ such that, for every $\mu > \mu_c$, the problem

$$\begin{cases} -u'' = (a^+ - \mu a^-)u^2 & \text{in } (0,1), \\ u(0) = u(1) = 0, \end{cases} \tag{1.5}$$

possesses, for every $\mu > \mu_c$, at least, $2^{n+1} - 1$ positive solutions if $a(x)$ is given by (1.3). However, this result does not solve the conjecture of Gómez-Reñasco and López-Gómez [29] according with it there is a $\lambda_c < \pi^2$ such that, for every $\lambda < \lambda_c$, (1.1) possesses, at least,

$$\sum_{j=1}^{n+1} \binom{n+1}{j} = 2^{n+1} - 1$$

positive solutions; among them, $n+1$ with a single peak around each of the maxima of $a(x)$, $\frac{(n+1)n}{2}$ with two peaks, and, in general, $\frac{(n+1)!}{j!(n+1-j)!}$ with j peaks for every $j \in \{1, ..., n+1\}$. For instance, when $n = 1$, then $a(x) = \sin(3\pi x)$ and, according to our numerical experiments, (1.1) indeed has, for sufficiently negative λ, three positive solutions: one with a bump on the left, one with a bump on the right, and another one with two bumps (see Figure 3a). Note that, essentially, Corollary 1.4.2 of Feltrin [24] establishes that (1.1) possesses $2^{n+1} - 1$ positive solutions provided $\lambda = 0$ and $\|a^-\|_\infty$ is sufficiently large, though it does not give any information for $\lambda < 0$. Thus, after two decades, the conjecture of [29] seems to remain open. For the purpose of this paper, we formulate here this conjecture in the following manner:

Conjecture 1.1. *Suppose that $a(x)$ possesses $n+1$ intervals where it is positive separated away by n intervals where it is negative. Then, there exists $\lambda_c < \pi^2$ such that, for every $\lambda < \lambda_c$, the problem (1.1) admits, at least, $2^{n+1}-1$ positive solutions.*

The main goal of this paper is to gain some insight, on this occasion of a dynamical nature, into that conjecture and to face, by the first time, the ambitious problem of ascertaining the global topological structure of the set of positive solutions of (1.1). As a direct consequence of our numerical experiments for the special choice (1.4), it becomes apparent the optimality of [24, Cor. 1.4.2], in the sense that, for sufficiently small $\mu > 0$, the problem (1.5) might have less than $2^{n+1}-1$ positive solutions.

Throughout most of this paper, we will assume that, much like for the special choice (1.3), $a(x)$ satisfies

(H_a) The open sets

$$\Omega_- := a^{-1}((-\infty, 0)) \quad \text{and} \quad \Omega_+ := a^{-1}((0, \infty))$$

consist of finitely many (non-trivial) intervals, I_j^-, $j \in \{1, ..., r\}$, and I_i^+, $i \in \{1, ..., s\}$, respectively, and a vanishes at the ends of these intervals in such a way that each interior interval $I_i^{\pm}$ is surrounded by two intervals of the form $I_j^{\mp}$, much like it happens with the special choice (1.3). In such case, we will denote, $I_j^- = (\alpha_j, \beta_j)$, with $\alpha_j < \beta_j$ for all $j \in \{1, ..., r\}$, and $I_i^+ = (\gamma_i, \varrho_i)$, with $\gamma_i < \varrho_i$ for all $i \in \{1, ..., s\}$.

As these intervals are adjacent and interlacing, $|r - s| \leq 1$. Under this assumption, our main analytical results can be summarized as follows. Theorem 3.1 establishes that, for any family of positive solutions of (1.1), $\{(\lambda, u_\lambda)\}_{\lambda<0}$,

$$\lim_{\lambda \downarrow -\infty} u_\lambda(x) = 0 \quad \text{for all } \ x \in \Omega_- = \bigcup_{j=1}^{r} I_j^- \tag{1.6}$$

uniformly in compact subsets of Ω_-. Theorem 3.2 establishes that there exists $T > 0$ such that, as soon as $u_0 \geq 0$ is a subsolution of (1.1), the unique solution of (1.2), denoted by $u(x, t; u_0, \lambda)$, is defined in $[0, T]$ as $\lambda \downarrow -\infty$ and satisfies, for every $t \in [0, T]$ and $x \in \Omega_-$,

$$\lim_{\lambda \downarrow -\infty} u(x, t; u_0, \lambda) = 0. \tag{1.7}$$

Moreover, this behavior is inherited by the intervals I_i^+ where $u_0 = 0$, as soon as u_0 also vanishes at the adjacent I_j^-'s, as established by the next result.

Theorem 1.1. *Suppose that $u_0 \gneq 0$ is a subsolution of (1.1) such that $u_0 = 0$ on some interior I_i^+ for some $i \in \{1, ..., s\}$, as well as on its adjacent intervals, say I_j^- and I_{j+1}^-, i.e.,*

$$u_0 = 0 \quad \text{in } \ I_j^- \cup I_i^+ \cup I_{j+1}^- = (\alpha_j, \beta_j) \cup (\beta_j, \alpha_{j+1}) \cup (\alpha_{j+1}, \beta_{j+1}).$$

Then, there exists $T = T(u_0) > 0$ such that, for every $t \in [0, T]$ and $x \in (\alpha_j, \beta_{j+1})$,

$$\lim_{\lambda \downarrow -\infty} u(x, t; u_0, \lambda) = 0. \tag{1.8}$$

Moreover, (1.8) holds uniformly in compact subintervals of (α_j, β_{j+1}). A similar result holds true for $I_1^+ = (0, \varrho_1)$ and $I_s^+ = (\gamma_s, 1)$.

By a simple combinatorial argument, Theorem 1.1 provides us with a further evidence supporting the conjecture of [29]. Actually, it proves it under an additional assumption.

Indeed, suppose that $a(x)$ satisfies (H_a) with $r = n \geq 1$ and $s = n+1$ and, for every $i \in \{1, ..., n+1\}$, let $\theta_{\{\lambda,i\}}$ be a positive solution of

$$\begin{cases} -u'' = \lambda u + a^+(x)u^2 & \text{in } (\gamma_i, \varrho_i), \\ u(\gamma_i) = u(\varrho_i) = 0, \end{cases} \tag{1.9}$$

and consider the subsolution of (1.1) defined through

$$u_0 := \begin{cases} \theta_{\{\lambda,i\}} & \text{in } I_i^+, \qquad i \in \{1, ..., n+1\}, \\ 0 & \text{in } I_j^-, \qquad j \in \{1, ..., n\}. \end{cases}$$

Suppose that $u(x, t; u_0, \lambda)$ is globally bounded in time as $\lambda \downarrow -\infty$. Then, Theorem 3.3 shows that there exists $\lambda_c < 0$ such that (1.1) has $2^{n+1} - 1$ positive solutions for every $\lambda < \lambda_c$. But the extremely challenging problem of ascertaining whether or not $u(x, t; u_0, \lambda)$ is globally bounded as $\lambda \downarrow -\infty$ remains open in this paper.

Throughout this paper, for any $a(x)$ with $n+1$ positive bumps separated away by negative ones, we use a code with $n+1$ digits in $\{0, 1\}$, where 1 means that the solution has a bump localized at the nodal interval indicated by its position in the code, whereas 0 means that no bump in that position exists. Thus, when, e.g., $a(x) = \sin(3\pi x)$, we have positive solutions in Figure 3a represented by 2-digit codes, where 00 stands for the trivial solution, 10 stands for a solution with a single bump on the left, 01 stands for a solution with one single bump on the right, and 11 stands for a positive solution with both bumps around each of the interior maxima of $a(x)$. At the end of this code, called the *type of the solution* in this paper, we will always add a positive integer within parenthesis, the *Morse index*, i.e., the dimension of the unstable manifold of the positive solution as a steady state of the associated parabolic problem (1.2). The dimension of the unstable manifold of a given steady state solution, say u, equals the number of negative eigenvalues, τ, of the linearized problem

$$\begin{cases} -v'' = \lambda v + 2a(x)u(x)v + \tau v & \text{in } (0, 1), \\ v(0) = v(1) = 0. \end{cases} \tag{1.10}$$

Although there is a huge amount of literature on bump and multi-bump solutions for nonlinear Schrödinger equations (see, e.g., Ambrosetti, Badiale and Cingolani [4], del Pino and Felmer [20, 21], Dancer and Wei [19], Wei [64], Wang and Zeng [63], Byeon and Tanaka [12], among many others), in the existing literature $a(x)$ always is a positive function. So, none of these results can be applied in our general context, which explains why the conjecture of [29] remains open.

This paper is organized as follows. Section 2 collects the available information concerning the global structure of the set of positive solutions of (1.1) paying attention to the detail as some of these results, rather topological, are not well known by experts yet. In Section 3 we prove Theorem 1.1 by using the theory of metasolutions (see, e.g., [42]). Then, we infer from it Theorem 3.3. Finally, in Sections 4, 5 and 6 we present and discuss the results of our numerical experiments in cases $n = 1$, $n = 2$ and $n = 3$, respectively. In Section 7 we analyze the more sophisticate case when a is given by (1.4) using $\mu \geq 1$ as the secondary bifurcation parameter. In Section 8 we shortly discuss the necessary numerics to implement the numerical experiments of this paper. The paper ends with a final discussion carried out in Section 9. Discussing the results of our numerical experiments in this short general presentation seems inappropriate. The readers should enjoy them in their own sections.

2. Global structure of the component $\mathscr{C}^+$

This section analyzes the local and global behaviors of the component of positive solutions $\mathscr{C}^+$ introduced in Section 1. The next result, of a technical nature, allows us to express, equivalently, (1.1) as a fixed point equation for a compact operator. As the proof is elementary, we omit it herein.

Lemma 2.1. *For every $f \in \mathcal{C}[0,1]$, the function*

$$u(x) = \int_0^x (s-x)f(s)\,ds - x\int_0^1 (s-1)f(s)\,ds \tag{2.1}$$

provides us with the unique solution of the linear boundary value problem

$$\begin{cases} -u'' = f \quad in\ \ [0,1], \\ u(0) = u(1) = 0. \end{cases} \tag{2.2}$$

According to Lemma 2.1, we introduce the linear integral operator $K : \mathcal{C}[0,1] \to \mathcal{C}^2[0,1]$ defined, for every $f \in \mathcal{C}[0,1]$, by

$$Kf(x) := \int_0^x (s-x)f(s)\,ds - x\int_0^1 (s-1)f(s)\,ds, \quad x \in [0,1]. \tag{2.3}$$

Subsequently, for every integer $n \geq 0$, we denote by $\mathcal{C}_0^n[0,1]$ the closed subspace of the real Banach space $\mathcal{C}^n[0,1]$ consisting of all functions $u \in \mathcal{C}^n[0,1]$ such that $u(0) = u(1) = 0$, and denote $\mathcal{C}[0,1] := \mathcal{C}^0[0,1]$, $\mathcal{C}_0[0,1] := \mathcal{C}_0^0[0,1]$. The next result collects a pivotal property of the integral operator K.

Lemma 2.2. *$K : \mathcal{C}[0,1] \to \mathcal{C}_0^2[0,1]$ is linear and continuous.*

Proof: As the integral is linear, K is linear. Moreover, setting $u := Kf$, we have that

$$u'(x) = -\int_0^x f(s)\,ds - \int_0^1 (s-1)f(s)\,ds \quad \text{and} \quad u''(x) = -f(x)$$

for all $x \in [0,1]$. Thus,

$$\|u\|_\infty \leq 3\|f\|_\infty, \quad \|u'\|_\infty \leq 2\|f\|_\infty, \quad \|u''\|_\infty \leq \|f\|_\infty.$$

Therefore, for every $f \in \mathcal{C}[0,1]$,

$$\|Kf\|_{\mathcal{C}^2[0,1]} \leq 6\|f\|_\infty,$$

which ends the proof. □

Subsequently, we consider the canonical injection

$$\jmath : \mathcal{C}_0^2[0,1] \hookrightarrow \mathcal{C}_0^1[0,1]. \tag{2.4}$$

Thanks to the Ascoli–Arzelà theorem, it is a linear compact operator. Thus,

$$\mathcal{K} := \jmath K|_{\mathcal{C}_0^1[0,1]} :\ \mathcal{C}_0^1[0,1] \to \mathcal{C}_0^1[0,1], \tag{2.5}$$

also is a linear compact operator. Using $\mathcal{K}$, the problem (1.1) can be expressed as a fixed point equation for a compact operator, because u solves (1.1) if, and only if,

$$u = \mathcal{K}(\lambda u + au^2).$$

Note that $R[\mathcal{K}] \subset \mathcal{C}_0^2[0,1]$, by the definition of $\mathcal{K}$. Thus, the solutions of (1.1) are the zeroes of the nonlinear operator $\mathfrak{F} : \mathbb{R} \times \mathcal{C}_0^1[0,1] \to \mathcal{C}_0^1[0,1]$ defined by

$$\mathfrak{F}(\lambda, u) := u - \mathcal{K}(\lambda u + au^2), \qquad (\lambda, u) \in \mathbb{R} \times \mathcal{C}_0^1[0,1]. \tag{2.6}$$

Setting

$$\mathfrak{L}(\lambda)u := u - \lambda\mathcal{K}u, \quad \mathfrak{N}(\lambda, u) := -\mathcal{K}(au^2), \qquad (\lambda, u) \in \mathbb{R} \times \mathcal{C}^1_0[0,1], \tag{2.7}$$

it is apparent that

$$\mathfrak{F}(\lambda, u) = \mathfrak{L}(\lambda)u + \mathfrak{N}(\lambda, u)$$

satisfies the general structural requirements of Chapters 2 and 6 of [39], because $\mathfrak{L}(\lambda)$ is an analytic compact perturbation of the identity map on $\mathcal{C}^1_0[0,1]$, I, and the nonlinearity is completely continuous, i.e., continuous and compact, and, being a polynomial, also is analytic. In particular, $\mathfrak{L}(\lambda)$ is Fredholm of index zero for all $\lambda \in \mathbb{R}$, and $\mathfrak{F}$ is a compact perturbation of the identity map that it is real analytic in $(\lambda, u) \in \mathbb{R} \times \mathcal{C}^1_0[0,1]$. Thus, the main theorems of Crandall and Rabinowitz [16, 17], as well as the unilateral global bifurcation theorem of López-Gómez [39, Th. 6.4.3], can be applied.

The generalized spectrum, $\Sigma(\mathfrak{L})$, of the Fredholm curve $\mathfrak{L}(\lambda)$ defined in (2.7) consists of the set of $\lambda \in \mathbb{R}$ for which $u = \lambda\mathcal{K}u$ for some $u \in \mathcal{C}^1_0[0,1]$, $u \neq 0$. Differentiating twice with respect to x, this fixed point equation can be equivalently expressed as

$$\begin{cases} -u'' = \lambda u \quad \text{in } [0,1], \\ u(0) = u(1) = 0. \end{cases} \tag{2.8}$$

Thus,

$$\Sigma(\mathfrak{L}) = \Big\{\sigma_n \equiv (n\pi)^2 \ : \ n \in \mathbb{N}, \ n \geq 1\Big\}.$$

Moreover,

$$N[\mathfrak{L}(\lambda_n)] = \text{span}\,[\psi_n], \qquad \psi_n(x) = \sin(n\pi x), \quad x \in [0,1].$$

Subsequently, in order to apply the main theorem of [16] at $\sigma_n = (n\pi)^2$, we fix $n \geq 1$ and, adopting the notations of [39, Ch. 2], we set $(\lambda_0, \varphi_0) \equiv (\sigma_n, \psi_n)$. Then,

$$N[\mathfrak{L}_0] = \text{span}\,[\varphi_0], \qquad \mathfrak{L}_0 \equiv \mathfrak{L}(\lambda_0) = I - \sigma_n\mathcal{K}, \qquad \mathfrak{L}_1 \equiv \mathfrak{L}'(\lambda_0) = -\mathcal{K},$$

and the following transversality condition holds

$$\mathfrak{L}_1(N[\mathfrak{L}_0]) \oplus R[\mathfrak{L}_0] = \mathcal{C}^1_0[0,1]. \tag{2.9}$$

On the contrary, assume that $\mathfrak{L}_1\varphi_0 \in R[\mathfrak{L}_0]$. Then, there exists $u \in \mathcal{C}^1_0[0,1]$ such that

$$-\mathcal{K}\varphi_0 = \mathfrak{L}_1\varphi_0 = \mathfrak{L}_0 u = u - \sigma_n\mathcal{K}u$$

and hence, differentiating twice with respect to x, it becomes apparent that

$$-\varphi_0 = -u'' - \sigma_n u.$$

Consequently, multiplying by φ_0 and integrating in $(0,1)$ yields

$$-\int_0^1 \varphi_0^2\,dx = \int_0^1 [(-u'' - \sigma_n u)\varphi_0]\,dx = \int_0^1 [(-\varphi_0'' - \sigma_n\varphi_0)u]\,dx = 0,$$

which is impossible. This shows (2.9). Therefore, as a direct application of the main theorem of Crandall and Rabinowitz [16], the following result of a local nature holds.

Theorem 2.1. *For any given integer $n \geq 1$, let Y denote the closed subspace of $\mathcal{C}^1_0[0,1]$ defined by*

$$Y := \Big\{w \in \mathcal{C}^1_0[0,1] \ : \ \int_0^1 w(x)\psi_n(x)\,dx = 0\Big\}.$$

Then, there exist $\eta > 0$ and two analytic maps $\lambda_n : (-\eta, \eta) \to \mathbb{R}$ and $y_n : (-\eta, \eta) \to Y$ such that

- *$\lambda_n(0) = \sigma_n$, $y_n(0) = 0$;*
- *$\mathfrak{F}(\lambda_n(s), s(\psi_n + y_n(s))) = 0$ for all $s \in (-\eta, \eta)$; and*

- *the solutions of the curve* $(\lambda_n(s), s(\psi_n + y_n(s)))$, $|s| < \eta$, *are the unique zeroes of* $\mathfrak{F}$, *besides* $(\lambda, 0)$, *in a neighborhood of* $(\sigma_n, 0)$ *in* $\mathbb{R} \times \mathcal{C}^1_0[0,1]$.

Since $y_n(0) = 0$, the function $u(s) = s(\psi_n + y_n(s)) \in \mathcal{C}^2_0[0,1]$ has the same nodal behavior as ψ_n for sufficiently small $s \neq 0$, because $y_n(s) \sim 0$ in $\mathcal{C}^1_0[0,1]$ and the zeroes of ψ_n are simple. Therefore, by Theorem 2.1, it is apparent that, for every $n \geq 1$, (1.1) has a curve of solutions with $n-1$ zeroes bifurcating from $u = 0$ at $\lambda = \sigma_n$, regardless the nature of the weight function $a \in \mathcal{C}[0,1]$. In particular, by the local uniqueness result at $(\sigma_n, 0)$, the positive solution of (1.1) can only bifurcate from $u = 0$ at the critical value of the parameter $\sigma_1 = \pi^2$. Next, we will analyze the local nature of this bifurcation from $(\lambda, u) = (\sigma_1, 0)$. Setting $D_1 := \lambda_1'(0)$, $D_2 := \lambda_1''(0)$, $w_1 := y_1'(0)$ and $w_2 := y_1''(0)$, we have that

$$\lambda_1(s) = \sigma_1 + sD_1 + s^2 D_2 + O(s^3), \qquad y_1(s) = sw_1 + s^2 w_2 + O(s^3),$$

as $s \to 0$. By Theorem 2.1, we already know that

$$\begin{aligned} -s(\psi_1 + sw_1 + s^2 w_2 + O(s^3))'' = [\sigma_1 + sD_1 + s^2 D_2 + O(s^3) \\ + a(x)s(\psi_1 + sw_1 + s^2 w_2 + O(s^3))]s(\psi_1 + sw_1 + s^2 w_2 + O(s^3)) \end{aligned}$$

for $s \simeq 0$. Thus, dividing by s yields

$$\begin{aligned} -(\psi_1 + sw_1 + s^2 w_2 + O(s^3))'' = [\sigma_1 + sD_1 + s^2 D_2 + O(s^3) \\ + a(x)s(\psi_1 + sw_1 + s^2 w_2 + O(s^3))](\psi_1 + sw_1 + s^2 w_2 + O(s^3)). \end{aligned} \tag{2.10}$$

Particularizing (2.10) at $s = 0$, yields to $-\psi_1'' = \sigma_1 \psi_1$, which holds true by the definition of ψ_1. Identifying terms of the first order in s, it follows from (2.10) that

$$-w_1'' = \sigma_1 w_1 + (D_1 + a(x)\psi_1)\psi_1. \tag{2.11}$$

Therefore, multiplying by ψ_1 this equation and integrating in $(0,1)$ yields

$$D_1 = -\frac{\int_0^1 a(x)\psi_1^3(x)\,dx}{\int_0^1 \psi_1^2(x)\,dx} = -2\int_0^1 a(x)\sin^3(\pi x)\,dx. \tag{2.12}$$

If $D_1 \neq 0$, then, since $a(x)$ changes the sign, the *bifurcation direction*, $D = D_1$, can take any value, either positive, or negative. Actually, the bifurcation to positive solutions is supercritical if $D > 0$, while it is subcritical if $D < 0$. If $D_1 = 0$, then we need to compute D_2. Suppose $D_1 = 0$. Then, similarly as above, we can collect terms of the second order in s from (2.10) to get

$$-w_2'' = \sigma_1 w_2 + D_2\psi_1 + a(x)w_1\psi_1$$

and hence,

$$D_2 = -\frac{\int_0^1 a(x)w_1(x)\psi_1^2(x)\,dx}{\int_0^1 \psi_1^2(x)\,dx} = -2\int_0^1 a(x)w_1(x)\sin^2(\pi x)\,dx. \tag{2.13}$$

Thus, to get the exact value of D_2, we need to determine $w_1(x)$. It is the unique solution of (2.11), subject to Dirichlet boundary conditions, in the closed subspace Y. Since $D_1 = 0$, the general solution of (2.11) is given by

$$\begin{aligned} w_1(x) = \cos(\pi x)\left(c_1 + \frac{1}{\pi}\int_0^x a(s)\sin^3(\pi s)\,ds\right) \\ + \sin(\pi x)\left(c_2 - \frac{1}{\pi}\int_0^x a(s)\sin^2(\pi s)\cos(\pi s)\,ds\right). \end{aligned}$$

As $0 = w_1(0) = c_1$, after some adjustment we find that

$$w_1(x) = c_2\sin(\pi x) + \frac{1}{\pi}\int_0^x a(s)\sin^2(\pi s)\sin(\pi s - \pi x)\,ds.$$

To find out c_2, we recall that $y_1(s) \in Y$ for $s \simeq 0$. Since Y is closed, this entails that

$$w_1 = \lim_{s\to 0} \frac{y_1(s)}{s} \in Y.$$

Thus,

$$\begin{aligned} 0 &= \int_0^1 w_1(x)\sin(\pi x)\, dx \\ &= c_2 \int_0^1 \sin^2(\pi x)\, dx + \int_0^1 \frac{\sin(\pi x)}{\pi} \int_0^x a(s)\sin^2(\pi s)\sin(\pi s - \pi x)\, ds\, dx \end{aligned}$$

and therefore,

$$c_2 = -2\int_0^1 \frac{\sin(\pi x)}{\pi} \int_0^x a(s)\sin^2(\pi s)\sin(\pi s - \pi x)\, ds\, dx.$$

This way we can compute the *bifurcation direction* $D = D_2$ when $D_1 = 0$. This situation arises in Sections 5, 6. Should it be $D_2 = 0$, then it is necessary to use higher order terms of $\lambda_1(s)$ and $y_1(s)$.

Next, we will use the Schauder formula for determining the Leray–Schauder degree $\mathrm{Deg}\,(\mathfrak{L}(\lambda), B_R)$, $R > 0$, for every $\lambda \in \mathbb{R} \setminus \Sigma(\mathfrak{L})$, where B_R stands for the open ball of radius R centered at the origin in the real Banach space $\mathcal{C}_0^1[0,1]$. According to it, we already know that

$$\mathrm{Deg}\,(\mathfrak{L}(\lambda), B_R) = (-1)^{m(\mathfrak{L}(\lambda))}, \tag{2.14}$$

where $m(\mathfrak{L}(\lambda))$ stands for the sum of the algebraic multiplicities of the negative eigenvalues of $\mathfrak{L}(\lambda)$. To determine $m(\mathfrak{L}(\lambda))$, we will find out all the values of $\mu \in \mathbb{R}$ for which there exists $u \in \mathcal{C}_0^1[0,1]$, $u \neq 0$, such that

$$\mathfrak{L}(\lambda)u = u - \lambda\mathcal{K}u = \mu u. \tag{2.15}$$

Since $\mathfrak{L}(\lambda)$ is invertible for all $\lambda \in (0, \sigma_1)$, by the homotopy invariance of the degree,

$$d_1 \equiv \mathrm{Deg}\,(\mathfrak{L}(\lambda), B_R) \quad \text{is constant on } \ \lambda \in (0, \sigma_1).$$

Similarly, for every $k \geq 2$,

$$d_{k+1} \equiv \mathrm{Deg}\,(\mathfrak{L}(\lambda), B_R) \quad \text{is constant on } \ \lambda \in (\sigma_k, \sigma_{k+1}).$$

The equation (2.15) can be expressed as

$$\mathcal{K}u = \frac{1-\mu}{\lambda}u,$$

or, equivalently, by inverting $\mathcal{K}$,

$$-u'' = \frac{\lambda}{1-\mu}u \quad \text{in } \ [0,1].$$

Note that, due to (2.15), $\mathcal{K}u = 0$ if $\mu = 1$, because $\lambda > 0$, and hence $u = 0$. Thus, $\mu \neq 1$ and hence, we can divide by $1 - \mu$. Consequently, there should exist some integer $n \geq 1$ such that

$$\frac{\lambda}{1-\mu} = \sigma_n$$

for some $n \geq 1$. Therefore, the set of (classical) eigenvalues of $\mathfrak{L}(\lambda)$ is given by

$$\sigma(\mathfrak{L}(\lambda)) = \Big\{\mu_n := 1 - \frac{\lambda}{\sigma_n} \ : \ n \in \mathbb{N},\ n \geq 1\Big\}. \tag{2.16}$$

On the other hand, for every $\lambda > 0$ and any integer $n \geq 1$, the eigenvalue $\mu_n := 1 - \frac{\lambda}{\sigma_n}$ is an algebraically simple eigenvalue of $\mathfrak{L}(\lambda) = I - \lambda\mathcal{K}$, because

$$N[I - \lambda\mathcal{K} - \mu_n I] = \text{span}\,[\psi_n] \quad \text{and} \quad \psi_n \notin R[I - \lambda\mathcal{K} - \mu_n I]. \tag{2.17}$$

Indeed, arguing by contradiction, assume that, for some $u \in \mathcal{C}_0^1[0,1]$,

$$\psi_n = u - \lambda\mathcal{K}u - \mu_n u = (1 - \mu_n)u - \lambda\mathcal{K}u.$$

Then,

$$(1 - \mu_n)u = \lambda\mathcal{K}u + \psi_n \in \mathcal{C}_0^2[0,1]$$

and, since $\mu_n \neq 1$, $u \in \mathcal{C}_0^2[0,1]$. Thus, differentiating twice with respect to x yields

$$-(1 - \mu_n)u'' = \lambda u - \psi_n'' = \lambda u + \sigma_n\psi_n.$$

Equivalently, by definition of μ_n,

$$-\frac{\lambda}{\sigma_n}u'' - \lambda u = \sigma_n\psi_n$$

and hence,

$$-u'' - \sigma_n u = \frac{\sigma_n^2}{\lambda}\psi_n.$$

Finally, multiplying by ψ_n and integrating in $(0,1)$, we find that

$$\frac{\sigma_n^2}{\lambda}\int_0^1 \psi_n^2 = \int_0^1 [(-u'' - \sigma_n u)\psi_n] = 0,$$

which is impossible. This ends the proof of (2.17). Therefore, (2.14) becomes

$$\text{Deg}\,(\mathfrak{L}(\lambda), B_R) = (-1)^{n(\lambda)}, \tag{2.18}$$

where $n(\lambda)$ stands for the number of negative eigenvalues of (2.16). Assume $\lambda < \sigma_1$. Then, $\frac{\lambda}{\sigma_1} < 1$ and, since $\sigma_n \geq \sigma_1$ for each $n \geq 1$, we find that

$$1 - \frac{\lambda}{\sigma_n} \geq 1 - \frac{\lambda}{\sigma_1} > 0.$$

Thus, $n(\lambda) = 0$ and (2.18) entails $\text{Deg}\,(\mathfrak{L}(\lambda), B_R) = 1$. Assume $\sigma_1 < \lambda < \sigma_2$. Then,

$$1 - \frac{\lambda}{\sigma_1} < 0 < 1 - \frac{\lambda}{\sigma_2} < 1 - \frac{\lambda}{\sigma_3} < \cdots$$

and hence, $n(\lambda) = 1$. Therefore, by (2.18), $\text{Deg}\,(\mathfrak{L}(\lambda), B_R) = -1$. Obviously, every time that λ crosses an additional eigenvalue σ_n, $n(\lambda)$ increases by 1. Therefore, for every integer $k \geq 1$,

$$\text{Deg}\,(\mathfrak{L}(\lambda), B_R) = \begin{cases} 1 & \text{if } \lambda \in (\sigma_{2k}, \sigma_{2k+1}), \\ -1 & \text{if } \lambda \in (\sigma_{2k+1}, \sigma_{2k+2}). \end{cases} \tag{2.19}$$

Consequently, according to [39, Th. 6.2.1], the next result holds. We are denoting by $\mathcal{S}$ the set of non-trivial solutions of (1.1), i.e.,

$$\mathcal{S} = \{(\lambda, u) \in \mathfrak{F}^{-1}(0) \ : \ u \neq 0\} \cup (\{(\sigma_n, 0) \ : \ n \geq 1\} \subset \mathbb{R} \times \mathcal{C}_0^1[0,1],$$

where $\mathfrak{F}(\lambda, u)$ is the operator introduced in (2.6).

Theorem 2.2. *For every $n \geq 1$, there exists a component of $\mathcal{S}$, $\mathscr{C}_n$, such that $(\sigma_n, 0) \in \mathscr{C}_n$. Moreover, for sufficiently small $\varepsilon > 0$,*

$$B_\varepsilon(\sigma_n, 0) \cap \mathscr{C}_n = \{(\lambda_n(s), s(\psi_n + y_n(s))) \ : \ s \sim 0\},$$

where $(\lambda_n(s), s(\psi_n + y_n(s)))$, $s \sim 0$, is the analytic curve given by Theorem 2.1.

As the nodes of the solutions of (1.1) are simple, it is easily seen that the number of nodes of the solutions of (1.1) vary continuously in $\mathbb{R} \times \mathcal{C}_0^1[0,1]$ and hence, since the solutions of $\mathscr{C}_n$ bifurcating from $u = 0$ at $\lambda = \sigma_n$ possess $n-1$ interior nodes in $(0,1)$, $\mathscr{C}_n \setminus \{(\sigma_n, 0)\}$ consists of solutions with $n-1$ interior nodes. Therefore,

$$\mathscr{C}_n \cap \mathscr{C}_m = \emptyset \quad \text{if } n \neq m.$$

Consequently, thanks to the global alternative of Rabinowitz [60], $\mathscr{C}_n$ is unbounded in $\mathbb{R} \times \mathcal{C}_0^1[0,1]$ for each integer $n \geq 1$. Note that $\mathscr{C}^+$ is the subcomponent of $\mathscr{C}_1$ consisting of the positive solutions $(\lambda, u) \in \mathscr{C}_1$. According to [39, Th. 6.4.3], $\mathscr{C}^+$ also is unbounded in $\mathbb{R} \times \mathcal{C}_0^1[0,1]$. A further rather standard compactness argument, whose details are omitted here, shows that actually $\mathscr{C}^+$ is unbounded in $\mathbb{R} \times \mathcal{C}_0[0,1]$. This information can be summarized into the next result.

Theorem 2.3. *The component $\mathscr{C}^+$ is unbounded in $\mathbb{R} \times \mathcal{C}_0[0,1]$. Moreover, $\lambda = \pi^2$ if $(\lambda, 0) \in \bar{\mathscr{C}}^+$. Furthermore, $\mathscr{C}^+$ bifurcates supercritically from $u = 0$ at $\lambda = \pi^2$ if $D > 0$, while it does it subcritically if $D < 0$, where D is given by* (2.12) *or* (2.13).

In addition, by the a priori bounds of Amann and López-Gómez [3], the next result holds.

Theorem 2.4. *The component $\mathscr{C}^+$ is uniformly bounded on any compact subinterval of $\lambda \in \mathbb{R}$, and* (1.1) *cannot admit a positive solution for sufficiently large λ. Thus,*

$$(-\infty, \pi^2) \subset \mathcal{P}_\lambda(\mathscr{C}^+).$$

Moreover, if (1.1) *admits a positive solution, (λ_0, u_0), with $\lambda_0 > \pi^2$, then it admits at least two positive solutions for every $\lambda \in (\pi^2, \lambda_0)$.*

These findings can be complemented with the theory of Gómez-Reñasco and López-Gómez [29, 30], later refined in [42], up to characterize the existence of linearly stable positive solutions of (1.1) thorough the sign of D. Indeed, by [42, Cor. 9.10], any positive solution of (1.1) is linearly unstable if $D \leq 0$, and actually, due to [42, Pr. 9.2], (1.1) cannot admit a positive solution (λ, u) with $\lambda \geq \pi^2$ in such case. Thus,

$$\mathcal{P}_\lambda(\mathscr{C}^+) = (-\infty, \pi^2)$$

if $D \leq 0$. Moreover, (1.1) admits some stable positive solution if, and only if, $D > 0$ and, in such case, the results of [42, Sec. 9.2-4], provide us with the next one.

Theorem 2.5. *Assume $D > 0$. Then, there exists $\lambda_t > \pi^2$ such that* (1.1) *cannot admit a positive solution if $\lambda > \lambda_t$, and*

$$\mathcal{P}_\lambda(\mathscr{C}^+) = (-\infty, \lambda_t].$$

Moreover,

(a) *Any positive solution of* (1.1) *with $\lambda \leq \pi^2$ is linearly unstable.*
(b) *For every $\lambda \in (\pi^2, \lambda_t]$, the minimal positive solution of* (1.1)*, $(\lambda, \theta_\lambda^{\min})$, is the unique stable positive solution of* (1.1)*. Moreover, these solutions are linearly stable if $\lambda \in (\pi^2, \lambda_t)$. Thus, they are local exponential attractors of* (1.2)*.*
(c) *For every $\lambda \in (\pi^2, \lambda_t)$,* (1.1) *possesses, at least, two positive solutions: one linearly stable and another one unstable.*
(d) *$(\lambda_t, \theta_{\lambda_t}^{\min})$ is the unique positive solution of* (1.1) *at $\lambda = \lambda_t$, and it is linearly neutrally stable. Moreover, the set of positive solutions of* (1.1) *in a neighborhood of $(\lambda_t, \theta_{\lambda_t}^{\min})$ consists of a quadratic subcritical turning point whose lower half-curve is filled in by linearly stable positive solutions, while its upper half-curve consists of unstable solutions with one-dimensional unstable manifold.*

(e) *The map* $\lambda \to \theta_\lambda^{\min}$, $(\sigma_1, \lambda_t) \to \mathcal{C}_0^1[0,1]$, *is analytic and*

$$\lim_{\lambda \uparrow \lambda_t} \theta_\lambda^{\min} = \theta_{\lambda_t}^{\min}.$$

The numerical experiments carried out in this paper confirm and illuminate these findings complementing them. Note that the *exchange stability principle* of Crandall and Rabinowitz [17] only provides us with the linearized stability of the minimal positive solution for $\lambda > \pi^2$ sufficiently close to π^2, while the existence and the uniqueness of the stable positive solution established by Theorem 2.5 inherits a global character. Very recently, it has been established by Fernández-Rincón and López-Gómez [27] that choosing a a nonlinearity of the type u^p for some $p \geq 2$ in (1.1) is imperative for the validity of Theorem 2.5, regardless the nature of the boundary conditions that might be of general type. This explains why in this paper we are focusing attention on the particular example (1.1).

3. Behavior of the solutions of (1.1) and (1.2) as $\lambda \downarrow -\infty$

The next result provides us with the point-wise behavior of the positive solutions of (1.1) in the open set Ω_-.

Theorem 3.1. *For every* $\lambda < \pi^2$, *let* u_λ *be a positive solution of* (1.1). *Then,*

$$\lim_{\lambda \downarrow -\infty} u_\lambda(x) = 0 \quad \textit{for all } x \in \Omega_- \tag{3.1}$$

uniformly on compact subintervals of Ω_-.

Proof. Pick an arbitrary $x_0 \in \Omega_-$. As Ω_- is open, there exists $\varepsilon > 0$ such that

$$0 < x_0 - 4\varepsilon < x_0 + 4\varepsilon < 1 \quad \text{and} \quad [x_0 - 4\varepsilon, x_0 + 4\varepsilon] \subset \Omega_-.$$

Since a is continuous, we have that

$$\omega := \max_{|x - x_0| \leq 4\varepsilon} a(x) < 0.$$

Let $\ell_\lambda^{\min}$ denote the minimal positive solution of the singular problem

$$\begin{cases} -\ell'' = \lambda \ell + a(x)\ell^2 & \text{in} \quad (x_0 - 4\varepsilon, x_0 + 4\varepsilon), \\ \ell(x_0 - 4\varepsilon) = \ell(x_0 + 4\varepsilon) = \infty, \end{cases} \tag{3.2}$$

whose existence is guaranteed by, e.g., [42, Ch. 3], and set

$$B := \|\ell_\lambda^{\min}\|_{\mathcal{C}[x_0 - 2\varepsilon, x_0 + 2\varepsilon]}.$$

Then, the restriction of the function $\ell_\lambda^{\min}$ to the interval $[x_0 - 2\varepsilon, x_0 + 2\varepsilon]$ provides us with a positive subsolution of the regular problem

$$\begin{cases} -u'' = \lambda u + \omega u^2 & \text{in} \quad (x_0 - 2\varepsilon, x_0 + 2\varepsilon), \\ u(x_0 - 2\varepsilon) = u(x_0 + 2\varepsilon) = B. \end{cases} \tag{3.3}$$

As $\omega < 0$, any sufficiently large constant, $M > B$, provides us with a supersolution of (3.3) such that

$$\ell_\lambda^{\min} < M \quad \text{in} \quad [x_0 - 2\varepsilon, x_0 + 2\varepsilon].$$

Thus, thanks to, e.g., [42, Th. 2.4], (3.3) possesses a unique positive solution, $\theta_{[\lambda, B]}$, such that

$$\ell_\lambda^{\min} \leq \theta_{[\lambda, B]} \leq M \quad \text{in} \quad [x_0 - 2\varepsilon, x_0 + 2\varepsilon].$$

Moreover, according to the proof of [42, Th 3.2], $\theta_{[\lambda, B]}$ is symmetric about x_0, and, for every $\lambda \in \mathbb{R}$, the point-wise limit

$$L_\lambda := \lim_{\xi \uparrow \infty} \theta_{[\lambda, \xi]}$$

is increasing and, thanks to the uniqueness result of [40], it provides us with the unique positive solution of the singular problem

$$\begin{cases} -u'' = \lambda u + \omega u^2 & \text{in } (x_0 - 2\varepsilon, x_0 + 2\varepsilon), \\ u(x_0 - 2\varepsilon) = u(x_0 + 2\varepsilon) = \infty. \end{cases}$$

Since L_λ is symmetric about x_0, it is apparent that

$$L_\lambda(x_0) = \min_{(x_0-2\varepsilon, x_0+2\varepsilon)} L_\lambda. \tag{3.4}$$

On the other hand, by [42, Th. 2.4], we already know that $\theta_{[\lambda,\xi]} < \theta_{[\mu,\xi]}$ if $\lambda < \mu$. Thus, letting $\xi \uparrow \infty$ yields

$$L_\lambda \leq L_\mu \quad \text{in } [x_0 - 2\varepsilon, x_0 + 2\varepsilon].$$

Subsequently, we consider the auxiliary function

$$\varphi(x) := \sin \frac{\pi(x - x_0 + \varepsilon)}{2\varepsilon}, \qquad x \in [x_0 - \varepsilon, x_0 + \varepsilon].$$

It has been chosen to satisfy

$$\begin{cases} -\varphi'' = \left(\frac{\pi}{2\varepsilon}\right)^2 \varphi & \text{in } (x_0 - \varepsilon, x_0 + \varepsilon), \\ \varphi(x_0 - \varepsilon) = \varphi(x_0 + \varepsilon) = 0. \end{cases} \tag{3.5}$$

Thus, multiplying the differential equation

$$-L_\lambda'' = \lambda L_\lambda + \omega L_\lambda^2 \quad \text{in } [x_0 - \varepsilon, x_0 + \varepsilon]$$

by φ and integrating in $(x_0 - \varepsilon, x_0 + \varepsilon)$ yields

$$-\int_{x_0-\varepsilon}^{x_0+\varepsilon} L_\lambda'' \varphi \, dx = \lambda \int_{x_0-\varepsilon}^{x_0+\varepsilon} L_\lambda \varphi \, dx + \omega \int_{x_0-\varepsilon}^{x_0+\varepsilon} L_\lambda^2 \varphi \, dx. \tag{3.6}$$

On the other hand, integrating by parts, we find that

$$\int_{x_0-\varepsilon}^{x_0+\varepsilon} L_\lambda'' \varphi \, dx = \int_{x_0-\varepsilon}^{x_0+\varepsilon} (L_\lambda' \varphi)' \, dx - \int_{x_0-\varepsilon}^{x_0+\varepsilon} L_\lambda' \varphi' \, dx = -\int_{x_0-\varepsilon}^{x_0+\varepsilon} L_\lambda' \varphi' \, dx,$$
$$\int_{x_0-\varepsilon}^{x_0+\varepsilon} L_\lambda \varphi'' \, dx = \int_{x_0-\varepsilon}^{x_0+\varepsilon} (L_\lambda \varphi')' \, dx - \int_{x_0-\varepsilon}^{x_0+\varepsilon} L_\lambda' \varphi' \, dx.$$

Consequently, by (3.5),

$$\begin{aligned} -\int_{x_0-\varepsilon}^{x_0+\varepsilon} L_\lambda'' \varphi \, dx = \int_{x_0-\varepsilon}^{x_0+\varepsilon} L_\lambda' \varphi' \, dx &= \int_{x_0-\varepsilon}^{x_0+\varepsilon} (L_\lambda \varphi')' \, dx - \int_{x_0-\varepsilon}^{x_0+\varepsilon} L_\lambda \varphi'' \, dx \\ &= L_\lambda(x_0 + \varepsilon)\varphi'(x_0 + \varepsilon) - L_\lambda(x_0 - \varepsilon)\varphi'(x_0 - \varepsilon) + \left(\tfrac{\pi}{2\varepsilon}\right)^2 \int_{x_0-\varepsilon}^{x_0+\varepsilon} L_\lambda \varphi \, dx. \end{aligned}$$

Thus, since $\omega < 0$, substituting in (3.6) yields

$$\begin{aligned} \left[\left(\tfrac{\pi}{2\varepsilon}\right)^2 - \lambda \right] \int_{x_0-\varepsilon}^{x_0+\varepsilon} L_\lambda \varphi \, dx &= \omega \int_{x_0-\varepsilon}^{x_0+\varepsilon} L_\lambda^2 \varphi \, dx + L_\lambda(x_0 - \varepsilon)\varphi'(x_0 - \varepsilon) - L_\lambda(x_0 + \varepsilon)\varphi'(x_0 + \varepsilon) \\ &< L_\lambda(x_0 - \varepsilon)\varphi'(x_0 - \varepsilon) - L_\lambda(x_0 + \varepsilon)\varphi'(x_0 + \varepsilon). \end{aligned}$$

Therefore, since

$$L_\lambda(x_0 - \varepsilon)\varphi'(x_0 - \varepsilon) - L_\lambda(x_0 + \varepsilon)\varphi'(x_0 + \varepsilon) > 0,$$

we can infer from the previous estimate that

$$\lim_{\lambda \downarrow -\infty} \int_{x_0-\varepsilon}^{x_0+\varepsilon} L_\lambda \varphi \, dx = 0. \tag{3.7}$$

Consequently, owing to (3.4) and (3.7), it becomes apparent that

$$\lim_{\lambda\downarrow-\infty} L_\lambda(x_0) = 0. \tag{3.8}$$

Note that, since

$$\ell_\lambda^{\min} \le \theta_{[\lambda,B]} \le L_\lambda \quad \text{in } (x_0 - 2\varepsilon, x_0 + 2\varepsilon),$$

(3.8) implies that

$$\lim_{\lambda\downarrow-\infty} \ell_\lambda^{\min}(x_0) = 0. \tag{3.9}$$

Similarly, for every $x \in [x_0 - \varepsilon, x_0 + \varepsilon]$, we have that

$$[x - \varepsilon, x + \varepsilon] \subset [x_0 - 2\varepsilon, x_0 + 2\varepsilon]$$

and hence, the restriction of $\ell_\lambda^{\min}$ to the interval $[x-\varepsilon, x+\varepsilon]$ provides us with a subsolution of

$$\begin{cases} -u'' = \lambda u + \omega u^2 & \text{in } (x - \varepsilon, x + \varepsilon), \\ u(x - \varepsilon) = u(x + \varepsilon) = B. \end{cases} \tag{3.10}$$

Consequently, reasoning as above, it becomes apparent that

$$\ell_\lambda^{\min} \le L_{\lambda,x} \quad \text{in } (x - \varepsilon, x + \varepsilon), \tag{3.11}$$

where $L_{\lambda,x}$ stands for the unique positive solution of the singular problem

$$\begin{cases} -u'' = \lambda u + \omega u^2 & \text{in } (x - \varepsilon, x + \varepsilon), \\ u(x - \varepsilon) = u(x + \varepsilon) = \infty. \end{cases}$$

By the uniqueness and the radial symmetry of $L_{\lambda,x}$ about x, we find that

$$L_{\lambda,x}(y) = L_\lambda(x_0 - x + y) \quad \text{for all } y \in (x - \varepsilon, x + \varepsilon).$$

Thus, it follows from (3.11) that

$$\ell_\lambda^{\min}(x) \le L_{\lambda,x}(x) = L_\lambda(x_0) \quad \text{for all } x \in (x_0 - \varepsilon, x_0 + \varepsilon).$$

Therefore, due to (3.8), we find that

$$\lim_{\lambda\downarrow-\infty} \ell_\lambda^{\min} = 0 \quad \text{uniformly in } (x_0 - \varepsilon, x_0 + \varepsilon).$$

A compactness argument ends the proof. □

Throughout the rest of this section, we will assume that $a(x)$ satisfies (H_a). Then, for every $j \in \{1, ..., r\}$, some of the following (excluding) options occurs. Either (i) $0 < \alpha_j < \beta_j < 1$, or (ii) $0 = \alpha_j < \beta_j < 1$, or (iii) $0 < \alpha_j < \beta_j = 1$. Subsequently, we will denote by $\ell_{\lambda,j}^{\min}$ the minimal positive solution of the singular problem

$$\begin{cases} -u'' = \lambda u + a(x)u^2 & \text{in } (\alpha_j, \beta_j), \\ u(\alpha_j) = \infty, \ \ u(\beta_j) = \infty, \end{cases} \tag{3.12}$$

if (i) holds, or the minimal positive solution of

$$\begin{cases} -u'' = \lambda u + a(x)u^2 & \text{in } (\alpha_j, \beta_j), \\ u(0) = 0, \ \ u(\beta_j) = \infty, \end{cases} \tag{3.13}$$

if (ii) holds, or the minimal positive solution of

$$\begin{cases} -u'' = \lambda u + a(x)u^2 & \text{in } (\alpha_j, \beta_j), \\ u(\alpha_j) = \infty, \ \ u(1) = 0, \end{cases} \tag{3.14}$$

in case (iii). Their existence is guaranteed, e.g., by [42, Ch. 3].

The proof of Theorem 3.1 reveals that actually the next result holds.

Corollary 3.1. *Under assumption* (H$_a$)*, for every* $j \in \{1, ..., r\}$ *and* $x \in (\alpha_j, \beta_j)$*,*

$$\lim_{\lambda \downarrow -\infty} \ell^{\min}_{\lambda,j}(x) = 0, \tag{3.15}$$

uniformly in compact subsets of (α_j, β_j)*.*

Conversely, Theorem 3.1 follows from Corollary 3.1 taking into account that, thanks to the maximum principle,

$$u_\lambda \leq \ell^{\min}_{\lambda,j} \qquad \text{in } (\alpha_j, \beta_j) \tag{3.16}$$

for all $j \in \{1, ..., r\}$.

The behavior of the positive solutions of (1.1) as $\lambda \downarrow -\infty$ in Ω_- described by Theorem 3.1 is mimicked by the positive solutions of its parabolic counterpart (1.2), as soon as the initial datum u_0 be a subsolution of (1.1). To state this result, we need to introduce some of notation. We will denote by $u(x, t; u_0, \lambda)$ the unique solution of (1.2), and by $T_{\max} = T_{\max}(u_0, \lambda) \in (0, +\infty]$ its maximal existence time. As for every $\lambda < \mu$ the solution $u(x, t; u_0, \mu)$ is a strict supersolution of (1.2), owing to the parabolic maximum principle,

$$u(x, t; u_0, \lambda) < u(x, t; u_0, \mu) \tag{3.17}$$

for all $x \in (0, 1)$ and $t \in [0, T_{\max}(u_0, \mu))$. Thus,

$$T_{\max}(u_0, \mu) \leq T_{\max}(u_0, \lambda) \quad \text{for all } \lambda < \mu. \tag{3.18}$$

Therefore, the limit

$$T_{\max}(u_0) \equiv \lim_{\lambda \downarrow -\infty} T_{\max}(u_0, \lambda) \in (0, \infty] \tag{3.19}$$

is well defined.

Theorem 3.2. *Suppose that* $u_0 \gneq 0$ *is a subsolution of* (1.1)*. Then, for every* $x \in \Omega_-$ *and* $t \in (0, T_{\max}(u_0))$*,*

$$\lim_{\lambda \downarrow -\infty} u(x, t; u_0, \lambda) = 0. \tag{3.20}$$

Moreover, the limit is uniform on compact subsets of Ω_-*.*

Proof. Pick $t \in (0, T_{\max}(u_0))$. By (3.18) and (3.19), there exists $\mu < 0$ such that $t \in (0, T_{\max}(u_0, \mu))$ for all $\lambda < \mu$. Moreover, since u_0 is a subsolution of (1.1), by Sattinger [61], $u(x, t; u_0, \lambda)$ is a subsolution of (1.1) for all $t \in [0, T_{\max}(u_0, \lambda))$; equivalently, $u(x, t; u_0, \lambda)$ is non-decreasing for all $t \in [0, T_{\max}(u_0, \lambda))$. In particular, for every $j \in \{1, ..., r\}$, the restriction of $u(\cdot, t; u_0, \lambda)$ to the interval $I_j^- = (\alpha_j, \beta_j)$ provides us with a positive subsolution of the singular boundary value problem (3.12) if (i) holds, (3.13) if (ii) holds, or (3.14) if (iii) holds. Thus, by the maximum principle, we find that

$$u(x, t; u_0, \lambda) \leq \ell^{\min}_{\lambda,j} \quad \text{in } [\alpha_j, \beta_j]. \tag{3.21}$$

Finally, (3.20) follows easily from (3.21) and Corollary 3.1. □

Since (3.20) holds for every $t \in (0, T_{\max}(u_0))$, letting $t \downarrow 0$ in (3.20), after inter-exchanging the two limits, it seems that a necessary condition so that $u_0 \gneq 0$ can be a subsolution of (1.1) as $\lambda \downarrow -\infty$ should be

$$u_0 \equiv 0 \quad \text{in } \Omega_- = \cup_{j=1}^r I_j^-,$$

which explains why all subsolutions of (1.1) that we will consider later satisfy this requirement.

Finally, we are ready to deliver the proof of Theorem 1.1. We will actually prove that one can take $T(u_0) = T_{\max}(u_0)$.

Proof of Theorem 1.1. First, suppose that I_i^+ is an interior interval. Note that $I_i^+ = (\gamma_i, \varrho_i) = (\beta_j, \alpha_{j+1})$. Choose ε sufficiently small so that $\alpha_j + \varepsilon < \beta_{j+1} - \varepsilon$. Then, by Corollary 3.1,

$$\lim_{\lambda\downarrow-\infty} \ell^{\min}_{\lambda,j}(\alpha_j + \varepsilon) = \lim_{\lambda\downarrow-\infty} \ell^{\min}_{\lambda,j+1}(\beta_{j+1} - \varepsilon) = 0. \tag{3.22}$$

Moreover, by (3.16), for every $t \in (0, T_{\max}(u_0))$, there is $\mu < 0$ such that $t \in (0, T_{\max}(u_0, \mu))$ and, for each $\lambda < \mu$,

$$u(x, t; u_0, \lambda) \le \ell^{\min}_{\lambda,h}(x) \quad \text{for all } \ x \in (\alpha_h, \beta_h), \ \ h \in \{j, j+1\}. \tag{3.23}$$

Thus, by (3.22) and (3.23),

$$\lim_{\lambda\downarrow-\infty} u(\alpha_j + \varepsilon, t; u_0, \lambda) = \lim_{\lambda\downarrow-\infty} u(\beta_{j+1} - \varepsilon, t; u_0, \lambda) = 0. \tag{3.24}$$

On the other hand, note that, as soon as the condition

$$\lambda + au(\cdot, t; u_0, \lambda) \le 0 \quad \text{in } \ [\alpha_j + \varepsilon, \beta_{j+1} - \varepsilon] \tag{3.25}$$

holds, we have that

$$\frac{\partial u}{\partial t} = \frac{\partial^2 u}{\partial x^2} + \lambda u + au^2 \le \frac{\partial^2 u}{\partial x^2} \quad \text{in } \ [\alpha_j + \varepsilon, \beta_{j+1} - \varepsilon].$$

Since $u_0 = 0$ in $[\alpha_j, \beta_{j+1}]$, by continuity, there exists $T(\lambda) > 0$ such that (3.25) holds for all $t \in [0, T(\lambda)]$. Actually, by (3.17), (3.25) holds for every $t \in [0, T(\mu)]$ if $\lambda < \mu$. Consequently, setting $T \equiv T(\mu)$ and

$$Q_T \equiv (\alpha_j + \varepsilon, \beta_{j+1} - \varepsilon) \times [0, T],$$

the parabolic maximum principle implies that

$$\max_{\bar{Q}_T} u = \max_{\partial_L Q_T} u,$$

where $\partial_L Q_T$ stands for the *lateral boundary* of the parabolic cylinder Q_T,

$$\partial_L Q_T \equiv (\{\alpha_j + \varepsilon, \beta_{j+1} - \varepsilon\} \times [0, T]) \cup ([\alpha_j + \varepsilon, \beta_{j+1} - \varepsilon] \times \{0\}).$$

Therefore, since $u_0 = 0$ in $[\alpha_j, \beta_{j+1}]$,

$$\begin{aligned} \max_{\bar{Q}_T} u &= \max_{t\in[0,T]} \max\{u(\alpha_j + \varepsilon, t; u_0, \lambda), u(\beta_{j+1} - \varepsilon, t; u_0, \lambda)\} \\ &= \max\{u(\alpha_j + \varepsilon, T; u_0, \lambda), u(\beta_{j+1} - \varepsilon, T; u_0, \lambda)\} \end{aligned} \tag{3.26}$$

because, since it is a subsolution of (1.1), $u(x, t; u_0, \lambda)$ is increasing in time.

Subsequently, we choose $\eta > 0$ arbitrary. Then, there exists $\mu = \mu(\eta) < 0$ such that, for every $\lambda < \mu$,

$$\lambda + \|a\|_\infty \eta < \frac{\lambda}{2} < 0.$$

Thanks to (3.24), shortening μ if necessary, we also have that, for every $\lambda < \mu$,

$$\max\{u(\alpha_j + \varepsilon, T; u_0, \lambda), u(\beta_{j+1} - \varepsilon, T; u_0, \lambda)\} < \eta.$$

Thus, (3.26) implies that

$$\max_{\bar{Q}_T} u < \eta,$$

and hence,

$$\lambda + a(x)u(x, T; u_0, \lambda) < \lambda + \|a\|_\infty \eta < \frac{\lambda}{2} < 0 \quad \text{in } \ [\alpha_j + \varepsilon, \beta_{j+1} - \varepsilon].$$

Therefore, u must remain bellow the level η in $[\alpha_j + \varepsilon, \beta_{j+1} - \varepsilon]$ for all time where it is defined. As $\eta > 0$ is arbitrary, the proof is completed in this case.

This proof can be easily adapted to cover the case when $0 \in \bar{I}_1^+$, or $1 \in \bar{I}_s^+$. Indeed, suppose, for instance, that $I_1^+ = (0, \varrho_1)$. Then, $I_1^- = (\varrho_1, \beta_1)$ and, whenever $u_0 = 0$ in $[0, \beta_1]$, the parabolic maximum principle can be applied in the interval $[0, \beta_1 - \varepsilon]$, instead of in $[\alpha_j + \varepsilon, \beta_{j+1} - \varepsilon]$, to get the same result. This ends the proof. □

In the rest of this section, we assume that $a(x)$ satisfies (H_a) with $s = n+1$ and $r = n$, like the special choice (1.3) with $n \in \mathbb{N}$, $n \geq 1$. Suppose

$$I_i^+ = (\gamma_i, \varrho_i), \qquad i \in \{1, ..., n+1\},$$

and, for every $i \in \{1, ..., n+1\}$, let $\theta_{\{\lambda,i\}}$ be a positive solution of

$$\begin{cases} -u'' = \lambda u + a^+(x)u^2 & \text{in } (\gamma_i, \varrho_i), \\ u(\gamma_i) = u(\varrho_i) = 0. \end{cases} \tag{3.27}$$

on the component $\mathscr{C}^+$ of this problem. The existence has been already discussed in Section 2 and follows from the a priori bounds of [3]. The uniqueness might be an open problem even in the special case when

$$a^+(x) = \mu_i \sin \frac{\pi(x - \gamma_i)}{\varrho_i - \gamma_i}, \qquad x \in [\gamma_i, \varrho_i], \tag{3.28}$$

for some constant $\mu_i > 0$. As, for every $\lambda < 0$, the change of variable $u \equiv -\lambda U$ transforms (3.27) in

$$\begin{cases} -\varepsilon U'' = -U + a^+(x)U^2 & \text{in } (\gamma_i, \varrho_i), \\ U(\gamma_i) = U(\varrho_i) = 0, \end{cases} \tag{3.29}$$

with $\varepsilon = -1/\lambda$, it turns out that the problem of the uniqueness of the positive solution of (3.27) as $\lambda \downarrow -\infty$ is equivalent to the problem of the uniqueness of the positive solution for the singular perturbation problem (3.29) as $\varepsilon \downarrow 0$. Although there is a huge amount of literature on multi-peak solutions for Schrödinger type equations like (3.29) (see, e.g., Ambrosetti, Badiale and Cingolani [4], del Pino and Felmer [20, 21], Dancer and Wei [19], and Wei [64]), the experts still seem to be focusing most of their efforts into the problem of the existence of multi-bump solutions, rather than on the problem of their uniqueness (see, e.g., the recent paper of Le, Wei and Xu [36]).

Our numerical experiments suggest that the problem (3.27), with the special choice (3.28), possesses a unique positive solution, $\theta_{\lambda,i}$, in the component $\mathscr{C}^+$ for every $\lambda < \pi^2$. Moreover, $\theta_{\lambda,i}$ is symmetric about the central point of (γ_i, ϱ_i), $z_i := (\gamma_i + \varrho_i)/2$, where $a^+(x)$ reaches its maximum value in I_i^+, and it has a single peak at z_i. Actually,

$$\mathscr{C}^+ = \left\{(\lambda, \theta_{\lambda,i}) \ : \ \lambda < \left(\tfrac{\pi}{\varrho_i - \gamma_i}\right)^2\right\}$$

consists of symmetric solutions about z_j, because we could not find any secondary bifurcation point along the curve $\mathscr{C}^+$. Figure 1 shows the global bifurcation diagram of positive solutions of (3.27) for the choice (3.28), with $\mu_i = 1$, after re-scaling the problem to the entire interval $[0, 1]$. We are plotting the parameter λ, in abscisas, versus the derivative of the solution at the origin, $u'(0)$, in ordinates. As for $\lambda < -600$, $\theta'_{\lambda,i}(0)$ is very small, in this range of values of λ it is hard to differentiate $\mathscr{C}^+$ from the λ-axis. The component $\mathscr{C}^+$ bifurcates subcritically from $u = 0$ at $\lambda = \pi^2$ and, according to [3], satisfies $\mathcal{P}_\lambda(\mathscr{C}^+) = (-\infty, \pi^2)$. It consists of symmetric solutions about 0.5 with a single peak at 0.5.

Figure 2 shows the plots of the solutions of $\mathscr{C}^+$ corresponding to $\lambda = -100$, $\lambda = -683$ and $\lambda = -1695$, respectively. Not surprisingly, the smaller is the value of λ, the more concentrated is the mass of $\theta_{\lambda,i}$ at 0.5. The three solutions plotted in Figure 2 have been previously re-scaled

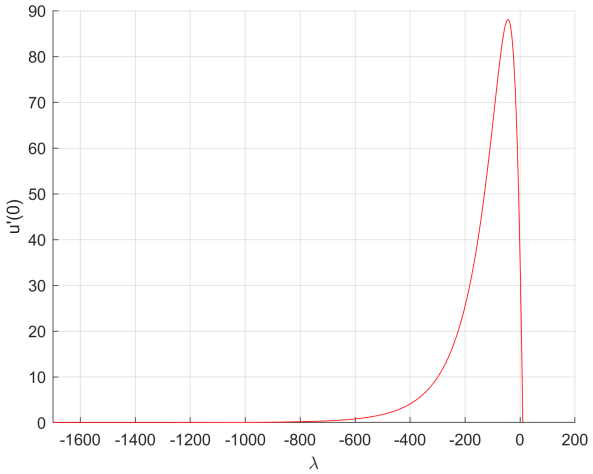

FIGURE 1. Global bifurcation diagram of (3.27)–(3.28).

to the interval $[0,1]$ from the original interval $[\gamma_i, \varrho_i]$ in such a way that 0.5 corresponds to z_i. Actually, according to our numerical experiments, it becomes apparent that, for every $x \in [\gamma_i, \varrho_i]$,

$$\lim_{\lambda \downarrow -\infty} \theta_{\lambda,i}(x) = \begin{cases} +\infty & \text{if } x = z_i, \\ 0 & \text{if } x \neq z_i, \end{cases}$$

which is a rather genuine behavior of this type of superlinear elliptic boundary value problems.

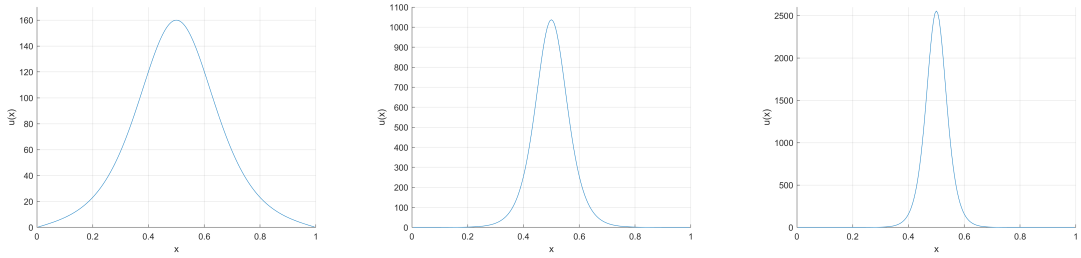

(A) $\lambda = -100$ (B) $\lambda = -683$ (C) $\lambda = -1695$

FIGURE 2. Three positive solutions of the component $\mathscr{C}^+$.

Subsequently, we will consider the subsolution of (1.1) defined by

$$\underbrace{\underline{u}_{1\ldots1}}_{n+1} := \begin{cases} \theta_{\lambda,i} & \text{in } [\gamma_i, \varrho_i], \ \ i \in \{1, ..., n+1\}, \\ 0 & \text{in } [0,1] \setminus \bigcup_{i=1}^{n+1} [\gamma_i, \varrho_i]. \end{cases} \tag{3.30}$$

The fact that it provides us with a weak subsolution of (1.1) is a direct consequence of a result of Berestycki and Lions [7]. Thus, making the choice $u_0 := \underline{u}_{1\ldots1}$ and using the theory of Sattinger [61], $u(x,t;u_0,\lambda)$ must be a subsolution of (1.1) for all $t \in I_{\max}(u_0,\lambda) = [0, T_{\max}(u_0,\lambda))$. Equivalently, $u(x,t;u_0,\lambda)$ is non-decreasing for all $t \in I_{\max}(u_0,\lambda)$. In particular,

$$u_0 \leq u(\cdot,t;u_0,\lambda) \ \text{ in } \ [0,1] \ \text{ for all } \ t \in I_{\max}(u_0,\lambda). \tag{3.31}$$

Then, the following result holds, though it remains an open problem to ascertain whether, or not, the condition (3.32) holds.

Theorem 3.3. *Suppose* (H_a) *with* $s = n+1$ *and* $r = n$, *and* $u_0 \equiv \underline{u}_{1...1}$. *Assume, in addition, that there exists* $\mu > 0$ *such that, for every* $\lambda < \mu$, $T_{\max}(u_0, \lambda) = \infty$ *and there is a constant* $C(\lambda) > 0$ *such that*

$$u(x,t;u_0,\lambda) \leq C(\lambda) \ \text{ for all } \ (x,t) \in [0,1] \times [0,\infty). \tag{3.32}$$

Then, there exists $\lambda_c < 0$ *such that* (1.1) *has, for every* $\lambda < \lambda_c$, $2^{n+1} - 1$ *positive solutions.*

Proof. Under these assumptions, thanks to the main theorem of Langlais and Phillips [35], for every $\lambda < \mu$ the point-wise limit

$$\theta_{\{\lambda,(1,...,1)\}} := \lim_{t\uparrow\infty} u(\cdot,t;u_0,\lambda)$$

provides us with a positive solution of (1.1) such that $u_0 \leq \theta_{\{\lambda,(1,...,1)\}}$. Thus, for every $i \in \{1,...,n+1\}$,

$$\theta_{\lambda,i} \leq \theta_{\{\lambda,(1,...,1)\}} \quad \text{in } \ I_i^+ = (\gamma_i, \varrho_i),$$

while, thanks to Theorem 3.1,

$$\lim_{\lambda\downarrow-\infty} \theta_{\{\lambda,(1,...,1)\}} = 0 \quad \text{in } \bigcup_{j=1}^{n} I_j^-.$$

In particular, for sufficiently negative $\lambda < 0$, the positive solution $\theta_{\{\lambda,(1,...,1)\}}$ has, at least, one peak on each of the $n+1$ intervals (γ_i, ϱ_i), $i \in \{1,...,n+1\}$.

Now, for every $(d_1,\ldots,d_{n+1}) \in \{0,1\}^{n+1}$ such that $\sum_{i=1}^{n+1} d_i \leq n$, we consider the initial data

$$\tilde{u}_0 := \underline{u}_{(d_1,...,d_{n+1})} \equiv \begin{cases} d_i\theta_{\{\lambda,i\}} & \text{in } \ I_i^+, \qquad i \in \{1,...,n+1\}, \\ 0 & \text{in } \ I_j^-, \qquad j \in \{1,...,n\}, \end{cases}$$

having, at least, $\sum_{i=1}^{n+1} d_i \leq |n|$ peaks. Arguing as before, it becomes apparent that $u(x,t;\tilde{u}_0,\lambda)$ is a subsolution of (1.1) for all $t \in I_{\max}(\tilde{u}_0,\lambda)$. Moreover, by the parabolic maximum principle, since $\tilde{u}_0 \leq u_0$, we have that, for every $x \in [0,1]$ and $t \in I_{\max}(\tilde{u}_0,\lambda)$,

$$u(x,t;\tilde{u}_0,\lambda) \leq u(x,t;u_0,\lambda).$$

Thus, $T_{\max}(\tilde{u}_0,\lambda) = \infty$ and, for sufficiently negative λ, $u(x,t;\tilde{u}_0,\lambda)$ is increasing in time and bounded above. Hence,

$$\theta_{\{\lambda,(d_1,...,d_{n+1})\}} \equiv \lim_{t\uparrow\infty} u(\cdot,t;\tilde{u}_0,\lambda) \leq \lim_{t\uparrow\infty} u(\cdot,t;u_0,\lambda) \equiv \theta_{\{\lambda,(1,...,1)\}}$$

provides us with a positive solution of (1.1) such that, according to Theorems 1.1 and 3.1,

$$\lim_{\lambda\downarrow-\infty} \theta_{\{\lambda,(d_1,...,d_{n+1})\}} = 0 \quad \text{in } \bigcup_{j=1}^{n} I_j^- \cup \bigcup_{i\in Z} I_i^+$$

where

$$Z \equiv \{i \in \{1,...,n+1\} : d_i = 0\}.$$

Since,

$$0 < \theta_{\{\lambda,i\}} \leq \theta_{\{\lambda,(d_1,...,d_{n+1})\}} \quad \text{in } \ I_i^+ \ \text{ for all } \ i \in \{1,...,n+1\} \setminus N,$$

a genuine combinatorial argument ends the proof, as these solutions differ as $\lambda \downarrow -\infty$. □

4. The case $n = 1$

Throughout this section, we assume that

$$a(x) = \sin(3\pi x), \qquad x \in [0, 1].$$

Then, the global bifurcation diagram of the positive solutions of (1.1) looks like shows Figure 3b. Our numerical experiments suggest that the set of positive solutions of (1.1) consists of the component $\mathscr{C}^+$, which bifurcates supercritically from $u = 0$ at $\lambda = \pi^2$, because

$$D_1 = -2\int_0^1 a(x)\sin^3(\pi x)\,dx = -2\int_0^1 \sin(3\pi x)\sin^3(\pi x)\,dx = \frac{1}{4} > 0.$$

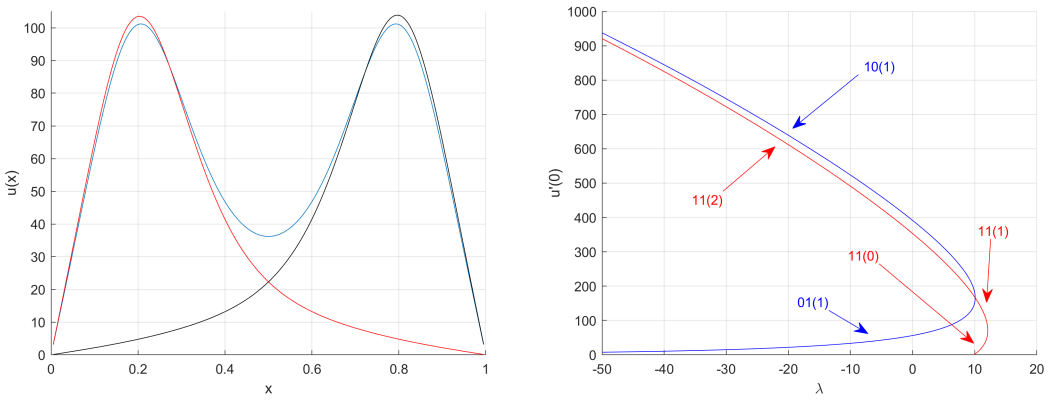

(A) Positive solutions for $\lambda \approx -21$: 10(1) in red, 01(1) in black, and 11(2) in blue.

(B) Global bifurcation diagram.

FIGURE 3. Numerical results for $a(x) = \sin(3\pi x)$.

This component exhibits a turning point at $\lambda_t \approx 12.1$, and a secondary bifurcation at $\lambda_s \approx 10.1$, as shown in the global bifurcation diagram plotted in Figure 3b. In this and in all subsequent global bifurcation diagrams we are plotting the parameter λ, in abscisas, versus the derivative of the solution at the origin, $u'(0)$, in ordinates. This allows to differentiate between all admissible positive solutions. By the symmetries of the problem, the reflection about 0.5 of any positive solution of (1.1) provides with another solution, though there is no way to differentiate between such solutions if, instead of plotting λ versus $u'(0)$, we plot λ versus the L_p-norm of the solutions for some $p \geq 1$. Should we proceed in this way, we could not differentiate between, e.g., the solutions of types 01(1) and 10(1), as they have the same L_p-norms for all $p \geq 1$ (see the plots of these solutions in Figure 3a).

According to Theorem 2.5, $\mathcal{P}_\lambda(\mathscr{C}^+) = (-\infty, \lambda_t]$ and, for every $\lambda \in (\pi^2, \lambda_t]$, the minimal positive solution of (1.1) is the unique stable positive solution of (1.1). Actually, for every $\lambda \in (\pi^2, \lambda_t)$, the minimal solution is linearly asymptotically stable and hence, its Morse index equals zero. Moreover, by Theorem 2.5, $(\lambda_t, \theta^{\min}_{\lambda_t})$ is the unique positive solution at λ_t, it is linearly neutrally stable, and it is a quadratic subcritical turning point of the component $\mathscr{C}^+$. The solutions on the upper half curve through the subcritical turning point $(\lambda_t, \theta^{\min}_{\lambda_t})$ have one-dimensional unstable manifold, and actually are of type 11(1) until λ reaches the secondary bifurcation point, λ_s, where they became unstable with Morse index two and type 11(2) for any further smaller value of λ.

At $\lambda = \lambda_s$, two (new) secondary branches of positive solutions with respective types 01(1) and 10(1) bifurcate subcritically. Naturally, $u'(0) \approx 0$ for the solutions of type 01(1), while

$u'(0)$ is large for those of type 10(1), as confirmed by our numerical experiments. These three branches seem to be globally defined for all further smaller values of λ, $\lambda < \lambda_s$.

In full agreement with Conjecture 1.1, the problem (1.1) has three positive solutions for every $\lambda < \lambda_s$. Figure 3a shows the plots of these solutions at a value $\lambda \approx -21$. Note that the number of peaks of the solutions coincides with the dimension of their respective unstable manifolds for all $\lambda < \lambda_s$.

5. The case $n = 2$

Throughout this section we have chosen

$$a(x) = \sin(5\pi x), \qquad x \in [0, 1].$$

By Conjecture 1.1, we expect to have $2^3 - 1 = 7$ positive solution for sufficiently negative λ. The global bifurcation diagram computed in this case has been plotted in Figure 4.

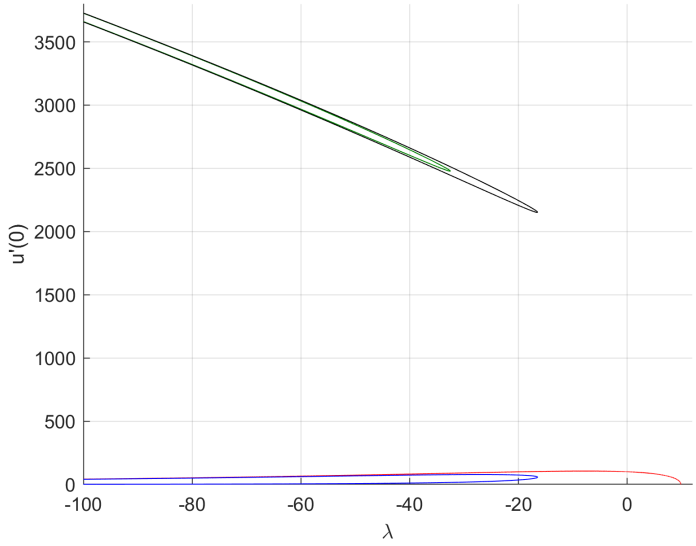

Figure 4. Global bifurcation diagram for $a(x) = \sin(5\pi x)$.

It consists of 4 components, 3 global folds isolated from $u = 0$, plus $\mathscr{C}^+$, which in this occasion bifurcates subcritically from $u = 0$ at $\lambda = \pi^2$, because

$$D_1 = 2\int_0^1 \sin(5\pi x)\sin^3(\pi x)\,dx = 0$$

and

$$D_2 = -2\int_0^1 w_1(x)\sin(5\pi x)\sin^2(\pi x)\,dx = -\frac{5}{256\pi^2} < 0.$$

None of these components, neither $\mathscr{C}^+$ nor any of the three folds plotted in Figure 4, exhibited any secondary bifurcation along it.

Figure 5 shows two magnifications of the most significant pieces of the global bifurcation diagram plotted in Figure 4 together with the superimposed types of the solutions along each of the solution curves plotted on it. Precisely, Figure 5a shows a zoom of the two superior

global folds plotted in Figure 4 around their respective turning points. These solutions look larger in these global bifurcation diagram because

$$\lim_{\lambda\downarrow-\infty} u'_\lambda(0) = +\infty$$

for any positive solution (λ, u_λ) having mass in $(0, 0.2)$. Figure 5a shows the types of the positive solutions along each of the half-branches of the two folds. They change from type 100(1) to type 110(2) as they cross the turning point of the exterior component, while they are changing from type 101(2) to type 111(3) as the turning point of the interior folding is crossed.

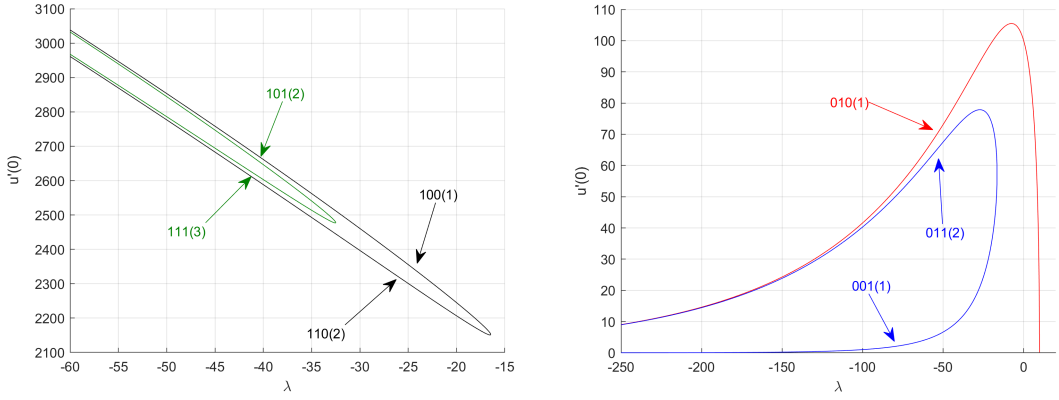

(A) Upper part magnification. (B) Lower part magnification.

FIGURE 5. Two significant magnifications of Figure 4.

Not surprisingly, since $\mathscr{C}^+$ does not exhibit any secondary bifurcation along it, all the solutions of $\mathscr{C}^+$ that we have computed are of type 010(1), in complete agreement with the exchange stability principle of Crandall and Rabinowitz [17], because $u = 0$ is linearly stable for all $\lambda < \pi^2$.

Lastly, the solutions along the interior folding in Figure 5b change type from 001(1) to 011(2) when the turning point of this components is switched on. Moreover, for sufficiently negative λ, (1.1) admits 7 positive solutions, with respective types

$$001(1), \qquad 010(1), \qquad 100(1), \qquad 101(2), \qquad 110(2), \qquad 011(2), \qquad 111(3),$$

in full agreement with Conjecture 1.1. In particular, in any circumstances, the number of peaks of these solutions, when they exist, equals their respective Morse indices.

6. THE CASE $n = 3$

Throughout this section we make the choice

$$a(x) = \sin(7\pi x), \qquad x \in [0, 1].$$

According to Conjecture 1.1, we expect to have $2^4 - 1 = 15$ positive solution for sufficiently negative λ. Since

$$D_1 = -2\int_0^1 \sin(7\pi x)\sin^3(\pi x)\,dx = 0$$

and

$$D_2 = -2\int_0^1 w_1(x)\sin(7\pi x)\sin^2(\pi x)\,dx = \frac{1}{128\pi^2} > 0,$$

the component $\mathscr{C}^+$ bifurcates supercritically from $u = 0$ at $\lambda = \pi^2$, and exhibits a secondary bifurcation at $\lambda_s \approx -2.85$. It has been plotted in Figure 6a, which shows a significant piece of the global bifurcation diagram of the positive solutions of (1.1).

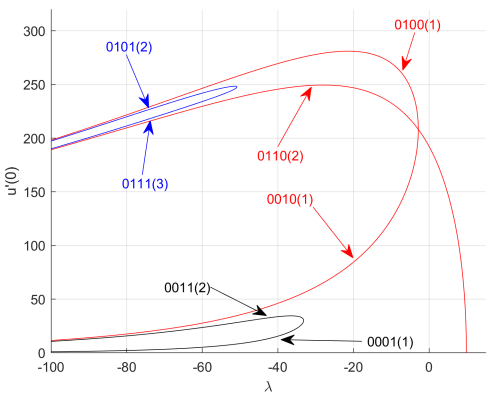

(A) Small positive solutions.

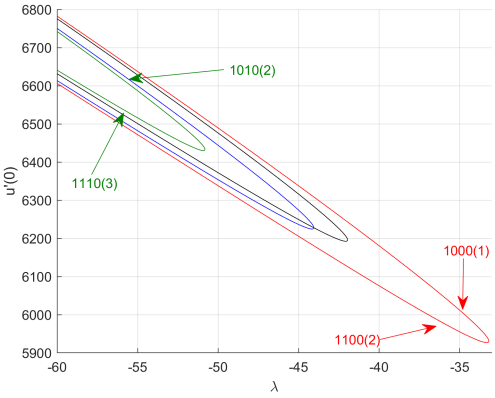

(B) Large positive solutions.

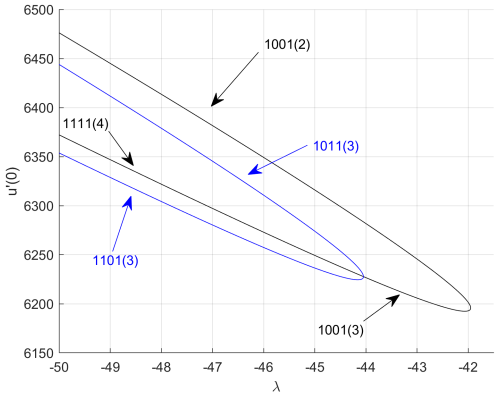

(C) A magnification of Figure 6b.

FIGURE 6. Scattered bifurcation diagrams for $a(x) = \sin(7\pi x)$.

Figure 6 consists of Figures 6a, 6b and 6c, where we are plotting, separately, the most significant branches of positive solutions that we have computed in our numerical experiments. By simply looking at the ordinate axis in Figures 6a and 6b, it is easily realized the ultimate reason why we are plotting these components in two separate figures. Whereas for those plotted on the left $u'(0) < 3 \cdot 10^2$, for those plotted on the right we have that $u'(0) > 59 \cdot 10^2$. So, plotting them in the same global bifurcation diagram would have pushed down against the λ-axis all the branches on the left, much like in Figure 4, but straightening this pushing effect. Figure 6c shows a zoom of the secondary bifurcation arising in Figure 6b, to detail the types of the positive solutions around it.

Since $\mathscr{C}^+$ bifurcates from $u = 0$ supercritically, by the exchange stability principle, [17], its solutions have Morse index zero until they reach the turning point. The bifurcation is very vertical in this case, hence, it is hard to determine for which λ the turning point occurs. Anyway, Morse index increases to one as we pass the turning point and it remains the same until we reach the bifurcation point at $\lambda_s \approx -2.85$, where the Morse index becomes two for any smaller value of λ. By Theorem 2.1, the solutions $(\lambda, u) \in \mathscr{C}^+$ with $\lambda \approx \pi^2$ have the form

$s(\sin(\pi x) + y(s))$ for some $s > 0$, $s \approx 0$. Thus, they have a single peak around 0.5. Once crossed λ_s, these solutions are of type 0110(2). The solutions along the bifurcated branches have types 0100(1) and 0010(1), respectively. So, this piece of the global bifurcation diagram seems to be generated by the two internal positive bumps of the weight function $a(x)$. Besides the component $\mathscr{C}^+$, Figure 6a shows two additional global subcritical folds. The solutions on the lower half-branch of the inferior folding have type 0001(1) and change to type 0011(2) on its upper half-branch, as the turning point of this component is crossed. Similarly, the solutions on the lower half-branch of the superior folding have type 0111(3) and change to type 0101(2) on the upper one. All those solutions can be generated, very easily, by taking into account that its type must begin with a 0, because $u'(0)$ is small, while the remaining three digits should cover all the possible combinations of three elements taken from $\{0, 1\}$. Thus, counting $u = 0$, we have a total of $2^3 = 8$ solutions for sufficiently negative λ.

Analogously, Figure 6b shows all solutions with $u'(0)$ sufficiently large, whose types must begin with 1. Thus, it also shows a total of $2^3 = 8$ solutions. According to our numerical experiments, these solutions are distributed into three components. Namely, two isolated global subcritical folds, plus a third component consisting of two interlaced subcritical folds, which is the component magnified and plotted in Figure 6c. The bifurcation along this component occurs at $\lambda_s \approx -44.05$.

According to these findings, based on a series of rather systematic numerical experiments, the sum of the four digits of the type of the solutions, i.e., their number of peaks, always provide us with the dimensions of their unstable manifolds, except for the solutions in a right neighborhood of the two bifurcation points on Figures 6a and 6c, where the solutions have types 0000(1) and 1001(3), respectively. Nevertheless, for sufficiently negative λ, this is a general rule.

In Figure 7 we have plotted a series of solutions of types 0111 and 0101 along the superior

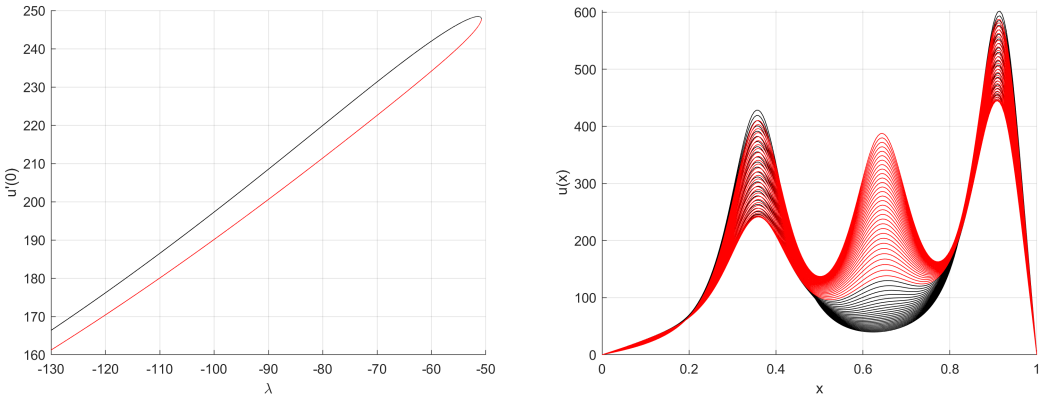

(A) The blue upper fold of Figure 6a.

(B) Plots of solutions of type 0111(3) (red) and 0101(2) (black) on the branch plotted on the left.

FIGURE 7. Plots of solutions (right) along the branch (left) from Figure 6a.

fold (blue branch) of Figure 6a. The solutions on the lower half-branch are of type 0111, because they exhibit three peaks, and have been plotted in Figure 7b using red color. As the turning point is approached, the peaks of these solutions decrease until the central one is almost glued as the turning point is crossed. Once switched the turning point, the solutions need some additional, very short, room for becoming of type 0101 pure, since the central peak still persists for a while, as it is illustrated in Figure 7b, where those solutions have been

plotted in black color. Essentially, as the turning point is switched, the external peaks of the 0111 solutions increase, while the central peak is glued.

7. The case $n = 2$ with an additional parameter μ

In this section, we make the following choice

$$a(x) := \begin{cases} \mu \sin(5\pi x) & \text{if} \quad x \in [0, 0.2) \cup (0.8, 1], \\ \sin(5\pi x) & \text{if} \quad x \in [0.2, 0.8], \end{cases} \tag{7.1}$$

where $\mu \geq 1$ is regarded as a secondary bifurcation parameter for (1.1). The behavior of this model for $\mu = 1$ has been already described in Section 5. The bifurcation direction is

$$D_1 = -\frac{\sqrt{\frac{1}{2}\left(5-\sqrt{5}\right)}\left(5-\sqrt{5}\right)^2(\mu-1)}{128\pi} < 0$$

for all $\mu > 1$ and hence, the bifurcation is always subcritical.

According to our numerical experiments, as we increase the value of μ, the global bifurcation diagram remains very similar to the one plotted in Figures 4 and 5, up to reaching the critical value $\mu_1 \approx 3.895$, where the global structure of the bifurcation diagram changes. Figures 8a and 8b plot the corresponding global bifurcation diagram for $\mu = 3.5$ and $\mu = 3.89$, respectively, whose global structure, topologically, coincides with the one already computed in Section 5 for $\mu = 1$.

Essentially, as μ separates away from $\mu = 1$ increasing towards $\mu = \mu_1$, the two subcritical folds lying in the upper part of the global bifurcation diagram plotted in Figure 4 are getting closer approaching the peak of the corresponding component $\mathscr{C}^+ \equiv \mathscr{C}^+_\mu$, as well as the global subcritical folding beneath, as sketched in Figure 8.

According to our numerical experiments, at the critical value of the parameter μ_1, the set of positive solutions of (1.1) consists of two components, instead of four, because three of the previous four components of the problem for $\mu < \mu_1$ are now touching at a single point playing the role of a sort of *organizing center* with respect to the secondary parameter μ, whereas the upper interior supercritical folding remains separated away from $\mathscr{C}^+_{\mu_1}$. Naturally, $\mathscr{C}^+_{\mu_1}$ consists of $\lim_{\mu\uparrow\mu_1} \mathscr{C}^+_\mu$ plus the limits of the previous exterior upper folds and folds beneath $\mathscr{C}^+_\mu$ for $\mu < \mu_1$.

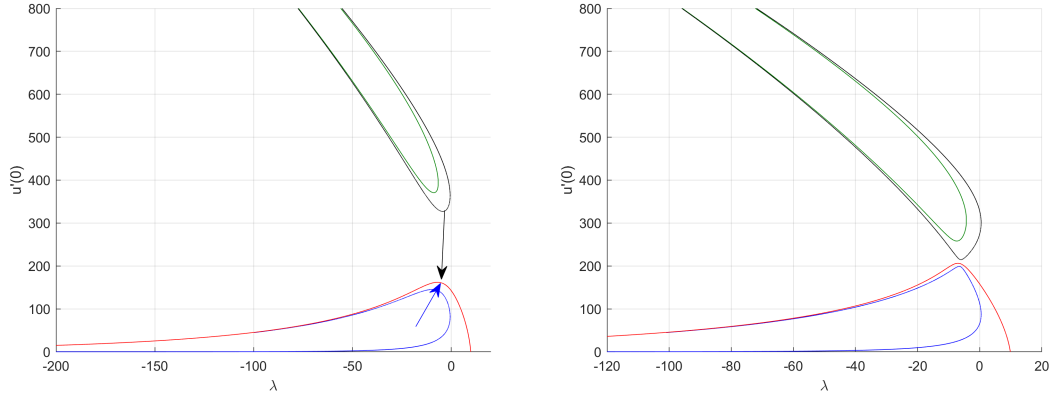

(A) $\mu = 3.5 < \mu_1$ (B) $\mu = 3.89 < \mu_1$

FIGURE 8. Global bifurcation diagrams for $\mu < \mu_1$.

The numerics suggests that, as μ increases separating away from μ_1, the touching point of the old three components spreads out into two secondary bifurcation points from the new component $\mathscr{C}_\mu^+$, in such a way that the "previous" folds do now bifurcate from $\mathscr{C}_\mu^+$ at these two bifurcation values with respect to the primary parameter λ, say $\lambda_1(\mu) > \lambda_2(\mu)$, as illustrated in Figure 9a, where it becomes apparent how the old upper interior folding component still remains separated away from $\mathscr{C}_\mu^+$. Essentially, the upper half-branch of the old folding above $\mathscr{C}_\mu^+$ together with the lower half-branch of the old interior folding provide us with the branch bifurcating from $\mathscr{C}_\mu^+$ at $\lambda_2(\mu)$, for $\mu > \mu_1$, whereas the lower half-branch of the old folding above $\mathscr{C}_\mu^+$ together with the upper half-branch of the old interior folding provide us with the new branch bifurcating from $\mathscr{C}_\mu^+$ at $\lambda_1(\mu)$. And this situation persists for all $\mu \in (\mu_1, \mu_2)$, where $\mu_2 \approx 3.925$. The bigger is μ in the interval (μ_1, μ_2), the more separated stay the two bifurcation values $\lambda_1(\mu)$ and $\lambda_2(\mu)$ and the more approaches the exterior upper fold to the component $\mathscr{C}_\mu^+$. The separation between the bifurcation values is very well illustrated by the next table that provides us with the corresponding values of $\lambda_1(\mu)$ and $\lambda_2(\mu)$ for three values of μ in (μ_1, μ_2):

μ	3.9	3.91	3.92
$\lambda_1(\mu)$	-5.1186	-4.4513	-3.9938
$\lambda_2(\mu)$	-7.5845	-8.4129	-9.0284

TABLE 1. $\lambda_i(\mu)$ for three values of $\mu \in (\mu_1, \mu_2)$.

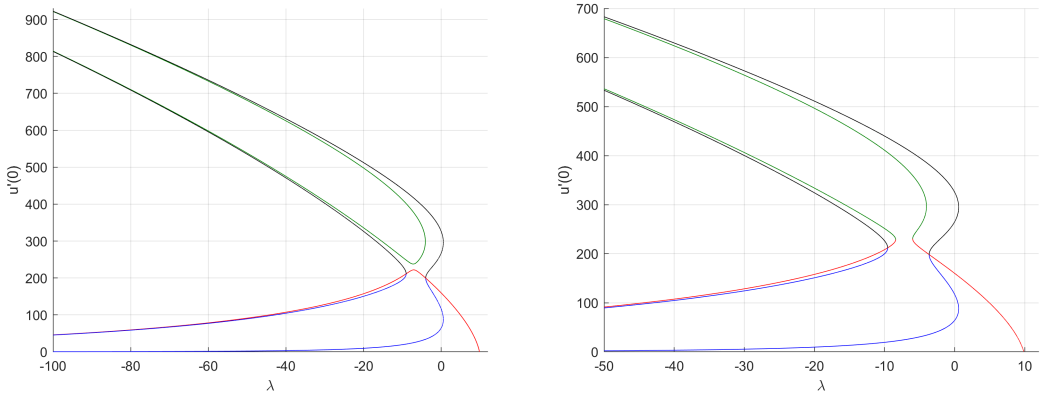

(A) $\mu_1 < \mu = 3.92 < \mu_2$ (B) $\mu_2 < \mu = 3.93$

FIGURE 9. Two significant global bifurcation diagrams

And this situation persists, until μ reaches the critical value μ_2, where, according to the numerics, the exterior folding touches $\mathscr{C}_{\mu_2}^+$ at a single point, in such a way that the set of positive solutions of (1.1) consists of the single component $\mathscr{C}_{\mu_2}^+$. As $\mu > \mu_2$ separates away from μ_2, our numerical experiments provide us with the global bifurcation diagram plotted in Figure 9b, where, once again, the set of positive solutions of (1.1) consists of two components, $\mathscr{C}_\mu^+$ plus a global subcritical fold with a bifurcated secondary branch with the structure of a global subcritical folding. Thus, a new re-organization of the previous solution branches has occurred through a sort of mutual re-combination.

The global bifurcation diagrams remained topologically equivalent for all values of $\mu > \mu_2$ for which we computed them. Figures 9b and 10a plot them for $\mu = 3.93$ and $\mu = 4.5$, respectively. In both cases, the set of positive solutions consists of $\mathscr{C}_\mu^+$ plus two global subcritical folds that meet at a single point, which can be viewed as a secondary bifurcation point from any of them. This structure persists for any further larger values of μ. Figure 10b shows a magnification of the most significant parts of Figure 10a superimposing the individual types of the solutions together with the dimensions of their unstable manifolds.

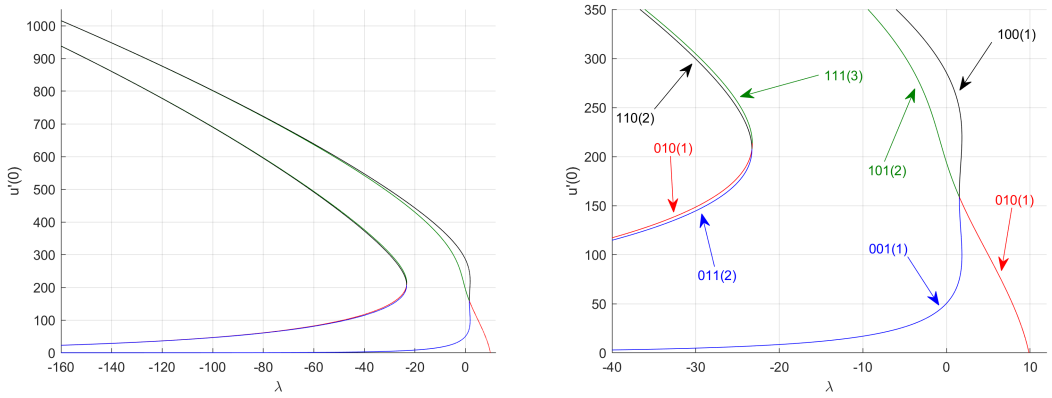

(A) $\mu_2 < \mu = 4.5$ (B) A zoom of the plot on the left

FIGURE 10. Global bifurcation diagram for $\mu > \mu_2$

In full agreement with Conjecture 1.1, for every $\mu \geq 1$, there exists $\lambda(\mu) < 0$ such that (1.1) has $2^3 - 1 = 7$ positive solutions for every $\lambda \leq \lambda(\mu)$. For the choice $\mu = 4.5$, $\lambda(\mu) \approx -23.27$ equals the λ-coordinate of the bifurcation point of the global subcritical folds. Note that, for this special choice, (1.1) possesses three solutions at $\lambda = 0$.

Figure 11 plots a series of solutions with types 100 and 001 along the blue/black branch

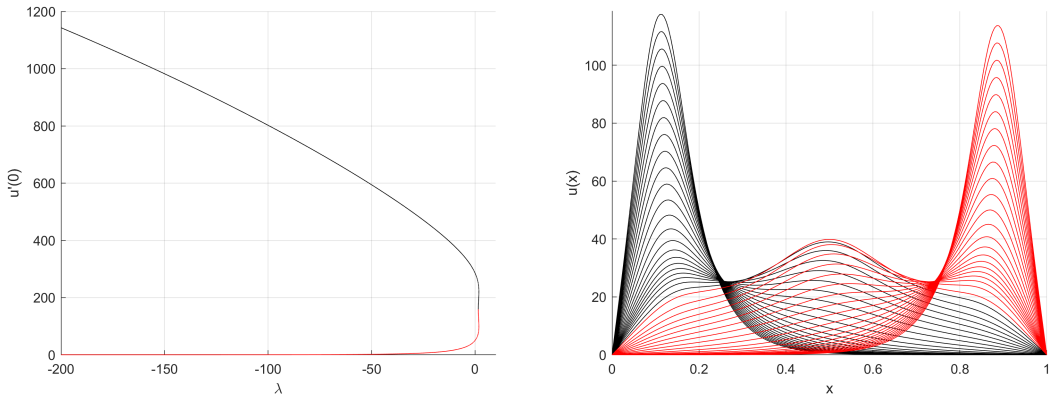

(A) The branch bifurcating from $\mathscr{C}_\mu^+$. (B) Plots of solutions 001(1) and 100(1) on the left.

FIGURE 11. Plots of solutions (right) along the branch (left) from Figure 10a.

of Figure 10b that is part of the component $\mathscr{C}_\mu^+$, which has been isolated in Figure 11a.

According to our numerical experiments, the solutions on the lower half-branch are of type 001; they have been plotted using red color. As the branching point is approached (see Figure 10b), the right peak diminishes and the solution looks like the first eigenfunction $\sin(\pi x)$. At the branching point, the solution changes its old type to 100. These solutions have been plotted using black color. The peak on the left starts to increase as we separate away from the bifurcation value.

8. Numerics of bifurcation problems

To discretize (1.1) we have used two methods. To compute the small positive solutions bifurcating from $u = 0$ we implemented a pseudo-spectral method combining a trigonometric spectral method with collocation at equidistant points, as in Gómez-Reñasco and López-Gómez [29, 32], López-Gómez, Eilbeck, Duncan and Molina-Meyer [43], López-Gómez and Molina-Meyer [45, 46, 47], López-Gómez, Molina-Meyer and Tellini [48], López-Gómez, Molina-Meyer and Rabinowitz [49], and Fencl and López-Gómez [26]. This gives high accuracy at a rather reasonable computational cost (see, e.g., Canuto, Hussaini, Quarteroni and Zang [14]). However, to compute the large positive solutions we have preferred a centered finite differences scheme, which gives high accuracy at a lower computational cost, as it is runs much faster in computing global solution branches in the bifurcation diagrams.

The pseudo-spectral method is more efficient and versatile for choosing the shooting direction from the trivial solution in order to compute the small positive solution of $\mathscr{C}^+$, as well as to detect the bifurcation points along the solution branches. Its main advantage in accomplishing this task comes from the fact that it provides us with the true bifurcation values from the trivial solution, while the scheme in differences only gives a rough approximation to these values. A pioneering reference on these methods is the paper of Eilbeck [23], which was seminal for the research teams of the second author.

For computing all the global subcritical folds arisen along this paper, we adopted the following, rather novel, methodology. Once computed $\mathscr{C}^+$, including all bifurcating branches from the primary curve emanating from $u = 0$ at $\lambda = \pi^2$, one can ascertain the types of the solutions in $\mathscr{C}^+$ for sufficiently negative λ. As, due to Conjecture 1.1 and the argument supporting it in Section 1, we already know that (1.1) admits $2^{n+1} - 1$ positive solutions for sufficiently negative λ, together with their respective types, we can determine the types of all solutions of (1.1) for λ sufficiently negative that remained outside the component $\mathscr{C}^+$. Suppose, e.g., that we wish to compute the solution curve containing the positive solutions of type 011(2) in Figure 10b. Then, we consider as the initial iterate, u_0, for the underlying Newton method some function with a similar shape. If the choice is sufficiently accurate, after finitely many iterates, whose number depends on how far away stays from the true solution the initialization u_0, the Newton scheme should provide us with the first positive solution on that particular component. Once located the first point, our numerical path-following codes provide us with the entire solution curve almost algorithmically though the code developed by Keller and Yang [34] to treat the turning points of these folds as if they were regular points treated with the implicit function theorem.

The huge complexity of some of the computed bifurcation diagrams, as well as their deepest quantitative features, required an extremely careful control of all the steps in the involved subroutines. This explains why the available commercial bifurcation solver packages, such as AUTO-07P, are almost un-useful to deal with differential equations, like the one of (1.1), with heterogeneous coefficients. As noted by Doedel and Oldeman in [22, p.18],

"given the non-adaptive spatial discretization, the computational procedure here is not appropriate for PDEs with solutions that rapidly vary in space, and care must be taken to recognize spurious solutions and bifurcations."

This is nothing than one of the main problems that we found in our numerical experiments, as the number of critical points of the solutions increases according to the dimensions of their unstable manifolds, and the solutions grew up to infinity as $\lambda \downarrow -\infty$ within the intervals of $\operatorname{supp} a^+$, while, due to Theorem 3.1, they decayed to zero on the intervals where $a(x)$ is negative. Naturally, for all numerical methods is a serious challenge to compute solutions exhibiting simultaneously internal and boundary layers, where the gradients can oscillate as much as wish for sufficiently negative λ.

For general Galerkin approximations, the local convergence of the solution paths at regular, turning and simple bifurcation points was proven by Brezzi, Rappaz and Raviart in [8, 9, 10] and by López-Gómez, Molina-Meyer and Villareal [50] and López-Gómez, Eilbeck, Duncan and Molina-Meyer in [43] for codimension two singularities in the context of systems. In these situations, the local structure of the solution sets for the continuous and the discrete models are known to be equivalent.

The global continuation solvers used to compute the solution curves of this paper, as well as the dimensions of the unstable manifolds of all the solutions filling them, have been built from the theory on continuation methods of Allgower and Georg [2], Crouzeix and Rappaz [18], Eilbeck [23], Keller [33], López-Gómez [37] and López-Gómez, Eilbeck, Duncan and Molina-Meyer [43].

9. Final discussion

Our systematic numerical experiments have confirmed that the following features should be true for a general $a(x)$ with $\operatorname{supp} a^+$ consisting of $n+1$ intervals separated away by n intervals where a is negative:

- As $\lambda \downarrow -\infty$, (1.1) has, at least, $2^{n+1}-1$ positive solutions. Theorem 3.3 has shown it under condition (3.32). It remains an open problem ascertaining whether, or not, (3.32) holds. Actually, for the special choice (1.3), it should have exactly $2^{n+1}-1$.
- As $\lambda \downarrow -\infty$, the Morse index of any positive solution u of type $d_1 d_2 \cdots d_{n+1}$, $d_j \in \{0,1\}$, is given by
$$\mathscr{M}(u) := \sum_{j=1}^{n+1} d_j.$$
- The eventual symmetric character of the solutions cannot be lost along any of the components of the set of solutions, unless a bifurcation point is crossed. Thus, each fold consists of either symmetric solutions around 0.5, or asymmetric ones.

Note that in the special case when $a(x)$ is given by (1.3), $a(0.5) < 0$ if n is odd, while $a(0.5) > 0$ if n is even. Moreover, according to our numerical experiments, the component $\mathscr{C}^+$ does not admit any bifurcation point if $n = 2$, whereas it admits one if $n \in \{1, 3\}$. Thus, one might be tempted to believe that, in general, $\mathscr{C}^+$ should not have any bifurcation point if $a(0.5) < 0$. Our numerical experiments in Section 7 show that, for the special choice

$$a(x) := \begin{cases} 4.5\sin(5\pi x) & \text{if} \quad x \in [0, 0.2) \cup (0.8, 1], \\ \sin(5\pi x) & \text{if} \quad x \in [0.2, 0.8], \end{cases} \tag{9.1}$$

the component $\mathscr{C}^+$ has a bifurcation point (see Figure 10b), though $a(0.5) < 0$. Thus, one should be extremely careful in conjecturing anything from either numerical experiments, or

heuristical considerations, as they might drive, very easily, to extract false conjectures (see Sovrano [62]).

According to the numeric of Section 7, the problem

$$\begin{cases} -u'' = a(x)u^2 \quad \text{in } (0,1), \\ u(0) = u(1) = 0, \end{cases} \tag{9.2}$$

for the special choice (9.1) has, exactly, three positive solutions, and it should not admit anymore, by consistency with the structure of the global bifurcation diagram (see Figure 10b). Thus, Corollary 1.4.2 of Feltrin [24] is optimal in the sense that it cannot be satisfied for sufficiently small $\mu > 0$. Precisely, it does not hold when $\mu = 1$ for the special choice (9.2). Since (1.1) still possesses $2^3 - 1 = 7$ positive solutions for sufficiently negative $\lambda < 0$, this example also shows the independence between the conjecture of [29] and the multiplicity results of Feltrin and Zanolin [25] and Feltrin [24].

For every $\mu \in (3.895, 3.925)$, the component $\mathscr{C}^+$ of (1.1) for the choice

$$a(x) := \begin{cases} \mu \sin(5\pi x) & \text{if} \quad x \in [0, 0.2) \cup (0.8, 1], \\ \sin(5\pi x) & \text{if} \quad x \in [0.2, 0.8], \end{cases} \tag{9.3}$$

exhibits two bifurcation points along it. This might be the first example of this nature documented in the abundant literature on superlinear indefinite problems.

As, generically, higher order bifurcations break down by the eventual asymmetries of the weight functions, as discussed in Chapter 7 of [39] and in [56], we conjecture that

- Generically, when $a(x)$ is asymmetric about 0.5, the set of positive solutions of (1.1) consists of the component $\mathscr{C}^+$ plus n supercritical folds, $\mathscr{D}_j$, $j \in \{1, ..., n\}$, in such a way that, as $\lambda \downarrow -\infty$, (1.1) admits, at least, one solution in $\mathscr{C}^+$ and two solutions in $\mathscr{D}_j$ for each $j \in \{1, ..., n\}$.

The global bifurcation diagram plotted in Figure 5 being a paradigm of this global topological behavior.

The analysis of the reorganization in components of the positive solutions of (1.1) carried out in Section 7 for the special choice (9.3) when μ increases from 3.89 up to reach the value $\mu = 3.93$ reveals the high complexity that the global bifurcation diagrams of (1.1) might have when $a(x)$ changes of sign a large number of times by incorporating the appropriate control parameters into the problem. Getting any insight into this problem is a challenge.

References

[1] S. Alama and G. Tarantello, Elliptic problems with nonlinearities indefinite in sign, *J. Funct. Anal.* **141** (1996), 159–215.

[2] E. L. Allgower and K. Georg, *Introduction to Numerical Continuation Methods*, SIAM Classics in Applied Mathematics 45, SIAM, Philadelphia, 2003.

[3] H. Amann and J. López-Gómez, A priori bounds and multiple solutions for superlinear indefinite elliptic problems, *J. Diff. Eqns.* **146** (1998), 336–374.

[4] A. Ambrosetti, M. Badiale and S. Cingolani, Semiclassical states of nonlinear Schrödinger equations, *Arch. Rat. Mech. Anal.* **140** (1997), 285–300.

[5] H. Berestycki, I. Capuzzo-Dolcetta and L. Nirenberg, Superlinear indefinite elliptic problems and nonlinear Liouville theorems, *Topol. Methods Nonl. Anal.* **4** (1994) 59–78.

[6] H. Berestycki, I. Capuzzo-Dolcetta and L. Nirenberg, Variational methods for indefinite superlinear homogeneous elliptic problems, *Nonl. Diff. Eqns. Appl.* **2** (1995), 553–572.

[7] H. Berestycki and P. L. Lions, Some applications of the method of super and subsolutions, in *Bifurcation and nonlinear eigenvalue problems* (Proc., Session, Univ. Paris XIII, Villetaneuse, 1978), pp. 16–41, Lecture Notes in Mathematics 782, Springer, Berlin, 1980.

[8] F. Brezzi, J. Rappaz and P. A. Raviart, Finite dimensional approximation of nonlinear problems, part I: Branches of nonsingular solutions, *Numer. Math.* **36** (1980), 1–25.
[9] F. Brezzi, J. Rappaz and P. A. Raviart, Finite dimensional approximation of nonlinear problems, part II: Limit points, *Numer. Math.* **37** (1981), 1–28.
[10] F. Brezzi, J. Rappaz and P. A. Raviart, Finite dimensional approximation of nonlinear problems, part III: Simple bifurcation points, *Numer. Math.* **38** (1981), 1–30.
[11] G. Buttazzo, M. Giaquinta and S. Hildebrandt, *One-dimensional Variational Problems*, Clarendon Press, Oxford, 1998.
[12] J. Byeon and K. Tanaka, Semi-classical standing waves for nonlinear Schrödinger equations at structurally stable critical points of the potential, *J. Eur. Math. Soc.* **15** (2013), 1859–1899.
[13] S. Cano-Casanova and J. López-Gómez, Properties of the principal eigenvalues of a general class of nonclassical mixed boundary value problems, *J. Dif. Eqns.* **178** (2002), 123–211.
[14] C. Canuto, M. Y. Hussaini, A. Quarteroni and T. A. Zang, *Spectral Methods in Fluid Mechanics*, Springer, Berlin, Germany, 1988.
[15] S. Cingolani and M. Lazzo, Multiple positive solutions to nonlinear Schrödinger equations with competing potential functions, *J. Diff. Eqns.* **160** (2000), 118–138.
[16] M. G. Crandall and P. H. Rabinowitz, Bifurcation from simple eigenvalues, *J. Funct. Anal.* **8** (1971), 321–340.
[17] M. G. Crandall and P. H. Rabinowitz, Bifurcation, perturbation of simple eigenvalues and linearized stability, *Arch. Rat. Mech. Anal.* **52** (1973), 161–180.
[18] M. Crouzeix and J. Rappaz, *On Numerical Approximation in Bifurcation Theory*, Recherches en Mathématiques Appliquées 13, Masson, Paris, 1990.
[19] E. N. Dancer and J. Wei, On the effect of domain topology in a singular perturbation problem, *Top. Meth. Nonl. Anal.* **11** (1998), 227–248.
[20] M. del Pino and P. Felmer, Semi-classical states for nonlinear Schrödinger equations, *J. Funct. Anal.* **149** (1997), 245–265.
[21] M. del Pino and P. Felmer, Multipeak bound states for nonlinear Schrödinger equations, *Ann. Inst. Henri Poincaré* **15** (1998), 127–149.
[22] E. J. Doedel and B. E. Oldeman, AUTO-07P: Continuation and bifurcation software for ODEs, 2012, http://www.dam.brown.edu/people/sandsted/auto/auto07p.pdf.
[23] J. C. Eilbeck, The pseudo-spectral method and path-following in reaction-diffusion bifurcation studies, *SIAM J. Sci. Stat. Comput.* **7** (1986), 599–610.
[24] G. Feltrin, *Positive Solutions to Indefinite Problems, A Topological Approach*, Frontiers in Mathematics, Birkhäuser, 2018.
[25] G. Feltrin and F. Zanolin, Multiple positive solutions for a superlinear problem: a topological approach, *J. Diff. Equ.* **259** (2015), 925–963.
[26] M. Fencl and J. López-Gómez, Nodal solutions of weighted indefinite problems, *J. Evol. Equ.* https://doi.org/10.1007/s00028-020-00625-7.
[27] S. Fernández-Rincón and J. López-Gómez, The Picone identity: A device to get optimal uniqueness results and global dynamics in Population Dynamics, *Nonlinear Analysis RWA, in press*, arXiv:1911.05066v2 [math.AP] 20 Nov 2019.
[28] M. Gaudenzi, P. Habets and F. Zanolin, A seven-positive-solutions theorem for a superlinear problem, *Adv. Nonlinear Stud.* **4** (2004), 149–164.
[29] R. Gómez-Reñasco and J. López-Gómez, The effect of varying coefficients on the dynamics of a class of superlinear indefinite reaction diffusion equations, *J. Diff. Eqns.* **167** (2000), 36–72.
[30] R. Gómez-Reñasco and J. López-Gómez, The uniqueness of the stable positive solution for a class of superlinear indefinite reaction diffusion equations, *Diff. Int. Eqns.* **14** (2001), 751–768.
[31] R. Gómez-Reñasco and J. López-Gómez, The effect of varying coefficients on the dynamics of a class of superlinear indefinite reaction diffusion arising in population dynamics, unpublished preprint 1999. Numerical experiments incorporated to Chapter 9 of [42].
[32] R. Gómez-Reñasco and J. López-Gómez, On the existence and numerical computation of classical and non-classical solutions for a family of elliptic boundary value problems, *Nonl. Anal. TMA* **48** (2002), 567–605.
[33] H. B. Keller, *Lectures on Numerical Methods in Bifurcation Problems*, Tata Insitute of Fundamental Research, Springer, Berlin, Germany, 1986.
[34] H. B. Keller and Z. H. Yang, A direct method for computing higher order folds, *SIAM J. Sci. Stat.* **7** (1986), 351–361.

[35] M. Langlais and D. Phillips, Stabilization of solutions of nonlinear and degenerate evolution equations, *Nonlinear Anal.* **9** (1985), 321-–333.

[36] Y. Le, J. Wei and H. Xu, Multi-bump solutions of $-\Delta u = K(x)u^{\frac{n+2}{n-2}}$ on lattices in $\mathbb{R}^n$, *J. reine angew. Math.* **743** (2018), 163–211.

[37] J. López-Gómez *Estabilidad y Bifurcación Estática. Aplicaciones y Métodos Numéericos*, Cuadernos de Matemática y Mecánica, Serie Cursos y Seminarios 4, Santa Fe, R. Argentina, 1988.

[38] J. López-Gómez, Varying bifurcation diagrams of positive solutions for a class of superlinear indefinite boundary value problems, *Trans. Amer. Math. Soc.* **352** (2000), 1825–1858.

[39] J. López-Gómez, *Spectral Theory and Nonlinear Functional Analysis*, CRC Press, Boca Raton, 2001.

[40] J. López-Gómez, Uniqueness of radially symmetric large solutions, *Disc. Cont. Dyn. Systems Supplement* (2007), 677–686.

[41] J. López-Gómez, *Linear Second Order Elliptic Operators*, World Scientific Publishing, 2013.

[42] J. López-Gómez, *Metasolutions of Parabolic Equations in Population Dynamics*, CRC Press, Boca Raton, 2016.

[43] J. López-Gómez, J. C. Eilbeck, K. Duncan and M. Molina-Meyer, Structure of solution manifolds in a strongly coupled elliptic system, *IMA J. Numer. Anal.* **12** (1992), 405–428.

[44] J. López-Gómez and M. Molina-Meyer, Bounded components of positive solutions of abstract fized point equations: mushrooms, loops and isolas, *J. Diff. Eqns.* **209** (2005), 416–441.

[45] J. López-Gómez and M. Molina-Meyer, Superlinear indefinite systems: Beyond Lotka Volterra models, *J. Differ. Eqns.* **221** (2006), 343–411.

[46] J. López-Gómez and M. Molina-Meyer, The competitive exclusion principle versus biodiversity through segregation and further adaptation to spatial heterogeneities, *Theor. Popul. Biol.* **69** (2006), 94–109.

[47] J. López-Gómez and M. Molina-Meyer, Modeling coopetition, *Math. Comput. Simul.* **76** (2007), 132–140.

[48] J. López-Gómez, M. Molina-Meyer and A. Tellini, Intricate dynamics caused by facilitation in competitive environments within polluted habitat patches, *Eur. J. Appl. Maths.* doi:10.1017/S0956792513000429 (2014), 1–17.

[49] J. López-Gómez, M. Molina-Meyer and P. H. Rabinowitz, Global bifurcation diagrams of one node solutions in a class of degenerate bundary value problems, *Disc. Cont. Dyn. Sys. B* **22** (2017), 923–946.

[50] J. López-Gómez, M. Molina-Meyer and M. Villareal, Numerical coexistence of coexistence states, *SIAM J. Numer. Anal.* **29** (1992), 1074–1092.

[51] J. López-Gómez and P. Omari, Global components of positive bounded variation solutions of a one-dimensional indefinite quasilinear Neumann problem, *Adv. Nonlinear Stud.* **19** (2019) 437–473.

[52] J. López-Gómez and P. Omari, Characterizing the formation of singularities in a superlinear indefinite problem related to the mean curvature operator, *J. Differ. Equ.* **269** (2020), 1544–1570.

[53] J. López-Gómez and P. Omari, Regular versus singular solutions in a quasilinear indefinite problem with an asymptotically linear potential, *Adv. Nonlinear Stud.* https://doi.org/10.1515/ans-2020-2083.

[54] J. López-Gómez, P. Omari, S. Rivetti, Positive solutions of one-dimensional indefinite capillarity-type problems, *J. Differ. Equ.* **262** (2017) 2335–2392.

[55] J. López-Gómez, P. Omari and S. Rivetti, Bifurcation of positive solutions for a one-dimensional indefinite quasilinear Neumann problem, *Nonlinear Anal.* **155** (2017) 1–51.

[56] J. López-Gómez and A. Tellini, Generating an arbitrarily large number of isolas in a superlinear indefinite problem, *Nonl. Anal.* **108** (2014), 223–248.

[57] J. López-Gómez, A. Tellini and F. Zanolin, High multiplicity and complexity of the bifurcation diagrams of large solutions for a class of superlinear indefinite problems, *Commun. Pure Appl. Anal.* **13** (2014), 1–73.

[58] L. Nirenberg, A strong maximum principle for parabolic equations, *Comm. Pure Appl. Maths.* **6** (1953), 167–177.

[59] J. Mawhin, D. Papini and F. Zanolin, Boundary blow-up for differential equations with indefinite weight, *J. Diff. Eqns.* **188** (2003), 33–51.

[60] P. H. Rabinowitz, Some global results for nonlinear eigenvalue problems, *J. Funct. Anal.* **7** (1971), 487–513.

[61] D. H. Sattinger, *Topics in stability and bifurcation theory*, Lecture Notes in Mathematics, Vol. 309. Springer-Verlag, Berlin–New York, 1973.

[62] E. Sovrano, A negative answer to a conjecture arising in the study of selection-migration models in population genetics, *J. Math. Biol.* **76** (2018), 1655–1672.

[63] X. Wang and B. Zeng, On concentration of positive bound states of nonlinear Schrödinger equations with competing potential functions, *SIAM J. Math. Anal.* **28** (1997), 633–655.

[64] J. Wei, On the construction of single-peaked solutions to a singularly perturbed semilinear Dirichlet problem, *J. Diff. Eqns.* **129** (1996), 315–333.

Department of Mathematics and NTIS, Faculty of Applied Sciences, University of West Bohemia, Univerzitní 8, 30100, Plzen, Czech Republic
Email address: fenclm37@ntis.zcu.cz

Institute of Inter-disciplinar Mathematics (IMI) and Department of Analysis and Applied Mathematics, Complutense University of Madrid, Madrid 28040, Spain
Email address: Lopez_Gomez@mat.ucm.es